UNIVERSITY OF NAPLES "FEDERICO II"

Ph.D Program in

Structural, Geothechnical and Seismic Engineering

XXXII CYCLE

Coordinator Prof. Eng.: Luciano Rosati

Tropeano Francesca

Ph.D. Thesis

CABLE SYSTEMS AND TENSILE STRUCTURES

Tutor: Prof. Arch. Ottavia Corbi

2020

To all my family, who is always supporting me, constantly.

To my sweet cousin Susanna: don't lose your passion for studying

and your determination to make your dreams come true.

Believe in yourself.

And in loving memory of my grandpa Mario, my friends Pino and Emilia.

You are my angels.

Acknowledgements

Thanks to my cousin Ilaria, you are a sister for me, and your smile and positivity were and are a safe place. My little Miriam: you are stronger than you think, follow your dreams!

My Uncle Gianfranco, always by my side and helping me in every technological and non-technological difficulty.

Finally, my thanks go to my friends, near and far who have always supported me in these years: Thank you very much. In particular thanks to you Ivan for always being ready to listen and to endure me, to you Andrea for the lucidity you gave me in the most difficult moments, and to you Valeria for having shared anxiety and misadventures even at a distance.

Thanks to you, grandpa Mario, for having educated and taught me to face the difficulties always with the right determination. I dedicate my doctorate to you.

Thanks to everyone close to me, it would be impossible to name you all. You know who you are.

Napoli, March 2020

Francesca

CABLE SYSTEMS AND TENSILE STRUCTURES

ABSTRACT

The present dissertation focuses on and investigates the behaviour of the structural category referred to as tensile structures, paying particular attention to the cable ones.

During the years the design of the structures has been conducted to lighter systems and the tensile structures rapidly increased thanks to their advantages as technical and time construction. To the other side, since the particular response to the external solicitation, the mechanical behaviour of these structures encouraged the researchers to find analytical and numerical methods proper to study, describe and analyze them.

In this research, once identified and described the different typologies of tensile structures, specific issues related to the statics of cable ones are dealt with an enhanced analysis of the current methodologies used to solve and manage these structural systems.

Composed of seven chapters, after an introduction about the issue and the main goal, the thesis starts from a recognition of the several types belonging to the analyzed structural categories, including cable, membrane, tensegrity and tensairity structures. One reports the features of each of them, highlighting the differences through some existing architectural examples, from the ancient to nowadays time.

Subsequently, the attention is paid to statics of cable structures including simple cables, cables with opposite curvature and cable nets.

Starting from a literature review, the selected approaches are analytically developed and demonstrated, focusing on both equilibrium and form-finding problems and highlighting advantages and disadvantages of each method, to have a suitable background to develop and introduce proper calculus models to solve the non-linear relationships characterizing these structures.

The study aims to deal with the main problems concerning the cable systems, as find the equilibrated and compatible configuration under external loads' action without the small displacements assumption, governing the non-linear relationship between forces and displacements, and taking into account the relevance of the deformations. Moreover, a fundamental scope of this research is to develop procedures suitable both in 2D and 3D cases, for several kinds of cable structures, and possible future computational implementation.

Related to these main goals, different procedures are proposed and described. Basing on the optimization approaches, one refers to the Total Potential Energy, finding the solution through a constrained minimization concerning the Kuhn-Tucker conditions. The method is applied to a 2D structure and a numerical example is reported to highlight the main features of the proposed methodology.

Moreover, the static response of plane and three-dimensional structures is evaluated by a calculus model under large displacements and in matrix form.

The non-linear relationship between forces and displacements is identified and then it is solved through a step by step procedure, linearizing the equation governing the problem at each infinitesimal load's step.

Firstly developed for a 2D structure, the approach is extended to a three-dimensional one highlighting its worth for several types of these systems.

Finally, an overview of the dynamic effects of tensile cable structure is explained, applying a modal analysis to a study case.

1. INTRODUCTION

In the last decades, the tensile structures application field has undergone a rapid spread. The requirement to realize functional buildings with less use of material and time has let to searching for and designing light constructions in order to overcome structural limits, thanks to the introduction and development of innovative materials and technologies both in temporary and permanent architectures (*D.S. Wakefield,1999*).

The lightness is one of the features diversifying these structures from other types of structural systems and therefore the structural and unstructural elements are chosen in order to minimize the self-weight.

Firstly, the constructions of big span roofs have been realized without intermediate supports (*T.T. Lan,1999*). During the years this type of structures have been used for smaller spaces as well as for vertical closings, floorings, canopies, and real buildings (hangars, arenas, exhibition pavilions), presenting a number of configurations and technologies.

The particular features such as lightness, high resistance, elastic behaviour, and pretensioning possibility, allow some versatile applications (*M. Salehi Ahmad Abas, 2013*) but, on the other side, show a high geometric non linearity that deeply affects their static behavior (*L. Liao, 2010*). Therefore, the detailed analysis of these structural systems is primary to ensure the stability of any component, in order to prevent the exceeding of admissible stresses during the pretension process and the overloads' application.

This is also the reason why many researches have been directing the gaze more and more to statics of these systems (*A.S. Kwan, 1998*), mainly framing behaviour models and methodologies within the two classes of force and displacements methods (*T.T. Lan, 1999*), under the understanding that, in these structures, the assumed configurations influence their equilibrium and that, therefore, finding the suitable geometry is fundamental.

First studies refer to reinforced concrete shell structures aiming at optimizing their shape taking the maximum advantage of the material, minimizing or making null the bending forces; however, due to the impossibility to reduce the thickness without

activating instability phenomena, other structural typologies, like tensile structures, have been developed, with components subject only by axial forces, and null bending.

Several typologies belong to this category of structures and are usually divided in plane (cable systems, cables with opposite curvature) and spatial (cable nets, membranes, *tensegrity* structures, *tensairity* structures). One may identify their evolution through three main historical periods (Fig. 1.1), according to Dong with special reference to spatial systems: ancient, pre-modern, and modern (*Dong, 2012*).
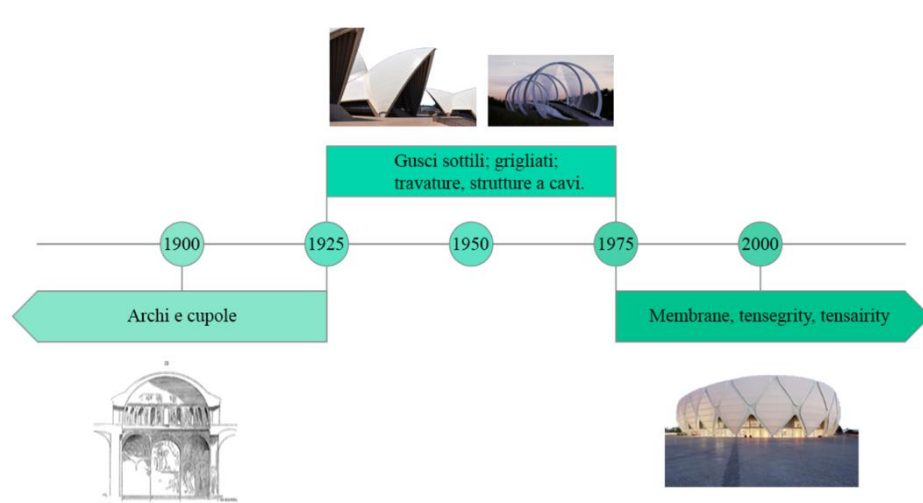
Figure 1.1: Historical evolution of the structures.

Cable structures are referred to when the cables or the cable systems represent the carrier elements (*Y. Liu et al., 2015*).

Ropes were used since ancient times as structural components, when climbing plants and lianas were employed for building hammocks and suspended bridges (*T. Kawada,2010*), or again for realizing boats for over thousand years (*R. Carter, 2006*).

The development of ropes as structural elements coincides with the evolution of construction materials, from the vegetable fibers to the modern high resistance steel for two main reasons: the first one concerns the will of overcoming increasingly larger spans, the second one, instead, is related to the need of new and complex configurations

(*Y. Liu,2015*), leading to the use of textile and plastic materials to build rooftops, facades and entire buildings (Fig. 1.2).

Figure 1.2: Some tensile structures' typologies.

Therefore, the interest about these structures has been strongly increasing both in the constructions and research field, where much attention has been paid also to the different behaviour under overloads and wind actions. To this regard some empiric studies have been conducted, in some cases underestimating the effects of the above-mentioned actions but arriving, anyway, to some solutions that highlight the behavioural features of these structural systems, where the importance of the strains causes the impossibility of application of the principle of effects' superposition.

During the years, several approaches and methodologies have been developed mainly referring to the catenary, finite element methods or energy approaches (*Y.C. Toklu, et al.,2017*).

The solving approaches for tensile structures' problems have been evolving and changing, related to the computer advent, allowing to find procedures with easier

compilation and such as to have minimum computational weight in order to identify the solution of the static problem of the structure with reference also to wind actions. Two main typical features affect these problems: the first one concerns the lightness; since, often, the self-weight of the structure is of the same order as the wind thrust acting on it; the second one is concerned with the deformability. As for cables' anchoring, the adoption of large spans and the use of pretensioning in cables also causes the increase of the drag value in the anchoring so that the boundary elements affect significantly the static operation of the whole structure. Within cable systems, the tensile ones are the most suitable to solve the problem of big span roofs, and the deformability can be considered a feature and a potentiality as well.

Many important academic studies on tensile structure have been developed by Frei Otto also including complex systems aimed to contain an entire city. Several types of tensile structures have been classified. With reference to cases where the carrier structure is represented only by cables (Fig. 1.3), one may distinguish simple cable systems, opposite curvature cable systems and cable nets.

According to the definition given for the first time at the IASS symposium 2004 in France (*IASS Symposium 2004, Montpellier,2004*), tensile structures can be identified as textile or plastic membranes (Fig. 1.4), *tensegrity* structures (tension+integrity) (Fig. 1.5), composed of tension (cables) and compression elements (struts), *tesairity* (tension+air+integrity) (Fig. 1.6) composed of beams, cables and membranes.

Figure 1.3: Cable structure; Zubizuri Bridge, Bilbao (Spain), S. Calatrava.
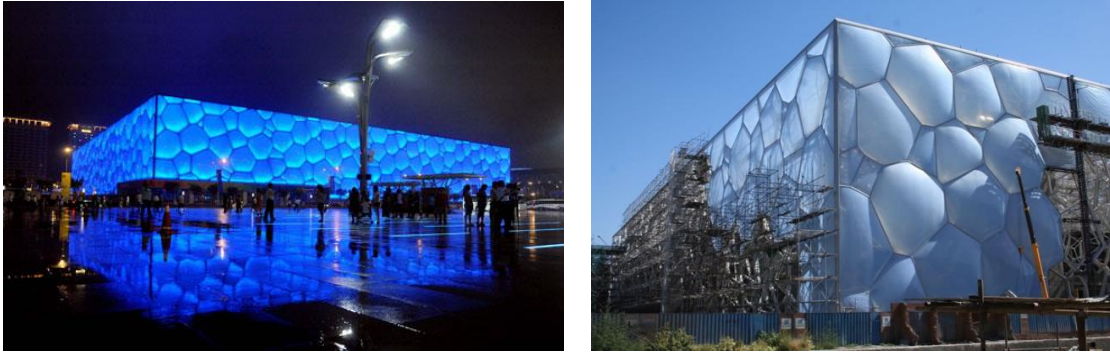
Figure 1.4: Membrane Structure; Watercube, Pechino (China), PTW Architects.

Figure 1.5: Tensegrity Structure; Kurilpa Bridge, Queensland (Australia), Ove Arup & Partners.

Figure 1.6: Tensairity Structure; Garage di Montreux Station, Montreux (Swiss), R. Luscher.

1.1 Structural classifications and general features

Cable systems represent a large variety of structures and some of them present features not too dissimilar from rigid covers. However, systems with cables as structural elements, can be considered one of the most important structural schemes within tensile components.

The relevance of steel cables as structural elements has been highlighted in the design and building of suspended or cable stayed bridges (Fig. 1.7-8), whose structural and architectural model represents a reference for the design of several tensile structures.

Many reinforced concrete or steel large span roofs, where the carrier parts are the cables, belong to the latter case.

However, there are a number of issues to be accounted for, one also relevant to bridge structures, and in particular the problem of wind oscillations, leading to the need of bracings. This problem turns relatively important in suspended bridges, where, because of larger spans, wide oscillation phenomena may lead to the collapse of the structure, as in the famous event of Tacoma Narrow Bridge in Washington.

Other problems concern the anchoring. Since the cables are the only structural elements, there is the need to fix the boundary with strong anchoring systems. For a long time, big supports have been realized in order to absorb the cables' pull forces, causing some aesthetic problems and for this reason often they are arranged under the ground level.

Further project benchmarks for the design of roofs concerns cable-stayed bridges (Fig.1.7-8), especially in the USA, where the ropes branch out from supporting elements that can be made of steel or reinforced concrete, and reach predefined locations at the extrados of the roof, also acting like bracings in most cases. Thanks to this solution, big overhangs with small thickness may be realized.
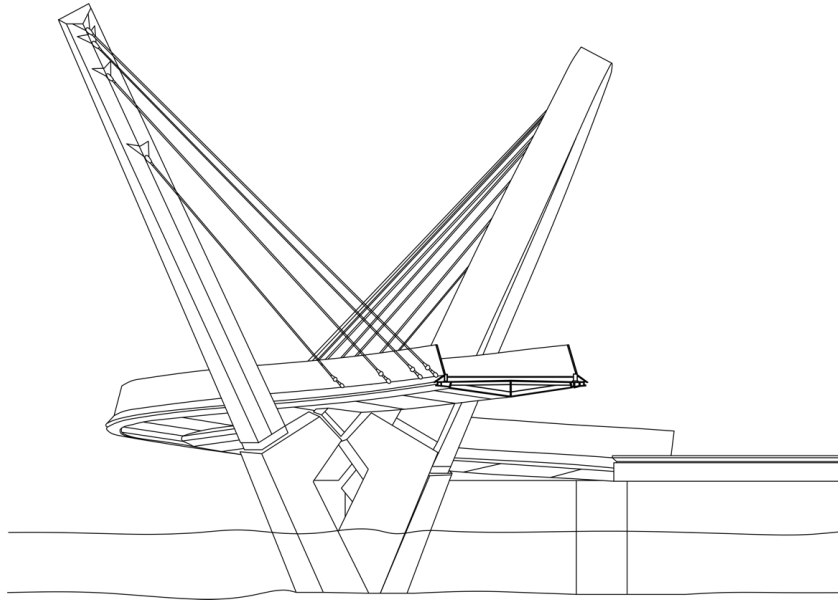
Figure 1.7: Cable-stayed bridge: Queen Elizabeth Quay Bridge; Perth (Australia),
Arup Associates.
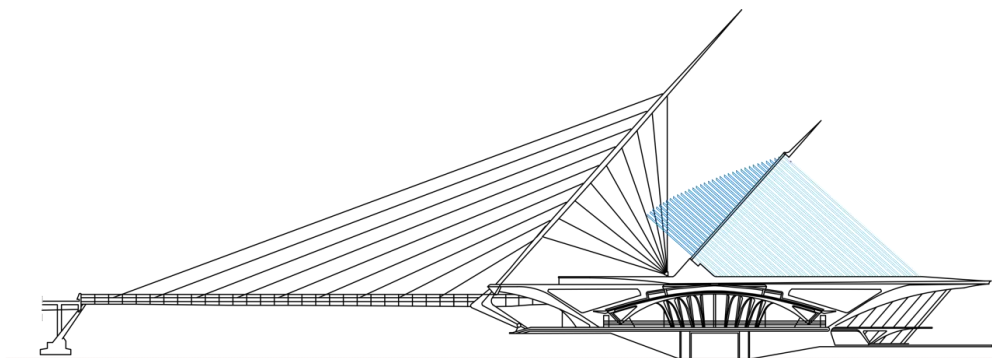
Figure 1.8: Cable- stayed bridge: Milwaukee Museum, Milwaukee (Wisconsin),
Santiago Calatrava.

The static of these structures can be further improved building some double overhangs; in this way the cables' drag force is balanced, and the supporting structures can be made smaller.

In literature four main subclasses of cable structures are identified:

Cable systems: where the single element, or several elements are linked to each other in series or radially and the load acts in the plane. This type of structures is used for moorings, curtains or tower tie-rods, e.g. in a project for an archive in a mine in Croatia, by David Garcia Studio (Fig. 1.9).
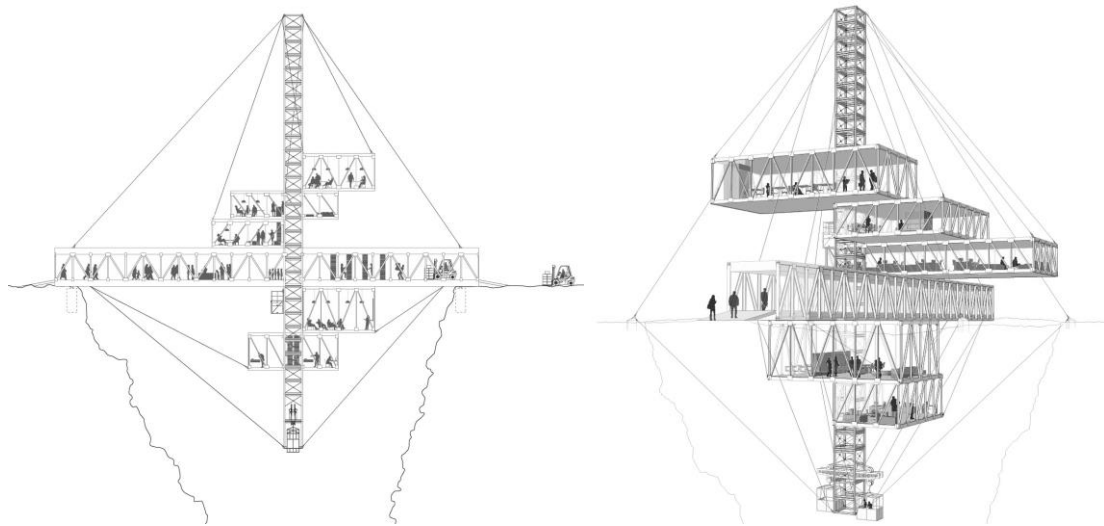
Figure 1.9: The Dead Websites Archive; Crnopac (Croatia), design of David Garcia Studio.

Cable trusses: also known as cables with opposite curvature, where the elements present opposite concavities and they are linked to each other in the plane. The loads act in the same plane; usually the cable trusses are used as supporting roofs; an example is shown in Fig. 1.10 relevant to the roof built in Wainlin, (Belgium) for a gas station, designed by Philyppe Samyn and Associées.
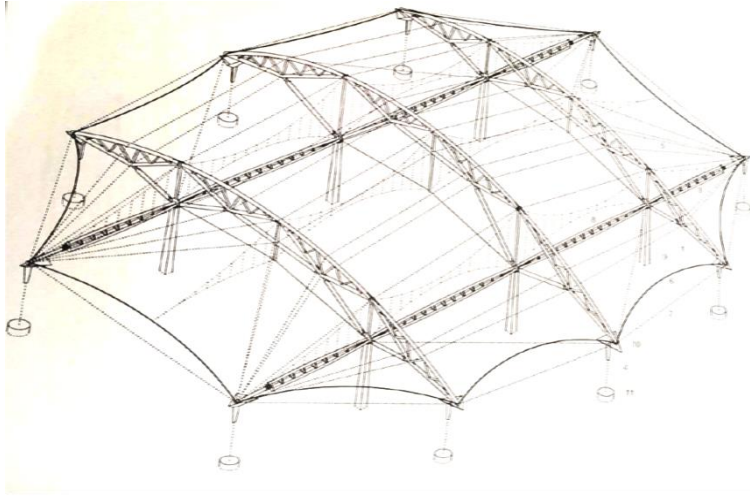
Figure 1.10: Gas Station covering, Wanlin (Belgium), Philyppe Samyn and Associés
(from "Atlante delle tensotrutture", Schock, Hans-Joackim,Torino 2001)

Cable-nets: the pretensioned elements are linked to each other to form a surface where the loads act orthogonally; these structures are typically used for roofs o suspended nets (Fig. 1.11).
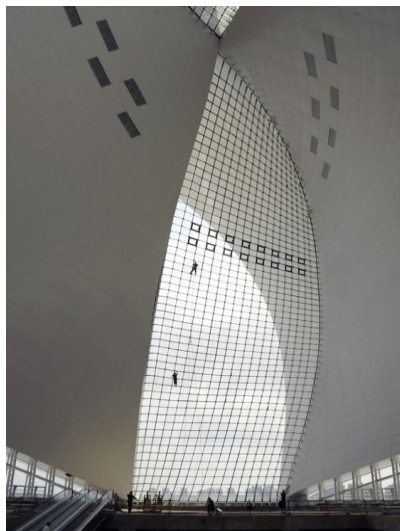
Figure 1.11: Maritime Museum, Lingang New City, (China), von Gerkan, Marg und Partner; SIAD.

Cable-nets system: the elements are linked to each other to develop a three-dimensional structure, such as the "trawl nets". These systems are mainly used in urban regeneration design or temporary buildings. Some examples are shown in Fig. 1.12-13.

Figure 1.12: Harmonic Motion/Rete di draghi, Temporary artwork MACRO, Roma (Italy), Toshiko Horiuki MacAdams.
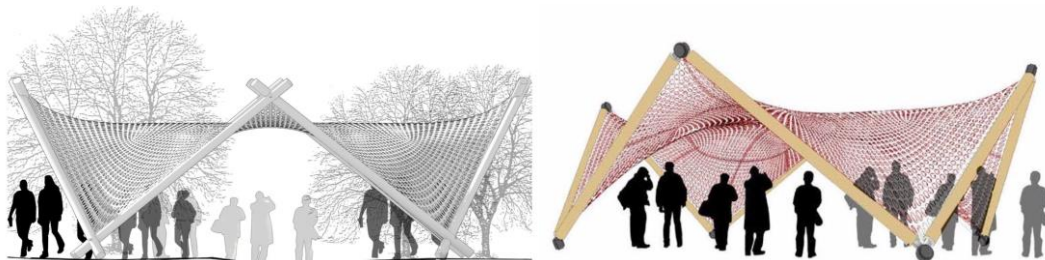
Figure 1.13: Hamaca Dream, New York (USA), designed by R. C. Ramos, J. Del Valle.

In the following Par.1.2-1.4 the features of the different categories are better described and deepened through examples of existing buildings in order to highlight the main differences, which are further analysed in the subsequent paragraphs.

1.2 Cable systems
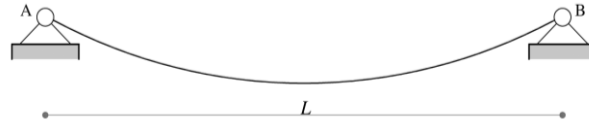
Figure 1.14: Representative scheme of the simple cable.

In Par. 1.1 some features of suspended rigid roofs have been highlighted, considering, mainly, the cases where the cables act as supports, that are external in the mentioned cases. The roof is then basically hanging from the cables. In Fig. 1.14 a scheme of this structural system is represented. In this kind of structure, if the tilt of the cable is large, a high value of normal stress is attained compared to the pull axial component.

There are many interesting cases where the cable is not external but integrated within the roof, thus acting as supporting element but also affecting its configuration, like in cases when one has a number of suspended cables, arranged in a modular sequence, and appropriately covered.

These structural and architectural schemes, thus, differ from the previously described ones, also allowing to cover a number of spaces with different shapes, from the squared to circular, or elliptical ones. This can be done by adequate position and assemblage of the cables according to two main basic arrangements:

Row scheme, typical of squared plants, where roofs present cylindrical shapes.

Radius scheme, usually used for circular plant spaces and similar ones, thus allowing shapes with overturned shells.

In the case of suspended cables, one should observe that the strain caused by the application of loads is relevant for two main reasons: the first one depends on the pull force endured by the cables; the second one, instead, depends on the circumstance that the loads' funicular is very far from the original configuration, thus causing the cover to follow the cables' deformation. Furthermore, some oscillation phenomena may

superpose, like in case of vacuum of the superior surface of the roof with an upward lift, which is the most worrisome effect. In order to account for this, some ballasting may be placed on the roof to offset the wind effects and to stabilize the configuration of the roof. The ballasting weight, actually, is able to increase the pull of permanent loads compared to the overloads' one, thus reducing at the same time the cable strain. However, even in this case there may be also some negative feature, since the response of the self-weight to the upward lift decreases with the increasing of the cause, producing a response which is no longer elastic.

The other side, placing the ballasting on the structure, it gets heavier and diminishes its performance.

To better understand the features and the behaviour of this kind of tensile structure, more details about the different arrangements are required. Starting from the row arrangements, other two subcategories can be identified. The first one is one of the most used schemes and it is characterized by the row arrangement of the cables where some transverse connection are introduced, helping the placement of the cover, increasing the distribution of the loads on the cables, and, thus, reducing the strains.

In the second arrangement, besides the transverse connections, their fixing is provided at the ends by adopting some boundary trusses. In this way the connecting elements act as bracings making unnecessary the ballasting. Nevertheless, this may be added in order to increase the cables' pull force even before the overloads' application, allowing the strain reduction.

Similar results may be obtained through the application of cables' pretension. This technique makes an improvement with relation to the ballasting placement, but in the same time shows some limits with regards to external actions, which modify the state of the cables, thus affecting the structure configuration. To solve this problem, often, the cables are fixed through tie-rods at points at the interior or exterior to the covered space.

As concerns radius tensile structures, the most important feature to deal with is concerned on how to find a way to absorb the high horizontal pull force transmitted by the cables to the external boundary. Since, if the boundary follows the loads' funicular curve then it undergoes only to compressive forces, thus, the most common structural configuration in radius tensile structures is characterized by two rings placed on the inner and outer boundaries of the cables. The first ring is in compression and the second

one in tension. Moreover, the inner second ring may also act as lightening and ventilation element as well as separator of the cables anchoring that converge in it.

These two typologies of cable arrangements fall within the general field of suspended shell roofs. Actually, in these kinds of roofs cables are immersed into concrete, making the structure monolithic, and accomplishing to the structural function, accounting both for compression and tangential stresses and moreover considerably containing the cable strains typical of suspended cables. Although some criticism was emerging in particular with reference to thin vaults, from the studies of Frei Otto, nevertheless, the advantages of suspended shells with respect to ordinary tensile structures have been largely demonstrated, since they reach the equilibrium conditions regardless of shape or overloads, with an elastic response. Moreover, thin vaults work only in compression and therefore they are dimensioned based on these stresses, whence, for large spans, the thicknesses result to be great, and the solutions are more expensive than in the case of the suspended shells, which allow to obtain thin thickness for significant spans.

Much attention is to be paid to the particular precompressive technique of the examined roofs, which regards the cable ballasting through the application of overloads lightly greater than those ones predicted for the structure. The application of these loads induces a tension in the cables; then, the loads are removed when the concrete is stiffen and, through the subsequent shortening of the cables, some compression is generated in the concrete, allowing to finally reduce the risk of cracks.

Since a problem may occur concerning boundary structures, that are solicited by the cable pull force, reaching maximum stresses, the boundary structures are required to assume with the shape of the loads' funicular in such a way to mainly work in compression, and diminish bending stresses, which are dangerous for the entire structure. Although the risk of cracks' occurrence may be then generally contained, this is not true for those shells following a negative Gauss shape, where more expensive solutions are often required with substitution of cable with steel profiles.

1.3 Opposite curvature cable systems
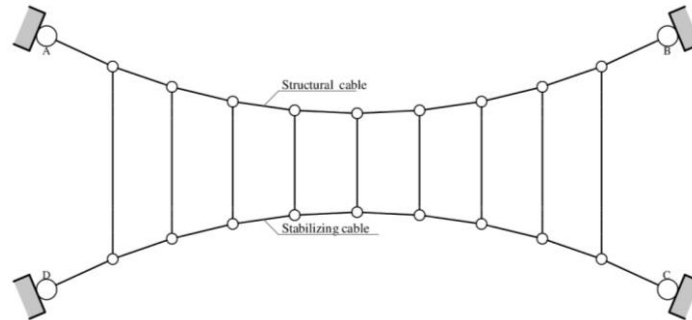
Figure 1.15: Scheme of a tensile structure with opposite curvature.

As above mentioned, a method for simple cable stiffening consists of fixing the structural cable to tie rods linked at defined points of the cover perimeter (Fig. 1.15). However, this operation may lead to some problems making hard its realization. An alternative has been proposed by Jawerth for the Ice Palace roof in Stockholm, where a plane system of cables with opposite curvatures is presented, linked to each other through diagonal elements.

In particular, the system is composed by a structural cable with an upward concavity linked, through diagonal elements, to another cable with opposite curvature, belonging to the same plane. The latter is recognized as tension cable since it is in tension before the application of the loads, producing a pretension state.

Consequently, when the overload acts, the additional load starts to decreases and thus the strain of the tension cable diminishes reducing the internal forces of the structural cable. In terms of equilibrium, the increase of internal stress is lower than that one that would occur under the only action of the overload.

Thus, this system affects also the deformability of the structural cable, which is further reduced by the diagonal elements that balance also the horizontal components of the external load.

The effectiveness of these structures is even more appreciated when a total inversion of loads is achieved, which may occur e.g. for a vacuum on the external surface. In this case, a particular reticular structure forms whose elements are all in tension, thus removing instability problems. Hence, it is possible to reach large spans, although with some limits in the anchoring.

Actually, upon changing of overloads, the pull horizontal component is constant and equal to the pretension one; increasing the overloads the cable undergoes an elongation and a decrease of the mutual action with the opposite cable, diminishing its tension. Whence the rise of the horizontal pull component is balanced by the decrease of the opposite cable tension. For this reason, the analyzed scheme may be considered a self-stiffened system and hence heavy ballasting is not necessary. Nevertheless, some pretensioning may be still assumed.

Starting from the Jawerth system, other schemes based on it have been proposed, basically diversified through different arrangements of the connecting elements, oblique or vertical ones.

Nevertheless, the Jawerth system is more effectiveness than other proposed ones.

As concerns the design, there are two main arrangements, as described in Par.1.1:

Row represented in Fig.1.16. and **Radius** in Fig. 1.17.

Figure 1.16: Tensile structure with opposite curvature in row arrangement.
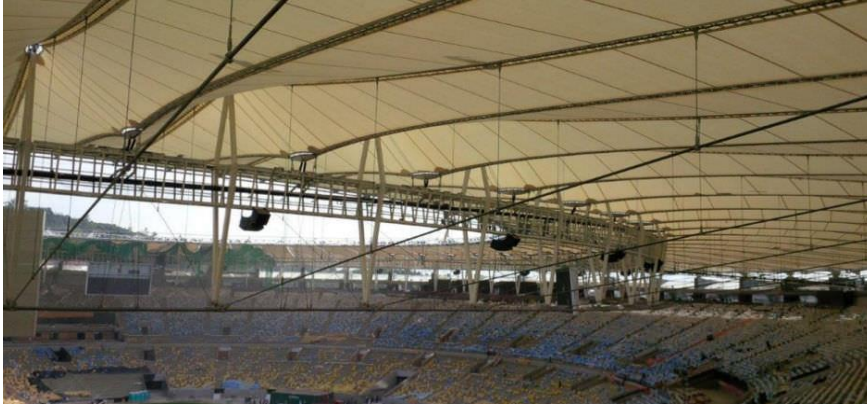
Figure 1.17: Radius arrangement of tensile structure with opposite curvature.

1.4 Cable nets and Cable-nets systems
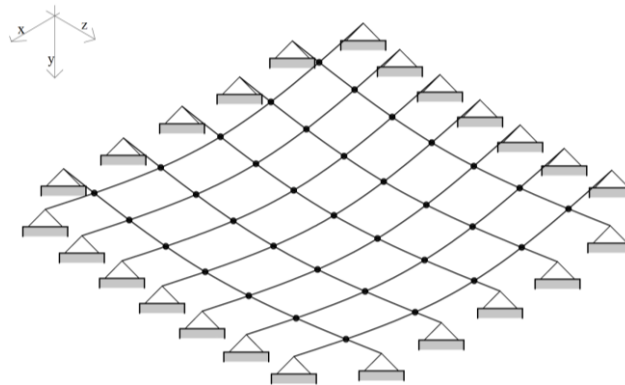
Figure 1.18: Cable-nets scheme.

Another kind of cable structure is represented by a system of cable-nets as shown in Fig. 1.18.

The cables have both structural and bracing function with all other components as coverings. In this case the optimal shape can be selected for optimal use of steel by removing compressive stresses and reducing the resisting section.

The cable-nets tensile structure can be considered as derived from opposite curvature systems. Actually, as above specified in Par. 1.2, in plane structures with opposite curvatures, the carrying and tensioning cables are arranged in the same plane.

On the contrary, in cable-nets the elements belong to different planes, and most of times to vertical planes, orthogonal to each other, whence the cables show upward or downward concavities with mutual intersections. Actually, the described systems may be regarded as three-dimensional extensions of those ones proposed by Jawerth. Other advantages, from the static point of view, are related to the aesthetic feature, allowing to select many different shapes, such as the saddle one.

Even in this kind of cable structure, the pretension is applied for stiffening., as proposed by Renè Sarger. Since cables intersect at certain points, the pretension of some cables leads to the pretension of the entire surface, and therefore, to the overall three-dimensional stiffening. Actually, in the nets the stiffening is in all the directions. As concerns the boundary structures, as mentioned one tends to have their curved shape matching the funicular of cables' drag forces.

The most adopted cable-nets refer to two orders schemes, whence more articulated systems can be realized, e.g. tents.

In Fig 1.18, typical cable-nets tents are shown, where it is possible to distinguish carrying and tensile cables, since cables with the same curvature belong to parallel planes. More complex situations are presented in Fig.1.19-20, where the same cable shows different curvatures, or the curvature of the same cable changes its sign and belongs to different planes.
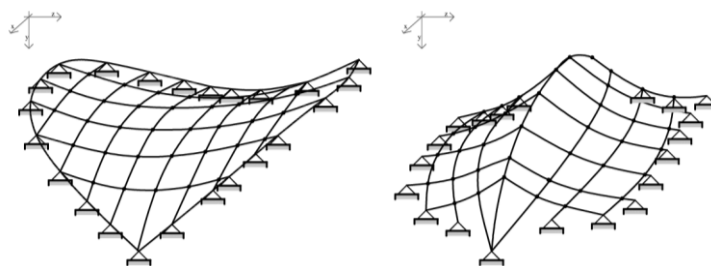
Figure 1.19: Scheme of different types of configurations of cable-nets.
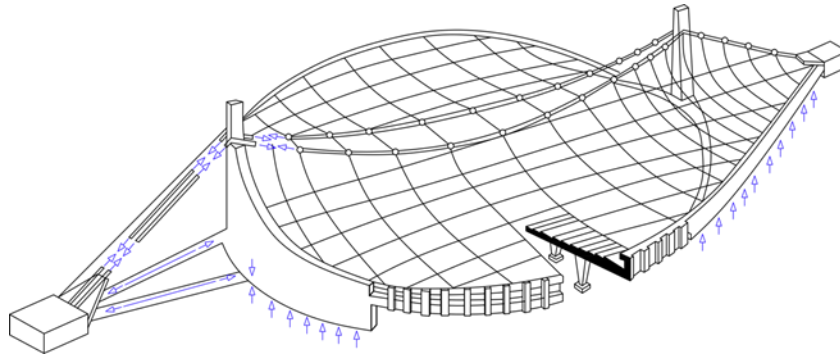
Figure 1.20: Structural scheme of National Gymnasium for Tokyo Olympics- Kenzo Tange.

Cable-nets can be also composed by several orders, for examples three, four and so on ones, moving more and more away from the basic configuration. Increasing the number of cables' orders, it is possible identify a continuous scheme. This structural system leads to roofs characterized by textile materials tensioned at their ends by supporting elements, in such a way to generate at any point a negative Gauss curvature.

The scientific and technological progress has pushed towards the use of less fleeting textile materials, gradually substituting the traditional sheets with materials with improved performance with regards also to environmental attacks. Particular attention on tends tensile structures was paid by Frei Otto, who proposed and showed several kinds and shapes of roofs in his opera "*Tensile Structures*", obtained with these structural systems (*F. Otto, 1972*).

In the design of tensile structures, a complex problem related to boundary structures must be dealt with, in particular concerning the transfer of stresses and external loads to the ground. However, there are several systems available, as shown in Fig. 1.21. One of the most used and simple ones is characterized by the vertical elements acting as struts transmitting the cables' drag forces to the ground. This scheme mainly has been used in rectangular plant roofs. Other types are characterized by vertical elements linked to each other by transversal ones along the funicular of cables' pull forces. Often these systems present angular points, in particular when the connecting elements are represented by two big arches.
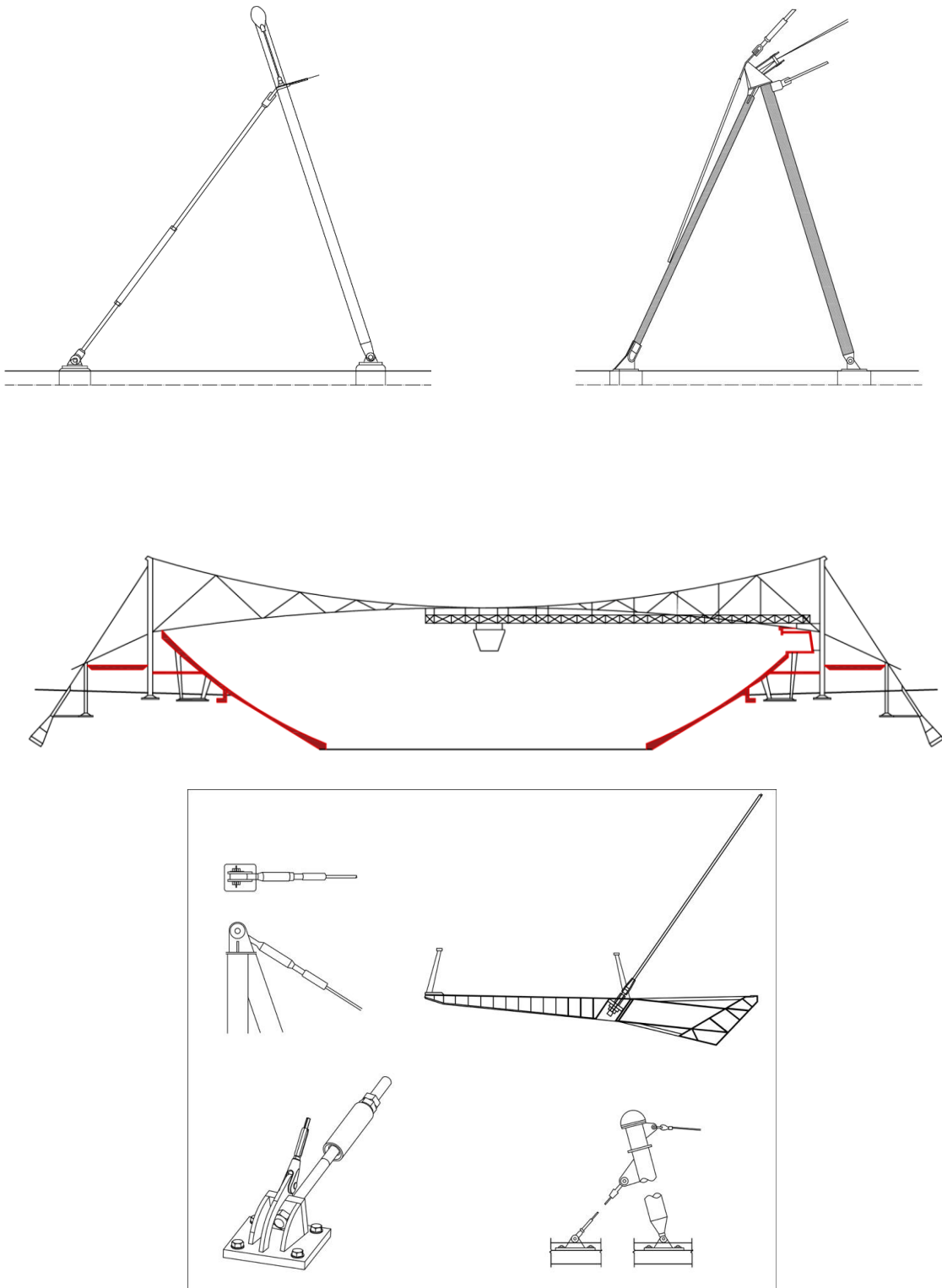
Figure 1.21: Scheme of main types of anchoring for cable structures.

Nevertheless, to obtain a more balanced system, a unique big ring may be chosen to replace the above-mentioned arches, avoiding the angular points and giving to vertical

elements the only role to transmit the external loads to the ground. Also, in this case, in order to have an optimal behaviour of the boundary ring, it should be shaped in order to follow the middle line of the pull forces' funicular but thus risking changing the shape in plant from the one required for the roof.

2. STATICS OF TENSILE STRUCTURES

2.1 Some historical background

The growing up spread of tensile structures has been developing hand to hand with the search and study of rigorous calculus methods in order to deal with the problems related to their statics.

As known, the rope is considered as an element without bending stiffness and incapable to resist compression and bending stresses. Therefore, to reach the equilibrium under tension stresses, the cable needs to adapt its shape to the acting loads.

From the literature, these kinds of systems are referred as *hypostatic* since forces are depending on deformations. The relevant static calculus is hard to solve, because the small displacements hypothesis is not valid and consequently also the superposition effects principle does not hold since the displacement components affect the unknown forces.

The case of the simple cable is one of the first problems rigorously treated by the modern mechanical studies and solved through the first elements of infinitesimal analysis *(M. Quagliaroni, 2010)*. In Table 2.1 a number of studies are summarized, developed during the centuries.

Table 2.1: Historical evolution of the rope studies

Year	Author	
1452-1519	*L. Da Vinci*	*First studies about the ropes*
1614	*Beeckman*	*Suspended bridge with parabolic profile.*
1638	*G. Galilei*	*Unstretching parabola*
1646	*Huygens*	*Revaluation of the Galileo unstretching parabola*
1679	*G. Pardies*	*He considers that the Galileo parabola is wrong.*
1691	*Huygens, Leibniz, Bernoulli*	*Unstretching catenary*
1891	*Routh*	*Elastic Catenary*
1975	*M. Irvine*	*Elastic catenary under point loads*

In the following Par. 2.2 some analytical solutions of the problem are showed.

2.2 Cables'equilibrium

The similarity between the exact profile of the cable and the parabolic one is known and, in case of tensioned cables, the consequent approximation of the cable segment to the distance between the supports is quite intuitive (Fig. 2.1).
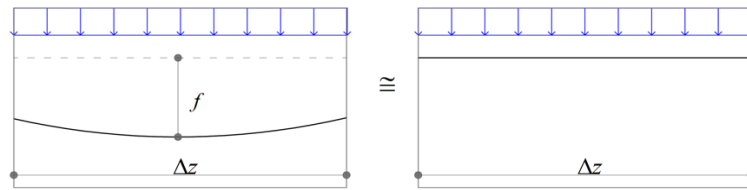
Figure 2.1: Simple cable- approximation of the cable segment with the distance between the supports.

Let consider the simple cable suspended from its two ends, identified in the points A and B, and subjected to the distributed vertical and horizontal loads, respectively *P* and *Q*. The self-weight is supposed negligible and *H* is the pull horizontal component of the drag force **T** (Fig. 2.2). Considering the reference system (*Oyz*) and the segment of the cable shown in Fig. 2.3, the equilibrium equations for vertical and horizontal translations are
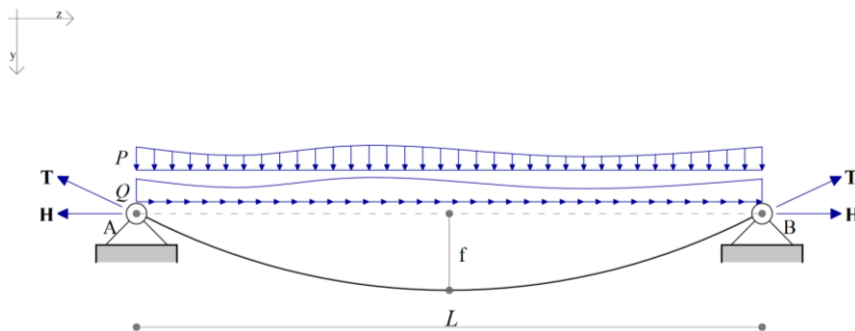
Figure 2.2: Simple cable.
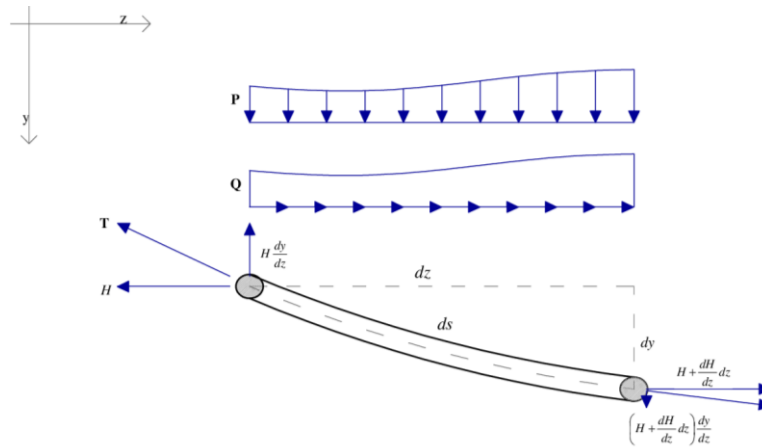
Figure 2.3: Cable segment.

$$\frac{d}{dz}\left(H\frac{dy}{dz}\right) + P = 0 \tag{2.2.1}$$

$$\frac{dH}{dz} + Q = 0 \tag{2.2.2}$$

Assuming acting only the vertical loads (Fig.2.4), and $H = \text{const}$
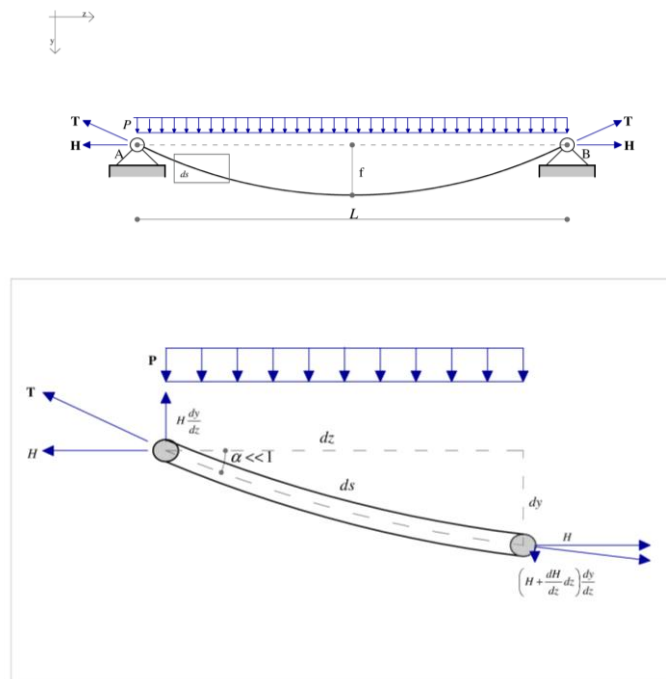
Figure 2.4: Simple cable under the action of the vertical load P.

Eq. (2.2.1) turns into

$$H\frac{d^2 y}{dz^2} = -P \tag{2.2.3}$$

and, assuming yet P = const, by integrating Eq. (2.2.3), one gets

$$Hy = -P\frac{z^2}{2} + C_1 z + C_2 \tag{2.2.4}$$

Once computed the integration constants C_1 and C_2, and imposed the passage of the cable through the A and B points, one may evaluate y

$$y = \frac{P}{2H} z(L - z) \tag{2.2.5}$$

Therefore, the H component can be computed after introducing the compatibility equation

$$\ell = \ell_o + \Delta\ell_o \tag{2.2.6}$$

where

ℓ is the length of the cable in the deformed shape

ℓ_o is the initial length of the cable

$\Delta\ell_o$ is the length variation due to the load application

L is the cable supports' distance.

Moreover the cable length ℓ is defined by

$$\ell = \int_0^L \sqrt{1 + \left(\frac{dy}{dz}\right)^2}\, dz \cong \int_0^L \left[1 + \frac{1}{2}\left(\frac{dy}{dz}\right)\right] dz = \int_0^L dz + \frac{1}{2}\int_0^\ell \left(\frac{dy}{dz}\right) dz = L + \frac{8}{3}\frac{f^2}{L} \tag{2.2.7}$$

where f denotes the deflection.

Assuming a very small tilt, one has

$$T \cong H \rightarrow \Delta\ell_o = \frac{HL}{EA}$$

and therefore, from Eq. (2.1.5) for $z = \dfrac{L}{2}$, one gets

$$f = \frac{PL^2}{8H} \tag{2.2.8}$$

whence

$$H = \frac{PL^2}{8f} \tag{2.2.9}$$

Remembering Eq. (2.2.6) and Eq. (2.2.7)

$$\begin{cases} \ell = \ell_o + \Delta\ell_o \\ \ell = L + \dfrac{8}{3}\dfrac{f}{L} \end{cases}$$

one gets

$$\ell_o + \Delta\ell_o = L + \frac{8}{3}\frac{f^2}{L} \tag{2.2.10}$$

with $\Delta\ell_o = \dfrac{HL}{EA}$

By substituting H obtained from Eq (2.2.9), one gets

$$\ell_0 + \frac{PL^3}{8fEA} = \ell + \frac{8}{3}\frac{f^2}{L} \tag{2.2.11}$$

$$\ell_o + \frac{PL^3}{8fEA} - \left(L + \frac{8}{3}\frac{f^2}{L}\right) = 0 \tag{2.2.12}$$

$$L + \frac{8}{3}\frac{f^2}{L} - \ell_o - \frac{PL^3}{8fEA} = 0 \tag{2.2.13}$$

and by multiplying for $\dfrac{3}{8}fL$

$$f^3 - (\ell_o - L)\frac{3}{8}fL - \frac{3}{64}\frac{PL^4}{EA} = 0 \tag{2.2.14}$$

Hence

$$f^3 - \frac{3}{8}fL(\ell_0 - L) - \frac{3}{64}\frac{PL^4}{EA} = 0 \tag{2.2.15}$$

Once identified the deflection f, H can be computed by Eq. (2.2.9) and then y is obtained by substituting H in Eq. (2.2.5).

Let assume to apply a distributed vertical load ΔP added to the acting one, producing a pull increasing ΔH. The cable points undergo other downward displacements in the y direction.

These displacements are identified by v; to satisfy the equilibrium, Eq. (2.2.3) turns into

$$(H + \Delta H)\frac{d^2(y + v)}{dz^2} = -P - \Delta P \tag{2.2.16}$$

By developing the products and remembering Eq. (2.2.3), Eq. (2.2.16) can written again as

$$\Delta H \frac{d^2 y}{dz^2} + \left(H + \Delta H\right)\frac{d^2 v}{dz^2} = -\Delta P \tag{2.2.17}$$

Eq. (2.2.17) is referred to the equilibrium configuration reached after the vertical load increasing. It is clear that, if ΔP is proportional to P, one may write the equilibrium referring to the undeformed configuration of the cable, because $y = y(z)$ represents a funicolar curve of ΔP.

Eq. (2.2.17) can be written again as

$$\Delta H \frac{d^2 y}{dz^2} = -\Delta P \tag{2.2.18}$$

Therefore, the variation of the produced horizontal component is

$$\Delta H = \frac{\Delta P L^2}{8f} \tag{2.2.19}$$

Analysing Eq. (2.2.17) one can put in evidence that the terms $\dfrac{d^2 y}{dz^2}$ and $\dfrac{d^2 v}{dz^2}$ are respectively the initial and final curvatures and to large H and $\dfrac{d^2 y}{dz^2}$ correspond small variations of $\dfrac{d^2 v}{dz^2}$.

By reporting the data on a graph, where P is reported on the x-axis and f on the y-axis, considering

$$\ell_0 = L \tag{2.2.20}$$

and hence

$$f = \sqrt[3]{\frac{3}{64} \frac{PL^4}{EA}} \tag{2.2.21}$$

it is clear that to the increasing of the load P a smaller increasing of the deflection corresponds (Fig. 2.5).
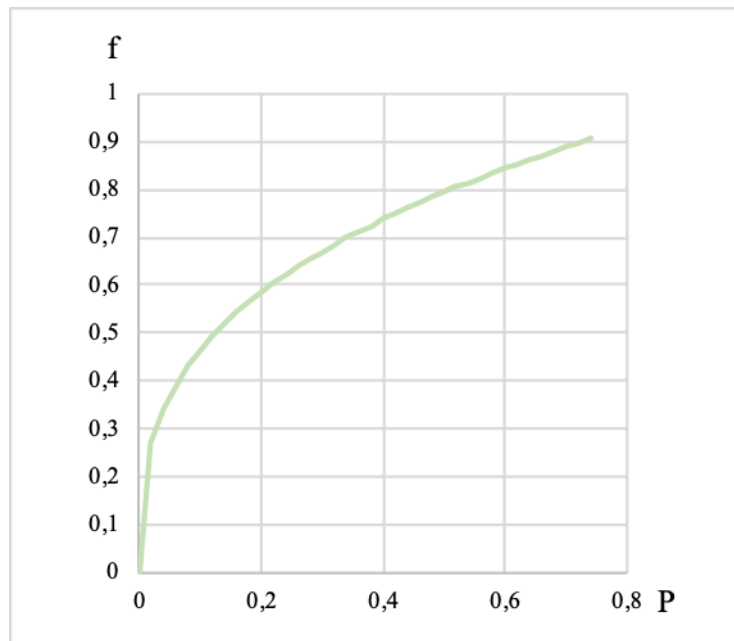
Figure 2.5: Graph of deflection f vs load P.

Therefore, it is clear that the ballasting cannot be chosen arbitrarily, but, on the contrary, it depends on the deflection of the roof established during the design phase.

Given f, the load P can be defined

$$P = \frac{64}{3}\frac{EA}{L^4}\left[f^3 - \frac{3}{8}L(\ell_o - L)f\right] \tag{2.2.22}$$

Considering Eq. (2.2.22), it is possible to compute the maximum value of P that is compatible with the assumed roof deflection, based on (2.2.20)

$$P_{\max} = \frac{64}{3}\frac{EA}{L^4}f^3 \tag{2.2.23}$$

Consequently, after identified $P_{\max}$ according to Eq. (2.2.9), it is possible to determine the maximum value of H, substituting Eq. (2.2.23) into Eq. (2.2.9)

$$H_{\max} = \frac{P_{\max}L^2}{8f} = \frac{64}{3}\frac{EA}{L^4}f^3\frac{L^2}{8f} = \frac{8}{3}\frac{EAf^2}{L^2} \tag{2.2.24}$$

This limit condition occurs when the initial length L_o corresponds exactly to ℓ, that is the distance between the two ends A and B.

Increasing the load P and the component ΔH in order to not change the deflection, it should be $\ell_o < L$; thus the ballasting should be associated to the preliminary tensioning of the cables

$$H_0 = EA\frac{L - \ell_o}{\ell_o} \tag{2.2.25}$$

There are several advantages related to the pretensioning of cables. Let consider the case when the pretensioning is applied through some vertical cables suitably pretensioned. From a static point of view, this system behaves like a cable with opposite curvature. The vertical cables, if conveniently outdistanced from each other, are able to realize a parabolic shape of the cable where the deflection f is equal to the one derived from the application of a vertical load P equal to the action transmitted by the vertical elements to the cable.

Moreover, when the external load is applied, the cable would tend to go downward diminishing the cables action and therefore behaving as if placed on an elastic ground. However, much attention should be paid to this feature, because it is possible that the actions of the vertical elements are nullified by the downward external load. To avoid this circumstance, the tensioning should be well calibrated in such a way to prevent waving phenomena of the cable for any intensity of the applied external load.

2.3 An approach to static analysis of cable systems and nets

Cable systems are usually classified in simple cables and cable nets, with, in the latter case, the subcategories of plane and spatial nets.

The first ones represent the carrying elements of suspended roofs and they are solicited in a unique direction (*F. Otto, F.Schleyer, 1972*).

2.3.1   Single cable

One considers the free simple cable in a three-dimensional reference system, as shown in Fig. 2.6, where the axes are identified through the unit vectors $\mathbf{e}_x, \mathbf{e}_y, \mathbf{e}_z$.

Let suppose the examined cable without bending stiffness, and described by the curve

$$\mathbf{r}(t) : x(t)\mathbf{e}_x + y(t)\mathbf{e}_y + z(t)\mathbf{e}_z \tag{2.3.1}$$

where t is a scalar variable.

In case of tensioned cables, it is convenient to select one of the fixed coordinates as variable; hence choosing x as scalar variable, Eq. (2.3.1) assumes the form

$$\mathbf{r}(x) : x\mathbf{e}_x + y(x)\mathbf{e}_y + z(x)\mathbf{e}_z \tag{2.3.2}$$
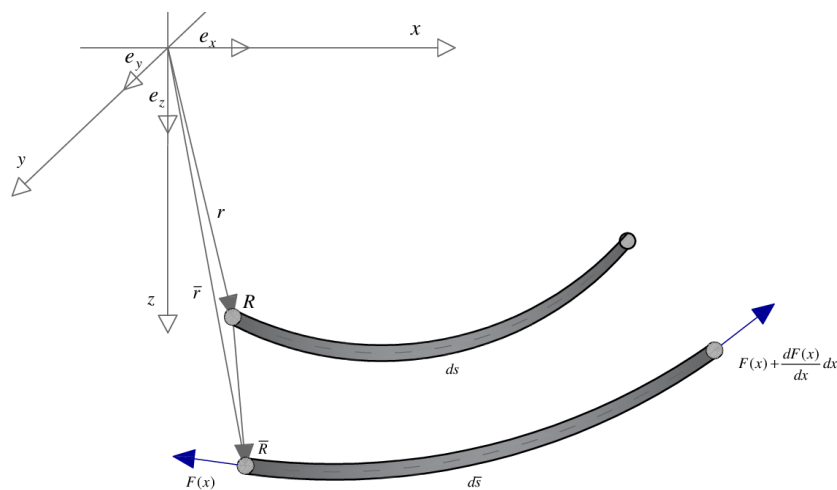
Figure 2.6: Single unstiffened cable in (Oxyz)

Therefore, one may consider the position vector $\mathbf{r}(x)$ of the cable in components

$$\mathbf{r}(x) = \begin{bmatrix} x \\ y(x) \\ z(x) \end{bmatrix} \tag{2.3.3}$$

This vector must be unique and at least two times differentiable. Therefore, the initial unloaded configuration has been identified.

Let assume that any overload or heat variation can act on the cable or that it may undergo some ends' displacements, leading to a configuration change and therefore a position change of the cable.

Thus, considering the displacement vector

$$\mathbf{U}(x) = \begin{bmatrix} u(x) \\ v(x) \\ w(x) \end{bmatrix} \tag{2.3.4}$$

the updated position is defined by

$$\bar{\mathbf{r}}(x) = \mathbf{r}(x) + \mathbf{U}(x) = \begin{bmatrix} x + u(x) \\ y(x) + v(x) \\ z(x) + w(x) \end{bmatrix} = \begin{bmatrix} \bar{x}(x) \\ \bar{y}(x) \\ \bar{z}(x) \end{bmatrix} \tag{2.3.5}$$

After first and second time derivation, one gets

$$\bar{\mathbf{r}}'(x) = \begin{bmatrix} 1 + u'(x) \\ y'(x) + v'(x) \\ z'(x) + w'(x) \end{bmatrix} \tag{2.3.6}$$

$$\bar{\mathbf{r}}''(x) = \begin{bmatrix} u''(x) \\ y''(x) + v''(x) \\ z'(x) + w''(x) \end{bmatrix} = \begin{bmatrix} \bar{x}''(x) \\ \bar{y}''(x) \\ \bar{z}''(x) \end{bmatrix} \tag{2.3.7}$$

One may recognize two cable states:

The first state of initial pretension is described by $\mathbf{r}(x)$ and identifies the curve under the self weight $\mathbf{g}(x)$ or any other dead load; in this case the generated stresses are marked by the g subscript.

The second state is identified by $\bar{\mathbf{r}}(x)$, and describes the curve also subject to the overloads (as shown in Fig. 2.7), that is under the load condition

$$\mathbf{q}(x) = \mathbf{g}(x) + \mathbf{P}(x) \qquad (2.3.8)$$

with

$\mathbf{g}(x)$ the dead load

$\mathbf{P}(x)$ the overload

$\mathbf{q}(x)$ the total external load given by superposition of dead loads and overloads.

Analogously, the q subscript identifies the dependence on this load condition.
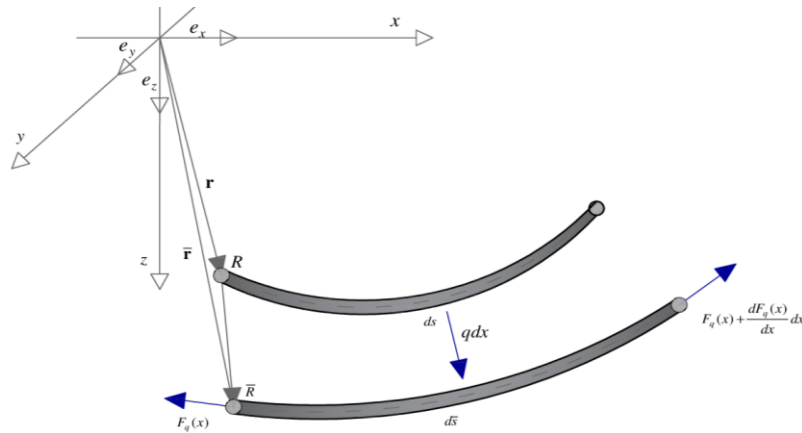
Figure 2.7: Free loaded cable in the space.

Thus, omitting the explicit dependence on the variables, under the load conditions shown in Fig. 2.7, the equilibrium can be set in the form

$$-\mathbf{F}_q + \left(\mathbf{F}_q + \frac{d\mathbf{F}_q}{dx}dx\right) + \mathbf{q}dx = \mathbf{0}$$

$$\frac{d\mathbf{F}_q}{dx} + \mathbf{q} = \mathbf{0} \qquad (2.3.9)$$

with $\mathbf{F_q}$ the internal drag force in the cable generated by $\mathbf{q}$.

Since no bending moments are admitted in the cable, it is necessary that

$$\bar{\mathbf{r}}' \times \mathbf{F}_q = \mathbf{0} \tag{2.3.10}$$

or, in other form,

$$\mathbf{F}_q = F_q \frac{\bar{\mathbf{r}}'}{\bar{r}'} \tag{2.3.11}$$

where F_q the intensity of $\mathbf{F}_q$.

These equilibrium conditions are imposed with reference to the deformed configuration.

Let then consider only the horizontal component H_q of the drag force, anyway tilted on the x-axis,

$$H_q = \mathbf{F}_q \cdot \mathbf{e}_x \tag{2.3.12}$$

Therefore Eq. (2.3.12) can be rewritten as

$$H_q = \frac{F_q}{\bar{r}'} \bar{\mathbf{r}}' \cdot \mathbf{e}_x \tag{2.3.13}$$

Considering

$$\bar{\mathbf{r}}' \mathbf{e}_x = 1 + u' \tag{2.3.14}$$

and being $u' \ll 1$, one gets

$$H_q = \frac{F_q}{\bar{r}'} \tag{2.3.15}$$

Projecting on the axes Eq. (2.3.9), and taking into account Eq. (2.3.11) and Eq. (2.3.15), one gets

$$\begin{cases} H'_q + q_x = 0 \\ H_q \bar{y}'' + q_y - q_x \bar{y}' = 0 \\ H_q \bar{z}'' + q_z - q_x \bar{z}' = 0 \end{cases} \tag{2.3.16}$$

The dead load at the initial state only in the z-direction should be applied, passing from the three-dimensional reference system ($Oxyz$) to the plane one (Oxz) (Fig.2.8).
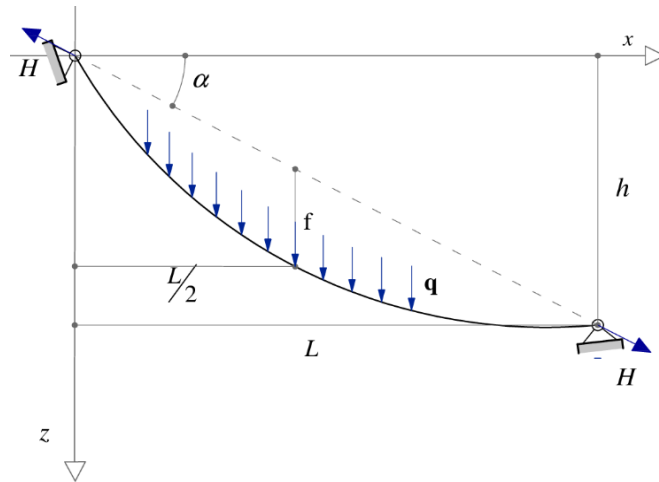
Figure 2.8: The cable in the plane (Oxz).

The cable position is identified through the position vector, given now

$$\mathbf{r} = \begin{bmatrix} x \\ 0 \\ z \end{bmatrix} \tag{2.3.17}$$

The dead load $\mathbf{g}$ is

$$\mathbf{g} = \begin{bmatrix} 0 \\ 0 \\ g \end{bmatrix} \tag{2.3.18}$$

and Eq. (2.3.16) assumes the following expression

$$\begin{cases} H'_q + P_x = 0 \\ H_q \bar{z}'' + q_z - q_x \bar{z}' = 0 \end{cases} \tag{2.3.19}$$

In the initial state $\mathbf{P} = \mathbf{0}$ and Eq. (2.3.19) can be still simplified, considering only the component H depending on the dead load $\mathbf{g}$

$$\begin{cases} H'_g = 0 \\ H_g \bar{z}'' + g_x = 0 \end{cases} \tag{2.3.20}$$

whence

$$H_g = \text{const} \qquad\qquad (2.3.21)$$

2.3.2   Elasticity conditions

Because of the effect of the overloads or of the heat loads, the cable length changes its initial state , which is described by the strain ε

$$\varepsilon = \frac{\bar{r}' - r'}{r'} \qquad\qquad (2.3.22)$$

Substituting Eq. (2.3.2) and Eq. (2.3.3), developing in series and neglecting the numerator greater than the second order, one gets

$$\varepsilon = \frac{\sqrt{(1+u')^2 + y'^2 + z'^2} - \sqrt{1 + y'^2 + z'^2}}{\sqrt{1 + y'^2 + z'^2}} \qquad\qquad (2.3.23)$$

$$\varepsilon = \frac{u' + yv' + z'w'}{1 + y'^2 + z'^2} + \frac{v'^2 + w'^2}{2(1 + y'^2 + z'^2)} \qquad\qquad (2.3.24)$$

From Eq. (2.3.24) it is possible to omit the second addend. Referring to the monoaxial stress state in the cables, the linear elasticity relation is applied and, taking into account that the cable self-weight is neglected, one gets

$$\varepsilon = \frac{F_p}{EA} + t_\varepsilon \qquad\qquad (2.3.25)$$

where

F_p is the force (positive in tension) undergone by the cable under the overload application

$t_\varepsilon = \alpha_t \Delta t$ is the expansion undergone by the cable for heat variation

α_t is the linear expansion coefficient

E is the elasticity modulus.

Substituting Eq. (2.3.24) into Eq. (2.3.25), it is possible to compute F_p

$$\varepsilon = \frac{u'+yv'+z'w'}{1+y'^2+z'^2} + \frac{v'^2+w'^2}{2(1+y'^2+z'^2)} = \frac{F_p}{EA} + t_\varepsilon$$

$$\frac{F_p}{EA} = \frac{u'+yv'+z'w'}{1+y'^2+z'^2} + \frac{v'^2+w'^2}{2(1+y'^2+z'^2)} - t_\varepsilon \qquad (2.3.26)$$

$$F_p = EA\left(\frac{u'+yv'+z'w'}{1+y'^2+z'^2} + \frac{v'^2+w'^2}{2(1+y'^2+z'^2)}\right) - t_\varepsilon EA$$

and, thereafter, the values of the pull horizontal components.

After neglecting the term $\dfrac{v'^2+w'^2}{2(1+y'^2+z'^2)}$ in Eq. (2.6.26), it turns into

$$F_p = \frac{EA(u'+yv'+z'w')}{1+y'^2+z'^2} - EAt_\varepsilon \qquad (2.3.27)$$

Moreover

$$H_p = \frac{F_p}{\bar{r}'} \qquad (2.3.28)$$

and, substituting Eq. (2.3.27)

$$H_p = \frac{EA(u'+yv'+z'w')}{(1+y'^2+z'^2)(1+y'^2+z'^2)^{1/2}} - \frac{EAt_\varepsilon}{(1+y'^2+z'^2)^{1/2}}$$

$$H_p = \frac{EA(u'+yv'+z'w')}{(1+y'^2+z'^2)^{3/2}} - \frac{EAt_\varepsilon}{(1+y'^2+z'^2)^{1/2}} \qquad (2.3.29)$$

Being $y = 0$, in the plane (Oxz) one gets

$$H_p = \frac{EA(u'+z'w')}{(1+z'^2)^{3/2}} - \frac{EAt_\varepsilon}{(1+z'^2)^{1/2}} \qquad (2.3.30)$$

2.3.3 Cable length

The cable length may be identified through arch length integration, distinguishing the initial state ℓ_g^o from the current state ℓ_q under the additional load and heat conditions

$$\ell_g^o = \int_0^L ds = \int_0^L r' dx = \int_0^L \sqrt{1 + y'^2 + z'^2} \, dx \tag{2.3.31}$$

$$\ell_q = \int_0^{L'} d\bar{s} = \int_0^{L'} \bar{r}' dx = \int_0^{L'} \sqrt{1 + \bar{y}'^2 + \bar{z}'^2} \, dx \tag{2.3.32}$$

Since the cable belongs to the plane (Oxz), $y' = 0$ and $\bar{y}' = v'$.

After computing the lengths into the two considered states, one may infer the variation

$$\Delta \ell = \ell_q - \ell_g^o \tag{2.3.33}$$

Making the suitable substitutions and considering constant H, E, A and t_ε, the length variation is given in the form

$$\Delta \ell = \frac{H_p}{EA} \int r'^2 \, dx + t_\varepsilon \ell_g \tag{2.3.34}$$

whence the problem should be dealt with for the elastic and inelastic case.

2.3.4   The inelastic cable

Once defined the deformations from the initial state, one has to identify the shape and the cable forces H and F. The cable subject only to the vertical loads may be analysed through graph methods. Hence, to better understand the non-linear behaviour of the examined case, a number of load conditions are considered, and specifically:

- **i) Constant vertical dead load**. In this case the self-weight of the cable is neglected. Actually, the cable is subject only to the dead load $q_z = \text{const}$, applied in the vertical direction.

- **ii) Self-weight.**: The contribution of the self-weight is taken into account in order to find the forces and the equilibrium configuration of the cable. The self-weight is assumed constant and referred to the unit length of the x-axis, $g_x = g_o = \text{const}$.

- **iii) Arbitrary vertical load.** An arbitrary load is applied in the vertical direction on the cable, with $q_x = 0$ and $H = \text{const}$.

- **iv) Arbitrary load.** In this case an arbitrary load and *H* depending on *x* are considered. The application points are identified in function only of the *x* coordinate.

- **v) Combination of dead load and overload.** The combination of the dead loads and the overloads is considered.

The analysis of the load conditions leads to the solution of the problem, identifying the forces *H* and the shape of the cable.

The first two cases refer to a well-known solving process and are here reported for completeness.

Furthermore, when the ratio between the deflection and the span of the cable is small, the stretching due to the overload **P** can be neglected, compared to the initial configuration. This allows some simplifications on the study of the shape and the stresses of the cable, and consequently the behaviour of the elastic cable under the external load **q** is easier to be analysed.

i) Constant vertical dead load

A uniform constant dead load is applied on the cable in the vertical direction, thus assuming

$$q_z = g = \text{const} \tag{2.3.35}$$

The solution is identified in the parabolic equation

$$z = \frac{g}{2H_g}\left(x^2 + C_1 x + C_2\right) \tag{2.3.36}$$

where C_1 and C_2 are the integration constants and their value is identified by substituting the ends' coordinates of the cable.

In the plane (*Oxz*), the above mentioned coordinates are

$$K_1 \equiv (x_1, 0, z_1) \equiv (0, 0, 0)$$
$$K_2 \equiv (x_2, 0, z_2) \equiv (x_L, 0, z_L)$$

and such that

$$x_2 - x_1 = L > 0 \tag{2.3.37}$$

Moreover the deflection is given in the form

$$d = \frac{g}{2H_g}\left(Lx - x^2\right) = 4f\left(\frac{x}{L} - \frac{x^2}{L^2}\right)$$ (2.3.38)

One assumes the maximum value of the middle term in order to calculate the pull horizontal component

$$H_g = \frac{gL^2}{8f}$$ (2.3.39)

One computes the length of the cable in the specific case when the angle $a = 0$ (Fig. 2.9) i.e. the cable ends are at the same height.
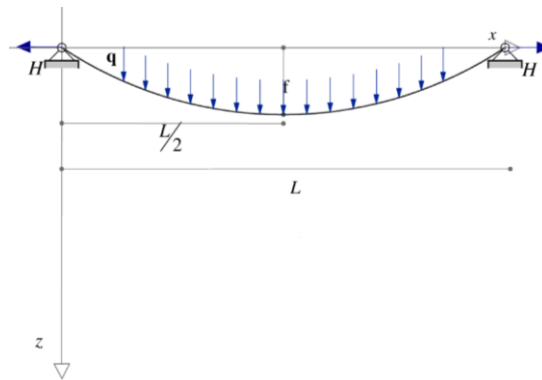
Figure 2.9: Cable with supports at the same height.

Comparing the deflection f with the span L, the cable length ℓ may be inferred.

Assuming $n = \frac{f}{L}$, the cable length is expressed in function of n and, hence, of the supports distance as

$$\ell = \frac{L}{2}\left(\sqrt{1+16n^2} + \frac{1}{4}arcsin4n\right)$$ (2.3.40)

Eq. (2.3.38) allows to identify the exact length of a cable with the ends at the same height.

ii) Self-weight

Let consider the self-weight g_o uniformly distributed along the cable curve referred to the x-axis unit length $g = g_o = \text{const}$.

Since

1. $\ell_g^o = \int ds = \int |r'| dx = \int \sqrt{1 + y'^2 + z'^2} \, dx$ $\qquad$ (2.3.41)

and, since the cable belongs to the plane (Oxz), one has $y'^2 = 0$

Then

$$\ell_g^0 = \sqrt{1 + z'^2} \qquad (2.3.42)$$

whence

$$g = g_0 \sqrt{1 + z'^2} \qquad (2.3.43)$$

Remembering that

$$H_g z'' + g = 0 \qquad (2.3.44)$$

and making the appropriate substitutions, the following expression is obtained

$$H_g z'' + g_0 \sqrt{1 + z'^2} = 0 \qquad (2.3.45)$$

whose general solution (catenary) is

$$z = -\frac{H_g}{g} \cos h \frac{g}{H_g}(x + C_1) + C_2 \qquad (2.3.46)$$

In case where $C_1 = 0$ and $C_2 = 0$, one gets

$$z = -\frac{H_g}{g} \cos h \frac{g}{H_g} x \qquad (2.3.47)$$

It follows that the origin of the cable is at a distance equal to $\dfrac{H_g}{g}$, beneath the curve vertix.

Therefore, the pull horizontal component can be obtained by the identified cable length once determined

$$\ell = \int_{x_1}^{x_2} \cos h \frac{g}{H_g}(x + C_1)dx \qquad (2.3.48)$$

iii) Arbitrary vertical load

Under this load condition, still considering constant the pull horizontal component, one introduces the moments M_y e M_z on the equivalent beam generated by the current load condition.

If the deflection is known, the H calculus is not particularly complex. Actually, in order to compute the length of the cable, one considers the shear stresses Q_y and Q_z acting on the equivalent beam.

With reference to Fig. 2.10, one infers
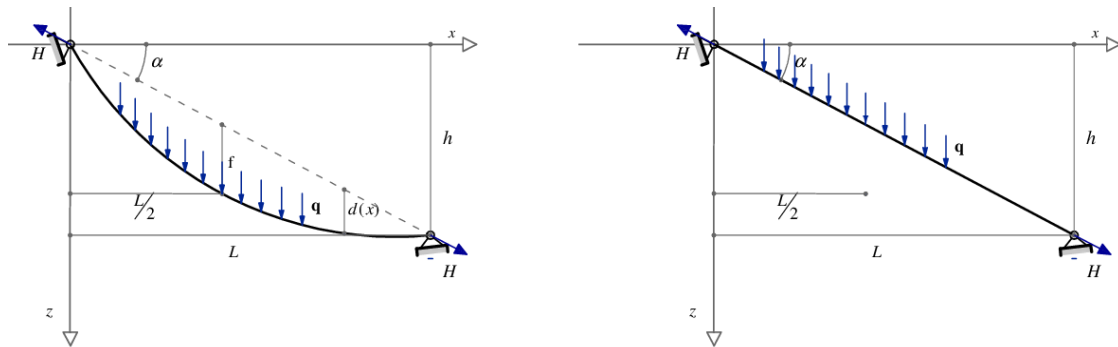
Figure 2.10: Simple cable and equivalent beam tilted on the horizontal axis in the plane (Oxz).

$$tan \; \alpha = \frac{h}{\ell} \qquad (2.3.49)$$

$$d = z - x \; tan\alpha \qquad (2.3.50)$$

$$\bar{d} = \bar{z} - x \; tan \; \alpha \qquad (2.3.51)$$

$$H_q v = M_y \qquad (2.3.52)$$

$$H_q \bar{d} = M_z \qquad (2.3.53)$$

One should notice that the moments' indexes in Eq. (2.3.52) – (2.3.53) do not identify the vector direction but the component of the load producing them.

Moreover, knowing that

$$Q_z = M'_z$$
$$Q_y = M'_y$$

(2.3.54)

one gets

$$\bar{z}' = \frac{Q_z}{H} + tan\alpha$$

(2.3.55)

and being $g_y = 0$

$$\bar{y}' = y' = \frac{Q_y}{H}$$

(2.3.56)

the deformed cable length can be computed as

$$\ell = \int \sqrt{1 + \left(\frac{Q_y}{H}\right)^2 + \left(\frac{Q_z}{H} + tan\alpha\right)^2} \, dx$$

(2.3.57)

Therefore, in the search of the equilibrium shape, if the length is known and the deflection is unknown, H and the cable geometry can be arbitrarily fixed. If comparing the values of the length resulting from Eq. (2.3.57), Eq. (2.3.31) and Eq. (2.3.33) they largely differ from the given value, then H is to be set again in order to get as close as possible to the expected value.

iv) Arbitrary load

One considers the load conditions q_x, q_y, q_z, whence $H \neq$ const.

The load is applied along the unknown cable line, and its application points are expressed only in function of x.

Thus, one proceeds to identify the pull horizontal component by the first of Eq. (2.3.16) inferring

$$H = H_o + \int_0^x P_x dx \tag{2.3.58}$$

where

H_o is a value previously computed and then corrected if necessary.

Once identified the horizontal component value of the stress in the beam, the new configuration assumed by the cable should be determined. For this reason, the remaining Eq. (2.3.16) are considered, where the ordinates along y and z are still expressed by their first derivatives.

Therefore, after integration, it is possible to identify the cable shape and subsequently the length by Eq. (2.3.31)-(2.3.32).

2.3.5   The elastic cable

In the case of elastic cable, in the analysis of forces and displacements of the cable the elastic stretching should be accounted for. Since the cable may be stretched, the deflection assumes values greater than in the unstretched case, and consequently the tensile pull force decreases.

The considered elasticity condition may be caused by the circumstance that the ends of the cable are blocked, preventing their displacements, or that they undergo some prefixed displacements or that the cable length changes according to its elongation.

The length as additional condition

As previously shown, the cable length, subject to dead loads, additional loads and heat variation, is given by

$$\ell_q = \int_{x_\ell}^{x_r} \sqrt{1 + v'^2 + z'^2}\, dx \tag{2.3.59}$$

$$\ell_q = \sqrt{1 + \left(\frac{Q_{yq}}{H_q}\right)^2 + \left(\frac{Q_{zq}}{H_q} + \tan\alpha\right)^2}\, dx \tag{2.3.60}$$

Remembering that Eq. (2.3.59) depends on the deformed cable coordinates, that may be inferred through the equilibrium conditions, Eq. (2.3.60) is referred to the auxiliary beam taking into account also the shear forces, as already emphasized.

Since in this case the cable is elastic, it undergoes a length variation $\Delta\ell$ depending on the horizontal components H_p, caused by the additional load and heat variation

$$\ell_q = \ell_g^o + \Delta\ell \tag{2.3.61}$$

And, after substitution of Eq. (2.3.34)

$$\Delta\ell = \frac{H_p}{EA}\int r'^2\,dx + t_\varepsilon \ell_g \tag{2.3.62}$$

$$\ell_q = \ell_g^o + \int \frac{H_p}{EA}\left(1 + z'^2\right)dx + \int t_\varepsilon dx \tag{2.3.63}$$

or when $q_x = 0$, and EA and t_ε are constant, one gets

$$\ell_q = \ell_g^o\left(1 + t_\varepsilon\right) + \frac{H_p}{EA}\int\left(1 + z'^2\right)dx \tag{2.3.64}$$

In these conditions the pull component H may be computed directly, but through iteration. Therefore, the value $H_q = H_g + H_p^{(1)}$ is fixed, assuming as known H_g and ℓ_g^o.

Starting from this value of H_q the relevant length ℓ_q^1 is calculated throught the ordinates' method described in the above. Hence a length value $^1\ell_q$ different from ℓ_q^1 is obtained.

Thus, one proceeds by fixing subsequent values of H up to convergence, satisfying the condition

$$^n\ell_q = \ell_q^n \tag{2.3.65}$$

In the case when $H = $ const, it is possible to refer to Eq. (2.3.24), always proceeding by iteration.

- **The span as additional condition**

Let now consider the case when only vertical loads act on the span of the cable. The pull horizontal component may be directly computed on the basis of the cable length by through a condition about displacements

$$\int u' dx = 0 \tag{2.3.66}$$

with

$$u' = -z'w' + \frac{H_p}{EA}(1+z'^2)^{\frac{3}{2}} + (1+z'^2)t_\varepsilon \tag{2.3.67}$$

Eq. (2.3.67) is inferred quite easily from Eq. (2.3.29)

$$H_p = \frac{EA(u'+yv'+z'w')}{(1+y'^2+z'^2)^{\frac{3}{2}}} - \frac{EAt_\varepsilon}{(1+y'^2+z'^2)^{\frac{1}{2}}} \tag{2.3.68}$$

$$H_p = \frac{u'EA}{(1+z'^2)^{\frac{3}{2}}} + \frac{z'w'EA}{(1+z'^2)^{\frac{3}{2}}} - \frac{EAt_\varepsilon}{(1+y'^2+z'^2)^{\frac{1}{2}}} =$$

$$\rightarrow u' = -z'w + \frac{H_p(1+z'^2)^{\frac{3}{2}}}{EA} + t_\varepsilon(1+z'^2)$$

Hence by integrating on the length, one gets

$$\int_{x_\ell}^{x_r} -z'w' + \frac{H_p}{EA}(1+z'^2)^{\frac{3}{2}} + (1+z'^2)t_\varepsilon dx = 0 \tag{2.3.69}$$

Decomposing the integral in Eq. (2.3.69) and assuming EA and t_ε constant, one gets

$$\int_{x_\ell}^{x_r} -z'w'dx + \frac{H_p}{EA}\int_{x_\ell}^{x_r}(1+z'^2)^{\frac{3}{2}}dx + t_\varepsilon\int_{x_\ell}^{x_r}(1+z'^2)dx = 0 \tag{2.3.70}$$

where

$$\ell_s = \int_{x_\ell}^{x_r}\left(1+z'^2\right)^{\frac{3}{2}}dx \tag{2.3.71}$$

$$\ell_t = \int_{x_\ell}^{x_r} \left(1 + z'^2\right) dx \tag{2.3.72}$$

$$\int_{x_\ell}^{x_r} -z'w' \, dx + \frac{H_p}{EA} \ell_s + t_\varepsilon \ell_t = 0 \tag{2.3.73}$$

Since

$$\int_{x_\ell}^{x_r} z'w' \, dx + \left[z'w\right]_{x_\ell}^{x_r} - \int_{x_\ell}^{x_r} z'' w \, dx = 0 \tag{2.3.74}$$

and remembering that

$$H_q z'' + g = 0 \tag{2.3.75}$$

one gets

$$H_q^2 \frac{\ell_s}{EA} + H_q \left[\frac{1}{H_g^2} \int_{x_\ell}^{x_r} g M_{zg} \, dx - H_g \frac{\ell_s}{EA} + t_\varepsilon \ell_t \right] - \frac{1}{H_g} \int_{x_\ell}^{x_r} g M_{zq} \, dx = 0 \tag{2.3.76}$$

where M_{zg} e M_{zq} denote the bendig moments depending to the load conditions **g** and **q**.

From Eq. (2.3.76), it is possible to achieve the horizontal tension component H_q.

Considering constant applied loads, the integral can be easily computed. Actually, remembering that the deflection under the dead load is

$$f = \frac{g\ell^2}{8H_g}, \quad n = \frac{f}{\ell} \tag{2.3.77}$$

Eq. (2.3.78) can be written as

$$H_q^2 \frac{\ell_s}{EA} + H_q \left[\frac{16n}{3} f - H_g \frac{\ell_s}{EA} + t_\varepsilon \ell_t \right] - \frac{2}{3} q\ell f = 0 \tag{2.3.78}$$

Eq. (2.3.71)-(2.3.72) in this case assume the value

$$\ell_t = L\left(1 + \frac{16}{3} n^2 + tan^2 \alpha\right) \tag{2.3.79}$$

and approximately

$$\ell_s \approx L \left(\frac{1 + 8n^2 + tan^2 \alpha}{cos \alpha} \right) \qquad (2.3.80)$$

Eq. (2.3.79)-(2.3.80) can be applied also for cable without a perfectly parabolic configuration. According to the above presented developments, the response of the cables, both in pretension state and under additional loads, is non-linear. The pretension represents a stress state, in equilibrium configuration, which the cable is subject to in order to make it stable and stiff under the overloads' application (*J.W. Leonard, 1988*).

The response of the element under pretension state is always non-linear, and the related equilibrium configuration depends on the applied pretension forces. The response to the overloads, instead, can be non-linear or almost-linear, according to the direction of application and the intensity of the load compared to the above-mentioned forces.

Hence, ought to the not strictly linear response, the effects of the two load conditions cannot be superposed, as already specified. So far, analytical methodologies for the single cable have been presented, highlighting the nature of the nonlinear behaviour of these structural elements, and allowing to find solutions, in most case approximated, suitable and implementable for several kinds of cable structures.

Therefore, it is important to understand how the cable geometry changes depending on the loads, not only because of their intensity, but also and especially of their application and arrangement.

Essentially two cases of uniformly distributed loads are considered: the one applied on the cable chord *L* with the ends at the same height as shown in Fig. 2.11 (b), and the other one acting on the arch of the curve as depicted in Fig. 2.11 (a), leading, in this case, to the catenary equation, which, in the limit case when the tilt is very small, tends to the simplified solution relevant to the first case.

(a)   *(b)*
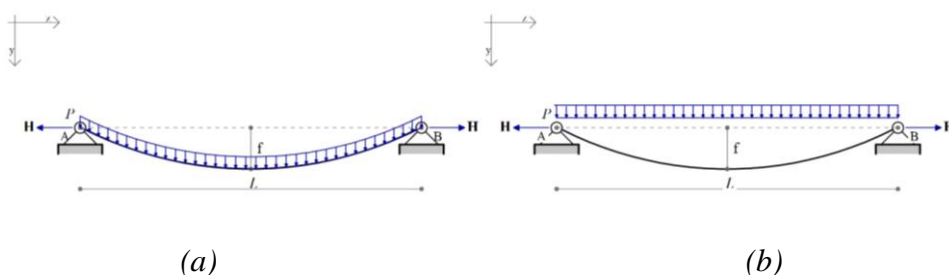
Figure 2.11: Uniform loads: (a) on the horizontal span and (b) along the length.

2.4 The cable as continuum or discrete element

On the basis of the previously introduced analytical methods, and in particular on the one relevant to the elastic catenary, a number of more recent approaches to the analysis of complex structures as suspended bridge (*D. Cobo Del Arco, A.C. Aparicio, 2001*) or three-dimensional cable structures have been developed *(Such et al, 2009)*. As previously highlighted, the advent of computer era has pushed towards the search of methods easy to compile. Matching the analytical solution of suspended cables with fixed ends with Finite Element methods (FE) formulations, and through the application of the Virtual Work Principle (VWP), a new formulation of catenary can be set up allowing to increase the solution accuracy and decrease the computational weight (*C.Wang et al, 2003*).   In order to simplify the governing problem equations and to allow easy CPU compilation, the cable can be modeled as continuous in Fig. 2.12 (a) or discrete element in Fig. 2.12 (b). In both cases, the equilibrium configuration is identified under the pretension state and as a consequence of the overloads' application through the identification of the tangent stiffness matrix and the forces vector.

(a)   *(b)*
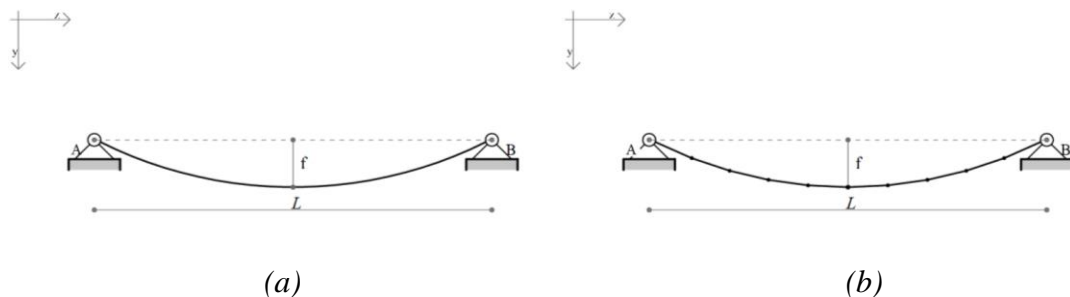
Figure 2.12: (a) Continuous and (b) discrete cable model.

It is easily perceivable that the cable discrete model can be obtained through the discretization of the continuous formulation, presenting a number of advantages such as to consider the nodal loads on the single cable segments, and to include both geometric and mechanical non linearity (*A. Shoostari et al, 2013*).

2.4.1   Continuum modelling of the cable (*CCC-Continuum Catenary Cable*)

Let consider a perfectly flexible cable under a uniformly distributed load (P_x, P_y, P_z)
applied along the three directions in the reference system (*Oxyz*), as shown in Fig.2.13.
Moreover, the cable is subject to a heat load Δt is assumed.

Geometrically the cable presents a constant cross-section area, and it is suspended
between the A and B points with coordinates

$$A \equiv (0,0,0)$$
$$B \equiv (\ell_x, \ell_y, \ell_z)$$
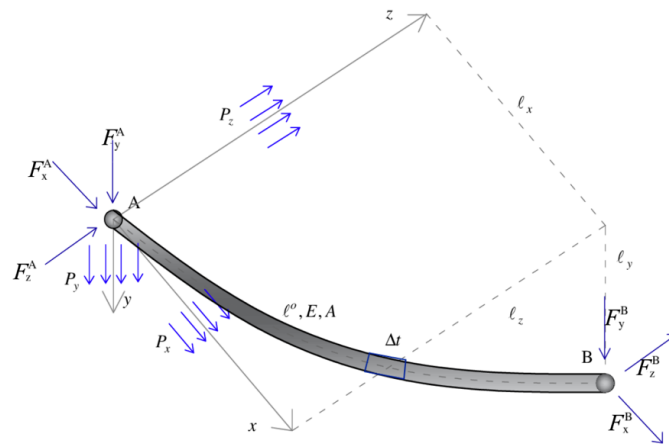
Figure 2.13: Continuous model of a cable under generic load conditions.

Denoting by *s* and *a* the lagrangian coordinates respectively in the undeformed and
deformed configurations, in the undeformed configuration

$$\begin{cases} x = x(s) = \displaystyle\int_0^s \frac{dx}{ds} ds \\[2em] y = y(s) = \displaystyle\int_0^s \frac{dy}{ds} ds \\[2em] z = z(s) = \displaystyle\int_0^s \frac{dz}{ds} ds \end{cases}$$

and in the deformed one

$$
\begin{cases}
x = x(a) = \int_0^a \dfrac{dx}{da}\, da \\[2em]
y = y(a) = \int_0^a \dfrac{dy}{da}\, da \\[2em]
z = z(a) = \int_0^a \dfrac{dy}{da}\, da
\end{cases}
$$

The equilibrium equations in the three directions are expressed by

$$
\begin{cases}
T\left(\dfrac{dx}{da}\right) = -\left(P_x s + F_x^A\right) \\[1.5em]
T\left(\dfrac{dy}{da}\right) = -\left(P_y s + F_y^A\right) \\[1.5em]
T\left(\dfrac{dz}{da}\right) = -\left(P_z s + F_z^A\right)
\end{cases}
\tag{2.4.1}
$$

where

F_x^A, F_y^A, F_z^A are the beam force components along the three axes at the node A

T is the cable stress

The stress T s given as a function of the lagrangian coordinate s by

$$
T(s) = \sqrt{\sum_i (P_i s + F_i^A)^2} \qquad \text{with } i = x, y, z
\tag{2.4.2}
$$

Furthermore, the stress T can be also expressed through the elasticity relation as a function of the strain, as

$$
T = EA\varepsilon
\tag{2.4.3}
$$

where

E is the elasticity modulus

A is the cross-section area

ε is the cable strain relevant to the component of the loads $\varepsilon_c = \left(\dfrac{da - ds}{ds}\right)$ and the one

of the heat $\varepsilon_t = -\alpha\Delta t$, with α denoting the thermal expansion coefficient.

Then Eq. (2.4.3) turns into

$$T = EA\left(\varepsilon_c + \varepsilon_t\right) = EA\left(\frac{da - ds}{ds} - \alpha\Delta t\right) = EA\left(\frac{da}{ds} - \frac{ds}{ds} - \alpha\Delta t\right)$$

$$T = EA\left(\frac{da}{ds} - 1 - \alpha\Delta t\right) \tag{2.4.4}$$

Linking the Cartesian and the lagrangian coordinates,

$$\begin{cases} x = x(s) = \int\limits_0^s \dfrac{dx}{ds}\,ds = \int\limits_0^s \dfrac{dx}{da}\dfrac{da}{ds}\,ds \\[2mm] y = y(s) = \int\limits_0^a \dfrac{dy}{ds}\,ds = \int\limits_0^s \dfrac{dy}{da}\dfrac{da}{ds}\,ds \\[2mm] z = z(s) = \int\limits_0^a \dfrac{dy}{ds}\,ds = \int\limits_0^s \dfrac{dz}{da}\dfrac{da}{ds}\,ds \end{cases} \tag{2.4.5}$$

Eq. (2.4.1) and Eq. (2.4.2) are then substituted in Eq. (2.4.5)

$$\frac{dx}{da} = \frac{-\left(P_x s + F_x^A\right)}{T} = \frac{-\left(P_x s + F_x^A\right)}{\sqrt{\sum\limits_i \left(P_i s + F_i^A\right)^2}}$$

$$\frac{dy}{da} = \frac{-\left(P_y s + F_y^A\right)}{T} = \frac{-\left(P_y s + F_y^A\right)}{\sqrt{\sum\limits_i \left(P_i s + F_i^A\right)^2}} \qquad \text{with} \quad i = x, y, z$$

$$\frac{dz}{da} = \frac{-\left(P_z s + F_z^A\right)}{T} = \frac{-\left(P_z s + F_z^A\right)}{\sqrt{\sum\limits_i \left(P_i s + F_i^A\right)^2}}$$

$$T = EA \frac{da}{ds} - EA - EA \alpha \Delta t$$

$$EA \frac{da}{ds} = T + EA + EA \alpha \Delta t$$

$$\frac{da}{ds} = \frac{T}{EA} + \frac{EA + EA \alpha \Delta t}{EA}$$

$$\frac{da}{ds} = \frac{T}{EA} + 1 + \alpha \Delta t$$

$$\begin{cases} \int_0^s \frac{dx}{da} \frac{da}{ds} ds = \int_0^s \frac{-\left(P_x s + F_x^A\right)}{\sqrt{\sum_i \left(P_i s + F_i^A\right)^2}} \left(\frac{\sqrt{\sum_i \left(P_i s + F_i^A\right)^2}}{EA} + 1 + \alpha \Delta t \right) ds \\[4mm] \int_0^s \frac{dy}{da} \frac{da}{ds} ds = \int_0^s \frac{-\left(P_y s + F_y^A\right)}{\sqrt{\sum_i \left(P_i s + F_i^A\right)^2}} \left(\frac{\sqrt{\sum_i \left(P_i s + F_i^A\right)^2}}{EA} + 1 + \alpha \Delta t \right) ds \quad \text{with } i = x, y, z \quad (2.4.6) \\[4mm] \int_0^s \frac{dz}{da} \frac{da}{ds} ds = \int_0^s \frac{-\left(P_z s + F_z^A\right)}{\sqrt{\sum_i \left(P_i s + F_i^A\right)^2}} \left(\frac{\sqrt{\sum_i \left(P_i s + F_i^A\right)^2}}{EA} + 1 + \alpha \Delta t \right) ds \end{cases}$$

Then the boundary conditions are applied

$$x(0) = y(0) = z(0) = 0 \tag{2.4.7}$$

$$\begin{aligned} x(\ell^o) &= \ell_x \\ y(\ell^o) &= \ell_y \\ z(\ell^o) &= \ell_z \end{aligned} \tag{2.4.8}$$

where

ℓ^o is the cable initial length.

By integrating along the element and using Eq. (2.4.7) and Eq. (2.4.8), the lengths' projection (ℓ_x, ℓ_y, ℓ_z) are obtained

$$\ell_i(F_x^A, F_y^A, F_z^A) =$$

$$-\frac{\ell^{o2}P_i}{EA} - \frac{\ell^{o2}F_i^A}{2EA} + \frac{(1+\alpha\Delta t)}{w^3}\left\{wP_i(T_1-T_2) + w^2F_i^A - bP_x\left[\begin{array}{c}\ln\left(\dfrac{b}{w}+T_1\right)+\\[2mm]-\ln\left(\ell^o w + \dfrac{b}{w}+T_2\right)\end{array}\right]\right\} \quad (2.4.9)$$

with

$$w = \sqrt{\sum_i P_i^2}; \ \ b = \sum_i f_i^A P_i; \ \ T_1 = T(0); \ \ T_2 = T(\ell^o)$$

In order to solve Eq. (2.4.9), the differential components of the cable stresses in the three directions are introduced, which, denoting

$$\ell_x = f(F_x^A, F_y^A, F_z^A)$$
$$\ell_y = g(F_x^A, F_y^A, F_z^A) \quad (2.4.10)$$
$$\ell_z = h(F_x^A, F_y^A, F_z^A)$$

are expressed in the form

$$d\ell_x = \frac{\partial f}{\partial F_x^A}dF_x^A + \frac{\partial f}{\partial F_y^A}dF_y^A + \frac{\partial f}{\partial F_z^A}dF_z^A$$

$$d\ell_y = \frac{\partial g}{\partial F_x^A}dF_x^A + \frac{\partial g}{\partial F_y^A}dF_y^A + \frac{\partial g}{\partial F_z^A}dF_z^A \quad (2.4.11)$$

$$d\ell_z = \frac{\partial h}{\partial F_x^A}dF_x^A + \frac{\partial h}{\partial F_y^A}dF_y^A + \frac{\partial h}{\partial F_z^A}dF_z^A$$

and writing Eq. (2.4.11) in matrix form

$$\begin{bmatrix}d\ell_x\\d\ell_y\\d\ell_z\end{bmatrix} = \begin{bmatrix}\dfrac{\partial\ell_x}{\partial F_x^A} & \dfrac{\partial\ell_x}{\partial F_y^A} & \dfrac{\partial\ell_x}{\partial F_z^A}\\[3mm]\dfrac{\partial\ell_y}{\partial F_x^A} & \dfrac{\partial\ell_y}{\partial F_y^A} & \dfrac{\partial\ell_y}{\partial F_z^A}\\[3mm]\dfrac{\partial\ell_z}{\partial F_x^A} & \dfrac{\partial\ell_z}{\partial F_y^A} & \dfrac{\partial\ell_z}{\partial F_z^A}\end{bmatrix}\begin{bmatrix}dF_x^A\\dF_y^A\\dF_z^A\end{bmatrix} \quad (2.4.12)$$

one gets in compact vector form

$$d\boldsymbol{\ell} = \mathbf{Q}d\mathbf{F} \quad (2.4.13)$$

where

$\mathbf{Q}$ is the compliance matrix.

The stiffness matrix $\mathbf{K}$ is got by

$$\mathbf{K} = \mathbf{Q}^{-1} \tag{2.4.14}$$

The stiffness matrix $\mathbf{K}$ in Eq. (2.4.14) is then embedded in the tangent stiffness matrix with six degrees of freedom

$$\mathbf{K}_T = \begin{bmatrix} -\mathbf{K} & \mathbf{K} \\ \mathbf{K} & -\mathbf{K} \end{bmatrix} \tag{2.4.15}$$

Finally, by identifying the force components at the B node

$$
\begin{aligned}
F_x^B &= -\left(P_x \ell^o + F_x^A\right) \\
F_y^B &= -\left(P_y \ell^o + F_y^A\right) \\
F_z^B &= -\left(P_z \ell^o + F_z^A\right)
\end{aligned}
\tag{2.4.16}
$$

the internal forces vector with six components is identified

$$\mathbf{F} = \left[F_x^A, F_y^A, F_z^A, F_x^B, F_y^B, F_z^B \right]^T \tag{2.4.17}$$

Then, once identified the tangent stiffness matrix and the internal forces vector, the cable length $\ell = \sqrt{\ell_x^2 + \ell_y^2 + \ell_z^2}$ is inferred.

2.4.2   Discrete modelling of the cable (*DCC-Discrete Catenary Cable*)

In discrete modelling, the cable is considered to be composed of several cable segments as shown in Fig. 2.14.
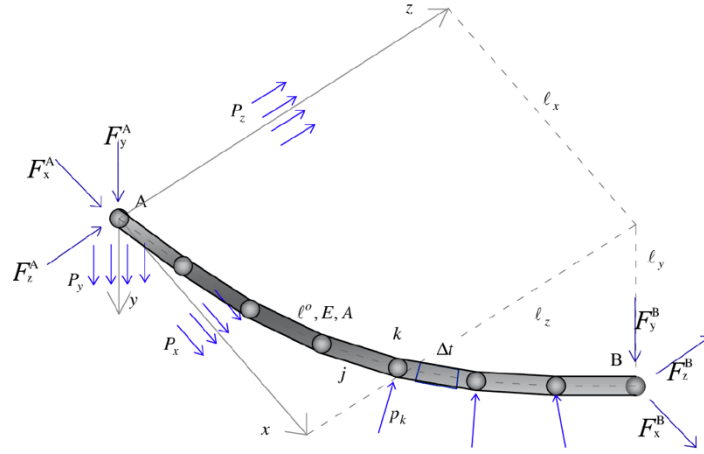
Figure 2.14: Discrete model of the cable with nodal load application.

Once denoted by m the number of cable segments and by ℓ^o the initial length of the entire cable, then the undeformed length of each segment is marked by ℓ^o_t

$$\ell^o_t = \frac{\ell^o}{m}$$

After denoting by ℓ_j the updated length of the jth element under the load p^k_i applied on the kth internal node in the ith direction, by x^j_i the jth component of the sub-element in the ith direction in the reference system, by T^j the jth sub-element stress, Eq. (2.4.1) turns into

$$T^j \left(\frac{\Delta x^j_i}{\ell_j} \right) = - \left(j\ell^o_t P_i + F^A_i + \sum_{k=1}^{j} p^k_i \right)$$ (2.4.18)

with

$i = x, y, z$
$j = 1 ... m$

and

$$\Delta x^j_i = x^{j+1}_i - x^j_i$$

Considering that

$$T_j = E_j A_j (\varepsilon_c^j - \varepsilon_t^j) = E_j A_j \left(\frac{\ell_j - \ell_t^o}{\ell_t^o} - \alpha \Delta t \right) = E_j A_j \left(\frac{\ell_j}{\ell_t^o} - 1 - \alpha \Delta t \right) \tag{2.4.19}$$

the x_i^j components can be computed

$$x_i^j = \sum_{k=1}^{j} \Delta x_i^k = \sum_{k=1}^{j} \frac{\Delta x_i^k}{\ell^k} \frac{\ell^k}{\ell_t^o} \ell_t^o \tag{2.4.20}$$

Substituting Eq. (2.4.18), (2.4.19) and Eq. (2.4.20), one gets

$$\ell_i \left(F_x^A, F_y^A, F_z^A \right) = -\ell_t^o \left(j \ell_t^o P_x + F_i^A + \sum_{k=1}^{j} p_j^k \right) \left(\frac{1}{E_j A_j} + \frac{1 + \alpha \Delta t}{T_j} \right) \tag{2.4.21}$$

After solving the system of equations in Eq.(2.4.21) by the differential components $\dfrac{\partial \ell_i}{\partial f_i^A}$, it is possible to identify the compliance matrix **Q**, besides the stiffness and tangent stiffness matrixes, in analogy with what reported in the previous Par.2.4.1. The internal forces vector **F** is then identified, thus allowing to identify the cable length as well.

In these first chapters, the main features of tensile structures have been highlighted, paying particular attention to the study of the simple cable. This problem has been dealt with a rigorous approach already during the XVII century with reference to the first elements of infinitesimal analysis, due to the non-linearity characterizing these structural elements that does not allow the application of effects' superposition.

Since then a number of solutions, mainly analytical, have been developed, such as those ones referring to the unstretchable catenary, unstretchable parabola, elastic catenary and overloaded catenary, and then considering the flexible cable.

During years, cable structures have been spreading in the construction field, including suspended bridges, cable-stayed bridges, coverings of big areas, as far as to play an important role in the free-form design thanks to the advent of new materials.

Thus, the interest in understanding their static behaviour, in addition to the dynamic one, has greatly increased. Starting from the solutions proposed from former mechanics, several approaches have been developed during years, also as a consequence of the advent of the computer era, aiming at simplifying the problem governing equations for allowing easy handling and computer programming.

New catenary cables have been considered as well, leading to the identification of the relevant entities, such as stiffness matrixes and internal forces vectors; cables have been modelled both as continuous or discrete elements, applying nodal loads. In this way, starting from these models, it is possible to analyse more complex structures, such as cable trusses or cable nets, that are deepened in Chapter 3.

3. 2D AND 3D SYSTEMS

3.1 Plane systems with opposite curvature

In this section, the static behaviour of plane systems with opposite curvature will be analysed.

This structural system can be considered as an evolution of the simple cable one (*K. Santoso, 2003*) since it is characterized by two elements with opposite curvatures, linked to each other by either vertical or diagonal cables. The upward cable has the carrying function, while the downward cable has the role to tent it. The connecting elements can absorb also compressive forces when the carrying cable presents a downward concavity (Fig.3.1).
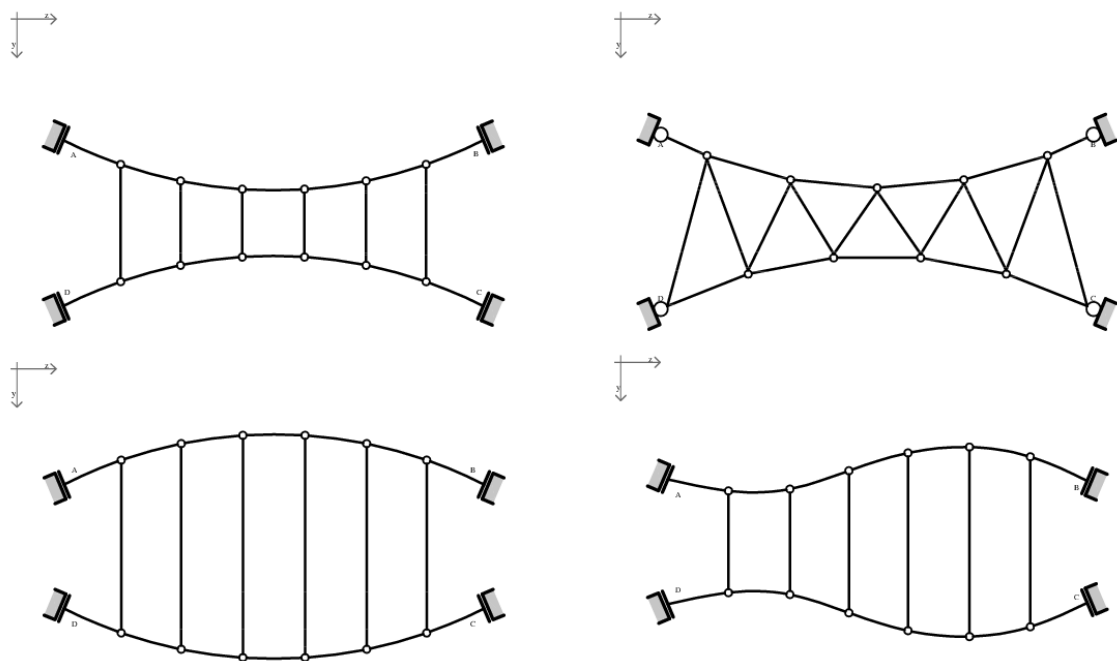
Figure 3.1: Schemes of different configurations of cables with opposite curvature.

The cable structures with opposite curvature can support loads that are directed in both the (upward and downward) directions in the plane, with the same stiffness (*K. Santaso, 2003*).

Moreover, it has also been shown that these systems are able to give a greater stability to the structure, actually, being able, under the same load conditions, to decrease the upward displacements of about 63,1%, the downward ones of 1,8%, and the total displacements of 29,4% with respect to the simple ones (*V. Goremikins, et al 2011*) (Fig. 3.2).
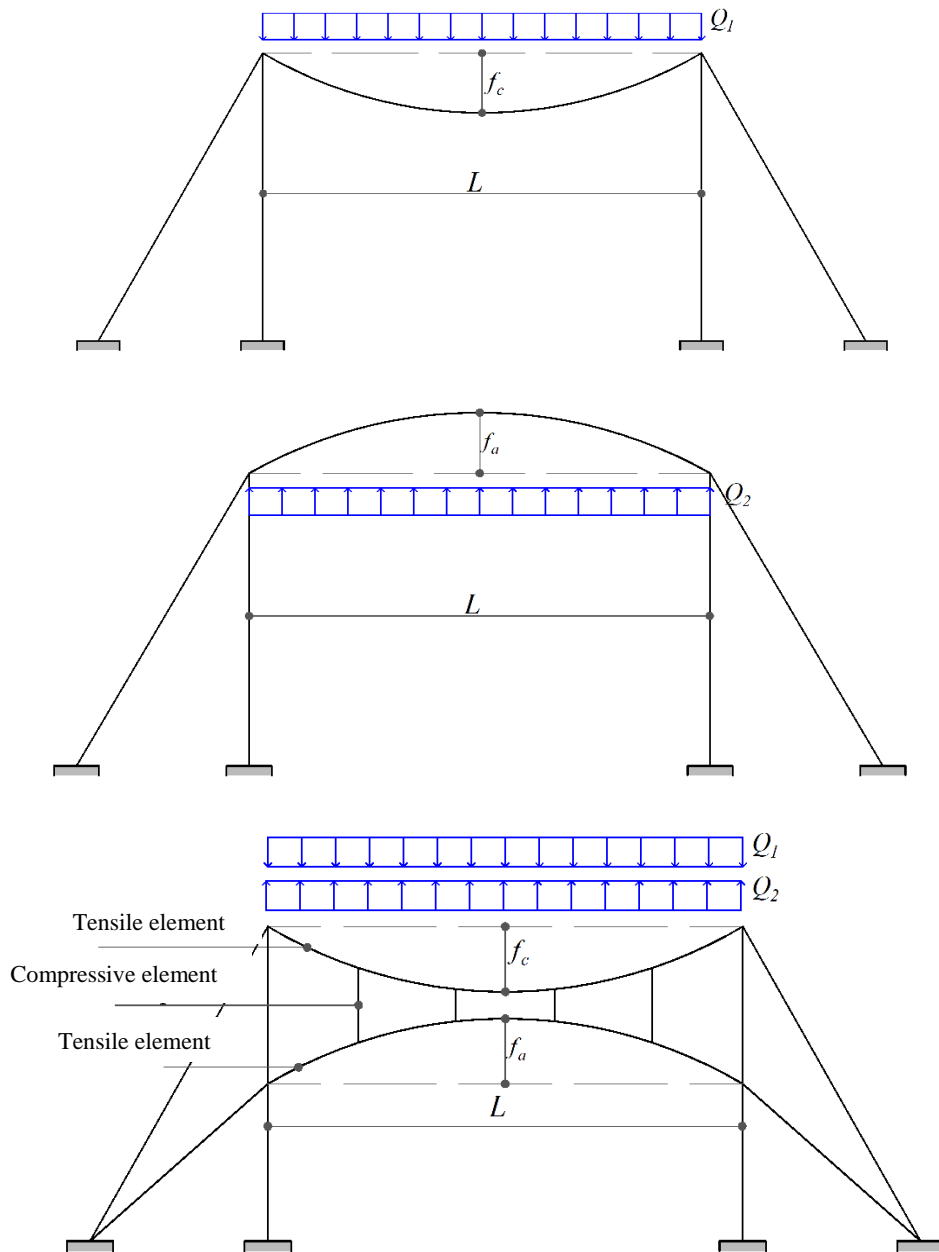
Figure 3.2: Cable systems with opposite curvature.

These structural typologies present several advantages, and they are particularly used for big span roofs and suspended bridges (*M. Raoof, T.J. Davies, 2004*).

A first example of cable structures with opposite curvature is represented by the Ice Palace in Stockholm by the Swedish engineer Jawerth (1960) (*Z. Chen, et al 2014*). Later, besides the applications for other roof systems, they be found in several engineering buildings (*M. Majowiecki, 2005*), and with different shapes.

Recently new systems have been developed, also composed of the union of frames (beams and piles) with cables with two different curvatures, that are interconnected in such a way to stabilize the entire structure under the load action.

Actually, thanks to the cables, the frame (Fig. 3.3) can resist both gravity overloads and wind pressure (*S. Lee, et al 2019*), compared to structures made of beams and single cables.
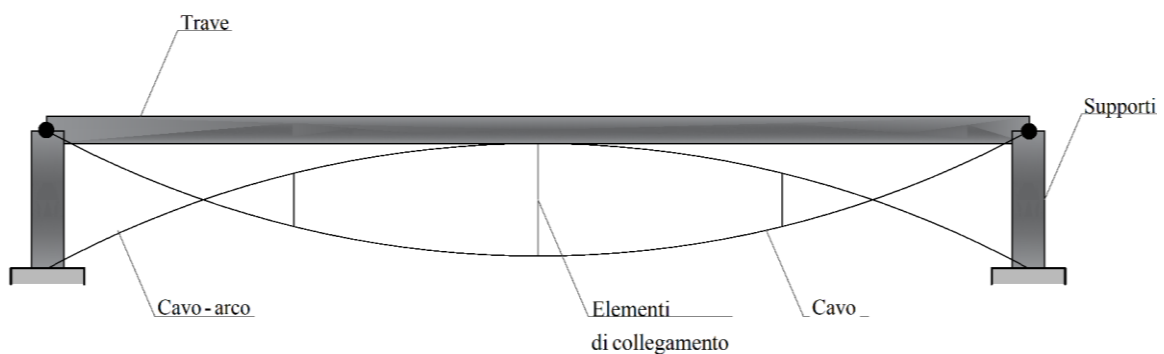
Figure 3.3: Tensile structure scheme composed of tensile cables and frames (S. Lee, 2019).

Several methods have been developed, starting from the first approaches proposed by Schleyer and Jawerth.

According to these studies, a methodology was developed based on the hypotheses of curtain behaviour and unextensibility of connecting cables, referring only to opposite

curvature systems linked by vertical elements, advantages of systems with diagonal connecting cables were highlighted by Jawerth.

Since one deals with articulated structures characterized by high non linearity in their geometry (*Z. Chen et al, 2014)*, the several analysis models developed during years have attempted to control the above-mentioned non linearity through different kinds of approaches.

Nonlinear FE models have been frequently used to highlight their performances with and without the overloads (*Huang et al,2007*). Actually, these structural systems can be regarded as discretized structures (*A. Sadaoui, et al., 2016*) allowing the development and the large spread of the above-mentioned models (*I. Talvik et al., 2001; Y. Kanno et al.,2002*).

To this regard a series of analyses has been led referring to bridge structures built with cables with opposite curvatures, considering also the non uniform load conditions, highlighting their deformation regime (*M.H. Huang, et al. 2008*).

Beyond FE approaches, several calculus models based on exact mathematic form expressions have been developed with the adoption of some approximations, such as: neglecting the second order terms in the equilibrium equations of the constituent cables in order to obtain the linearization of the problem and to solve the equilibrium under the overloads; or neglecting the self-weight of the cables and applying uniformly distributed loads along the span; or supposing the inclination of the chord very small and sometimes, assuming as continuous the connecting vertical elements (S. *Kmet et al., 2014*) (Fig. 3.4).
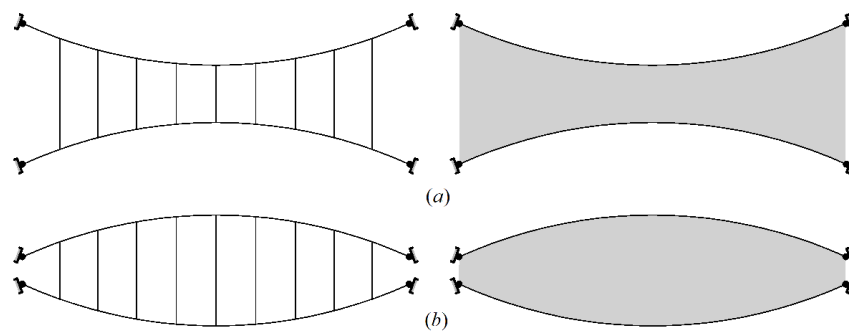
Figure 3.4: Biconcave (a) and Biconvex (b) geometric profiles with continuum modelling of the connection elements (S. Kmet et al., 2014).

Comparing the approaches, one may observe that in the case of the finite elements models some particular attention needs to be paid to the circumstance that some elements may be subject to compressive stresses; therefore, in this case the compressive stiffness of these elements must be deleted and the acting loads redistributed on the adjacent cables. However, if the number of compressed elements is high the structure is unstable, and the solution diverges. This case unlikely occurs in closed form models (*A. Sadaoui et al, 2016*).

As mentioned, one of the main issues in setting up the calculus models is represented by the aim of handling them quite easily for computational purposes However, one of the first calculus programs both for the linear and nonlinear analysis of these cable structures, was developed by Broughton and Ndumbaro and it is based on the Newton - Raphson technique taking into account both geometric and mechanical non linearity (*P. Broughton, P. Ndumbaro,1999).* The requested inputs concern the structural geometry, the elements' stiffness, the loads arrangement, the boundary conditions, and the pretension value.

Actually, the pretension plays a central role in tensile structures in general, and particularly in this type of structures because of lightness. The pretension represents the initial load that acts on the structure, and therefore on the cables, in order to have no elements in compression after the overloads' action.

Thus, the study of these structural typologies mainly concerns the geometry finding once known the pull forces, and the search and the identification of the static and deformative regime after the external loads' application.

It is important to remember that the pretensional forces must be identified with reference to the most dangerous load condition, checking that: the admissible stresses are not overpassed, the deflections respect the deformability of the material, and the internal forces in the cables is not null.

Referring to the pretension geometry, one assumes that the self-weight is negligible compared to the applied loads.

In the following, an analytical method for the analysis of plane structures with opposite curvature suitable for several typologies is described.

3.1.1   The pretension geometry

One refers to the structural scheme given in Fig.3.5, supposed to be subject to the self-stress state reached after the pretension.

In the scheme *1,2,3,...,k,...n* identify the *n* internal nodes, while A,B,C,D the boundary ones.
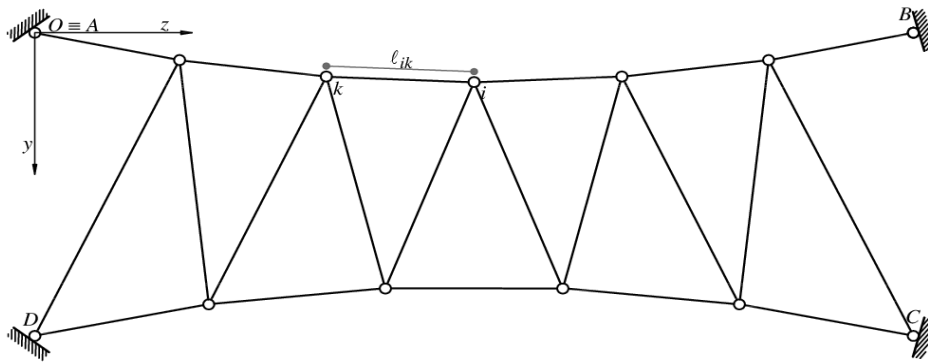
Figure 3.5: Scheme of a plane cable structure with opposite curvature- pretension geometry.

The kth internal node is referred to with coordinates z_k and y_k , and interconnected with the $i^{\text{th.}}$ node with coordinates z_i and y_i , through the cable segment with length ℓ_{ik} .

In synthesis

$$k \equiv (y_k, z_k)$$
$$i \equiv (y_i, z_i)$$

ℓ_{ik} is the cable segment length with ends *i-k*

$$\ell_{ik} = \sqrt{\Delta y_{ik}^2 + \Delta z_{ik}^2} \tag{3.1.1}$$

with

$$\Delta y_{ik} = y_i - y_k \tag{3.1.2}$$

$$\Delta z_{ik} = z_i - z_k \tag{3.1.3}$$

Then, being T_{ik}^o the internal forces in the generic cable i-k, and A_{ik} the cross section area, the equilibrium of the generic k^{th} node for the horizontal translation is

$$\sum_i T_{ik}^o \frac{\Delta z_{ik}}{\ell_{ik}} = 0 \qquad\qquad (3.1.4)$$

and for the vertical one

$$\sum_i T_{ik}^o \frac{\Delta y_{ik}}{\ell_{ik}} = 0 \qquad\qquad (3.1.5)$$

One should consider that it is impossible to always arbitrarily fix the geometry of the structure in order to find the associated forces regime satisfying Eq. (3.1.4) and Eq. (3.1.5). Actually, the node equilibrium cannot be generalized for any configuration, since the internal forces must be in tension.

Consequently, there is the requirement to find the configuration and therefore the pretensioned geometry respecting the above-mentioned conditions.

The problem of finding the pretensioned geometry can be dealt with in several modes: starting from the initial lengths ℓ_{ik}^o of the cable segments between the ith and k^{th} node, and the internal forces at the ends, that is the connection cables with external restraints that apply the pretension to the structure. Therefore the non-linear system in $2n$ equations and $2n$ unknown variables (y_k, z_k) is identified[1], that is not homogeneus because the coordinates of the end nodes A,B,C and D are known.

---

[1]Due to the constitutive law(cont.):

$$
\begin{cases}
\sum_i EA_{ik}\, \Delta z_{ik} \left(\dfrac{1}{\ell_{ik}^o} - \dfrac{1}{\sqrt{\Delta z_{ik}^2 + \Delta y_{ik}^2}} \right) = 0 \\[4mm]
\sum_i EA_{ik}\, \Delta y_{ik} \left(\dfrac{1}{\ell_{ik}^o} - \dfrac{1}{\sqrt{\Delta z_{ik}^2 + \Delta y_{ik}^2}} \right) = 0
\end{cases}
\qquad \forall \ \text{internal node } k \qquad\qquad (3.1.6)
$$

$$
T_{ik}^0 = EA_{ik}\, \frac{\ell_{ik} - \ell_{ik}^o}{\ell_{ik}^o}
$$

Substituting in Eq.(3.1.4 - 3.1.5), the translation equilibrium equations, one has

$$
\sum_i EA_{ik}\, \frac{\ell_{ik} - \ell_{ik}^o}{\ell_{ik}^o}\, \frac{\Delta z_{ik}}{\ell_{ik}} = 0
$$

$$
\sum_i EA_{ik}\, \frac{\ell_{ik} - \ell_{ik}^o}{\ell_{ik}^o}\, \frac{\Delta y_{ik}}{\ell_{ik}} = 0
$$

$$
\ell_{ik} = \sqrt{\Delta z_{ik}^2 + \Delta y_{ik}^2}
$$

hence for any internal node of the system, the equilibrium equation turns into

$$
\sum_i EA_{ik} \left(\frac{\sqrt{\Delta z_{ik}^2 + \Delta y_{ik}^2} - \ell_{ik}^o}{\ell_{ik}^o} \right) \frac{\Delta z_{ik}}{\sqrt{z_{ik}^2 + y_{ik}^2}} = 0
$$

$$
\sum_i EA_{ik}\, z_{ik} \left(\frac{\sqrt{\Delta z_{ik}^2 + \Delta y_{ik}^2}}{\ell_{ik}^o \sqrt{\Delta z_{ik}^2 + \Delta y_{ik}^2}} - \frac{1}{\sqrt{\Delta z_{ik}^2 + \Delta y_{ik}^2}} \right) = 0
$$

$$
\sum_i EA_{ik}\, z_{ik} \left(\frac{1}{\ell_{ik}^o} - \frac{1}{\sqrt{\Delta z_{ik}^2 + \Delta y_{ik}^2}} \right) = 0
$$

Similarly

$$
\sum_i EA_{ik} \left(\frac{\sqrt{\Delta z_{ik}^2 + \Delta y_{ik}^2} - \ell_{ik}^o}{\ell_{ik}^o} \right) \frac{y_{ik}}{\sqrt{\Delta z_{ik}^2 + \Delta y_{ik}^2}} = 0
$$

$$
\sum_i EA_{ik}\, y_{ik} \left(\frac{\sqrt{\Delta z_{ik}^2 + \Delta y_{ik}^2}}{\ell_{ik}^o \sqrt{\Delta z_{ik}^2 + \Delta y_{ik}^2}} - \frac{1}{\sqrt{\Delta z_{ik}^2 + \Delta y_{ik}^2}} \right) = 0
$$

$$
\sum_i EA_{ik}\, y_{ik} \left(\frac{1}{\ell_{ik}^o} - \frac{1}{\sqrt{\Delta z_{ik}^2 + \Delta y_{ik}^2}} \right) = 0
$$

Another method provides to write a system in $2n$ non-linear equations and in $2n$ unknown variables y_k and z_k to compute the initial length of the generic segment, by fixing the stresses T_{ik}^{o} [2] and therefore the pretension.

$$\begin{cases} \sum_i T_{ik}^{o} \dfrac{\Delta z_{ik}}{\ell_{ik}} = 0 \\[2mm] \sum_i T_{ik}^{o} \dfrac{\Delta y_{ik}}{\ell_{ik}} = 0 \end{cases} \quad \forall \text{ internal node } k \tag{3.1.7}$$

$$\ell_{ik}^{o} = \frac{\ell_{ik}}{1 + \dfrac{T_{ik}^{o}}{E_{ik} A_{ik}}} \tag{3.1.8}$$

ℓ_{ik}^{o} is the initial length of the generic cable segment i-k should have in order to achieve the final length ℓ_{ik} under the T_{ik}^{o} force.

In the above-described methods, one gets some systems that are quite difficult to solve because the systems are nonlinear with a large number of unknown variables. Considering and fixing the pull horizontal component

$$H_{ik}^{o} = \frac{|\Delta z_{ik}|}{\ell_{ik}} T_{ik}^{o} \tag{3.1.9}$$

in such a way the equilibrium condition along the z-axis[3] is satisfied by

---

$$T_{ik}^{o} = EA_{ik} \frac{\ell_{ik} - \ell_{ik}^{o}}{\ell_{ik}^{o}}$$

$$\ell_{ik}^{o} T_{ik}^{o} = EA_{ik} \left(\ell_{ik} - \ell_{ik}^{o} \right)$$

$$\ell_{ik}^{o} T_{ik}^{o} + EA_{ik} \ell_{ik}^{o} = EA_{ik} \ell_{ik}$$

[2] $\dfrac{\ell_{ik}^{o} T_{ik}^{o}}{EA_{ik}} + \ell_{ik}^{o} = \ell_{ik}$

$$\ell_{ik}^{o} \left(\frac{T_{ik}^{o}}{EA_{ik}} + 1 \right) = \ell_{ik}$$

it is expressed

$$\ell_{ik}^{o} = \frac{\ell_{ik}}{\left(1 + \dfrac{T_{ik}^{o}}{EA_{ik}} \right)}$$

in function of T_{ik}^{o}

$$\sum_i \frac{\Delta z_{ik}}{\left|\Delta z_{ik}\right|} H_{ik}^o = 0 \tag{3.1.10}$$

while the equilibrium along the y-axis[4] should satisfy

$$\sum_i \frac{\Delta y_{ik}}{\left|\Delta z_{ik}\right|} H_{ik}^o = 0 \tag{3.1.11}$$

In order to satisfy Eq. (3.1.11) it is sufficient that only the ordinates y_k are undtermined. Therefore z_k can be arbitrarly fixed, thus reducing the number of equations from $2n$ to n, and, hence, leading to the solution of a linear problem governed by n equations in n unknown variables y_k.

$$H_{ik}^o = \frac{\left|\Delta z_{ik}\right|}{\ell_{ik}} T_{ik}^o$$

$$\ell_{ik} H_{ik}^o = \left|\Delta z_{ik}\right| T_{ik}^o$$

$$T_{ik}^o = \frac{\ell_{ik} H_{ik}^o}{\left|\Delta z_{ik}\right|}$$

[3]
$$\sum_i T_{ik}^o \frac{\Delta z_{ik}}{\ell_{ik}} = 0$$

$$\sum_i \frac{\ell_{ik} H_{ik}^o}{\left|\Delta z_{ik}\right|} \frac{\Delta z_{ik}}{\ell_{ik}} = 0$$

$$\sum_i \frac{\Delta z_{ik}}{\left|\Delta z_{ik}\right|} H_{ik}^o = 0$$

$$H_{ik}^o = \frac{\left|\Delta z_{ik}\right|}{\ell_{ik}} T_{ik}^o$$

$$\ell_{ik} H_{ik}^o = \left|\Delta z_{ik}\right| T_{ik}^o$$

$$T_{ik}^o = \frac{\ell_{ik} H_{ik}^o}{\left|\Delta z_{ik}\right|}$$

[4]
$$\sum_i T_{ik}^o \frac{\Delta y_{ik}}{\ell_{ik}} = 0$$

$$\sum_i \frac{\ell_{ik} H_{ik}^o}{\left|\Delta z_{ik}\right|} \frac{\Delta y_{ik}}{\ell_{ik}} = 0$$

$$\sum_i \frac{\Delta y_{ik}}{\left|\Delta z_{ik}\right|} H_{ik}^o = 0$$

Therefore, one writes Eq. (3.1.11) for any internal node and, once identified the unknown variables, the internal forces can be computed by

$$T_{ik}^o = H_{ik}^o \sqrt{1 + \left(\frac{\Delta y_{ik}}{\Delta z_{ik}} \right)^2} \qquad \qquad (3.1.12)$$

Subsequently, by Eq. (3.1.8)

$$\ell_{ik}^o = \frac{\ell_{ik}}{1 + \dfrac{T_{ik}^o}{E_{ik} A_{ik}}} \qquad \qquad (3.1.8)$$

the initial lengths of any cable segment composing the system can be determined in order to identify the equilibrated and compatible configuration.

So far, the case where the examined structure is in a self-stress state has been supposed.

In the following Par. 3.2, the behaviour of the above-mentioned structure under the overloads' action is analysed.

3.1.2   The overloads' effect

The problem of the structure under the overloads' action is now dealt with. The loads act on the nodes in the same plane of the system as shown in Fig.3.6; therefore, the nodes undergo displacements in the reference axes directions (y, z).

Let suppose the cable segment straight, even if it stretches of $\Delta \ell_{ik}$ due to the nodal displacements.
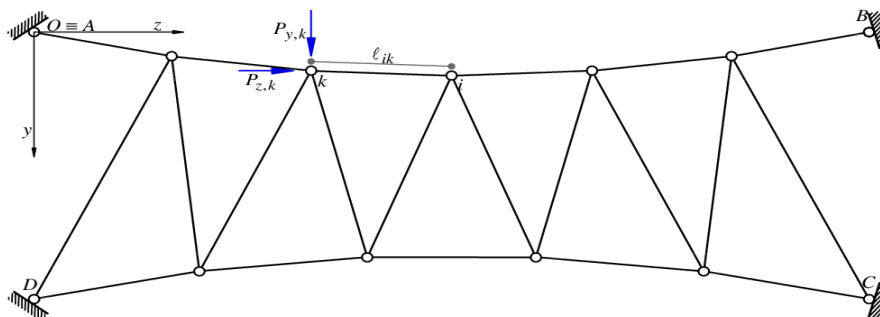
Figure 3.6: Static scheme of a plane cable structure in (Oyz).

Denoting by:

$P_{y,k}$ e $P_{z,k}$ the vertical and horizontal components of the applied nodal load respectively, assumed to be positive if their versus is concordant with the reference axes one.

v_k and w_k the vertical and horizontal components of the displacements respectively, assumed to be positive if their versus is concordant with the reference axes one

$$\Delta v_{ik} = v_i - v_k$$

$$\Delta w_{ik} = w_i - w_k$$

$\Delta \ell_{ik}$ the length variation of the cable segment starting from the length ℓ_{ik}

T_{ik} the pull in the cable due to the pretension and the applied overloads

Δt the heat variation;

α the thermal expansion coefficient;

Both Δt and α depend on the cables' materials.
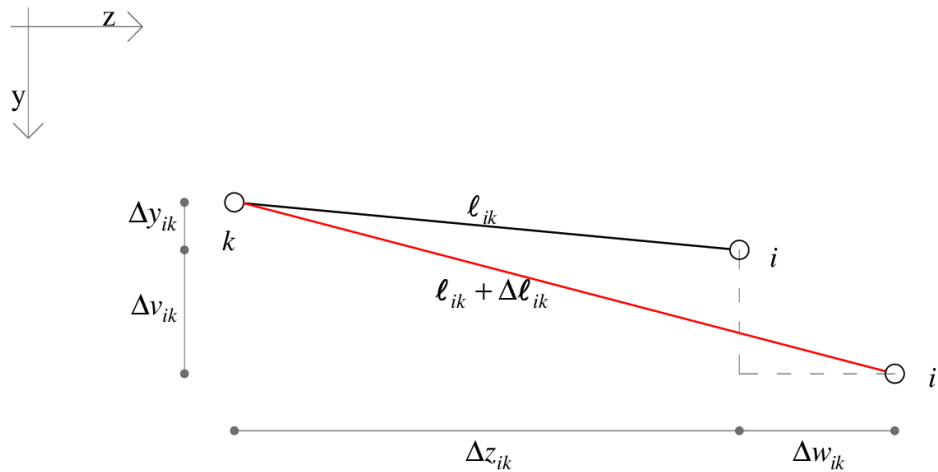
Figure 3.7: Deformed beam due to overloads.

Fig. 3.7 shows the initial and the deformed configuration of the cable, for which the equilibrium equations in the horizontal and vertical direction are respectively

$$\sum_i T_{ik} \frac{\Delta z_{ik} + \Delta w_{ik}}{\ell_{ik} + \Delta \ell_{ik}} + P_{z,k} = 0 \tag{3.1.9}$$

$$\sum_i T_{ik} \frac{\Delta y_{ik} + \Delta v_{ik}}{\ell_{ik} + \Delta \ell_{ik}} + P_{y,k} = 0 \tag{3.1.10}$$

Let denote by H_{ik} the pull horizontal component

$$H_{ik} = T_{ik} \frac{\left| \Delta z_{ik} + \Delta w_{ik} \right|}{\ell_{ik} + \Delta \ell_{ik}} \tag{3.1.11}$$

whence

$$T_{ik} = \frac{\ell_{ik} + \Delta \ell_{ik}}{\left| \Delta z_{ik} + \Delta w_{ik} \right|} H_{ik} \tag{3.1.12}$$

Substituting Eq. (3.1.12) in Eq. (3.1.9) and Eq. (3.1.10), the equilibrium equations to translation are

$$\sum_i H_{ik} \frac{\Delta z_{ik} + \Delta w_{ik}}{\left| \Delta z_{ik} + \Delta w_{ik} \right|} + P_{z,k} = 0 \tag{3.1.13}$$

$$\sum_i H_{ik} \frac{\Delta y_{ik} + \Delta v_{ik}}{\left| \Delta z_{ik} + \Delta w_{ik} \right|} + P_{y,k} = 0 \tag{3.1.14}$$

To identify the problem solution, the elastic-kinematic relations should be identified, that are the relations connecting the static components T_{ik} and H_{ik} with the kinematic ones v_{ik} and w_{ik} .

Thus, with reference to Fig. 3.7, one can infer

$$\begin{aligned}
\left(\ell_{ik} + \Delta \ell_{ik} \right)^2 &= \left(\Delta z_{ik} + \Delta w_{ik} \right)^2 + \left(\Delta y_{ik} + \Delta v_{ik} \right)^2 = \\
&= \ell_{ik}^2 + 2\Delta \ell_{ik} \ell_{ik} + \Delta \ell_{ik}^2 = \Delta z_{ik}^2 + 2\Delta z_{ik} \Delta w_{ik} + \Delta w_{ik}^2 + \Delta y_{ik}^2 + 2\Delta y_{ik} \Delta v_{ik} + \Delta v_{ik}^2
\end{aligned} \tag{3.1.15}$$

Furthermore, since

$$\ell_{ik}^2 = \Delta z_{ik}^2 + \Delta y_{ik}^2 \tag{3.1.16}$$

and then

$$2\Delta \ell_{ik} \ell_{ik} + \Delta \ell_{ik}^2 - \left[\Delta w_{ik}^2 + \Delta v_{ik}^2 + 2(\Delta z_{ik} \Delta w_{ik} + \Delta y_{ik} \Delta v_{ik}) \right] = 0 \tag{3.1.17}$$

solving for $\Delta\ell_{ik}$ [5] and simplifying, one gets

$$\Delta\ell_{ik} = \left\{ \ell_{ik}\sqrt{1+\frac{1}{\ell_{ik}^2}\left[\Delta w_{ik}^2 + \Delta v_{ik}^2 + 2(\Delta z_{ik}\Delta w_{ik} + \Delta y_{ik}\Delta v_{ik})\right]} - 1 \right\} \tag{3.1.18}$$

Moreover, always referring to Fig. 3.7, ℓ_{ik} can be expressed as

$$\ell_{ik} = |\Delta z_{ik}|\sqrt{1+\left(\frac{\Delta y_{ik}}{\Delta z_{ik}}\right)^2} \tag{3.1.19}$$

Thus, Eq. (3.1.18) turns into

$$\Delta\ell_{ik} = |\Delta z_{ik}|\sqrt{1+\left(\frac{\Delta y_{ik}}{\Delta z_{ik}}\right)^2}\left\{ \sqrt{1+\frac{1}{1+\left(\frac{\Delta y_{ik}}{\Delta z_{ik}}\right)^2}\left[\left(\frac{\Delta w_{ik}}{\Delta z_{ik}}\right)^2 + \left(\frac{\Delta v_{ik}}{\Delta z_{ik}}\right)^2 + 2\left(\frac{\Delta w_{ik}}{\Delta z_{ik}} + \frac{\Delta y_{ik}\Delta v_{ik}}{\Delta z_{ik}\Delta z_{ik}}\right)\right]} - 1 \right\} \tag{3.1.20}$$

Because of the constitutive law

$$\Delta\ell_{ik} = \frac{T_{ik} - T_{ik}^o}{EA_{ik}}\ell_{ik} + \alpha\Delta t\ell_{ik} \tag{3.1.21}$$

remembering Eq. (3.1.4) and Eq. (3.2.17), one gets

$$T_{ik} = \frac{\ell_{ik} + \Delta\ell_{ik}}{|\Delta z_{ik} + \Delta w_{ik}|}H_{ik} \tag{3.1.4}$$

$$\ell_{ik} = |\Delta z_{ik}|\sqrt{1+\left(\frac{\Delta y_{ik}}{\Delta z_{ik}}\right)^2} \tag{3.2.17}$$

$$(\ell_{ik} + \Delta\ell_{ik})^2 = (\Delta z_{ik} + \Delta w_{ik})^2 + (\Delta y_{ik} + \Delta v_{ik})^2$$

---

[5]
$$2\Delta\ell_{ik}\ell_{ik} + \Delta\ell_{ik}^2 = \left[\Delta w_{ik}^2 + \Delta v_{ik}^2 + 2(\Delta z_{ik}\Delta w_{ik} + \Delta y_{ik}\Delta v_{ik})\right]$$
$$2\Delta\ell_{ik}\ell_{ik} + \Delta\ell_{ik}^2 + \ell_{ik}^2 - \ell_{ik}^2 = \left[\Delta w_{ik}^2 + \Delta v_{ik}^2 + 2(\Delta z_{ik}\Delta w_{ik} + \Delta y_{ik}\Delta v_{ik})\right]$$
$$(\ell_{ik} + \Delta\ell_{ik})^2 - \ell_{ik}^2 = \left[\Delta w_{ik}^2 + \Delta v_{ik}^2 + 2(\Delta z_{ik}\Delta w_{ik} + \Delta y_{ik}\Delta v_{ik})\right]$$
$$(\ell_{ik} + \Delta\ell_{ik})^2 = \left[\Delta w_{ik}^2 + \Delta v_{ik}^2 + 2(\Delta z_{ik}\Delta w_{ik} + \Delta y_{ik}\Delta v_{ik})\right] + \ell_{ik}^2$$
$$\sqrt{(\ell_{ik} + \Delta\ell_{ik})^2} = \sqrt{\left[\Delta w_{ik}^2 + \Delta v_{ik}^2 + 2(\Delta z_{ik}\Delta w_{ik} + \Delta y_{ik}\Delta v_{ik})\right] + \ell_{ik}^2}$$
$$\Delta\ell_{ik} = \sqrt{\left[\Delta w_{ik}^2 + \Delta v_{ik}^2 + 2(\Delta z_{ik}\Delta w_{ik} + \Delta y_{ik}\Delta v_{ik})\right] + \ell_{ik}^2} - \ell_{ik}$$
$$\Delta\ell_{ik} = \ell_{ik}\left\{\sqrt{1+\frac{1}{\ell_{ik}^2}\left[\Delta w_{ik}^2 + \Delta v_{ik}^2 + 2(\Delta z_{ik}\Delta w_{ik} + \Delta y_{ik}\Delta v_{ik})\right]} - 1\right\}$$

$$T_{ik} = \frac{(\ell_{ik} + \Delta\ell_{ik})}{|\Delta z_{ik} + \Delta w_{ik}|} H_{ik} = \frac{H_{ik}}{\left|1 + \frac{\Delta w_{ik}}{\Delta z_{ik}}\right|} \sqrt{\left(\frac{\Delta z_{ik}}{\Delta z_{ik}} + \frac{\Delta w_{ik}}{\Delta z_{ik}}\right)^2 + \left(\frac{\Delta y_{ik}}{\Delta z_{ik}} + \frac{\Delta v_{ik}}{\Delta z_{ik}}\right)^2}$$

$$T_{ik} = \frac{(\ell_{ik} + \Delta\ell_{ik})}{|\Delta z_{ik} + \Delta w_{ik}|} H_{ik} = \frac{H_{ik}}{\left|1 + \frac{\Delta w_{ik}}{\Delta z_{ik}}\right|} \sqrt{\left(1 + \frac{\Delta w_{ik}}{\Delta z_{ik}}\right)^2 + \left(\frac{\Delta y_{ik}}{\Delta z_{ik}} + \frac{\Delta v_{ik}}{\Delta z_{ik}}\right)^2}$$

$$T_{ik} = \frac{(\ell_{ik} + \Delta\ell_{ik})}{|\Delta z_{ik} + \Delta w_{ik}|} H_{ik} = \frac{H_{ik}}{\left|1 + \frac{\Delta w_{ik}}{\Delta z_{ik}}\right|} \sqrt{\left(1 + \frac{\Delta w_{ik}}{\Delta z_{ik}}\right)^2 + \left(\frac{\Delta y_{ik}}{\Delta z_{ik}} + \frac{\Delta v_{ik}}{\Delta z_{ik}}\right)^2} \tag{3.1.21}$$

Taking into account Eq. (3.1.17), Eq. (3.1.18) and Eq. (3.2.10) and making the suitable substitutions in Eq. (3.1.19), one gets

$$\ell_{ik} = |\Delta z_{ik}| \sqrt{1 + \left(\frac{\Delta y_{ik}}{\Delta z_{ik}}\right)^2} \tag{3.1.17}$$

$$T_{ik}^o = H_{ik}^o \sqrt{1 + \left(\frac{\Delta y_{ik}}{\Delta z_{ik}}\right)^2} \tag{3.1.18}$$

$$T_{ik} = \frac{\ell_{ik} + \Delta\ell_{ik}}{|\Delta z_{ik} + \Delta w_{ik}|} H_{ik} \tag{3.1.10}$$

$$\Delta\ell_{ik} = \frac{T_{ik} - T_{ik}^o}{EA_{ik}} \ell_{ik} + \alpha\Delta t \ell_{ik} \tag{3.2.19}$$

$$\Delta\ell_{ik} =$$

$$= |\Delta z_{ik}| \sqrt{1 + \left(\frac{\Delta y_{ik}}{\Delta z_{ik}}\right)^2}$$

$$\left[\frac{H_{ik}}{EA_{ik}\left|1 + \frac{\Delta w_{ik}}{\Delta z_{ik}}\right|} \sqrt{\left(1 + \frac{\Delta w_{ik}}{\Delta z_{ik}}\right)^2 + \left(\frac{\Delta y_{ik}}{\Delta z_{ik}} + \frac{\Delta v_{ik}}{\Delta z_{ik}}\right)^2} - \frac{H_{ik}^o}{EA_{ik}} \sqrt{1 + \left(\frac{\Delta y_{ik}}{\Delta z_{ik}}\right)^2} + \alpha\Delta t \right]$$

$$\Delta\ell_{ik} =$$

$$= |\Delta z_{ik}| \sqrt{1 + \left(\frac{\Delta y_{ik}}{\Delta z_{ik}}\right)^2} \tag{3.1.22}$$

$$\left[\frac{H_{ik}}{E \, A_{ik} \left|1 + \frac{\Delta w_{ik}}{\Delta z_{ik}}\right|} \sqrt{\left(1 + \frac{\Delta w_{ik}}{\Delta z_{ik}}\right)^2 + \left(\frac{\Delta y_{ik}}{\Delta z_{ik}} + \frac{\Delta v_{ik}}{\Delta z_{ik}}\right)^2} - \frac{H_{ik}^0}{E \, A_{ik}} \sqrt{1 + \left(\frac{\Delta y_{ik}}{\Delta z_{ik}}\right)^2} + \alpha\Delta t \right]$$

To identify the searched elastic-kinematic relations, Eq.(3.1.17) is equalized to Eq. (3.1.22), obtaining H_{ik}. Hence, set the problem, one can proceed to the search of the solution, that can be hard to compute in this way. Thus, remembering that

$$\Delta v_{ik} = v_i - v_k$$

$$\Delta w_{ik} = w_i - w_k$$

$\Delta\ell_{ik}$ is the length variation of the cable segment obtained starting from the pretensioned length ℓ_{ik},

some simplifications may be applied, and in particular:

$$\frac{\Delta w_{ik}}{\Delta z_{ik}} << 1 \text{ e } \frac{\Delta v_{ik}}{\Delta z_{ik}} << 1 \ ,$$

which means that these ratios can be considered negligible, allowing to introduce the relevant changes in Eq. (3.1.11), Eq. (3.1.12), Eq. (3.1.21), Eq. (3.1.22).

$$\sum_i H_{ik} \frac{\Delta z_{ik} + \Delta w_{ik}}{|\Delta z_{ik} + \Delta w_{ik}|} + P_{z,k} = 0 \cong \sum_i \frac{\Delta z_{ik}}{|\Delta z_{ik}|} H_{ik} + P_{z,k} = 0$$

$$\sum_i H_{ik} \frac{\Delta y_{ik} + \Delta v_{ik}}{|\Delta z_{ik} + \Delta w_{ik}|} + P_{y,k} = 0 \cong \sum_i \frac{\Delta z_{ik}}{|\Delta z_{ik}|} H_{ik} \left(\frac{\Delta y_{ik}}{\Delta z_{ik}} + \frac{\Delta v_{ik}}{\Delta z_{ik}} \right) + P_{y,k} = 0$$

$$T_{ik} = \frac{(\ell_{ik} + \Delta\ell_{ik})}{|\Delta z_{ik} + \Delta w_{ik}|} H_{ik} \cong H_{ik} \sqrt{1 + \left(\frac{\Delta y_{ik}}{\Delta z_{ik}} \right)^2}$$

$$\Delta\ell_{ik} =$$

$$= |\Delta z_{ik}| \sqrt{1 + \left(\frac{\Delta y_{ik}}{\Delta z_{ik}} \right)^2} \left[\frac{H_{ik}}{E_{ik} A_{ik} \left| 1 + \frac{\Delta w_{ik}}{\Delta z_{ik}} \right|} \sqrt{\left(1 + \frac{\Delta w_{ik}}{\Delta z_{ik}} \right)^2 + \left(\frac{\Delta y_{ik}}{\Delta z_{ik}} + \frac{\Delta v_{ik}}{\Delta z_{ik}} \right)^2} - \right.$$
$$\left. + \frac{H_{ik}^0}{E_{ik} A_{ik}} \sqrt{1 + \left(\frac{\Delta y_{ik}}{\Delta z_{ik}} \right)^2} + \alpha\Delta t \right] \cong$$

$$\cong \Delta\ell_{ik} = |\Delta z_{ik}| \sqrt{1 + \left(\frac{\Delta y_{ik}}{\Delta z_{ik}} \right)^2} \left[\frac{H_{ik}}{E_{ik} A_{ik}} \sqrt{1 + \left(\frac{\Delta y_{ik}}{\Delta z_{ik}} \right)^2} - \right.$$
$$\left. + \frac{H_{ik}^o}{E_{ik} A_{ik}} \sqrt{1 + \left(\frac{\Delta y_{ik}}{\Delta z_{ik}} \right)^2} + \alpha\Delta t \right]$$

These equations then, after putting

$$k_{ik} = 1 + \left(\frac{\Delta y_{ik}}{\Delta z_{ik}} \right)^2 \tag{3.1.23}$$

$$\Delta H_{ik} = H_{ik} - H_{ik}^o \tag{3.1.24}$$

assume the expressions

$$\sum_i \frac{\Delta z_{ik}}{|\Delta z_{ik}|} \left(H_{ik}^o + \Delta H_{ik} \right) + P_{z,k} = 0 \tag{3.1.25}$$

$$\sum_i \frac{\Delta z_{ik}}{|\Delta z_{ik}|} \left(H_{ik}^o + \Delta H_{ik} \right) \left(\frac{\Delta y_{ik}}{\Delta z_{ik}} + \frac{\Delta v_{ik}}{\Delta z_{ik}} \right) + P_{y,k} = 0 \tag{3.1.26}$$

$$\Delta\ell_{ik} = \frac{\Delta z_{ik}}{k_{ik}^{1/2}} \left(\frac{\Delta w_{ik}}{\Delta z_{ik}} + \frac{\Delta v_{ik}}{\Delta z_{ik}} \frac{\Delta y_{ik}}{\Delta z_{ik}} \right) \tag{3.1.27}$$

$$T_{ik} = H_{ik} k_{ik}^{1/2} \tag{3.1.28}$$

$$\Delta \ell_{ik} = \left| \Delta z_{ik} \right| \left(k_{ik} \frac{\Delta H_{ik}}{EA_{ik}} + \alpha \Delta t k_{ik}^{1/2} \right) \tag{3.1.29}$$

$$\Delta \ell_{ik} = \left| \Delta z_{ik} \right| \left(k_{ik} \frac{\Delta H_{ik}}{EA_{ik}} + \alpha \Delta t k_{ik}^{1/2} \right) = \frac{\Delta z_{ik}}{k_{ik}^{1/2}} \left(\frac{\Delta w_{ik}}{\Delta z_{ik}} + \frac{\Delta v_{ik}}{\Delta z_{ik}} \frac{\Delta y_{ik}}{\Delta z_{ik}} \right)$$

whence

$$\Delta H_{ik} = \frac{EA_{ik}}{k_{ik}^{1/2}} \left[\left(\frac{\Delta w_{ik}}{\Delta z_{ik}} + \frac{\Delta v_{ik}}{\Delta z_{ik}} \frac{\Delta y_{ik}}{\Delta z_{ik}} \right) - \alpha \Delta t k_{ik} \right] \tag{3.1.30}$$

Furthermore, the pretension forces have to oppose the deformations of the structure; therefore, they may be supposed greater than internal forces induced by the external loads

$$H_{ik}^{o} \gg \Delta H_{ik} \tag{3.1.31}$$

Taking into account Eq. (3.1.31), and Eq. (3.1.16)-(3.1.17), the translation equilibrium equations, respectively in the horizontal[6] and vertical[7] direction, turn into

---

$$\sum_i \frac{\Delta z_{ik}}{\left| \Delta z_{ik} \right|} H_{ik}^{o} + \sum_i \frac{\Delta z_{ik}}{\left| \Delta z_{ik} \right|} \Delta H_{ik} + P_{z,k} = 0$$

but

[6] $\sum_i \dfrac{\Delta z_{ik}}{\left| \Delta z_{ik} \right|} H_{ik}^{o} = 0$

hence

$$\sum_i \frac{\Delta z_{ik}}{\left| \Delta z_{ik} \right|} \Delta H_{ik} + P_{z,k} = 0$$

[7](Cont.)

$$\sum_i \frac{\Delta z_{ik}}{|\Delta z_{ik}|} \Delta H_{ik} + P_{z,k} = 0 \tag{3.1.32}$$

$$\sum_i \frac{\Delta z_{ik}}{|\Delta z_{ik}|} \left(H_{ik}^o \frac{\Delta v_{ik}}{\Delta z_{ik}} + \Delta H_{ik} \frac{\Delta y_{ik}}{\Delta z_{ik}} \right) + P_{y,k} = 0 \tag{3.1.33}$$

Hence, now it is possible to write the two equilibrium equations for the n internal nodes, substituting the value of ΔH_{ik} obtained from Eq. (3.1.30), into the above-mentioned expressions; then the problem in the $2n$ unknown variables w_k and v_k is solved.

$$\sum_{\substack{i=1 \\ k=1}}^{n} \frac{\Delta z_{ik}}{|\Delta z_{ik}|} \Delta H_{ik} + P_{z,k} = 0 \tag{3.1.34}$$

$$\sum_{\substack{i=1 \\ k=1}}^{n} \frac{\Delta z_{ik}}{|\Delta z_{ik}|} \left(H_{ik}^o \frac{\Delta v_{ik}}{\Delta z_{ik}} + \Delta H_{ik} \frac{\Delta y_{ik}}{\Delta z_{ik}} \right) + P_{y,k} = 0 \tag{3.1.35}$$

with

$$\Delta H_{ik} = \frac{EA_{ik}}{k_{ik}^{1/2}} \left[\left(\frac{\Delta w_{ik}}{\Delta z_{ik}} + \frac{\Delta v_{ik}}{\Delta z_{ik}} \frac{\Delta y_{ik}}{\Delta z_{ik}} \right) - \alpha \Delta t k_{ik} \right] \tag{3.1.36}$$

$$\sum_i \frac{\Delta z_{ik}}{|\Delta z_{ik}|} \left(H_{ik}^o + \Delta H_{ik} \right) \left(\frac{\Delta y_{ik}}{\Delta z_{ik}} + \frac{\Delta v_{ik}}{\Delta z_{ik}} \right) + P_{y,k} = 0$$

$$\sum_i \frac{\Delta z_{ik}}{|\Delta z_{ik}|} \left(H_{ik}^o \frac{\Delta y_{ik}}{\Delta z_{ik}} + H_{ik}^o \frac{\Delta v_{ik}}{\Delta z_{ik}} + \Delta H_{ik} \frac{\Delta y_{ik}}{\Delta z_{ik}} + \Delta H_{ik} \frac{\Delta v_{ik}}{\Delta z_{ik}} \right) + P_{y,k} = 0$$

but

$$H_{ik}^o \frac{\Delta y_{ik}}{|\Delta z_{ik}|} = 0$$

and

$$\Delta H_{ik} \frac{\Delta v_{ik}}{\Delta z_{ik}} << 1$$

for the hypotheses

$$\frac{\Delta v_{ik}}{\Delta z_{ik}} << 1$$

$$\Delta H_{ik} << H_{ik}^o$$

Hence their product gives a neglegible quantity.

Therefore the equilibrium equation to vertical translation assumes the following expression

$$\sum_i \frac{\Delta z_{ik}}{|\Delta z_{ik}|} \left(H_{ik}^o \frac{\Delta v_{ik}}{\Delta z_{ik}} + \Delta H_{ik} \frac{\Delta y_{ik}}{\Delta z_{ik}} \right) + P_{y,k} = 0$$

One then proceeds by iteration, considering the terms $\Delta H_{ik} \dfrac{\Delta v_{ik}}{\Delta z_{ik}}$, neglected in the previous calculus phase, and adding them as fictitious loads to the external loads. Therefore v_k^* and w_k^* are computed and one proceeds this way until the results from two subsequent iterations present approximatively coinciding values, that is up to convergence.

$$
\begin{cases}
\displaystyle\sum_{\substack{i=1\\k=1}}^{n} \frac{\Delta z_{ik}}{|\Delta z_{ik}|} \Delta H_{ik} + P_{z,k} = 0 \\[3em]
\displaystyle\sum_{\substack{i=1\\k=1}}^{n} \frac{\Delta z_{ik}}{|\Delta z_{ik}|} \left(H_{ik}^o \frac{\Delta v_{ik}}{\Delta z_{ik}} + \Delta H_{ik} \frac{\Delta y_{ik}}{\Delta z_{ik}} \right) + P_{y,k} + P_{y,k}^* = 0
\end{cases}
$$

with

$$
\Delta H_{ik} = \frac{EA_{ik}}{k_{ik}^{1/2}} \left[\left(\frac{\Delta w_{ik}}{\Delta z_{ik}} + \frac{\Delta v_{ik}}{\Delta z_{ik}} \frac{\Delta y_{ik}}{\Delta z_{ik}} \right) - \alpha \Delta t k_{ik} \right]
$$

$$
P_{y,k}^* = \Delta H_{ik} \frac{\Delta v_{ik}}{\Delta z_{ik}} \ll 1
$$

$$
\rightarrow
\begin{cases}
\displaystyle\sum_{\substack{i=1\\k=1}}^{n} \frac{\Delta z_{ik}}{|\Delta z_{ik}|} \frac{EA_{ik}}{k_{ik}^{1/2}} \left[\left(\frac{\Delta w_{ik}}{\Delta z_{ik}} + \frac{\Delta v_{ik}}{\Delta z_{ik}} \frac{\Delta y_{ik}}{\Delta z_{ik}} \right) - \alpha \Delta t k_{ik} \right] + P_{z,k} = 0 \\[3em]
\displaystyle\sum_{\substack{i=1\\k=1}}^{n} \frac{\Delta z_{ik}}{|\Delta z_{ik}|} \left(H_{ik}^o \frac{\Delta v_{ik}}{\Delta z_{ik}} + \Delta H_{ik} \frac{\Delta y_{ik}}{\Delta z_{ik}} \right) + P_{y,k} + P_{y,k}^* = 0
\end{cases}
$$

$$
\rightarrow
\begin{cases}
\displaystyle\sum_{\substack{i=1\\k=1}}^{n} \frac{\Delta z_{ik}}{|\Delta z_{ik}|} \frac{EA_{ik}}{k_{ik}^{1/2}} \frac{\Delta w_{ik}}{\Delta z_{ik}} = -\sum_{\substack{i=1\\k=1}}^{n} \frac{\Delta z_{ik}}{|\Delta z_{ik}|} \frac{EA_{ik}}{k_{ik}^{1/2}} \left[\left(\frac{\Delta v_{ik}}{\Delta z_{ik}} \frac{\Delta y_{ik}}{\Delta z_{ik}} \right) - \alpha \Delta t k_{ik} \right] - P_{z,k} \\[3em]
\displaystyle\sum_{\substack{i=1\\k=1}}^{n} \frac{\Delta z_{ik}}{|\Delta z_{ik}|} \left(H_{ik}^o \frac{\Delta v_{ik}}{\Delta z_{ik}} + \Delta H_{ik} \frac{\Delta y_{ik}}{\Delta z_{ik}} \right) + P_{y,k} + P_{y,k}^* = 0
\end{cases}
$$

$$
\rightarrow
\begin{cases}
\displaystyle\sum_{\substack{i=1\\k=i}}^{n} \Delta w_{ik} = -\left(\sum_{\substack{i=1\\k=i}}^{n} \left[\left(\frac{\Delta v_{ik}}{\Delta z_{ik}} \frac{\Delta y_{ik}}{\Delta z_{ik}} \right) - \alpha \Delta t k_{ik} \right] \right) \Delta z_{ik} - \frac{P_{z,k}}{\displaystyle\sum_{\substack{i=1\\k=1}}^{n} \frac{\Delta z_{ik}}{|\Delta z_{ik}|} \frac{EA_{ik}}{k_{ik}^{1/2}}} \Delta z_{ik} \\[4em]
\displaystyle\sum_{\substack{i=1\\k=1}}^{n} \frac{\Delta z_{ik}}{|\Delta z_{ik}|} \left(H_{ik}^o \frac{\Delta v_{ik}}{\Delta z_{ik}} + \Delta H_{ik} \frac{\Delta y_{ik}}{\Delta z_{ik}} \right) + P_{y,k} + P_{y,k}^* = 0
\end{cases}
$$

paying attention to the second equation

$$\sum_{\substack{i=1 \\ k=1}}^{n} \frac{\Delta z_{ik}}{|\Delta z_{ik}|} \left(H_{ik}^{o} \frac{\Delta v_{ik}}{\Delta z_{ik}} + \Delta H_{ik} \frac{\Delta y_{ik}}{\Delta z_{ik}} \right) + P_{y,k} + P_{y,k}^{*} = 0$$

substituting

$$\Delta H_{ik} = \frac{EA_{ik}}{k_{ik}^{1/2}} \left[\left(\frac{\Delta w_{ik}}{\Delta z_{ik}} + \frac{\Delta v_{ik}}{\Delta z_{ik}} \frac{\Delta y_{ik}}{\Delta z_{ik}} \right) - \alpha \Delta t k_{ik} \right]$$

and

$$\sum_{\substack{i=1 \\ k=i}}^{n} \Delta w_{ik} = -\left(\sum_{\substack{i=1 \\ k=i}}^{n} \left[\left(\frac{\Delta v_{ik}}{\Delta z_{ik}} \frac{\Delta y_{ik}}{\Delta z_{ik}} \right) - \alpha \Delta t k_{ik} \right] + \frac{P_{z,k}}{\frac{\Delta z_{ik}}{|\Delta z_{ik}|} \frac{EA_{ik}}{k_{ik}^{1/2}}} \right) \Delta z_{ik}$$

one turns into

$$\sum_{\substack{i=1 \\ k=1}}^{n} \frac{\Delta z_{ik}}{|\Delta z_{ik}|} \left\{ H_{ik}^{o} \frac{\Delta v_{ik}}{\Delta z_{ik}} + \frac{EA_{ik}}{k_{ik}^{1/2}} \left[\left(\frac{\Delta w_{ik}}{\Delta z_{ik}} + \frac{\Delta v_{ik}}{\Delta z_{ik}} \frac{\Delta y_{ik}}{\Delta z_{ik}} \right) - \alpha \Delta t k_{ik} \right] \frac{\Delta y_{ik}}{\Delta z_{ik}} \right\} + P_{y,k} + P_{y,k}^{*} = 0$$

$$\sum_{\substack{i=1 \\ k=1}}^{n} \frac{\Delta z_{ik}}{|\Delta z_{ik}|} H_{ik}^{o} \frac{\Delta v_{ik}}{\Delta z_{ik}} - \sum_{\substack{i=1 \\ k=1}}^{n} \frac{\Delta z_{ik}}{|\Delta z_{ik}|} \frac{EA_{ik}}{k_{ik}^{1/2}} \left[\left(\frac{\Delta v_{ik}}{\Delta z_{ik}} \frac{\Delta y_{ik}}{\Delta z_{ik}} \right) - \alpha \Delta t k_{ik} \right] \frac{\Delta y_{ik}}{\Delta z_{ik}} +$$

$$-\sum_{\substack{i=1 \\ k=i}}^{n} \frac{\Delta z_{ik}}{|\Delta z_{ik}|} \frac{EA_{ik}}{k_{ik}^{1/2}} \frac{P_{z,k}}{\sum_{\substack{i=1 \\ k=i}}^{n} \frac{\Delta z_{ik}}{|\Delta z_{ik}|} \frac{EA_{ik}}{k_{ik}^{1/2}}} \frac{\Delta y_{ik}}{\Delta z_{ik}} + \sum_{\substack{i=1 \\ k=1}}^{n} \frac{\Delta z_{ik}}{|\Delta z_{ik}|} \frac{EA_{ik}}{k_{ik}^{1/2}} \left[\left(\frac{\Delta w_{ik}}{\Delta z_{ik}} + \frac{\Delta v_{ik}}{\Delta z_{ik}} \frac{\Delta y_{ik}}{\Delta z_{ik}} \right) - \alpha \Delta t k_{ik} \right] \frac{\Delta y_{ik}}{\Delta z_{ik}} =$$

$$= -P_{y,k} - P_{y,k}^{*}$$

simplifying one obtains

$$\sum_{\substack{i=1 \\ k=1}}^{n} \frac{\Delta z_{ik}}{|\Delta z_{ik}|} H_{ik}^{o} \frac{\Delta v_{ik}}{\Delta z_{ik}} - P_{z,k} \frac{\Delta y_{ik}}{\Delta z_{ik}} = -P_{y,k} - P_{y,k}^{*}$$

$$\sum_{\substack{i=1 \\ k=1}}^{n} \Delta v_{ik} = \left(P_{z,k} \frac{\Delta y_{ik}}{\Delta z_{ik}} - P_{y,k} - P_{y,k}^{*} \right) \frac{|\Delta z_{ik}|}{H_{ik}^{o}}$$

Once identified Δv_{ik}, it is substituted in the first equilibrium equation obtaining the updated value of Δw_{ik}. These values are denoted by v_{ik}^{*} and w_{ik}^{*} and the process is repeated up to convergence.

One should also consider that in the reported procedure, the displacement components of the connection nodes between the structure and the restraints are supposed known.

Denoting by M the connection nodes with the restraints (Fig. 3.8), one may infer that,
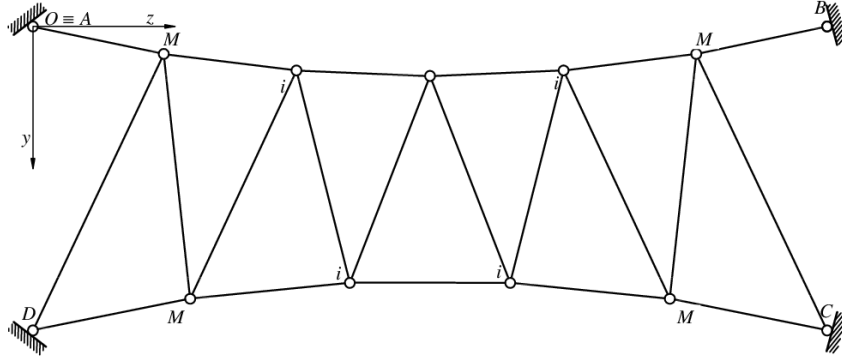
Figure 3.8: Cable structure with opposite curvature in the plane (Oyz), where M denote the connection nodes with the constrained ones.

through these nodes, the structure transmits on the restraint the horizontal and vertical reactions, given by

$$R_{z,M} = \sum_i \frac{\Delta z_{iM}}{|\Delta z_{iM}|} \Delta H_{iM} \tag{3.1.37}$$

$$R_{y,M} = \sum_i \frac{\Delta z_{iM}}{|\Delta z_{iM}|} \left(H_{iM}^0 \frac{\Delta v_{iM}}{\Delta z_{iM}} \Delta H_{iM} + \Delta H_{iM} \frac{\Delta y_{iM}}{\Delta z_{iM}} \right) \Delta H_{iM} \tag{3.1.38}$$

where i is the ith internal node connected to the node M through a cable segment.

If the fixed nodes are denoted by r, the displacements of M are

$$w_M = \sum_{j=1}^{r} \left(\overline{w}_{jM} R_{zj} + \overline{w}_{jM}' R_{vj} \right) \tag{3.1.39}$$

$$v_M = \sum_{j=1}^{r} \left(\overline{v}_{jM} R_{vj} + \overline{v}_{jM}' R_{0j} \right) \tag{3.1.40}$$

where

$\overline{w}_{jM}, \overline{w}_{jM}', \overline{v}_{jM}, \overline{v}_{jM}'$ are the influence coefficients.

These latter expressions, together with Eq. (3.1.32) and (3.1.33), complete the problem solution.

3.2 Cable nets

Spatial systems include a large range of structures; actually, referring to the literature, there are several definitions that can cause some confusion. However, among all, the definition given by the *Working Group of the International Association on Spatial Steel Structures* better describes these structures;

 "A space frame is a structural system assembled of linear elements so arranged that forces are transferred in a three-dimensional manner. In some cases, the constituent element may be two-dimensional. Macroscopically a space frame often takes the form of a flat or a curved surface".

To this typology a number of structures belong, such as membrane structures, suspend-domes, spatial structure presenting a dome shape and typical of gyms' coverings. *tensegrity* structures, *tensarity* structures and cable nets, the latter defined as *"a structure system in the form of a network of elements (as opposed to a continuous surface). Rolled, extruded or fabricated sections comprise the member elements. Another characteristic of latticed structural system is that their load-carrying mechanism is three dimensional in nature"* (ASCE).

According to Dong et al (*S. Dong et al., 2012*), the story of spatial structures can be divided into three main phases: ancient, pre-modern and modern. In particular, the first one refers to thin reinforced concrete shells, and the last one to cable nets, characterized by the use of light material and modern technologies: the combination of materials and different shapes, the application of the pretension and the new structural concepts are their fundamental features.

Moreover, based on the component elements, one may distinguish stiff spatial structures, composed of stiff members like beams, and flexible structures, when the constitutive elements are cables or membranes.

In this paragraph, with respect to flexible spatial structures, i.e. cable nets, that involve some additional complexity in the static calculus because of their geometric features, some examples are showed (Figs. 3.9-11).

Figure 3.9: Olympic Stadium, Monaco, Germany (1970); Frei Otto.

Figure 3.10: Diplomatic club heart tent, Riad, Saudi Arabia (1980); Frei Otto.
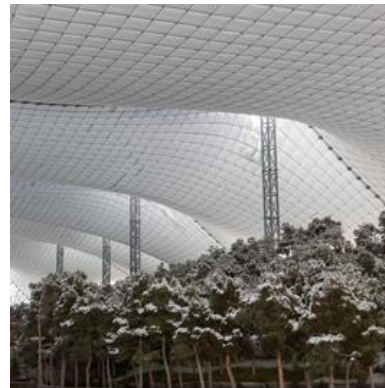
Figure 3.11: Tehran Birds Garde, Tehran, Iran (2017); Diba Group.

Cable nets may be considered as a derivation of the systems with opposite curvature, where the cables (the carrying one and the stabilizing one) are arranged in different vertical planes that usually intersect with each other orthogonally.

Basically the net shows two or more series of cables that stretch out homogeneously the generated surface in all directions. Compared to plane structures, in the cable-nets the external loads act in a plane different from the one of the cable, thus introducing some complexity on the calculus also ought to the increasing of the unknowns' number and therefore of the equations to solve.

Thus, the study of these structures has been motivating several researches and it is constantly evolving (*Such et al.,2009*). A lot of methods and theories have been developed about the geometry finding both under pretension and overloads applications.

The first solving approaches referred to two main theoretical approaches: the continuum and the discontinuous on., then modified during the years.

The discontinuous approach, initially introduced by Bandel (*H.K. Bandel, 1959*), is based on the writing of equilibrium and compatibility equations for each node composing the structure, and then solving the system.

The formulated equilibrium equations are linearized and controlled through compatibility ones, proceeding then to the application of iterative methods to find the solution.

The studies of Siev and Eidelman (*A. Siev, J. Eidelman, 1964*), Mollman and Mortensen (*H. Mollman, P.L. Mortensen, 1966*) are based on these theories, where horizontal loads and displacements are considered.

The continuous approach considers the structure as a membrane without stiffness for tangential stresses, reacting exclusively with normal tensile forces. Hence, it is supposed that the structure is characterized by a textile material obtained through the approach of the cables. Therefore, a continuum structure is achieved, involving differential equations and introducing the boundary equations.

This theory has been at the basis of several studies, such as the Eras and Helze's ones (*G.Eras, H.Elze,1963*), similar to the Bandel's discontinuous theory, that assumes only the action of vertical loads and therefore vertical nodal displacements to solve the problem; or to the Schleyer's approach (*F.K. Schleyer,1965*), which considers also the horizontal displacements, but only in the second approximation.

Subsequently, the methods have been divided into two macro-categories, basically referring to the nonlinear displacement methods or force density methods (FDM), used both in the form-finding and in the static problems, and therefore for searching for the equilibrium conditions.

Iterative methods which update the configuration at any step respecting the equilibrium conditions, belong to the first group. Argyris (*J.H. Argyris,1974*) was one of the first authors to use this method, for the design of the Olympic Stadium in Monaco; then it has been used also by Vilnay (*O.Vilnay, 1990*), and by Jayaraman and Knudson (*H. Jayaramam, W. Knudson, 1981*), who developed two-nodes finite elements on the basis of the elastic catenary equation. Finally, more recently, Andreu et al (*A. Andreu et al, 2006*), instead, used the deformable catenary within a FE method.

The *FDM*, originally developed by Scheck (*H. Scheck, 1974*) among others, has been widely used for several typologies of cable systems as far as for membranes.

However, the beginning of the computer era in the early sixties, led changes on the solving approaches referring to the static problems of these structures. Actually, methods easy to computationally implement were developed, such as the FE method, firstly developed under small displacements. Since cable nets usually undergo large displacements under the overloads' action, the FE method could not be used in its original formulation, but it was modified for structural nonlinear problem solutions, motivating a number of iterative methods for its application. Among these, the most suitable and reliable method for cable structures is the Newton-Raphson one (*Tibert, 1999*).

On the basis of these theories, a method for the nonlinear analysis of the examined structures has been proposed recently, referring to a variational formulation in curvilinear coordinates in the field of finite deformations. This study, after identifying the displacements as kinematic variables of the problem, through the *Virtual Work Principle* application (VWP) infers the relation between deformations and displacements, implementing, then, the finite elements method both for continuum elements and discontinuous ones (*Miquel et al, 2017*).

Again always under the perspective of methods easy to be computationally implemented, matrix methods have been proposed where the structure is analysed as a

discrete system and the governing problem equations are written in matrix formulation. These approaches are based on the classical displacement formulation, where the unknown variables are the kinematic components, or on the force formulation where the variables are identified in the cable forces. For programming purposes the most adopted is the displacement approach, since it is very versatile and can applied to several cable structures typologies, load conditions, stiffness variations (*Lan,1999*).

Other methods are based on the minimization of the Total Potential Energy through constrained procedures (*Toklu et al, 2017*).

In *Par. 3.3.1* a cable-nets system is analysed through an approach based on a membrane analogy, essentially based on writing the governing equilibrium and compatibility equations in an integral-differential form. Only at the second stage, some simplified hypotheses are introduced, in such a way to avoid neglecting some important parameters for the calculus and for the solution of the problem at the initial phase of the procedure.

The adopted membrane analogy is basically founded on regarding the net as a continuum, which exhibits an equivalent behaviour both in terms of stiffness and resistance; in this way the mechanical properties (stiffness, elasticity modulus, thin, Poisson coefficient, etc.) of the system under analysis are calculated on the equivalent membrane, referring to the continuous theory.

As for plane systems, starting from the pretensioned state, neglecting the self-weight, in the case of cable-nets the governing equilibrium equations are projected on the three axes, passing to a three-dimensional system.

3.2.1   The pretension geometry

With reference to the points in Fig. 3.12

$$k \equiv \left(x_k, y_k, z_k \right)$$
$$i \equiv \left(x_i, y_i, z_i \right)$$

One has as regards to equilibrium

$$
\begin{cases}
\displaystyle\sum_i T_{ik}^o \frac{\Delta x_{ik}}{\ell_{ik}} = 0 \\[3mm]
\displaystyle\sum_i T_{ik}^o \frac{\Delta y_{ik}}{\ell_{ik}} = 0 \\[3mm]
\displaystyle\sum_i T_{ik}^o \frac{\Delta z_{ik}}{\ell_{ik}} = 0
\end{cases}
\tag{3.2.1}
$$

where

$$
\begin{aligned}
\Delta x_{ik} &= x_i - x_k \\
\Delta y_{ik} &= y_i - y_k \\
\Delta z_{ik} &= z_i - z_k
\end{aligned}
\tag{3.2.2}
$$

and

$$
\ell_{ik} = \sqrt{\Delta x_{ik}^2 + \Delta y_{ik}^2 + \Delta z_{ik}^2}
\tag{3.2.3}
$$
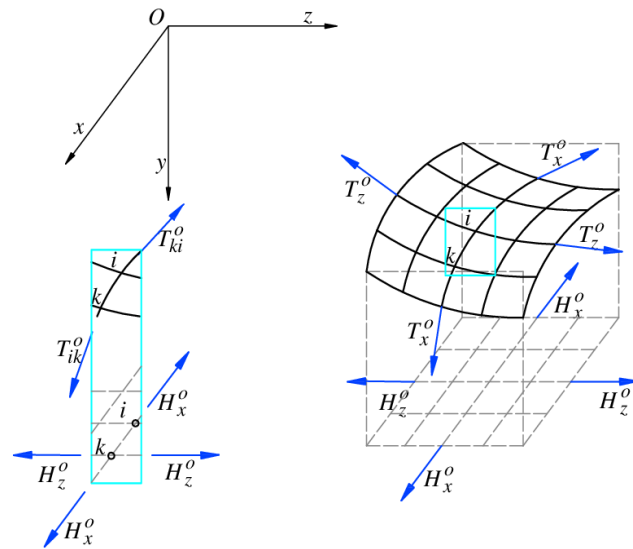
Figure 3.12: Cable-nets tensile structure scheme. Pretension geometry with details of the cable segment i-k.

Considering the pull horizontal components along the *x* and *z* axes

$$
H_{x,ik}^o = \frac{|\Delta x_{ik}|}{\ell_{ik}} T_{ik}^o
\tag{3.2.4}
$$

$$H_{z,ik}^0 = \frac{|\Delta z_{ik}|}{\ell_{ik}} T_{ik}^0 \tag{3.2.5}$$

one has, for equilibrium to horizontal translation,

$$H_{x,ik}^o = \frac{|\Delta x_{ik}|}{\ell_{ik}} T_{ik}^o \to T_{ik}^o = H_{x,ik}^o \frac{\ell_{ik}}{|\Delta x_{ik}|}$$

$$\sum_i T_{ik}^o \frac{\Delta x_{ik}}{\ell_{ik}} = 0 \to \sum_i H_{x,ik}^o \frac{\ell_{ik}}{|\Delta x_{ik}|} \frac{\Delta x_{ik}}{\ell_{ik}} = 0 \to \sum_i H_{x,ik}^o \frac{\Delta x_{ik}}{|\Delta x_{ik}|}$$

$$\sum_i \frac{\Delta x_{ik}}{|\Delta x_{ik}|} H_{x,ik}^o = 0 \tag{3.2.6}$$

$$\sum_i \frac{\Delta z_{ik}}{|\Delta z_{ik}|} H_{z,ik}^o = 0 \tag{3.2.7}$$

and, for vertical translation

$$\sum_i \frac{\Delta y_{ik}}{|\Delta x_{ik}|} H_{x,ik}^o = 0. \tag{3.2.8}$$

The latter Eq. (3.2.8) turns into[8]

$$\sum_i \frac{\Delta y_{ik}}{|\Delta z_{ik}|} H_{z,ik}^o = 0 \tag{3.2.9}$$

since

---

[8] With reference to

$$\sum_i \frac{\Delta y_{ik}}{|\Delta x_{ik}|} H_{x,ik}^o = 0$$

since

$$H_{x,ik}^o = \frac{|\Delta x_{ik}|}{|\Delta z_{ik}|} H_{z,ik}^o$$

one gets

$$\sum_i \frac{\Delta y_{ik}}{|\Delta x_{ik}|} \frac{|\Delta x_{ik}|}{|\Delta z_{ik}|} H_{z,ik}^o = 0 \implies \sum_i \frac{\Delta y_{ik}}{|\Delta z_{ik}|} H_{z,ik}^o = 0$$

$$T_{ik}^o = \frac{H_{x,ik}^o \ell_{ik}}{|\Delta x_{ik}|}$$

$$T_{ik}^o = \frac{H_{z,ik}^o \ell_{ik}}{|\Delta z_{ik}|}$$

$$\frac{H_{z,ik}^o \ell_{ik}}{|\Delta z_{ik}|} = \frac{H_{x,ik}^o \ell_{ik}}{|\Delta x_{ik}|}$$

$$H_{z,ik}^o = \frac{|\Delta z_{ik}|}{|\Delta x_{ik}|} H_{x,ik}^o$$

$$H_{x,ik}^o = \frac{|\Delta x_{ik}|}{|\Delta z_{ik}|} H_{z,ik}^o$$

$$H_{z,ik}^o = \sum_i \frac{|\Delta z_{ik}|}{|\Delta x_{ik}|} H_{x,ik}^o \qquad (3.2.10)$$

After Eq. (3.2.6), one can proceed fixing the initial length or forces, related to each other through the constitutive law

$$T_{ik}^o = EA_{ik} \frac{\ell_{ik} - \ell_{ik}^o}{\ell_{ik}^o} \qquad (3.2.11)$$

The system in $3n$ linear equations and in $3n$ unknown variables x_k, y_k, z_k is obtained

$$\begin{cases} \sum_i EA_{ik} \dfrac{\ell_{ik} - \ell_{ik}^o}{\ell_{ik}^o} \dfrac{\Delta x_{ik}}{\ell_{ik}} = 0 \\[2mm] \sum_i EA_{ik} \dfrac{\ell_{ik} - \ell_{ik}^o}{\ell_{ik}^o} \dfrac{\Delta y_{ik}}{\ell_{ik}} = 0 \\[2mm] \sum_i EA_{ik} \dfrac{\ell_{ik} - \ell_{ik}^o}{\ell_{ik}^o} \dfrac{\Delta z_{ik}}{\ell_{ik}} = 0 \end{cases} \qquad (3.2.12)$$

The pretension configuration is identified subsequently based on the fixed values of the lengths and initial forces.

The above introduced problem is hard to solve and moreover the forces cannot be computed by fixing arbitrarily the pretension geometry.

One proceeds fixing arbitrarily two of the unknown variables x_k and z_k, and the horizontal components of the pull components $H^o_{x,ik}$ and $H^o_{z,ik}$, in order to check the horizontal equilibrium Eq. (3.1.6) - (3.1.7)

$$\sum_i \frac{\Delta x_{ik}}{|\Delta x_{ik}|} H^o_{x,ik} = 0 \qquad (3.1.6)$$

$$\sum_i \frac{\Delta z_{ik}}{|\Delta z_{ik}|} H^o_{z,ik} = 0 \qquad (3.1.7)$$

In this way the number of unknown variables y_k is reduced from $3n$ to n, and they can be computed considering the third equilibrium equation for any internal node of the net

$$y_k \sum_i \frac{\Delta y_{ik}}{|\Delta z_{ik}|} H^o_{z,ik} = 0 \qquad (3.1.8)$$

The scheme shown in Fig. 3.12 is referred to, composed by a cable net with a plant parallel to the x and z axes. The elements composing the net, in this specific case, belong to planes parallel to the coordinate ones and orthogonal with each other.

In each node two cables belonging to different and orthogonal planes, interconnect; hence for any cable segment i-k, the contribute of only horizontal component of forces is different from zero. In order to satisfy Eq. (3.2.6) - (3.2.7), the horizontal component in each cable needs to be constant, because the force parallel to the z-axis does not contribute to balance the force parallel to the x one, being orthogonal to each other.

Consequently, at each node two cables are intersected, belonging to different planes and reciprocally orthogonal; then for any cable segment i-k there is one contribution of a single horizontal stress component ($H^o_{x,ik}$ or $H^o_{z,ik}$) different than zero.

In order to satisfy the equilibrium equations Eq. (2.6.6)-(2.6.7), the horizontal component for any cable must be constant, since the internal force along z cannot contribute to the equilibrium of the internal force along x because they are orthogonal, and vice versa.

Therefore, at the interconnection node a vertical force acts, resulting by the mutual action of the mentioned internal forces. Thus, the resulting equilibrium equation is given by the expression, in pretension phase and without any vertical load on the kth node

$$\sum_i \frac{\Delta y_{ik}}{|\Delta z_{ik}|} H_{z,ik}^o + \sum_i \frac{\Delta y_{ik}}{|\Delta x_{ik}|} H_{x,ik}^o = 0 \qquad (3.2.13)$$

One can be put in evidence that the values of $H_{z,ik}^o$ and $H_{x,ik}^o$ are fixed and chosen in order to satisfy Eq. (3.2.6) and (3.2.7), and considering the contribute of the unique horizontal component of the force, implying that it is constant for any cable segment. In this way the values of y_k are easily computable.

Hence, once identified the unknown variables, one can compute the values of the pull and the initial length for any cable segment in order to obtain the equilibrated and compatible solution.

3.2.2 The continuum approach and membrane analogy

The method is now essentially based on the continuous theory of the static behaviour of tensile cable-nets structures. One assumes a membrane model of the structure in order to reduce the algebraic nonlinear equations to differential ones, compared to the discontinuous theory.

With reference to Fig. 3.13, the surface element with dimensions δs_x, δs_z, whose plane projections are respectively δx and δz, in the initial state is undergone by the tensile

forces T_x^o and T_z^o per unit length of the cable, whose plane projections H_x^o and H_z^o are the horizontal components of the pretension drag forces per unit length. One gets[9]
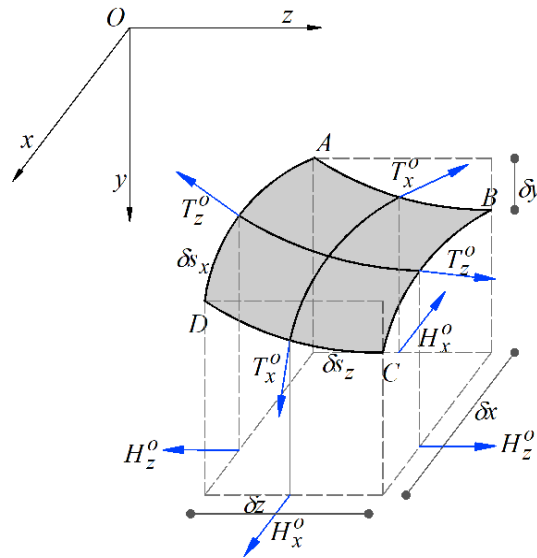
Figure 3.13: Geometry of a cable net assimilable to a membrane where δx and δz are the projections in plant of the cables respectively along the x and z axes; δy the height variation between the vertices A and B (similarly for D and C).

$$H_x^o = H_x^o(z)$$
$$H_z^o = H_z^o(x)$$

(3.2.14)

The pull forces per unit length of the cables along the z and x directions can be computed referring to the horizontal components in Eq. (3.2.14)

---

[9] with reference to the projection in plant

$$\frac{\partial H_x^o}{\partial x} = 0$$

$$\frac{\partial H_z^o}{\partial z} = 0$$

$$H_x^o \frac{\partial^2 y}{\partial x^2} + H_z^o \frac{\partial^2 y}{\partial z^2} = 0$$

from the first two

$$H_x^o(z)$$

$$H_z^o(x)$$

$$T_x^o = H_x^0 \frac{\delta z}{\delta x} \frac{\delta s_x}{\delta s_z}$$

$$T_z^o = H_z^0 \frac{\delta x}{\delta z} \frac{\delta s_z}{\delta s_x} \tag{3.2.15}$$

Taking into account

$$\delta s_x = \sqrt{\delta x^2 + \delta y^2} \rightarrow \delta s_x = \delta x \sqrt{1 + \left(\frac{\delta y}{\delta x}\right)^2}$$

$$\delta s_z = \sqrt{\delta y^2 + \delta z^2} \rightarrow \delta s_z = \delta z \sqrt{1 + \left(\frac{\delta y}{\delta z}\right)^2}$$

$$\delta s_x = \delta x \sqrt{1 + \left(\frac{\delta y}{\delta x}\right)^2}$$

$$\delta s_z = \delta z \sqrt{1 + \left(\frac{\delta y}{\delta z}\right)^2} \tag{3.2.16}$$

and substituting Eq. (3.2.16) in Eq. (3.2.15)

$$T_1^o = H_x^o \frac{\delta z}{\delta x} \frac{\delta x}{\delta z} \frac{\sqrt{1 + \left(\frac{\delta y}{\delta x}\right)^2}}{\sqrt{1 + \left(\frac{\delta y}{\delta z}\right)^2}} = H_x^o \sqrt{\frac{1 + \left(\frac{\partial y}{\partial x}\right)^2}{1 + \left(\frac{\partial y}{\partial z}\right)^2}}$$

$$T_2^o = H_z^o \frac{\delta x}{\delta z} \frac{\delta z}{\delta x} \frac{\sqrt{1 + \left(\frac{\delta y}{\delta z}\right)^2}}{\sqrt{1 + \left(\frac{\delta y}{\delta x}\right)^2}} = H_x^o \sqrt{\frac{1 + \left(\frac{\partial y}{\partial z}\right)^2}{1 + \left(\frac{\partial y}{\partial x}\right)^2}}$$

the forces can be expressed

$$T_x^o = H_x^o \sqrt{\frac{1 + \left(\frac{\partial y}{\partial x}\right)^2}{1 + \left(\frac{\partial y}{\partial z}\right)^2}}$$

$$T_z^o = H_x^o \sqrt{\frac{1 + \left(\frac{\partial y}{\partial z}\right)^2}{1 + \left(\frac{\partial y}{\partial x}\right)^2}} \tag{3.2.17}$$

Considering the infinitesimal surface equilibrium equation one gets[10]

$$H_x^o \frac{\partial^2 y}{\partial x^2} + H_z^o \frac{\partial^2 y}{\partial z^2} = 0 \qquad\qquad (3.2.18)$$

Therefore, the problem of identifying the pretension geometry reduces to the integration of Eq. (3.3.18), after imposing the boundary conditions. If they are homogeneous, the solution is of the type y (x, z) = 0, highlighting the feature that, for the tensile cable net, without loads, where the ends are at the same height, then the equilibrium configuration is certainly plane.

Another pretension geometric feature of nets can be deduced by Eq. (3.2.18), whence

$$\frac{\dfrac{\partial^2 y}{\partial x^2}}{\dfrac{\partial^2 y}{\partial z^2}} = -\frac{H_z^o}{H_x^o} \qquad\qquad (3.2.19)$$

Assuming H_x^o and H_z^o positive if in tension, the second derivatives, that are the curvatures presents opposite signs. This property clarifies the saddle configuration shown in Fig. 3.14 assumed by these structures.

---

[10] Due to equilibrium to translation along y is

$$\frac{\partial}{\partial s}\left(T \frac{\delta y}{\delta s} \right) ds$$

expressing in function of the horizontal components of the thrust H_x^o and H_z^o

$$d\left(H_x^o \frac{\delta s_x}{\delta x} \frac{\delta y}{\delta s_x} \right) + d\left(H_z^o \frac{\delta s_z}{\delta z} \frac{\delta y}{\delta s_z} \right)$$

$$\rightarrow H_x^o \partial\left(\frac{\partial y}{\partial x} \right) + H_z^o \partial\left(\frac{\partial y}{\partial z} \right)$$

$$\rightarrow H_x^o \left(\frac{\partial^2 y}{\partial x^2} \right) + H_z^o \left(\frac{\partial^2 y}{\partial z^2} \right)$$
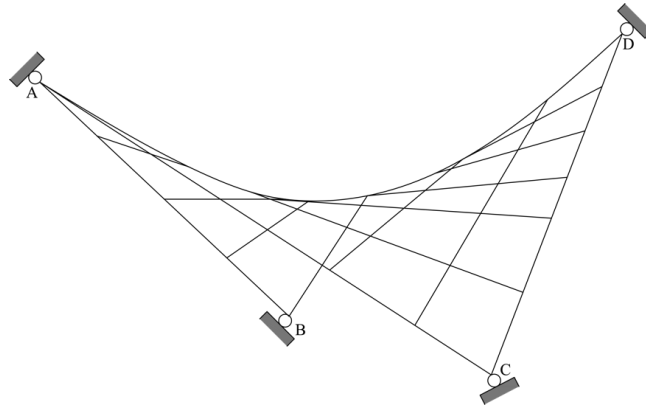
Figure 3.14: Saddle configuration scheme of a cable-net.

3.2.3   The overloads' effect

One considers the equivalent membrane and assumes the action of the external loads P_x, P_y, P_z applied per unit surface as shown in Fig. 3.15. Moreover, with reference to Fig. 3.15, $\delta u', \delta w', \delta u'', \delta w''$ denote the horizontal differential displacements compared to the node A, and $\delta v'$ the vertical one.
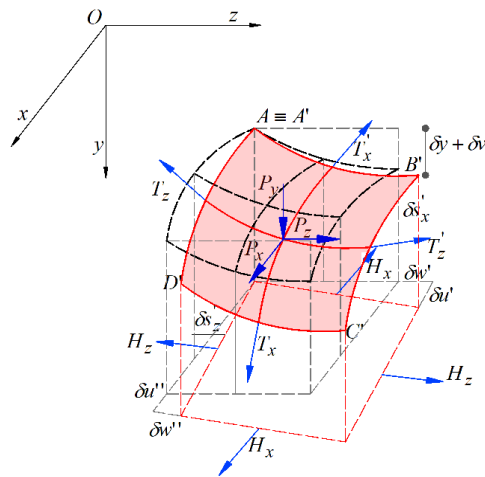
Figure 3.15: Cable nets tensile structures- external loads application. Deformed (in red) and undeformed (in black) configurations. $\delta u', \delta w', \delta u'', \delta w''$ denote the displacements along x and z respectively, $\delta v'$ the displacement along y compared to the height of point A.

Due to the action of the load the configuration changes, starting from the compatible and equilibrated one reached in the pretension phase. The surface element $\delta s_x \delta s_z$, with plant projection $\delta x \delta z$, turns into the surface element $\delta s'_x \delta s'_z$, whose projections in plant are no longer parallel to the coordinate axes (Fig. 3.15).

Consequently, the forces T_x^o and T_x^o assume the values T_x and T_z in order to balance the load and assume the new shape.

Specifying that *u, v, w* denote the displacement components along the three reference axes, considered positive forwards positive axes

$$T_x(H_x)$$

$$T_x(H_x) = H_x \frac{\delta z}{(\delta x + \delta u)} \frac{\delta s'_x}{\delta s'_z}$$

$$T_x(H_x) = H_x \frac{\delta z}{\delta x \left(1 + \dfrac{\delta u}{dx}\right)} \frac{\delta s'_x}{\delta s'_z}$$

$$T_x(H_x) = H_x \frac{\delta z}{\delta x \left(1 + \dfrac{\partial u}{\partial x}\right)} \frac{\delta s'_x}{\delta s'_z}$$

$$T_x(H_x) = H_x \frac{\delta z}{\delta x} \frac{\delta s'_x}{\delta s'_z \left(1 + \dfrac{\partial u}{\partial x}\right)}$$

$$T_z(H_z)$$

$$T_z(H_z) = H_z \frac{\delta x}{(\delta z + \delta w)} \frac{\delta s'_z}{\delta s'_x}$$

$$T_z(H_z) = H_z \frac{\delta x}{\delta z \left(1 + \dfrac{\delta w}{dz}\right)} \frac{\delta s'_z}{\delta s'_x} =$$

$$T_z(H_z) = H_z \frac{\delta x}{\delta z \left(1 + \dfrac{\partial w}{\partial z}\right)} \frac{\delta s'_z}{\delta s'_x}$$

$$T_z(H_z) = H_z \frac{\delta x}{\delta z} \frac{\delta s'_z}{\delta s'_x \left(1 + \dfrac{\partial w}{\partial z}\right)}$$

the forces are given by

$$T_x = H_x \frac{\delta z}{\delta x} \frac{\delta s'_x}{\delta s'_z \left(1 + \frac{\partial u}{\partial x}\right)}$$

$$T_z = H_z \frac{\delta x}{\delta z} \frac{\delta s'_z}{\delta s'_x \left(1 + \frac{\partial w}{\partial z}\right)}$$

(3.2.20)

where

H_x is the pull horizontal component, in the x direction, due to the loads' application

$$H_x \delta z = T_x \delta x \frac{\delta s'_z}{\delta s'_x} \left(1 + \frac{\partial u}{\partial x}\right)$$

(3.2.21)

H_z is the pull horizontal component, in the z direction, due to the loads'application

$$H_z \delta x = T_z dz \frac{\delta s'_x}{\delta s'_z} \left(1 + \frac{\partial w}{\partial z}\right)$$

(3.2.22)

Moreover, one gets

$$\delta s'_x = \sqrt{(\delta x + \delta u)^2 + (\delta y + \delta v)^2 + (\delta w)^2}$$

$$\delta s'_x = dx \sqrt{\left(1 + \frac{\partial u}{\partial x}\right)^2 + \left(\frac{\partial w}{\partial x}\right)^2 + \left(\frac{\partial y}{\partial x} + \frac{\partial v}{\partial x}\right)^2}$$

$$\delta s'_z = \sqrt{(\delta u)^2 + (\delta y + \delta v)^2 + (\delta z + \delta w)^2}$$

$$ds'_z = dz \sqrt{\left(\frac{\partial u}{\partial z}\right)^2 + \left(\frac{\partial y}{\partial z} + \frac{\partial v}{\partial z}\right)^2 + \left(1 + \frac{\partial w}{\partial z}\right)^2}$$

$$ds'_x = dx \sqrt{\left(1 + \frac{\partial u}{\partial x}\right)^2 + \left(\frac{\partial w}{\partial x}\right)^2 + \left(\frac{\partial y}{\partial x} + \frac{\partial v}{\partial x}\right)^2}$$

$$ds'_z = dz \sqrt{\left(1 + \frac{\partial w}{\partial z}\right)^2 + \left(\frac{\partial u}{\partial z}\right)^2 + \left(\frac{\partial y}{\partial z} + \frac{\partial v}{\partial z}\right)^2}$$

(3.2.23)

Here the directions of the forces are not parallel to the x and z axes, because of deformation. The equilibrium equations for the new surface element, and therefore the elastic-kinematic equations are set in order to identify the unknown variables of the problem.

Supposing negligible the first derivates compared to the unit, the equilibrium equations following the analytical developments

$$\frac{\partial H_x}{\partial x}\left(1 - \frac{\partial w}{\partial x}\frac{\partial u}{\partial z}\right) - H_x \frac{\partial^2 w}{\partial x^2}\frac{\partial u}{\partial z} + H_z \frac{\partial^2 u}{\partial z^2} - P_z \frac{\partial u}{\partial z} + P_x = 0$$

$$\frac{\partial H_x}{\partial x} - \frac{\partial H_x}{\partial x}\frac{\partial w}{\partial x}\frac{\partial u}{\partial z} - H_x \frac{\partial^2 w}{\partial x^2}\frac{\partial u}{\partial z} + H_z \frac{\partial^2 u}{\partial z^2} - P_z \frac{\partial u}{\partial z} + P_x = 0$$

but

$$\frac{\partial H_x}{\partial x}\frac{\partial w}{\partial x}\frac{\partial u}{\partial z} << 1$$

$$H_x \frac{\partial^2 w}{\partial x^2}\frac{\partial u}{\partial z} << 1$$

$$P_z \frac{\partial u}{\partial z} << 1$$

$$\frac{\partial H_x}{\partial x} + H_z \frac{\partial^2 u}{\partial z^2} + P_x = 0 \tag{3.2.24}$$

$$\frac{\partial H_z}{\partial z}\left(1 - \frac{\partial u}{\partial z}\frac{\partial w}{\partial x}\right) - H_z \frac{\partial w}{\partial x}\frac{\partial^2 u}{\partial z^2} + H_x \frac{\partial^2 w}{\partial z^2} - P_x \frac{\partial w}{\partial x} + P_z = 0$$

$$\frac{\partial H_z}{\partial z} - \frac{\partial H_z}{\partial z}\frac{\partial u}{\partial z}\frac{\partial w}{\partial x} - H_z \frac{\partial w}{\partial x}\frac{\partial^2 u}{\partial z^2} + H_x \frac{\partial^2 w}{\partial z^2} - P_x \frac{\partial w}{\partial x} + P_z = 0$$

but

$$\frac{\partial H_z}{\partial z}\frac{\partial u}{\partial z}\frac{\partial w}{\partial x} << 1$$

$$H_z \frac{\partial w}{\partial x}\frac{\partial^2 u}{\partial z^2} << 1$$

$$P_x \frac{\partial w}{\partial x} << 1$$

assume the form

$$\frac{\partial H_z}{\partial z} + H_x \frac{\partial^2 w}{\partial z^2} + P_z = 0 \tag{3.2.25}$$

$$\frac{\partial H_x}{\partial x}\left(\frac{\partial y}{\partial x} + \frac{\partial v}{\partial x}\right) + \frac{\partial H_z}{\partial z}\left(\frac{\partial y}{\partial z} + \frac{\partial v}{\partial z}\right) + H_x \frac{\partial^2 (y+v)}{\partial x^2} + H_z \frac{\partial^2 (y+v)}{\partial z^2} + P_y = 0 \tag{3.2.26}$$

One highlights that the terms in Eq. (3.2.24) $\frac{\partial \Delta H_x}{\partial x}$ e $H_z\left(\frac{\partial^2 u}{\partial z^2}\right)$ are the aliquot of the

load P_x absorbed respectively by the cables belonging to the planes parallel to the x and

z axes.

Assuming

$$P_x^* = H_z \frac{\partial^2 u}{\partial z^2} \tag{3.2.27}$$

as the aliquot of the load P_x absorbed by the cables in the z direction due to H_z, and similarly

$$P_z^* = H_x \frac{\partial^2 w}{\partial x^2} \tag{3.3.28}$$

the aliquot of the load P_z absorbed by the cables in the x direction due to H_x, Eq.(3.2.24-3.2.25) turn into

$$\frac{\partial H_x}{\partial x} + P_x + P_x^* = 0 \tag{3.2.29}$$

$$\frac{\partial H_z}{\partial x} + P_z + P_z^* = 0 \tag{3.2.30}$$

whence

$$\frac{\partial H_x}{\partial x} = -\left(P_x + P_x^*\right) \tag{3.2.31}$$

$$\frac{\partial H_z}{\partial z} = -\left(P_z + P_z^*\right) \tag{3.2.32}$$

Consequently, Eq. (3.2.26)

$$\frac{\partial H_x}{\partial x}\left(\frac{\partial y}{\partial x}+\frac{\partial v}{\partial x}\right)+\frac{\partial H_z}{\partial z}\left(\frac{\partial y}{\partial z}+\frac{\partial v}{\partial z}\right)+H_x\frac{\partial^2(y+v)}{\partial x^2}+H_z\frac{\partial^2(y+v)}{\partial z^2}+P_y=0$$

$$\frac{\partial H_x}{\partial x}\frac{\partial y}{\partial x}+\frac{\partial H_x}{\partial x}\frac{\partial v}{\partial x}+\frac{\partial H_z}{\partial z}\frac{\partial y}{\partial z}+\frac{\partial H_z}{\partial z}\frac{\partial v}{\partial z}+H_x\left(\frac{\partial^2 y}{\partial x^2}+\frac{\partial^2 v}{\partial x^2}\right)+H_z\left(\frac{\partial^2 y}{\partial z^2}+\frac{\partial^2 v}{\partial z^2}\right)+P_y=0$$

but

$$\frac{\partial H_x}{\partial x}\frac{\partial v}{\partial x}<<1$$

$$\frac{\partial H_z}{\partial z}\frac{\partial v}{\partial z}<<1$$

$$\frac{\partial H_x}{\partial x}\frac{\partial y}{\partial x}+\frac{\partial H_z}{\partial z}\frac{\partial y}{\partial z}+H_x\left(\frac{\partial^2 y}{\partial x^2}+\frac{\partial^2 v}{\partial x^2}\right)+H_z\left(\frac{\partial^2 y}{\partial z^2}+\frac{\partial^2 v}{\partial z^2}\right)+P_y=0$$

From Eq.(2.5.30) - (2.5.31=

$$-(P_x^*+P_x)\frac{\partial y}{\partial x}+-(P_z^*+P_z)\frac{\partial y}{\partial z}+H_x\left(\frac{\partial^2 y}{\partial x^2}+\frac{\partial^2 v}{\partial x^2}\right)+H_z\left(\frac{\partial^2 y}{\partial z^2}+\frac{\partial^2 v}{\partial z^2}\right)+P_y=0$$

$$-(P_x^*+P_x)\frac{\partial y}{\partial x}-(P_z^*+P_z)\frac{\partial y}{\partial z}+\left(H_x^o+\Delta H_x\right)\left(\frac{\partial^2 y}{\partial x^2}+\frac{\partial^2 v}{\partial x^2}\right)+\left(H_z^o+\Delta H_z\right)\left(\frac{\partial^2 y}{\partial z^2}+\frac{\partial^2 v}{\partial z^2}\right)+P_y=0$$

$$H_x^o\frac{\partial^2 y}{\partial x^2}+H_z^o\frac{\partial^2 y}{\partial z^2}+H_x^o\frac{\partial^2 v}{\partial x^2}+H_z^o\frac{\partial^2 v}{\partial z^2}+\Delta H_x\frac{\partial^2 y}{\partial x^2}+\Delta H_x\frac{\partial^2 v}{\partial x^2}+\Delta H_z\frac{\partial^2 y}{\partial z^2}+\Delta H_z\frac{\partial^2 v}{\partial z^2}-(P_x^*+P_x)\frac{\partial y}{\partial x}-(P_z^*+P_z)\frac{\partial y}{\partial z}+P_y=0$$

From Eq. (2.5.17)

$$H_x^o\frac{\partial^2 y}{\partial x^2}+H_z^o\frac{\partial^2 y}{\partial z^2}=0$$

$$H_x^o\frac{\partial^2 v}{\partial x^2}+H_z^o\frac{\partial^2 v}{\partial z^2}+\Delta H_x\frac{\partial^2 y}{\partial x^2}+\Delta H_x\frac{\partial^2 v}{\partial x^2}+\Delta H_z\frac{\partial^2 y}{\partial z^2}+\Delta H_z\frac{\partial^2 v}{\partial z^2}-(P_x^*+P_x)\frac{\partial y}{\partial x}-(P_z^*+P_z)\frac{\partial y}{\partial z}+P_y=0$$

Denoting by

$$P_y^*=\Delta H_x\frac{\partial^2 v}{\partial x^2}+\Delta H_z\frac{\partial^2 v}{\partial z^2} \tag{3.2.33}$$

One gets the following formulation

$$H_x^0\frac{\partial^2 v}{\partial x^2}+H_z^0\frac{\partial^2 v}{\partial z^2}+\Delta H\frac{\partial^2 y}{\partial x^2}-\left(P_x+P_x^*\right)\frac{\partial y}{\partial x}-\left(P_z+P_z^*\right)\frac{\partial y}{\partial z}+P_y+P_y^*=0 \tag{3.2.34}$$

with

$$\Delta H_x=\frac{EA_x}{k_x^{3/2}}\left(\frac{\partial u}{\partial x}+\frac{\partial y}{\partial x}\frac{\partial v}{\partial x}-\alpha\Delta t k_x\right)$$

$$\Delta H_z=\frac{EA_z}{k_z^{3/2}}\left(\frac{\partial w}{\partial z}+\frac{\partial y}{\partial z}\frac{\partial v}{\partial z}-\alpha\Delta t k_z\right) \tag{3.2.35}$$

$$\Delta H_x=H_x-H_x^0$$

$$\Delta H_z=H_z-H_z^0 \tag{3.2.36}$$

where

A_x and A_z are the cross-section areas per unit length obtained by the vertical plane with equation $z = const$ and $x = const$.

$$k_x = 1 + \left(\frac{\partial y}{\partial x}\right)^2$$
$$k_z = 1 + \left(\frac{\partial y}{\partial z}\right)^2$$

(3.2.37)

Δt and α are the thermal variation and coefficient, referred to the environment and material of the cable.

The formulated problem shows some calculus difficulties; thus, a number of simplified hypotheses are introduced in the first stage, neglecting some terms that are then reintroduced in the second phase.

By definition, P_x^* and P_z^* are

$$P_x^* = H_z \frac{\partial^2 u}{\partial z^2} \ll P_x$$

(3.2.38)

$$P_z^* = H_x \frac{\partial^2 w}{\partial x^2} \ll P_z$$

(3.2.39)

This is because the load aliquot $P_x (P_x^*)$ absorbed by the cables arranged in the planes parallel to the z axis is less than the one absorbed by the cables in the x direction. Then Eq. (3.2.38) holds. Similarly, the load aliquot $P_z (P_z^*)$ absorbed by the cables arranged in the planes parallel to x is assumed less than the one absorbed by the cables arranged in planes parallel to z; hence, Eq.(3.2.39) holds.

Then one can approximate $P_x^* = P_z^* = 0$.

Moreover, as previously specified for the system of cables with opposite curvature

$$\Delta H_x \ll H_x^0$$
$$\Delta H_z \ll H_z^0$$

(3.2.40)

and being from Eq. (3.2.33)

$$P_y^* = \Delta H_x \frac{\partial^2 v}{\partial x^2} + \Delta H_z \frac{\partial^2 v}{\partial z^2}$$

(3.2.41)

The contribution of P_y^* can be neglected in Eq. (3.2.34)

$$P_y^* \ll P_y$$

(3.2.42)

and, then, in the first approximation

$$P_x^* = P_y^* = P_z^* = 0$$

(3.2.43)

Hence the equilibrium equations turn into[11]

11

$$\frac{\partial H_x}{\partial x} + P_x + P_x^* = 0$$

$$\frac{\partial H_x}{\partial x} + P_x = 0$$

but

$$H_x = H_x^o + \Delta H_x$$

hence

$$\frac{\partial}{\partial x}\left(H_x^o + \Delta H_x\right) + P_x = 0$$

$$\frac{\partial H_x^o}{\partial x} + \frac{\partial \Delta H_x}{\partial x} + P_x = 0$$

however

$$\frac{\partial H_x^o}{\partial x} = 0$$

(cont.)

$$\frac{\partial \Delta H_x}{dx} + P_x = 0$$

$$\frac{\partial \Delta H_z}{dz} + P_z = 0 \qquad (3.2.44)$$

$$H_x^o \frac{\partial^2 v}{\partial x^2} + H_z^0 \frac{\partial^2 v}{\partial z^2} + \Delta H_x \frac{\partial^2 y}{\partial x^2} + \Delta H_z \frac{\partial^2 y}{\partial x^2} - \left(P_x\right)\frac{\partial y}{\partial x} - \left(P_z\right)\frac{\partial y}{\partial z} + P_y = 0$$

By integration of the first two Eq. (3.3.44) and carrying on with the relevant developments, one gets

$$\Delta H_x = f(z) - \int_{x'}^{x} P_x dx = 0$$

$$\qquad (3.2.45)$$

$$\Delta H_z = g(x) - \int_{z'}^{z} P_z dz = 0$$

Where $f(z)$ and $g(x)$ are two arbitrary functions to be identified through the boundary conditions, and x' and z' are the coordinates of the boundary points of the structure.

---

hence the equilibrium equation to the translation along x axis is

$$\frac{\partial \Delta H_x}{\partial x} + P_x = 0$$

$$\frac{\partial H_z}{\partial x} + P_z = 0$$

but

$$H_z = H_z^o + \Delta H_z$$

hence

$$\frac{\partial}{\partial z}\left(H_z^o + \Delta H_z\right) + P_z = 0$$

$$\frac{\partial H_z^o}{\partial z} + \frac{\partial \Delta H_z}{\partial z} + P_z = 0$$

however

$$\frac{\partial H_z^o}{\partial z} = 0$$

hence the equilibrium equation to the translation along the z axis is

$$\frac{\partial \Delta H_z}{\partial z} + P_z = 0$$

Actually, $f(z)$ and $g(x)$ are the values assumed by ΔH_x and ΔH_z at the boundary points with coordinates x' and z'.
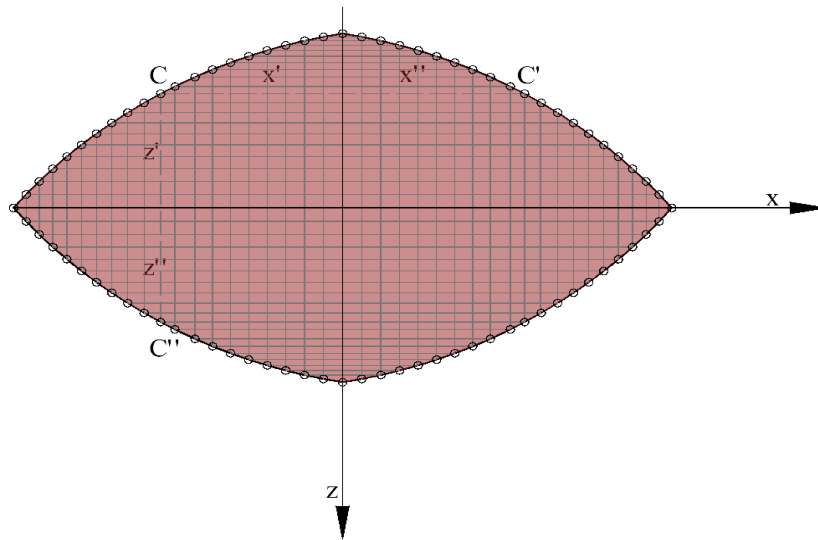
Figure 3.16: Projection in plant of the boundary of cable-net.

With reference to Fig. 3.16, it is possible to assume the above-mentioned coordinates in the following form

$$x' = x'(z)$$
$$z' = z'(x)$$

and in analogy

$$x'' = x''(z)$$
$$z'' = z''(x)$$

Taking into account Eq. (3.2.35)

$$\Delta H_x = \frac{EA_x}{k_x^{3/2}}\left(\frac{\partial u}{\partial x} + \frac{\partial y}{\partial x}\frac{\partial v}{\partial x} - \alpha\Delta t k_x\right)$$

$$\Delta H_z = \frac{EA_z}{k_z^{3/2}}\left(\frac{\partial w}{\partial z} + \frac{\partial y}{\partial z}\frac{\partial v}{\partial z} - \alpha\Delta t k_z\right)$$

(3.2.35)

one gets

$$\Delta H_x = \frac{EA_x}{k_x^{3/2}}\left(\frac{\partial u}{\partial x} + \frac{\partial y}{\partial x}\frac{\partial y}{\partial x} - \alpha\Delta t k_x\right) = f(z) - \int_{x'}^{x} P_x dx$$

$$\Delta H_z = \frac{EA_z}{k_z^{3/2}}\left(\frac{\partial u}{\partial z} + \frac{\partial y}{\partial z}\frac{\partial y}{\partial z} - \alpha\Delta t k_z\right) = g(x) - \int_{x'}^{x} P_z dz$$

(3.2.46)

that may be solved with reference to $\dfrac{\partial u}{\partial x}$ and $\dfrac{\partial w}{\partial z}$

$$\frac{\partial u}{\partial x} = \frac{k_x^{3/2}}{EA_x}\left[f(z) - \int_{x'}^{x} P_x dx\right] - \frac{\partial y}{\partial x}\frac{\partial v}{\partial x} + \alpha\Delta t k_x$$

$$\frac{\partial w}{\partial z} = \frac{k_z^{3/2}}{EA_z}\left[g(x) - \int_{z'}^{z} P_z dz\right] - \frac{\partial y}{\partial z}\frac{\partial v}{\partial z} + \alpha\Delta t k_z$$

(3.2.47)

Let assume now that u_c, v_c, w_c are the displacements of the constrained points due to the actions undergone by the structure caused by the action of the cable nets on it (that are assumed equal to zero).

The functions *u, v, w* to be identified, should comply with the following boundary conditions

$$u[x, y(x), z(x)] = u_C[x, y(x), z(x)]$$
$$v[x, y(x), z(x)] = v_C[x, y(x), z(x)]$$
$$w[x, y(x), z(x)] = w_C[x, y(x), z(x)]$$

(3.2.48)

The equalities concerning the horizontal displacements can be easily verified, imposing

$$u_{C''} - u_C = \Delta u(z) = \int_{x''}^{x'} \frac{\partial u}{\partial x} dx$$

$$w_{C''} - w_C = \Delta w(x) = \int_{z''}^{z'} \frac{\partial w}{\partial z} dz$$

(3.2.49)

where

$u_{C''}$ is the horizzontal displacement of the point C'' in the x direction

$w_{C''}$ is the horizontal displacement of the point C'' in the z direction

$\Delta u(z)$ is the relative displacement of the connecting points at the end of the cable along x

$\Delta w(x)$ is the relative displacement of the connecting points at the ends of the cables along z

Eq. (3.3.49) impose that the relative displacement of the fixed points along x and z of the boundary cables are equal to the displacements in the same directions of the ends of the same cables, with the possibility of rigid horizontal displacements.

To solve the problem for identifying the functions $u,\ v,\ w$, one assumes that the boundary is stiff, and therefore $u_C = v_C = w_C = 0$, and one gets

$$\int_{x''}^{x'}\frac{du}{dx}dx = 0$$
$$\int_{z''}^{z'}\frac{dw}{dz}dz = 0$$

$$(3.2.50)$$

Substituting $\dfrac{\partial u}{\partial x}$ and $\dfrac{\partial w}{\partial z}$ (Eq. 3.2.47) in Eq. (3.2.42)

$$\int_{x''}^{x'}\frac{k_x^{3/2}}{EA_x}\left[f(z)-\int_{x'}^{x}P_x dx\right]-\frac{\partial y}{\partial x}\frac{\partial v}{\partial x}+\alpha\Delta tk dx = 0$$
$$\int_{z''}^{z'}\frac{k_z^{3/2}}{EA_z}\left[g(x)-\int_{z'}^{z}P_z dz\right]-\frac{\partial y}{\partial z}\frac{\partial v}{\partial z}+\alpha\Delta tk dz = 0$$

$$(3.2.51)$$

one may identify the unknown functions $f(z)$ and $g(x)$, $\Delta H_x(z),\Delta H_z(x)$ after some developments. Starting from

$$\int_{x'}^{x''}\frac{k_x^{3/2}}{EA_x}\left[f(z)-\int_{x'}^{x}P_x dx\right]dx-\int_{x'}^{x''}\frac{\partial y}{\partial x}\frac{\partial v}{\partial x}dx+\int_{x'}^{x''}\alpha\Delta tk dx = 0$$

$$\frac{f(z)}{EA_x}\int_{x'}^{x''}k_x^{3/2}-\int_{x'}^{x''}\left[\frac{k_x^{3/2}}{EA_x}\int_{x'}^{x}P_x dx\right]dx+\int_{x'}^{x''}\alpha\Delta tk dx-\int_{x'}^{x''}\frac{\partial y}{\partial x}\frac{\partial v}{\partial x}dx = 0$$

one assumes

$$M(z) = \int\limits_{x'}^{x''} \left[\frac{k_x^{3/2}}{EA_x} \int\limits_{x'}^{x} P_x dx \right] dx - \int\limits_{x'}^{x''} \alpha \Delta t k dx$$

for the hypothesis of stiff boundary, the displacements are null, then

$$\int\limits_{x'}^{x''} \frac{\partial y}{\partial x} \frac{\partial v}{\partial x} dx = \left| \frac{\partial y}{\partial x} v \right|_{x'}^{x''} - \int\limits_{x'}^{x''} \frac{\partial v}{\partial x} v dx = -\int\limits_{x'}^{x''} \frac{\partial v}{\partial x} v dx$$

$$\frac{f(z)}{EA_x} \int\limits_{x'}^{x''} k_x^{3/2} dx - M(x) + \int\limits_{x'}^{x''} \frac{\partial v}{\partial x} v dx$$

and it is possible to get

$$f(z) = \left[M(z) - \int\limits_{x'}^{x''} \frac{\partial v}{\partial x} v dx \right] \frac{EA_x}{\int\limits_{x'}^{x''} k^{3/2}}$$

Analogously

$$\int\limits_{z'}^{z''} \frac{k_z^{3/2}}{EA_z} \left[g(x) - \int\limits_{z'}^{z} P_z dz \right] - \frac{\partial y}{\partial z} \frac{\partial v}{\partial z} + \alpha \Delta t k dz = 0$$

$$\frac{g(x)}{EA_z} \int\limits_{z'}^{z''} k_z^{3/2} dz - \int\limits_{z'}^{z''} \left[\frac{k_x^{3/2}}{EA_z} \int\limits_{z'}^{z} P_z dz \right] dx + \int\limits_{z'}^{z''} \alpha \Delta t k_z dz - \int\limits_{z'}^{z''} \frac{\partial y}{\partial z} \frac{\partial v}{\partial z} dz = 0$$

one assumes

$$N(x) = \int\limits_{z'}^{z''} \left[\frac{k_z^{3/2}}{EA_z} \int\limits_{z'}^{z} P_z dz \right] dz - \int\limits_{z'}^{z''} \alpha \Delta t k dz$$

and, for the hypothesis of stiff boundary, the displacements are null, then

$$\int\limits_{z'}^{z''} \frac{\partial y}{\partial z} \frac{\partial v}{\partial z} dx = \left| \frac{\partial y}{\partial z} v \right|_{z'}^{z''} - \int\limits_{z'}^{z''} \frac{\partial v}{\partial z} v dz = -\int\limits_{z'}^{z''} \frac{\partial v}{\partial z} v dz$$

$$\frac{g(z)}{EA_z} \int\limits_{z'}^{z''} k_z^{3/2} dz - N(x) + \int\limits_{z'}^{z''} \frac{\partial v}{\partial z} v dz$$

getting

$$g(z) = \left[N(x) - \int_{z'}^{z''} \frac{\partial v}{\partial z} v dz \right] \frac{EA_z}{\int_{z'}^{z''} k_z^{3/2}}$$

Assuming

$$F(z) = \frac{EA_x}{\int_{x'}^{x''} k^{3/2}}$$

$$G(x) = \frac{EA_z}{\int_{z'}^{z''} k_z^{3/2}}$$

One finally infers

$$\Delta H_x = F(z) \left[M(z) - \int_{x'}^{x''} \frac{\partial^2 y}{\partial x^2} v dx \right] - \int_{x'}^{x''} P_x dx$$

$$\Delta H_z = G(x) \left[N(x) - \int_{z'}^{z''} \frac{\partial^2 y}{\partial z^2} v dz \right] - \int_{z'}^{z''} P_z dz$$

(3.2.52)

Substituting Eq. (3.2.52) in the third equation of vertical translation equilibrium of Eq. (3.2.44) , one gets[12]

$$H_x^0 \frac{\partial^2 v}{\partial x^2} + H_z^0 \frac{\partial^2 v}{\partial z^2} - F(z) \frac{\partial^2 y}{\partial x^2} \int_{x'}^{x''} \frac{\partial^2 y}{\partial x^2} v dx - G(x) \frac{\partial^2 y}{\partial z^2} \int_{z'}^{z''} \frac{\partial^2 y}{\partial z^2} v dz + q(x,z) = 0 \qquad (3.2.53)$$

By integrating Eq. 3.2.52, the unknown displacement v is identified, which after substituted in Eq. (3.2.53), allows to identify $\Delta H_x, \Delta H_z$.

---

[12]
$$H_x^0 \frac{\partial^2 v}{\partial x^2} + H_z^0 \frac{\partial^2 v}{\partial z^2} + \left[F(z) \left[M(z) - \int_{x'}^{x''} \frac{\partial^2 y}{\partial x^2} v dx \right] - \int_{x'}^{x''} P_x dx \right] \frac{\partial^2 y}{\partial x^2} +$$

$$+ \left[G(x) \left[N(x) - \int_{z'}^{z''} \frac{\partial^2 y}{\partial z^2} v dz \right] - \int_{z'}^{z''} P_z dz \right] \frac{\partial^2 y}{\partial z^2} - (P_x) \frac{\partial y}{\partial x} - (P_z) \frac{\partial y}{\partial z} + P_y = 0$$

$$H_x^0 \frac{\partial^2 v}{\partial x^2} + H_z^0 \frac{\partial^2 v}{\partial z^2} - F(z) \frac{\partial^2 y}{\partial x^2} \int_{x'}^{x''} \frac{\partial^2 y}{\partial x^2} v dx - G(x) \frac{\partial^2 y}{\partial z^2} \int_{z'}^{z''} \frac{\partial^2 y}{\partial z^2} v dz + q(x,z) = 0$$

with

$$q(x,z) = F(z) \left(M(z) - \int_{x'}^{x''} P_x dx \right) \frac{\delta^2 y}{\delta x^2} + G(x) \left(N(x) - \int_{z'}^{z''} P_z dz \right) \frac{\partial^2 y}{\partial z^2} - (P_x) \frac{\partial y}{\partial x} - (P_z) \frac{\partial y}{\partial z} + P_y = 0$$

Then the values of u_c, v_c, w_c can be calculated, remembering that they were initially set equal to 0 in the first approximation.

Integrating Eq. (3.2.47), once known the displacements, one may compute the loads $P_x^* = P_y^* = P_z^*$, neglected till now. Thus Eq. (3.2.48), considering the above-mentioned loads, turn into

$$\frac{\partial u^*}{\partial x} = \frac{k_x^{3/2}}{EA_x}\left[f(z) - \int_{x'}^{x}\left(P_x + P_x^*\right)dx \right] - \frac{\partial y}{\partial x}\frac{\partial v^*}{\partial x} + \alpha\Delta t k_x$$

$$\frac{\partial w^*}{\partial z} = \frac{k_z^{3/2}}{EA_z}\left[g(x) - \int_{z'}^{z}\left(P_z + P_z^*\right)dz \right] - \frac{\partial y}{\partial z}\frac{\partial v^*}{\partial z} + \alpha\Delta t k_z$$

$$(3.2.55)$$

Following the procedure developed in the above one gets

$$f^*(z) = F(z)\left[M^*(z) - \int_{x'}^{x''}\frac{\partial v}{\partial x}v^*dx \right]$$

$$(3.2.56)$$

with

$$M^*(z) = \int_{x'}^{x''}\left[\frac{k_x^{3/2}}{EA_x}\int_{x'}^{x}P_x + P_x^*dx \right]dx + \left(\frac{\partial y}{\partial x}\right)_{x=x'}v_c - \left(\frac{\partial y}{\partial x}\right)_{x=x''}v_c' - \int_{x'}^{x''}\alpha\Delta t k_x dx + \Delta u(z)$$

$$(3.2.57)$$

$$g^*(z) = \left[N^*(x) - \int_{z'}^{z''}\frac{\partial v}{\partial z}vdz \right]\frac{EA_z}{\int_{z'}^{z''}k_z^{3/2}}$$

$$(3.2.58)$$

with

$$N^*(x) = \int_{z'}^{z''}\left[\frac{k_z^{3/2}}{EA_z}\int_{z'}^{z}P_z + P_z^*dz \right]dz + \left(\frac{\partial y}{\partial z}\right)_{z=z'}vc - \left(\frac{\partial y}{\partial z}\right)_{z=z''}vc'' - \int_{z'}^{z''}\alpha\Delta t k_z dz + \Delta w(x)$$

$$(3.2.59)$$

One go on to identify $\Delta H_x^*, \Delta H_z^*$, which, in analogy with what previously developed, are substituted in the vertical translation equilibrium equations, allowing to compute v^* in the second approximation

$$\Delta H_x = F(z)\left[M^*(z) - \int_{x'}^{x''}\frac{\partial^2 y}{\partial x^2}v^*dx \right] - \int_{x'}^{x''}P_x + P_x^*dx$$

$$\Delta H_z = G(x)\left[N^*(x) - \int_{z'}^{z''}\frac{\partial^2 y}{\partial z^2}v^*dz \right] - \int_{z'}^{z''}P_z + P_z^*dz$$

$$(3.2.60)$$

$$H_x^0\frac{d^2v}{dx^2} + H_z^0\frac{d^2v}{dz^2} - F(z)\frac{d^2y}{dx^2}\int_{x'}^{x''}\frac{d^2y}{dx^2}v^*dx - G(x)\frac{d^2y}{dz^2}\int_{z'}^{z''}\frac{d^2y}{dz^2}v^*dz + q(x,z) = 0$$

with

$$q(x,z) = F(z)\left(M^*(z) - \int\limits_{x'}^{x''} P_x + P_x^* dx\right)\frac{\partial^2 y}{\partial x^2} + G(x)\left(N^*(x) - \int\limits_{z'}^{z''} P_z + P_z^* dz\right)\frac{\partial^2 y}{\partial z^2} - $$

$$+ \left(P_x + P_x^*\right)\frac{\partial y}{\partial x} - \left(P_z + P_z^*\right)\frac{\partial y}{\partial z} + P_y + P_y^* = 0 \qquad (3.2.61)$$

One proceeds in this way up to convergence.

3.3 Bidirectional systems

Bidirectional structural schemes belong to the category of nets (Fig. 3.17-24), recognized in structural typologies characterized by two families of cables interconnected to each other, where the interconnection is exclusively between the ones belonging to different families. The scheme can be plane or spatial when the constitutive elements belong to different planes.

The increasing wish to lighten the modern buildings, aiming at the maximum construction transparency, have been proceeding together with the search of adequate supporting structures for wide glass windows, in order to bear both vertical and horizontal actions, like the wind actions (*Bedon, 2014*).

Hence, plane bidirectional schemes are usually adopted as supporting elements for glazed facades, minimizing the use of teel in order to maximize the lightness and transparency of the building.

3.3.1 General features

One of the first buildings with plane bidirectional scheme as support to the façade, was the Hotel Kempinski in Monaco (1989/1990) in Fig. 17, where the main structure consists of a net of two families of cables, with fixed nodes which bear the glass panels.
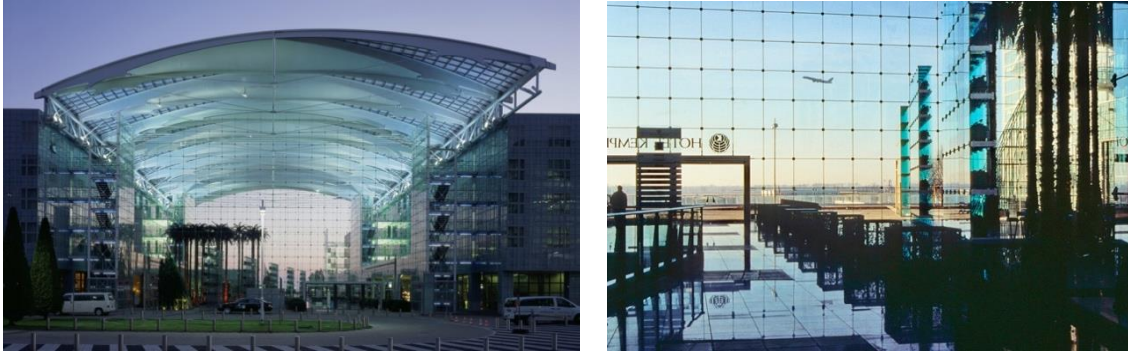
Figure 3.17: Hotel Kempinski Façade, Munich (Germany),(1989-1990).
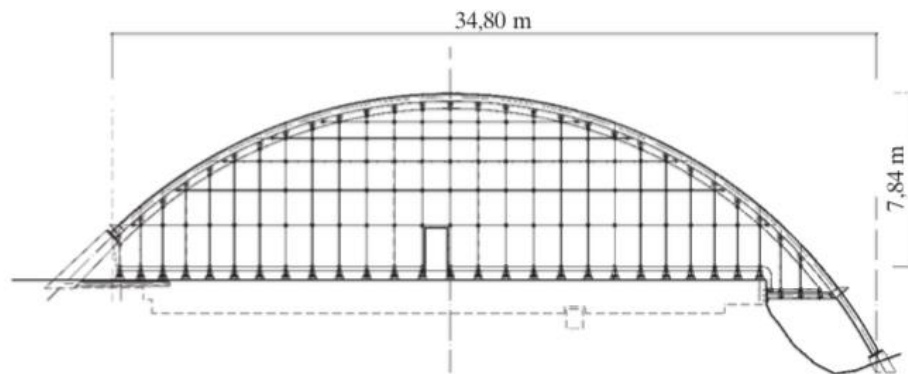
Figure 3.18: Protection system of ancient Roman ruins in Germany (2011): glazed façade supported by a plane bidirectional scheme.

Figure 3.19: Time Warner Center, New York (2003); the glazed facade is supported by a system of cables with springs at the base. They provide also a pretension state in the cables.

One of the advantages of the use of these systems lies in their stiffness and stability, obtained by the pretension applied to the constitutive cables. As above-mentioned, bidirectional schemes can be spatial too, acting as supporting systems or covering buildings with large spans (Figs. 3.21-23), also adopted for temporary installations or design buildings (Fig. 3.24). Thanks to the characterizing lightness, these covering systems give the possibility to avoid the arrangement of supporting elements (i.e. piles) in the inner spaces.

One of the first examples of spatial bidirectional schemes can be identified in the roof realized by Frei Otto, for the Munich Park (Fig. 3.20).

Figure 3.20: Olympic Park, Munich, Germany (1970); Frei Otto.
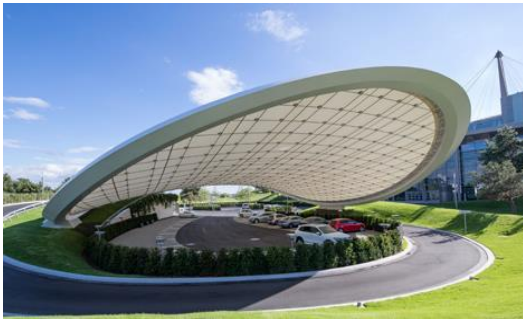
Figure 3.21: Autostadt Roof and Service Pavilion, Wolfsburg, Germany; Graft Architects.
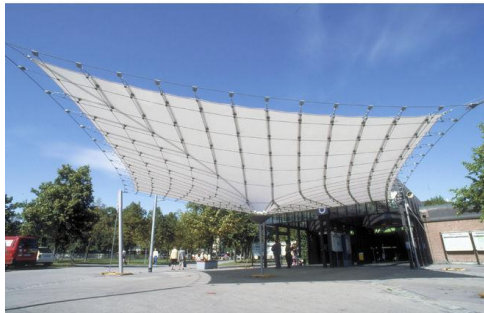
Figure 3.22: Bidirectional covering to support a membrane system.

Figure 3.23: Covering of an open theatre, Palma de Mallorca, Elias Torres, Martinez Lapena.
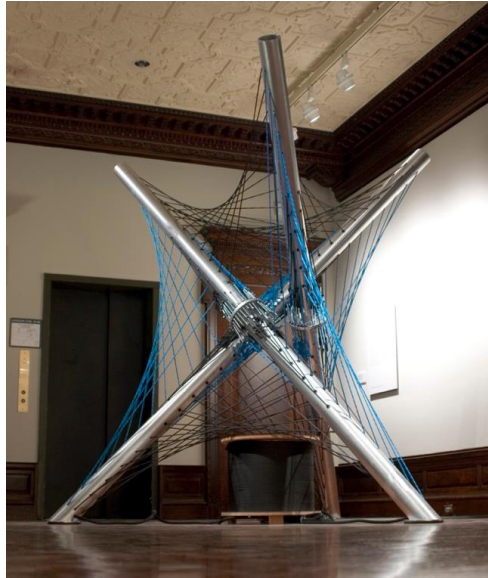
Figure 3.24: Rope and Sound; Squid-Lab.

As it can be highlighted from Figs.3.21-24, cable-nets in general and spatial bidirectional schemes in particular, can assume several configurations. As known, these structures belong to the category of the tensile ones (*M. Patelli, M. Quagliaroli, 2010*) and therefore they work only with axial forces. Thus, the stress state and the geometry are strictly connected to each other.

Hence, other problems concern the initial form-finding or the initial zero state, which requires the searching of the nodes position after the assembly of the structure, considering the cables forces or some related parameters as known.

3.3.2   Equilibrium of bidirectional systems

One of the most used approaches is represented by the FDM (*Force Density Method*), introduced by Scheck in the 1974 and then changed and conformed to the most modern typologies of structures as tensegrity (*Zang e Ohsaky, 2006*).

Thus, in this paragraph, a methodology for searching for the points' coordinates of a spatial bidirectional scheme, is described.
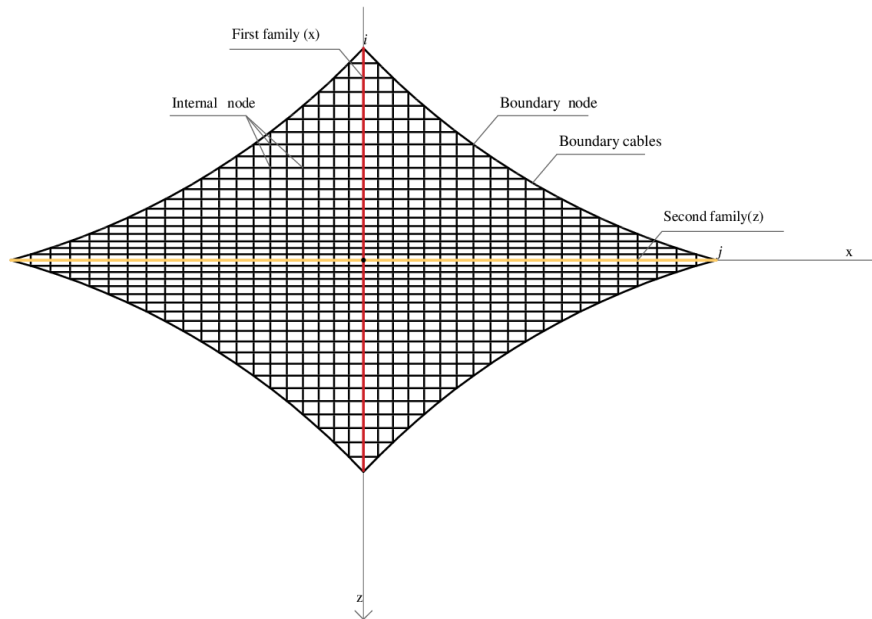
Figure 3.25: Plant of a bidirectional scheme with identification of two cables' families.

The method is based on the *walkthrough technique*[13] for solving equilibrium equations system, for a net composed by *n* cables along one direction and *m* in the other one, allowing to reduce the number of the above -mentioned equations.

On the basis of the methods available in literature about the initial configuration finding, one refers to those ones easier to be handled from a computational point of view, and in particular to the method developed by R.Avent (*R.R. Avent, 1969*), which was then extended to several study cases, such as nets with non stiff boundaries or without rectangular plants for finding the initial configuration, i.e. the nodes' coordinates under some identified conditions and under the pretension.

The method, based on the Avent's approach and on the *walkthrough technique*, solves the problem by reducing the number of equations, based on some simplified hypotheses:

the cables composing the structure are defined as beams but are able to transmit only tensile forces;

the nodes are point-like;

the loads are considered nodal;

---

[13] It consists of a technique, mostly used for algorithms' checks, aimed at validating the accuracy of the analysis models, based on the identification of the error but not on its correction, in order to improve results.

the Hooke law is valid (linear elastic material);
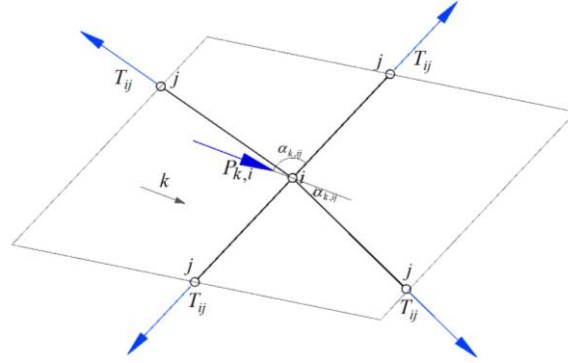
Figure 3.26: Nodal point in a bidirectional scheme.

With reference to Fig. 3.26, denoting by i the interconnection node of the structure, by j the adjacent ones, by $P_{k,i}$ the load acting on it in the k direction and by T_{ij} the force in the ij beam, the following relations hold, respectively for the translation equilibrium and compatibility

$$\sum_{j} T_{ij} \cos \alpha_{k,ij} = P_{k,i} \qquad (3.3.1)$$

where

$\alpha_{k,ij}$ is the inclination angle of the beam ij with respect to the k direction

$P_{k,i}$ is the component along the k direction of the load $\boldsymbol{P}_i$ acting on the node i

Eq. (3.4.1) can be rewritten as follows, introducing the kth coordinates of the nodes i and j and the length assumed by the beam after the pretension

$$\sum_{j} \frac{T_{ij}}{\ell_{ij}} \left(x_{k,j} - x_{k,i} \right) = P_{k,i} \qquad (3.3.2)$$

where

$x_{k,j}$ is the x-coordinate of the node j

$x_{k,i}$ is the x coordinate of the node i

ℓ_{ij} is the length of the beam ij after the pretension

Due to compatibility, instead, and by the constitutive law,

$$\frac{T_{ij}}{EA_{ij}} = \frac{\Delta \ell_{ij}}{\ell_{ij}}$$
(3.3.3)

with

E the Young modulus

A_{ij} the beam cross section area

$\Delta \ell_{ij}$ the length variation of the beam ij

ℓ_{ij} the pretensioned length of the beam

The equation highlights that the forces in the beams produce a length variation $\Delta \ell_{ij}$, because of the elasticity of the composing material.

The solution of the linear equations system may be achieved by partial differences, where the equilibrium equations composing the system and written for any node, have as unknown variables the coordinates of the node and of the adjacent nodes. However, this approach shows some limits, mainly complying with the possibility of application only for cable-nets with rectangular plant and stiffened boundaries, and subject only to vertical loads.

In the following one shows an approach aiming at accounting also for structures with non stiffened boundaries, without rectangular plant and with internal points at known height, but it is suitable only for bidirectional schemes.

Let refer to Fig. 3.25 where the generic interconnection node of a bidirectional scheme and the adjacent nodes are shown. Moreover, the length and the tension forces of the beams are indicated.

According to the Avent's method, the equilibrium equations are written for the interconnected node, where the unknown variables are the coordinates of the node itself and of the adjacent nodes.
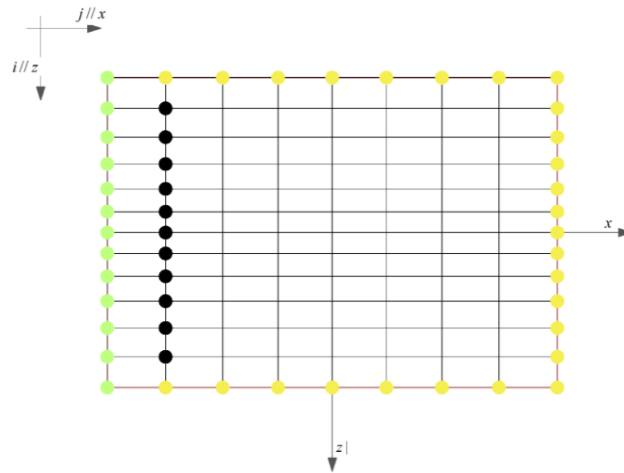
Figure 3.27: Plant details of a bidirectional scheme.
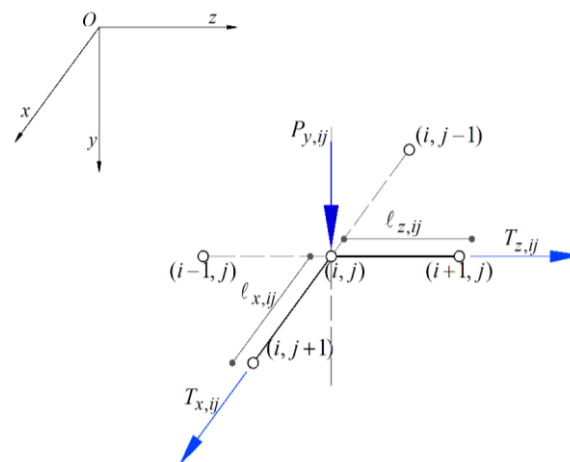
Figure 3.26: Node of a bidirectional scheme, where the two families are parallel to the x and z axis, subject to overload.

Denoting by

(i,j) the crossing point of the ith cable of the first family, with the jth of the second family

$x(i,j), y(i,j), z(i,j)$ the coordinates of the identified point by the ith and j^{th} cables of the two families

$T_{x,ij}$ the force in the beam of the first family

$\ell_{x,ij}$ the length of the cable of the first family

$T_{z,ij}$ the force in the cable of the second family

$\ell_{z,ij}$ the length of the cable in the second family

$D_x = \dfrac{T_{x,ij}}{\ell_{x,ij}}$ the density force in the x direction defined as the ratio between the length of

the cable segment along the acting direction

$D_z = \dfrac{T_{z,ij}}{\ell_{z,ij}}$ the density force in z direction

the equilibrium equation Eq. (3.3.2) is[14]

$$D_{x,ij}\left(y_{i,j+1} - y_{ij}\right) + D_{z,ij}\left(y_{i+1,j} - y_{ij}\right) + D_{x,i,j-1}\left(y_{i,j-1} - y_{ij}\right) + D_{z,i-1,j}\left(y_{i-1,j} - y_{ij}\right) = P_{y,ij} \quad (3.4.4)$$

which is nonlinear, because $\ell_{x,ij}$ and $\ell_{y,ij}$ depend on the points' coordinates.

The advantge of this approach is that the force density is assumed known rather than the

pretension one. Hence, $\dfrac{T_{x,ij}}{\ell_{x,ij}} = D_{x,ij}$ and $\dfrac{T_{z,ij}}{\ell_{z,ij}} = D_{z,ij}$ are known and Eq. (3.4.4) have

---

[14]

$$\frac{T_{x,ij}}{\ell_{x,ij}}\left(y_{i,j+1} - y_{ij}\right) + \frac{T_{z,ij}}{\ell_{z,ij}}\left(y_{i+1,j} - y_{ij}\right) + \frac{T_{x,i,j-1}}{\ell_{x,i,j-1}}\left(y_{i,j-1} - y_{ij}\right) + \frac{T_{z,i-1,j}}{\ell_{z,i-1j}}\left(y_{i-1,j} - y_{ij}\right) = P_{y,ij}$$

assuming

$$\frac{T_{x,ij}}{\ell_{x,ij}} = D_{x,ij}$$

$$\frac{T_{z,ij}}{\ell_{z,ij}} = D_{z,ij}$$

$$\frac{T_{x,i,j-1}}{\ell_{x,i,j-1}} = D_{x,i,j-1}$$

$$\frac{T_{z,i-1,j}}{\ell_{z,i-1,j}} = D_{z,i-1,j}$$

it obtains

$$D_{x,ij}\left(y_{i,j+1} - y_{ij}\right) + D_{z,ij}\left(y_{i+1,j} - y_{ij}\right) + D_{x,i,j-1}\left(y_{i,j-1} - y_{ij}\right) + D_{z,i-1,j}\left(y_{i-1,j} - y_{ij}\right) = P_{y,ij}$$

only y as unknown variables and therefore one may infer a recursive equation for the node $y_{i,j+1}$ [15]

$$y_{i,j+1} = y_{ij} + \frac{D_{z,ij}}{D_{x,ij}}\left(y_{i+1,j} - y_{ij}\right) - \frac{D_{x,i,j-1}}{D_{x,ij}}\left(y_{i,j-1} - y_{ij}\right) + \frac{D_{z,i-1,j}}{D_{x,ij}}\left(y_{i-1,j} - y_{ij}\right) + \frac{P_{y,ij}}{D_{x,ij}} \quad (3.3.5)$$

Similar conclusions can be achieved for $x(i,j+1)$ and $z(i,j+1)$.

Let anyway proceed with the y coordinate.

To identify the actual solution of the problem, the particular $\dot{y}(i,j)$ and homogeneous y_k^* solutions are searched for.

To find the particular solution one considers Fig.3.27, where the external points and some internal ones are identified.
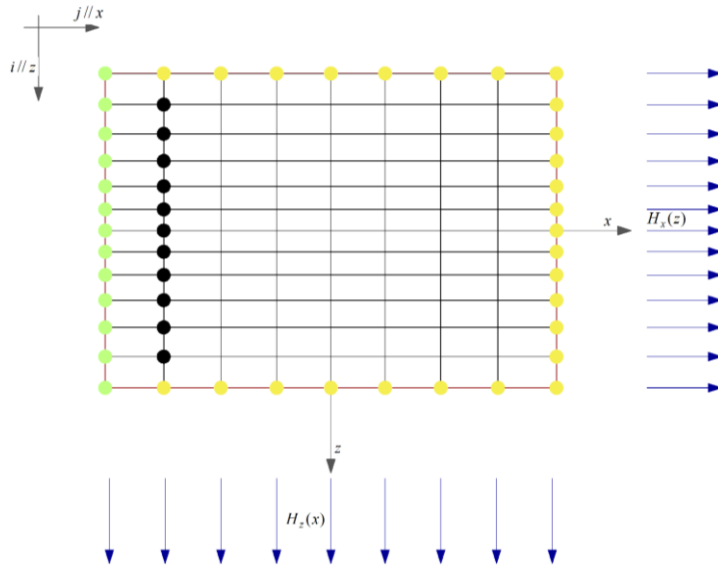
Figure 3.28: Plant of a bidirectional scheme and identification of the nodes.

---

[15]

$$D_{x,ij}\left(y_{i,j+1} - y_{ij}\right) + D_{z,ij}\left(y_{i+1,j} - y_{ij}\right) + D_{x,i,j-1}\left(y_{i,j-1} - y_{ij}\right) + D_{z,i-1,j}\left(y_{i-1,j} - y_{ij}\right) = P_{y,ij}$$

$$D_{x,ij}\,y_{i,j+1} - D_{x,ij}\,y_{ij} + D_{z,ij}\,y_{i+1,j} - D_{z,ij}\,y_{ij} + D_{x,i,j-1}\,y_{i,j-1} - D_{x,i,j-1}\,y_{ij} + D_{z,i-1,j}\,y_{i-1,j} - D_{z,i-1,j}\,y_{ij} = P_{y,ij}$$

$$y_{i,j+1} = y_{ij} - \frac{D_{z,ij}\,y_{i+1,j}}{D_{x,ij}} + \frac{D_{z,ij}\,y_{ij}}{D_{x,ij}} - \frac{D_{x,i,j-1}\,y_{i,j-1}}{D_{x,ij}} + \frac{D_{x,i,j-1}\,y_{ij}}{D_{x,ij}} - \frac{D_{z,i-1,j}\,y_{i-1,j}}{D_{x,ij}} + \frac{D_{z,i-1,j}\,y_{ij}}{D_{x,ij}} + \frac{P_{y,ij}}{D_{x,ij}}$$

$$y_{i,j+1} = y_{ij} + \frac{D_{z,ij}}{D_{x,ij}}\left(y_{i+1,j} - y_{ij}\right) - \frac{D_{x,i,j-1}}{D_{x,ij}}\left(y_{i,j-1} - y_{ij}\right) + \frac{D_{z,i-1,j}}{D_{x,ij}}\left(y_{i-1,j} - y_{ij}\right) + \frac{P_{y,ij}}{D_{x,ij}}$$

Starting from the boundary ones, for the cables in the x direction one attributes the coordinates only to the green nodes; while, for the cables in the z direction, the heights at both ends are assigned. One considers a sufficient number of internal points to which arbitrary coordinates are attributed and, through Eq. (3.3.6), the coordinates of all internal points and end ones along x are computed, thus composing the particular solution $\dot{y}(i, j)$ [16].

Then one proceeds to identify the homogeneous solution $y_k^*(i, j)$.

With reference to internal points (in black in Fig.3.27), the homogeneus solution is computed, nullyfing the heights of the boundary points and the contribution of the external load

$$y_{i,j+1} = y_{ij} + \frac{D_{z,ij}}{D_{x,ij}}\left(y_{i+1,j} - y_{ij}\right) - \frac{D_{x,i,j-1}}{D_{x,ij}}\left(y_{i,j-1} - y_{ij}\right) + \frac{D_{z,i-1,j}}{D_{x,ij}}\left(y_{i-1,j} - y_{ij}\right) + \frac{P_{y,ij}}{D_{x,ij}} \qquad (3.3.6)$$

$$y_{i,j+1} = y_{ij} + \frac{D_{z,ij}}{D_{x,ij}}\left(y_{i+1,j} - y_{ij}\right) - \frac{D_{x,i,j-1}}{D_{x,ij}}\left(y_{i,j-1} - y_{ij}\right) + \frac{D_{z,i-1,j}}{D_{x,ij}}\left(y_{i-1,j} - y_{ij}\right) \qquad (3.3.7)$$

Linearly independent heights are arbitrarily attributed in order to identify the heights of all points through Eq. (3.3.7).

The solution is given by the following relationship

$$y(i, j) = \dot{y}(i, j) + \sum_{1}^{m-2}{}_k \alpha_k y_k^*(i, j) \text{ [17]} \qquad (3.3.8)$$

with

$y(i, j)$ the complete solution $\qquad (3.3.9)$

The values α_k must be computed in order to identify the actual heights of the boundary points. Thus, denoted by (i_c, j_c) one of these points and by $y_c(i_c, j_c)$ its height, one has

$$y_c(i_c, j_c) = \dot{y}(i_c, j_c) + \sum_{1}^{m-2}{}_k \alpha_k y_k^*(i_c, j_c) \qquad (3.3.10)$$

From Eq. (3.3.10), α_k are inferred

$$\sum_{1}^{m-2}{}_k \alpha_k = \frac{y_c(i_c, j_c) - \dot{y}(i_c, j_c)}{y_k^*(i_c, j_c)} \qquad (3.3.11)$$

which, once substituted in Eq. (3.3.10), allow to identify the solution $y(i, j)$.

---

[16] The arbitrary values chosen to start the analysis do not satisfy the boundary conditions.

[17] *m-2* because in the omgeneus solution the points belonging to the two boundary cables are not considered; "*m*" is the number of the cables.

In the following, one reports some examples of equilibrium shapes' searches for bidirectional systems. Starting from defined topologies, several shapes are found considering different loads and density forces.

3.3.2.1 Anticlastic three-dimensional nets

One considers a squared grid firstly, without external loads with force densities varying at boundary and internal nodes with a ratio between 5:1-1:1. Then the effects of the external loads are evaluated.

First cases concern a topology scheme composed by $n = 36$ nodes (fixed and free nodes) and $m = 60$ branches.

Fig. 3.30 shows the anticlastic surface obtained considering null external loads and force densities ratio of 5:1 between external and internal branches. Then, the ratio has been modified to 2:1 in Fig. 3.31 and to 1:1 in Fig. 3.32. As one may notice, the curvature of the surface increases when the ratio diminishes.
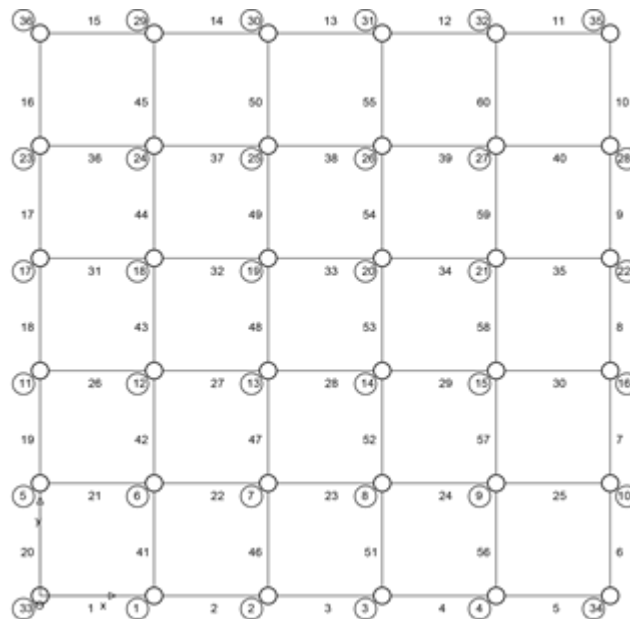
Figure 3.29: Topology scheme.
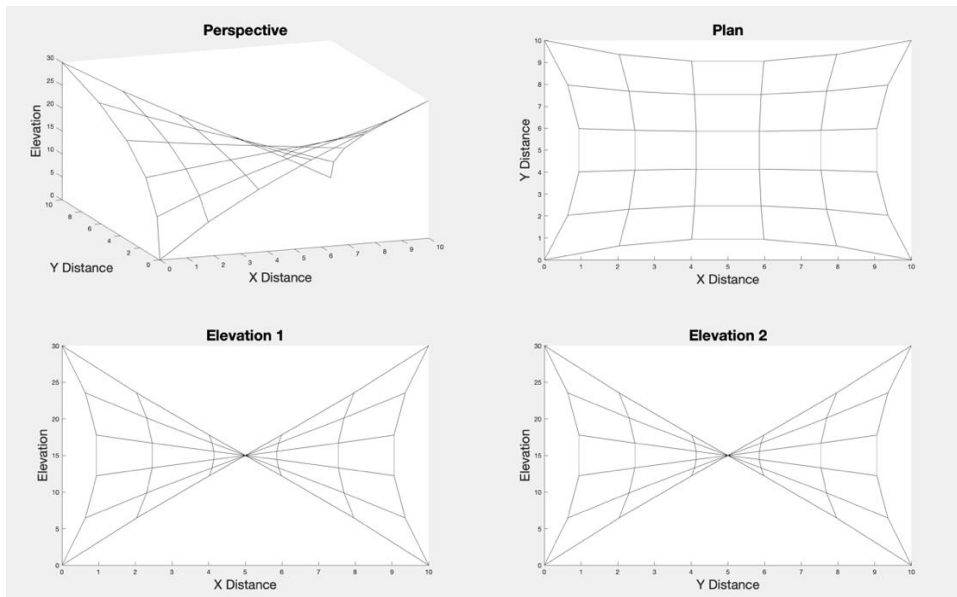
Figure 3.30: Equilibrium shape-ratio in edge to interior branches force densities is 5:1 and without external loads. Anticlastic surface.

(boundary branches q = 5; interior branches q = 1; external loads $P_x = 0$; $Py = 0$; $Pz = 0$*)*
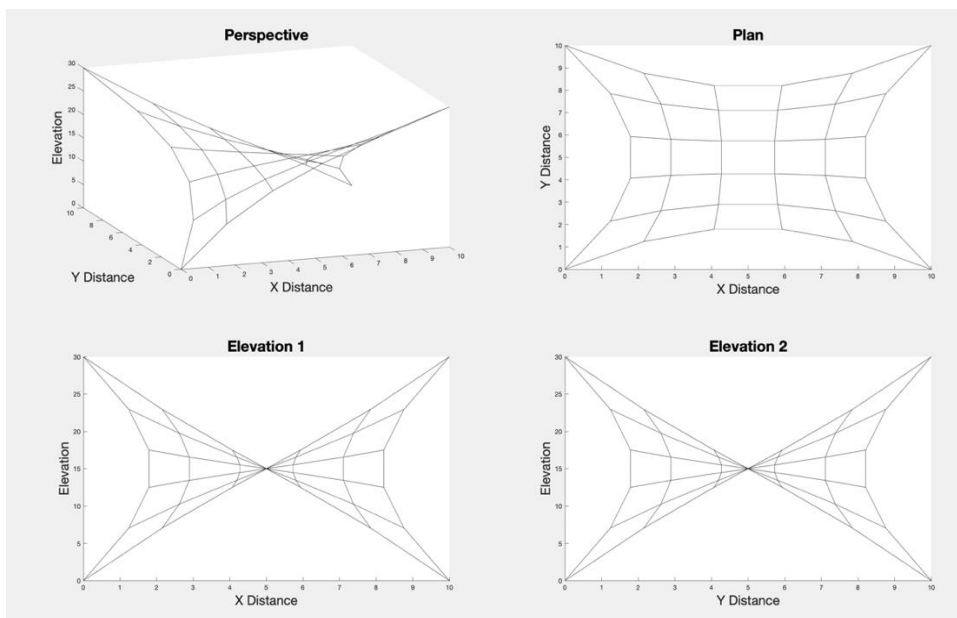
Figure 3.31: Equilibrium shape-ratio in edge to interior branches force densities is 2:1 and without external loads. Anticlastic surface.

(boundary branches q=2; interior branches q=1; external loads $P_x=0$;$P_y=0$;$P_z=0$*).*
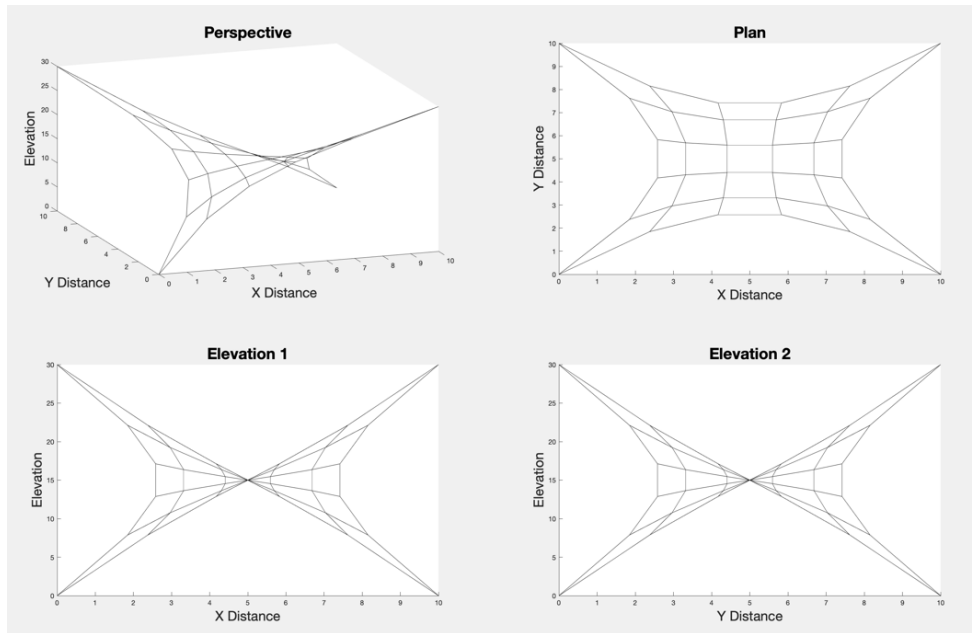
*Figure 3.32: Equilibrium shape-ratio in edge to interior branches force densities is 1:1
and without external loads. Anticlastic surface.*

(boundary branches q=1; interior branches q=1; external loads $P_x=0;P_y=0;P_z=0$).

3.3.2.2 Synclastic three-dimensional nets

Here, the effects of the overloads are analysed and the shapes obtained are shown in Fig. 3.33-34, when considering a force densities ratio of $q = 1:1$, and vertical loads $P_z = 2$ (Fig. 3.33) and $P_z = 4$ (Fig. 3.34) applied upward. One can notice that the surface turns into a Synclastic surface.
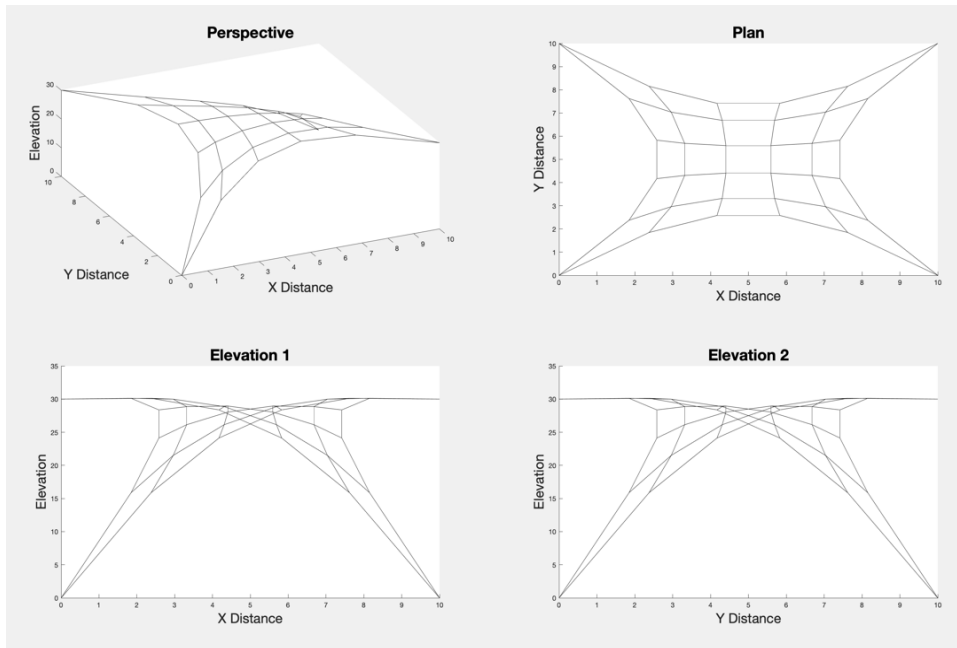
Figure 3.33: Equilibrium shape-ratio in edge to interior branches force densities is 1:1 and subject to vertical load P_z. Synclastic surface.
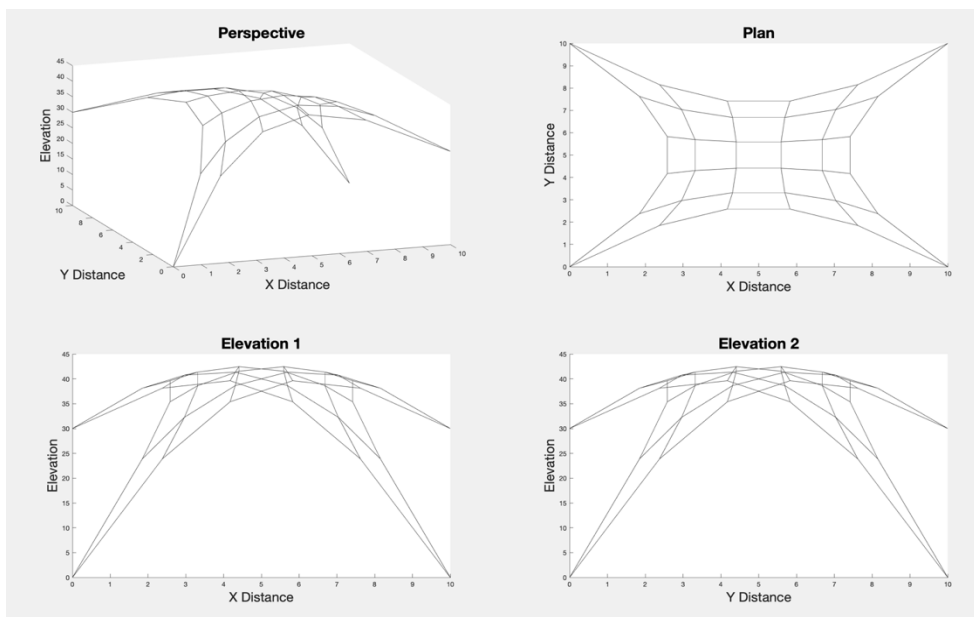
Figure 3.34: Equilibrium shape-ratio in edge to interior branches force densities is 1:1 and subject to vertical load P_z. Synclastic surface.

In Fig. 3.3 the four corners are fixed, keeping the ratio at $q = 1:1$, under the upward load $P_z = 4$.
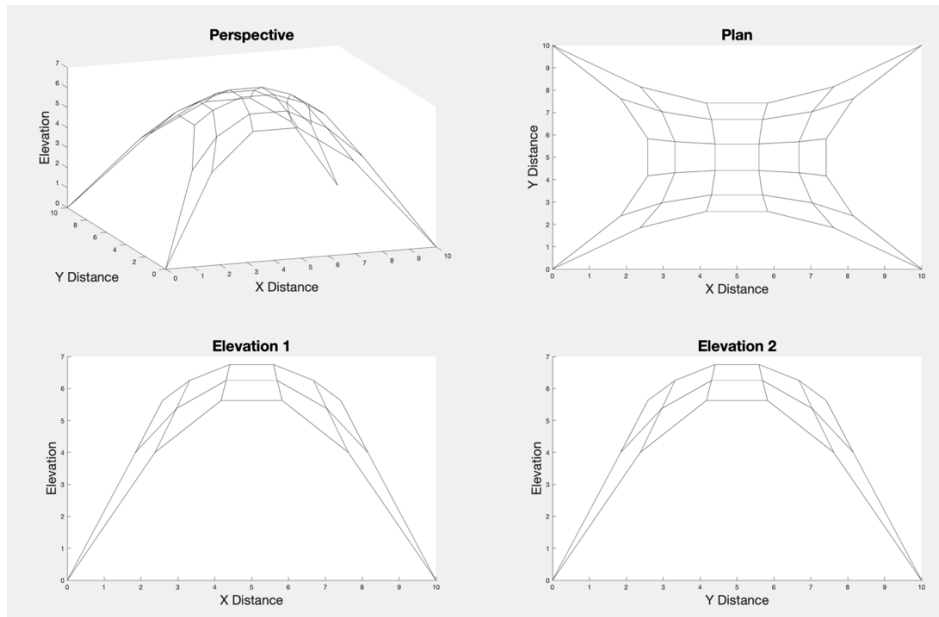
Figure 3.35: Equilibrium shape under vertical load P_z with unstraight edges. Ratio in the edge to the interior branches is 1:1.

3.3.2.3 Other equilibrium shapes

Considering the same topology (Fig. 3.29), in Fig. 3.34 the equilibrium shape of the structure is shown under a load condition $P_z= 4$ applied in the upward direction and with straight horizontal edges; the boundary straight branches are subject to force densities $q=100$, and the other ones to $q = 1$.
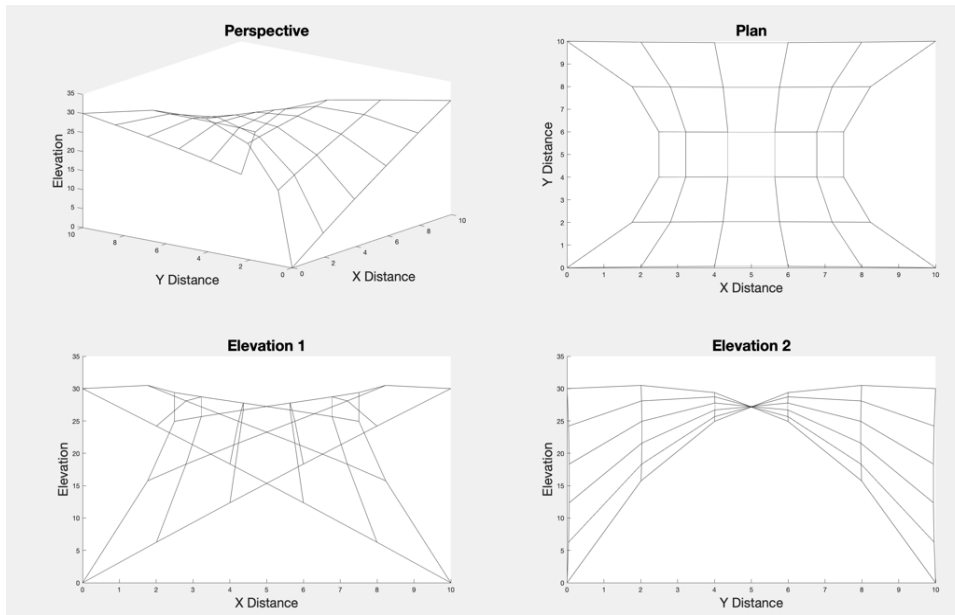
Figure 3.36: Equilibrium shape under vertical load P_z, with straight horizontal edges.

In Fig. 3.37 is represented the equilibrium shape, instead, considering the straight horizontal and vertical edges with q=100 for the external branches and q=1 for the internal ones. The load condition is $P_z=4$ applied upward.
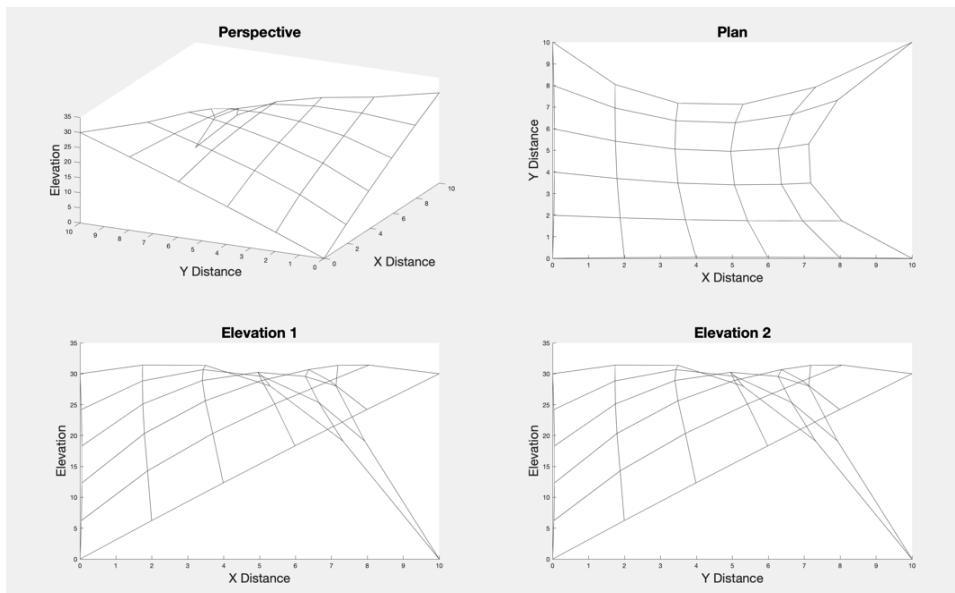
Figure 3.37: Equilibrium shape applying a vertical load P_z, with straight edges.

With reference to the topology scheme in Fig. 3.38, the equilibrium shape is obtained under a load $P_z = 1$ applied upward, external branches with $q = 100$ and the internal one with $q = 1$. Moreover, the edges are considered fixed and straight (Fig. 3.39).
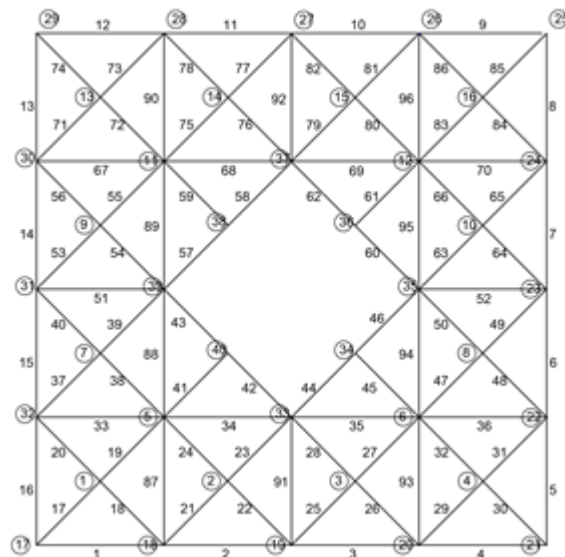
Figure 3.38: Topology scheme.
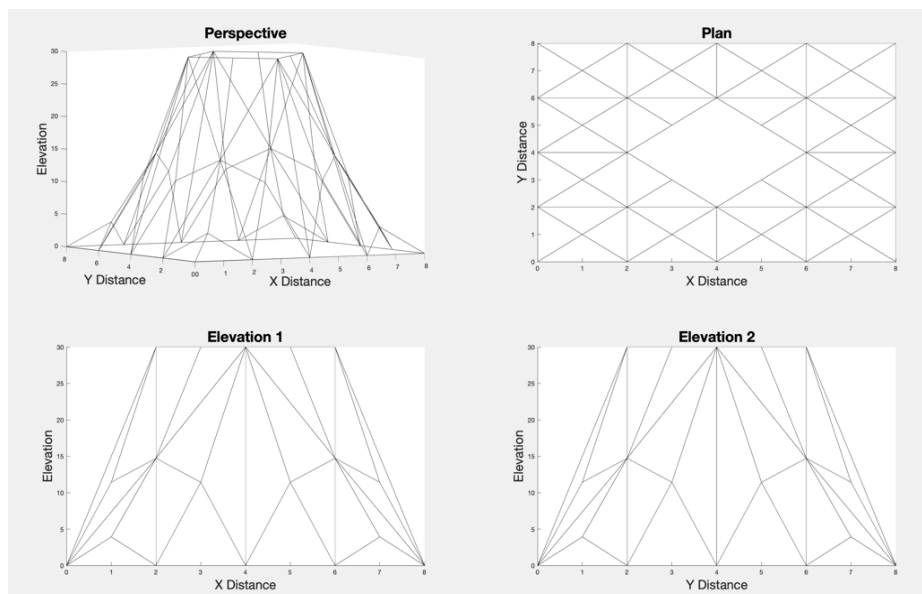
Figure 3.39: Equilibrium shape- fixed and straight edges under vertical loads P_z.

A scheme composed by $n = 39$ nodes and $m = 98$ branches is considered in Fig. 3.40. In this case the force densities ratio is 100:1 and the load applied is $P_z=1$ obtaining the equilibrium shape illustrated in Fig. 3.40.
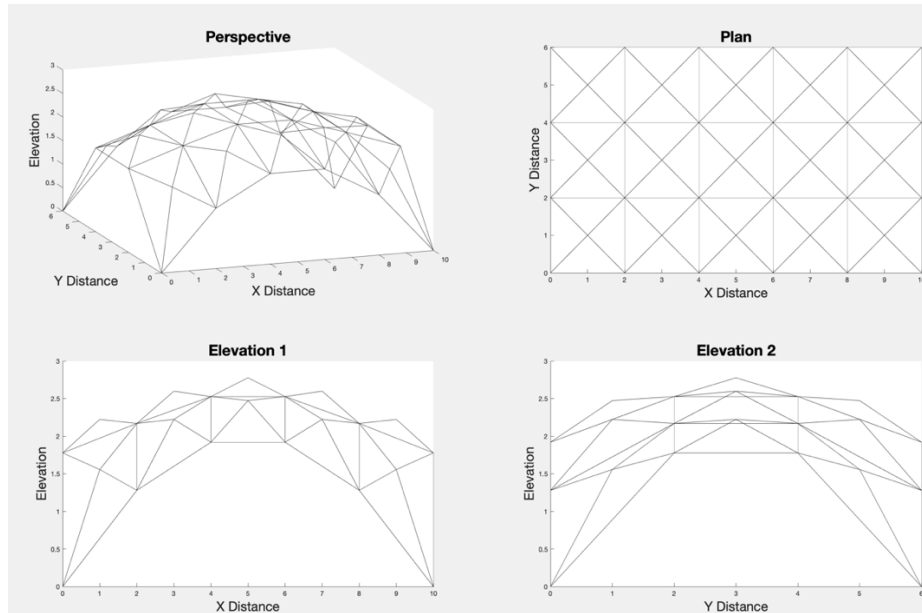
Figure 3.40: Equilibrium shape with fixed and straight edges.

The case with $P_z = -1$ applied in the downward direction is shown in Fig. 3.41, with $q = 100$ and $q = 1$ for the external and internal branches respectively.
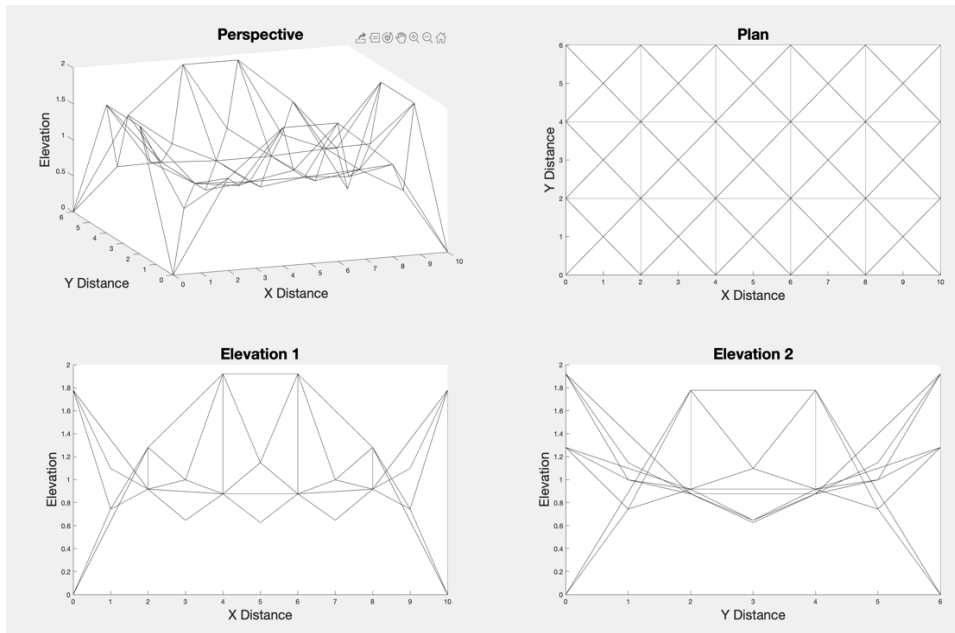
Figure 3.41: Equilibrium shape with fixed and straight edges.

Moreover the effects of the horizontal load $P_x = 1$ (applied towards positive x axis) and $P_y = 1$ (applied towards positive y axis) , and $P_z = 0$, are shown in Fig. 3.42 and Fig. 3.43 respectively. The ratio of force densities is 100:1.
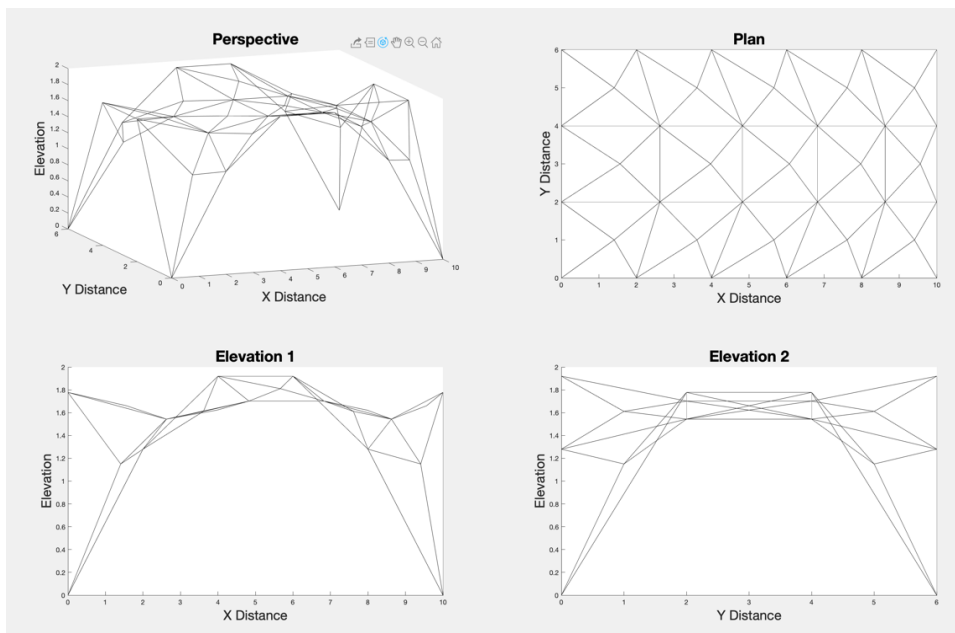
Figure 3.42: Equilibrium shape with fixed and straight edges.
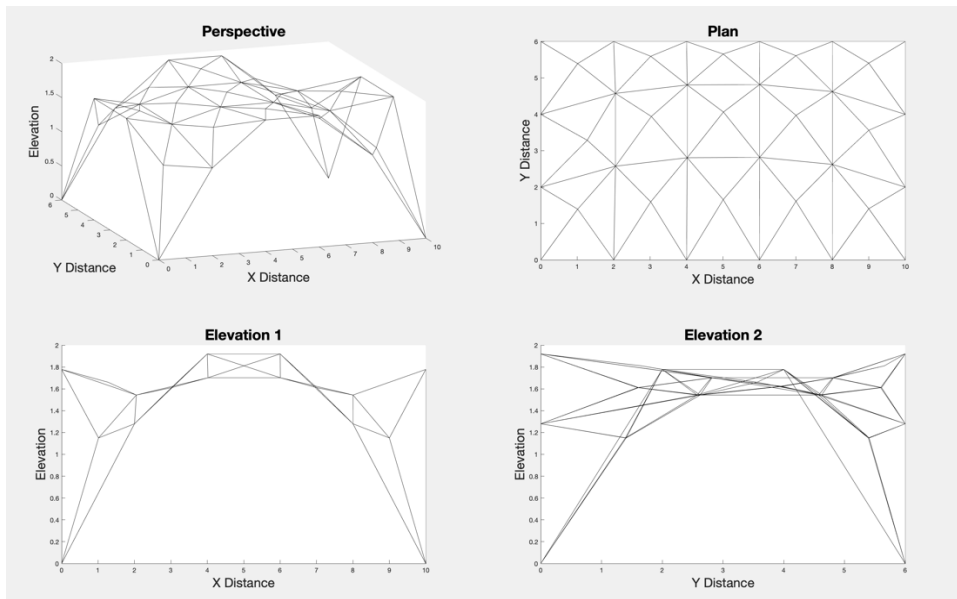
Figure 3.43: Equilibrium shape with fixed and straight edges.

Finally, the combination of loads $P_x = 1$ (applied towards positive *x* axis) and $P_z=1$ (applied upward), .and combination of $P_y = 1$ (applied towards positive *y* axis) and $P_z = 1$ (applied upward) are highlighted in the equilibrium shapes shown respectively in Fig. 3.44 and Fig. 3.45.
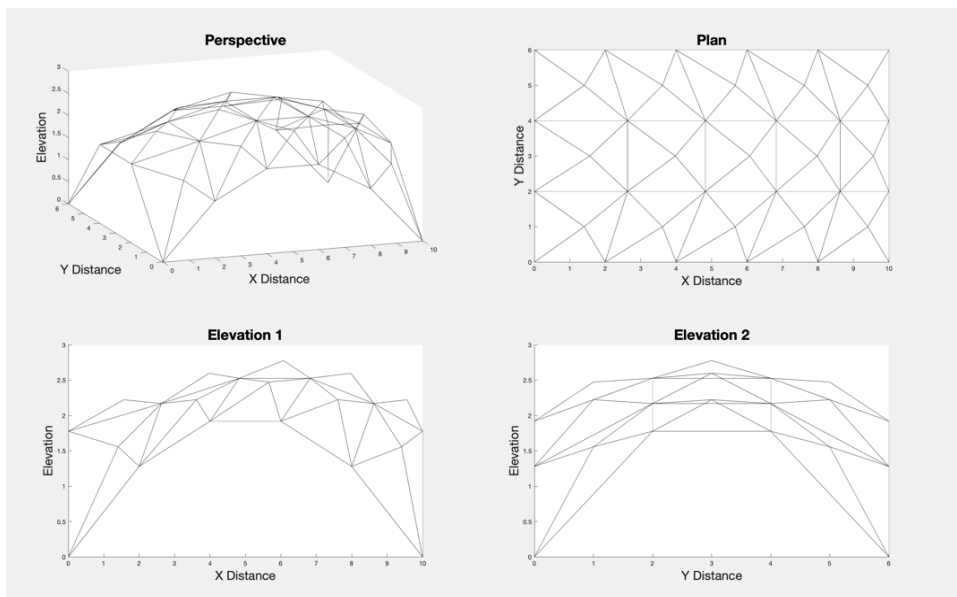
Figure 3.44: Equilibrium shape with fixed and straight edges.
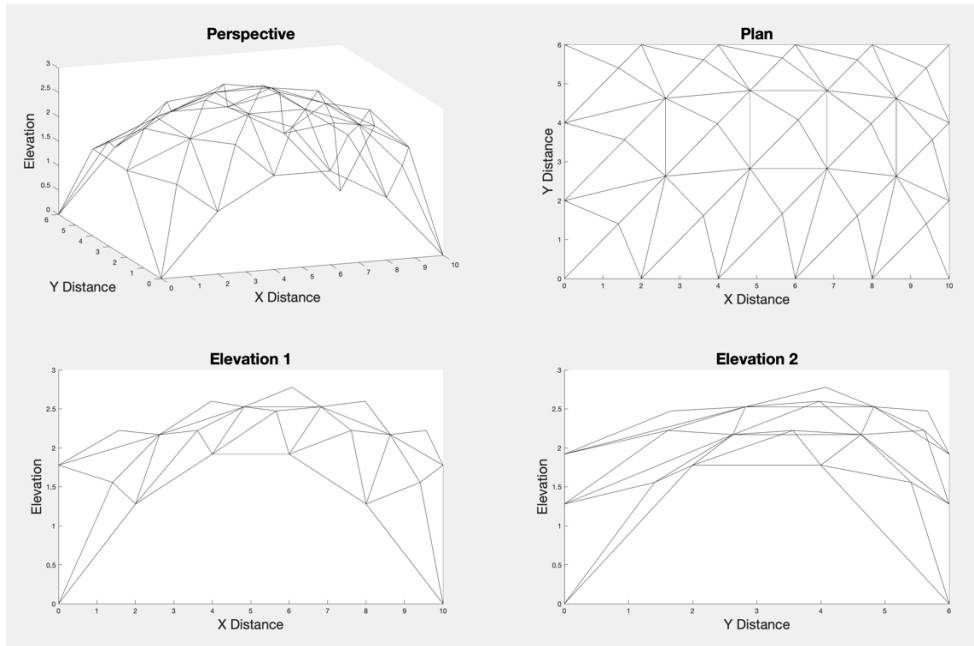
Figure 3.45: Equilibrium shape with fixed and straight edges.

In Fig. 3.47 the equilibrium shape of the topology scheme in Fig. 3.46 are shown, with the application of $P_z = 1$ upward and the force densities ratio equal to 100:1.
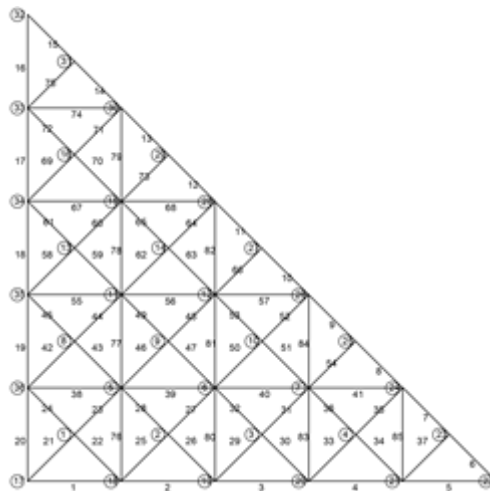
Figure 3.46:Topology scheme.
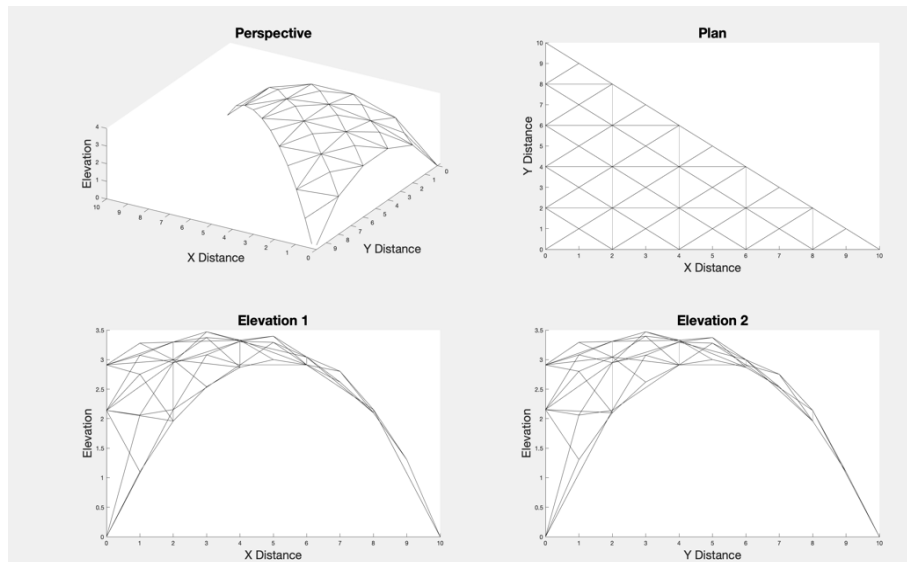
Figure 3.47: Equilibrium shape with fixed and straight edges.

4. ENERGY APPROACHES

One of the most important problems in the study of cable structures consists of identifying the equilibrium configuration under the overloads' application.

Moreover, the behaviour of these structures is described through suitable mathematical models. In most cases, they are formulated by differential equations solved by several approaches, such as the variational formulation belonging "*to the branch of mechanics, usually called analytical mechanics, which bases the entire study of equilibrium and motion on two fundamental scalar quantities, the kinetic energy and the potential energy*" (*Lan, 86*).

The configuration change is governed by large displacements leading to a number of difficulties in the analysis of the behaviour of these structures, due to the geometric and possibly mechanical non-linearity.

Therefore, the main approaches developed during the years can be divided into two types: the first ones are based mostly on the iterative processes, and the other ones are of the energetic kind. In this case, the minimum of the functional is searched for through constrained or unconstrained optimum methodologies.

These methods have been widely used in several field, in particular in the structural one. Actually, they can be adopted both for geometric and mechanical non-linearity, under large displacements and large strains hypotheses (*G.R. Monforton, N.M. El-Hakim, 1980*).

Consequently, energy approaches have been widely used for the analysis of elastic beams, shell structures, i.e. systems undergone by finite displacements, such as in the studies by Brogner (*F.K. Brogner,1965*), Mallet and Schimdt (*R.H. Mallet, L.A. Schimdt, 1967*), which have been later modified by the same Brogner in order to extend the application also to tension structures cases (*F.K. Brogner,1968*).

Then, Buchholdt, Das and Hill applied the approach on a cable-net structures referring to the *Gradient Method* (*H.A. Buchholdt et al, 1974*).

Monforton and El-Hakim (*Monforton and El-Hakim, 1980*) proposed an energetic approach for the analysis of truss and cable systems considering the geometric and mechanical non-linearity, and based on the Minimum Total Potential Energy Principle (TPE).

On this basis, new methods were developed by researchers during the years, such as those ones by Wang et al (*Wang et al., 2003*) where the authors implement the VWP for

a two nodes cable with a catenary profile, or that one by Kanno and Ohsaky (*Y. Kanno, M. Ohsaki, 2005*) who suggest a method based on the Minimum Complementary Energy Principle (CE), considering a cable-net structure with geometric and mechanical non-linearity.

Recently, Toklu et al (*Toklu et al, 2017*) proposed an energy minimization method through a *Total Potential Optimization* (TPO) technique and making recourse to Meta-Heuristic Algorithms (*Genetic Algorithm* (*GA*), *Particle Swarm Optimization* (*PSO*), *Ant Colony Optimization* (*ACO*), *Harmony Search Algorithm* (*HS*), *Firefly Algorithm* (*FA*), *Bat Algorithm* (*BA*)), rather than to the classical ones (*Gradient Method, Steepest Descent Method, Conjugate Gradient Method, Newton-Raphson, etc*) to search for the functionals' minimum.

The method is implemented for cable nets systems, selecting *Harmony Search* algorithm (*HS*) (*Geem et al.,2001*), inspired by the music and used in several optimization problems in the engineering field.

4.1 General Setup

So far one has emphasized that cable structures have been interesting the researchers mainly about their particular performance under the action of external loads, withstanding large displacements (*A. Pintea, G. Tarta, 2012*) and making it necessary to analyse their non-linear response in order to thoroughly describe their behaviour.

As well known, variational approaches are largely used in the engineering field because they allow to describe the mechanical principle by employing the mathematical variational problems.

According to the TPE for an elastic structure under conservative forces, the functional is given by the sum Π of the external loads' potential W and the strain energy U

$$\Pi = U + W \tag{4.1.1}$$

It depends on the configuration and therefore on the lagrangian coordinates of the system c_i

$$\Pi = \Pi(c_i) \tag{4.1.2}$$

For a three-dimensional continuum, under the above-mentioned conditions, the strain energy is given by

$$U = \frac{1}{2} \int_V \boldsymbol{\sigma} \cdot \boldsymbol{\varepsilon} \, dV \tag{4.1.3}$$

where

$\boldsymbol{\sigma}$ is the stress tensor

$\boldsymbol{\varepsilon}$ is the strain tensor

V is the volume of the body

and the loads' potential is given by

$$W = -\int_V \left(F_x u + F_y v + F_z w \right) dV - \int_S \left(P_x u + P_y v + P_z w \right) dS \tag{4.1.4}$$

where

P_x, P_y, P_z are the load components along the three reference axes

u, v, w are the displacement components along the three reference axes

F_x, F_y, F_z are the components of the mass forces

S, V are the body surface and volume

Hence, by substituting Eqs. (4.1.3)-(4.1.4) in Eq. (4.1.1), one gets

$$\Pi = \frac{1}{2} \int_V \boldsymbol{\sigma} \cdot \boldsymbol{\varepsilon} \, dV - \int_V \left(F_x u + F_y v + F_z w \right) dV - \int_S \left(P_x u + P_y v + P_z w \right) dS \tag{4.1.5}$$

For minimizing one writes down

$$\frac{d\Pi}{dc_i} = 0 \quad \forall c_i \tag{4.1.6}$$

The fundamental problem about the cable structures consists of identifying the displacements undergone by the structure and the internal forces developed due to the action of the external loads, thus of identifying the equilibrium configuration.

Nell'ambito dei metodi energetici il principio si basa sulla individuazione di un set di spostamenti che minimizzano l'energia potenziale totale.

The reference solution equation for these problems is typically given in the form

$$\mathbf{P} = \mathbf{K}\Delta\mathbf{u} + \mathbf{Z}\Delta\ell^* \tag{4.1.7}$$

where

P is the external load vector

K is the stiffness matrix

Δu is the displacements variation vector

$\mathbf{Z} = \mathbf{B}^{\mathrm{T}}\mathbf{C}^{-1}$ is the distortion matrix

$\Delta\ell^*$ is the elongation distortion vector.

Besides the more classical methodologies generally based on direct solving and handling of the mathematical relations, some additional paths have been outlined including the development of some special algorithms that allow to identify the solution, suitable both for linear and non linear problems.

4.2 Metaheuristic Algorithms

With the final objective of identifying a displacement set minimizing the energy functional, several methodologies have been developed over the years, some of them based on Metaheuristic Algorithms, where the TPE is assumed as objective functional and the displacements as unknown variables.

Metaheuristic Algorithms are based on the observation of natural events such as the natural selection, whence the *Genetic Algorithm* is developed, the social animal behaviour which led to the *Particle Swarm Optimization* (PSO) or even the musicians' method to compose the music, like for the *Harmony Search* (HS).

Focusing on the latter, this approach can be applied both in linear and non-linear problems, and is inspired by the approach adopted by the musicians to compose the harmony, when several possible combinations of notes are considered to find the right one.

Firstly proposed by Geem (*Geem et al., 2001*), during the years the HS method has been applied in different fields, including the structural design one. The algorithm can be summarized as follows. It starts from initializing a matrix called *Harmony Memory,* including sets of possible solutions. The size of this matrix, or *Harmony Memory Size* (HMS), can range, usually, between 50 and 100 (*X.Z. Gao et al, 2015*).

For example, considering a problem in *N*- dimension, the HM is set as follows

$$\mathbf{HM} = \begin{bmatrix} x_1^1 & x_2^1 & \dots & x_n^1 \\ x_1^2 & x_2^2 & \dots & x_n^2 \\ \vdots & & & \\ x_1^{HMS} & x_2^{HMS} & \dots & x_n^{HMS} \end{bmatrix}$$

(4.2.1)

where

$$[x_1^1 \ x_2^1 \ ... \ x_n^1]$$

$[x_1^{HMS} \ x_2^{HMS} \ ... \ x_n^{HMS}]$ are the solutions arbitrarily computed

The second step concerns the *improvisation* of a new solution given by $\begin{bmatrix} x_1^{'} & x_2^{'} & \cdots & x_n^{'} \end{bmatrix}$, where each element is obtained considering the Harmony Memory Considering Rate (HMCR), which is the probability to select an element of HM, as the element of a new solution. Furthermore, it can be modified taking into account the Pitching Adjust Rate (PAR), identifying the probability of a candidate from the HM to be mutated. Once a new solution is detected and evaluated, if its performances are better than the previous ones, then the worst element in the HM is replaced, otherwise it is cancelled. Finally, the previous steps are repeated until the convergence or the established criterion are reached.

This method has been largely applied in optimization problems. However, most of these problems are constrained optimization problems, where the objective is to identify the solution accommodating the imposed constraint, represented by equalities or inequalities, or both of them. Nevertheless, the original version of the HS method presents some difficulties to solve the constrained problems, because the solution should be found in the HM and sometimes its elements cannot satisfy the imposed conditions. Hence several variations of this approach have been developed in order to

improve its implementation. For example, the *Global-best Harmony Search* (GHS) by Omaran and Mahdavi (*M. Omaran, M. Mahdavi,2008*), or the *Dynamic Local Best Harmony Search* (DLHS), developed by Pan et al. (*Q.Pan. Et al, 2018*), where the HM is subdivided in other independent sub-HMs; or even the new self-adaptive Harmony Search (HS) proposed by Wang and Huang (*C.M. Wang,Y-F., Huang, 2009*). Moreover, a modified HS are available for cable structures, as described in the following.

The geometric features of the structures are defined, and in particular the number, the coordinates and the boundary conditions for each node; loads and pretension forces are applied. Then, a range of possible displacements is identified and evaluated. Among them the unknown variables of the problem are searched for.
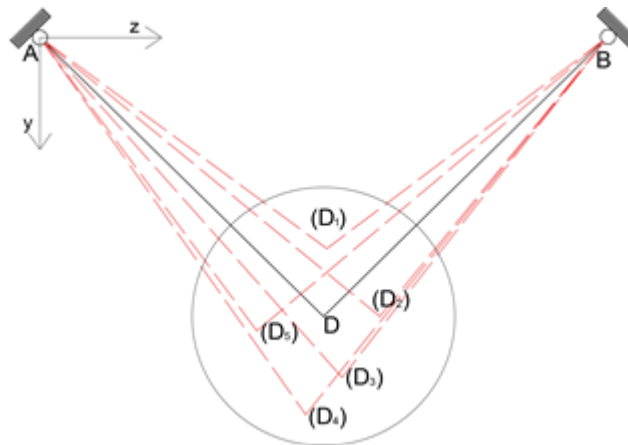
Figure 4.1: Possible nodal displacements' selection and relevant deformed configurations (in dashed line).

Therefore, the HM is obtained from unifying the Harmony Vector (HV) and the Harmony Memory Size (HMS). Each vector includes the nodes coordinates arbitrarily obtained, each one representing a new structure configuration under defined load conditions. Hence the strain energy, the work and the TPE can be computed.

Thus, the procedure consists of identifying several configurations, and computing the TPE for each one, up to determine the one who reaches the minimum energy value.

Hence, with reference to the above-mentioned structure one proceeds to identify a set of possible deformed configurations that are arbitrarily generated. The node coordinates are assembled into the HM, as vectors

$$\mathbf{HM} = \left[\left(x_j, y_j, z_j \right)_1 \quad \left(x_j, y_j, z_j \right)_2 \quad \left(x_j, y_j, z_j \right)_3 \quad \ldots \quad \left(x_j, y_j, z_j \right)_{HMS} \right] \qquad (4.2.2)$$

where

$$\left(x_j, y_j, z_j \right)_1 = \mathbf{HV_1}$$

$$\left(x_j, y_j, z_j \right)_2 = \mathbf{HV_2}$$

$$\left(x_j, y_j, z_j \right)_{HMS} = \mathbf{HV}_{HMS}$$

where $\mathbf{HV}$ denotes the Harmony Vector.

For each element of the structure the TPE is computed through the strain and loads' potential energy.

To this purpose one refers to the single k^{th} element ij connecting the ith and the jth nodes, with the initial length ℓ_{ij}^o given by

$$\ell_{ij}^o = \sqrt{\left(x_j - x_i \right)^2 + \left(y_j - y_i \right)^2 + \left(z_j - z_i \right)^2} \qquad (4.2.3)$$

with $\left(x_i, y_i, z_i \right)$ and $\left(x_j, y_j, z_j \right)$, respectively, the ends' i and j coordinates in the three-dimensional reference system $(Oxyz)$.

If one identifies $\left(u_i, v_i, w_i \right)$ and $\left(u_j, v_j, w_j \right)$ as the displacements of the i and j nodes in $(Oxyz)$, the updated length of the analysed beam is given by

$$\ell_{ij} = \sqrt{\left(x_j - x_i + u_j - u_i \right)^2 + \left(y_j - y_i + v_j - v_i \right)^2 + \left(z_j - z_i + w_j - w_i \right)^2} \qquad (4.2.4)$$

whence, the stretching $\Delta\ell_{ij}$ is

$$\Delta\ell_{ij} = \ell_{ij} - \ell_{ij}^\circ \qquad (4.2.5)$$

and, therefore, the uniform strain of the element is given by the ratio

$$\varepsilon_{ij} = \frac{\Delta\ell_{ij}}{\ell_{ij}^o} \qquad (4.2.6)$$

Generally speaking $\sigma_{ij} = \sigma_{ij}\left(\varepsilon_{ij} \right)$; supposing that the material has an elastic-linear behaviour, one has

$$\sigma_{ij} = E\varepsilon_{ij} \tag{4.2.7}$$

with E the Young modulus, then the strain energy in the kth element ij is

$$e_k = \frac{1}{2}E\varepsilon_{ij}^2 \tag{4.2.8}$$

and, in case of nonlinear behaviour, coincides with the subtended area of the $\sigma - \varepsilon$ graph, and therefore it is obtained through integration.

Then with reference to the global system, the TPE is given

$$\Pi = \sum_{k=1}^{m} e_k A_k \ell_k - \sum_{i=1}^{n}\left(P_{xi}u_i + P_{yi}v_i + P_{zi}w_i\right) \tag{4.2.9}$$

where

m is the number of beams

n is the number of nodes

and the index k is referred to the entities of the kth beam ij.

Referring to the structure in Fig.4.2, the Harmony Vectors (HVs) are defined considering the several positions assumed by the free node D due to the external loads action.
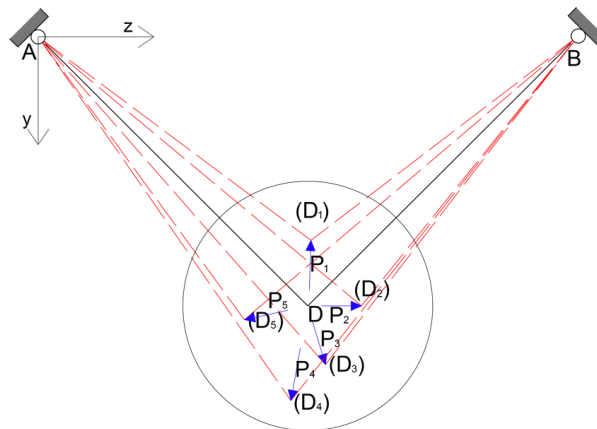
Figure 4.2: Undeformed cable system and deformed shape due the application of the external loads on the free node.

Hence the HVs are the following

$$\mathbf{HV}_1 = (y_D, z_D)_1$$
$$\mathbf{HV}_2 = (y_D, z_D)_2$$
$$\mathbf{HV}_3 = (y_D, z_D)_3 \qquad\qquad (4.2.10)$$
$$\mathbf{HV}_4 = (y_D, z_D)_4$$
$$\mathbf{HV}_5 = (y_D, z_D)_5$$

taking into account that $(y_D, z_D)_r$ denote the updated coordinates of the node D in any new configuration, respectively along the y and z reference axes, in the specific case with $r=1..5$.

Starting from the identified HVs, the initial Harmony Matrix (HM) and its size (HMS) can be assembled.

Actually, the HM is composed by the HVs

$$\mathbf{HM} = \begin{bmatrix} (y_D, z_D)_1 & (y_D, z_D)_2 & (y_D, z_D)_3 & (y_D, z_D)_4 & (y_D, z_D)_1 \end{bmatrix}$$
$$\qquad\qquad \mathbf{HV}_1 \qquad \mathbf{HV}_2 \qquad \mathbf{HV}_3 \qquad \mathbf{HV}_4 \qquad \mathbf{HV}_{HMS=5} \qquad (4.2.11)$$

hence, the TPE is computed for each beam of the system in the different configurations.

Therefore, one starts from defining the geometrical properties, computing the initial length and the updates

$$\ell^o_{AD} = \sqrt{(y_D - y_A)^2 + (z_D - z_A)^2} \qquad\qquad (4.2.12)$$

$$\ell^o_{BD} = \sqrt{(y_D - y_B)^2 + (z_D - z_B)^2} \qquad\qquad (4.2.13)$$

where

(y_A, z_A) are the coordinates of the node A in the plane system (Oyz)

(y_B, z_B) are the coordinates of the node B in (Oyz)

(y_D, z_D) are the coordinates of the node D in (Oyz)

Therefore, the deformed length is computed considering the displacement components of the free node D, in each new configuration. Thus denoting by $\left(v_{D_r}, w_{D_r} \right)$ with

r=1,...,5

respectively the vertical and horizontal components of the node D in the update configurations with $r = 1\ldots5$, the final lengths of the beams are identified by

$$\ell^1_{AD} = \sqrt{\left(y_D - y_A + v_{D_1} - v_A \right)^2 + \left(z_D - z_A + w_{D_1} - w_A \right)^2}$$

$$\ell^2_{AD} = \sqrt{\left(y_D - y_A + v_{D_2} - v_A \right)^2 + \left(z_D - z_A + w_{D_2} - w_A \right)^2}$$

$$\ell^3_{AD} = \sqrt{\left(y_D - y_A + v_{D_3} - v_A \right)^2 + \left(z_D - z_A + w_{D_3} - w_A \right)^2}$$

$$\ell^4_{AD} = \sqrt{\left(y_D - y_A + v_{D_4} - v_A \right)^2 + \left(z_D - z_A + w_{D_4} - w_A \right)^2}$$

$$\ell^5_{AD} = \sqrt{\left(y_D - y_A + v_{D_5} - v_A \right)^2 + \left(z_D - z_A + w_{D_5} - w_A \right)^2}$$

but

$\left(v_A, w_A \right) = \left(0,0 \right)$ (are the displacements components of node A) for the boundary conditions.

hence

$$\ell^1_{AD} = \sqrt{\left(y_D - y_A + v_{D_1} \right)^2 + \left(z_D - z_A + w_{D_1} \right)^2}$$

$$\ell^2_{AD} = \sqrt{\left(y_D - y_A + v_{D_2} \right)^2 + \left(z_D - z_A + w_{D_2} \right)^2}$$

$$\ell^3_{AD} = \sqrt{\left(y_D - y_A + v_{D_3} \right)^2 + \left(z_D - z_A + w_{D_3} \right)^2}$$

$$\ell^4_{AD} = \sqrt{\left(y_D - y_A + v_{D_4} \right)^2 + \left(z_D - z_A + w_{D_4} \right)^2}$$

$$\ell^5_{AD} = \sqrt{\left(y_D - y_A + v_{D_5} \right)^2 + \left(z_D - z_A + w_{D_5} \right)^2}$$

where ℓ^r_{AD} with $r = 1,\ldots,5$ denotes the updated length of the AD beam in each considered new configuration.

In the same way the final lengths of the BD beam are calculated

$$\ell^1_{AD} = \sqrt{\left(y_D - y_B + v_{D_1} - v_B\right)^2 + \left(z_D - z_A + w_{D_1} - w_B\right)^2}$$

$$\ell^2_{AD} = \sqrt{\left(y_D - y_B + v_{D_2} - v_B\right)^2 + \left(z_D - z_B + w_{D_2} - w_B\right)^2}$$

$$\ell^3_{AD} = \sqrt{\left(y_D - y_B + v_{D_3} - v_B\right)^2 + \left(z_D - z_B + w_{D_3} - w_B\right)^2}$$

$$\ell^4_{AD} = \sqrt{\left(y_D - y_B + v_{D_4} - v_B\right)^2 + \left(z_D - z_B + w_{D_4} - w_B\right)^2}$$

$$\ell^5_{AD} = \sqrt{\left(y_D - y_B + v_{D_5} - v_B\right)^2 + \left(z_D - z_B + w_{D_5} - w_B\right)^2}$$

but

$\left(v_B, w_B\right) = \left(0,0\right)$ (are the displacements components of node B) for the boundary conditions.

hence

$$\ell^1_{AD} = \sqrt{\left(y_D - y_B + v_{D_1}\right)^2 + \left(z_D - z_B + w_{D_1}\right)^2}$$

$$\ell^2_{AD} = \sqrt{\left(y_D - y_B + v_{D_2}\right)^2 + \left(z_D - z_B + w_{D_2}\right)^2}$$

$$\ell^3_{AD} = \sqrt{\left(y_D - y_B + v_{D_3}\right)^2 + \left(z_D - z_B + w_{D_3}\right)^2}$$

$$\ell^4_{AD} = \sqrt{\left(y_D - y_B + v_{D_4}\right)^2 + \left(z_D - z_B + w_{D_4}\right)^2}$$

$$\ell^5_{AD} = \sqrt{\left(y_D - y_B + v_{D_5}\right)^2 + \left(z_D - z_B + w_{D_5}\right)^2}$$

Since the length variation is given as the difference between the final and initial length, one calculate the elongations $\Delta\ell^r_{AD}$ and $\Delta\ell^r_{BD}$

$$\Delta\ell^1_{AD} = \ell^1_{AD} - \ell^o_{AD}$$
$$\Delta\ell^2_{AD} = \ell^2_{AD} - \ell^o_{AD}$$
$$\Delta\ell^3_{AD} = \ell^3_{AD} - \ell^o_{AD} \qquad (4.2.14)$$
$$\Delta\ell^4_{AD} = \ell^4_{AD} - \ell^o_{AD}$$
$$\Delta\ell^5_{AD} = \ell^5_{AD} - \ell^o_{AD}$$

$$\Delta \ell^1_{BD} = \ell^1_{BD} - \ell^o_{BD}$$

$$\Delta \ell^2_{BD} = \ell^2_{BD} - \ell^o_{BD}$$

$$\Delta \ell^3_{BD} = \ell^3_{BD} - \ell^o_{BD} \qquad (4.2.15)$$

$$\Delta \ell^4_{BD} = \ell^4_{BD} - \ell^o_{BD}$$

$$\Delta \ell^5_{BD} = \ell^5_{BD} - \ell^o_{BD}$$

and, then, the strains

$$\varepsilon^r_{AD} = \frac{\Delta \ell^r_{AD}}{\ell^o_{AD}} \quad \text{with} \quad r = 1...5 \qquad (4.2.16)$$

$$\varepsilon^r_{BD} = \frac{\Delta \ell^r_{BD}}{\ell^o_{BD}} \quad \text{with} \quad r = 1...5 \qquad (4.2.17)$$

whence, with reference to the stress-strain curve, one identifies the coupled stresses.
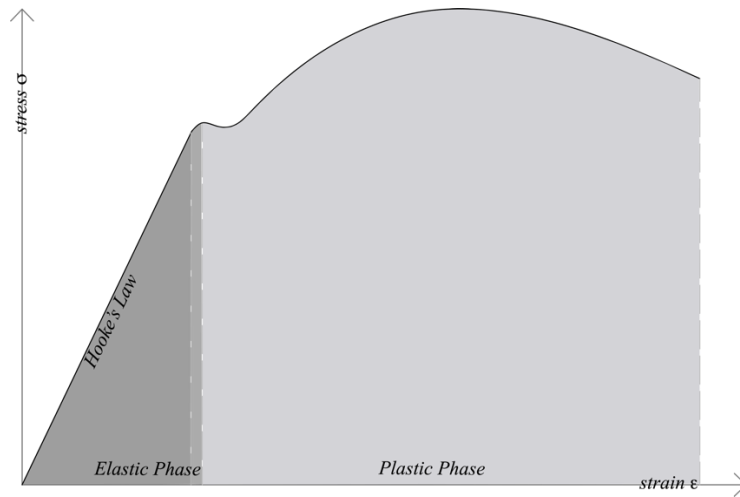
Figure 4.3: Stress-strain graph.

By referring to the linear elastic behaviour of the beams (Fig. 4.3) in Eq.(4.2.7)
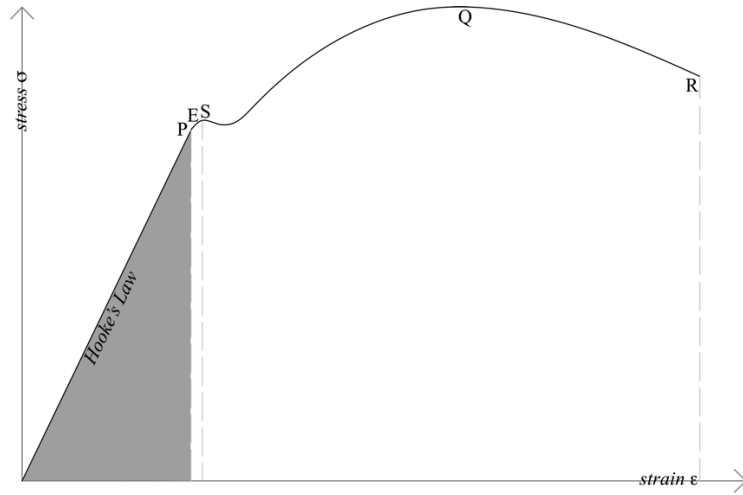
Figure 4.4: Stress-strain graph: linear-elastic behaviour.

the strain energy in the elements are given by

$$U_{AD}^r = \frac{1}{2}\sigma_{AD}^r \varepsilon_{AD}^r A_{AD} \ell_{AD}^r$$

$$U_{BD}^r = \frac{1}{2}\sigma_{BD}^r \varepsilon_{BD}^r A_{BD} \ell_{BD}^r$$

(4.2.18)

where

U_{AD}^r is the strain energy of the AD for each rth configuration

U_{BD}^r is the strain energy of the BD for each rth configuration

σ_{AD}^r is the stress of the AD coupled to strain ε_{AD}^r in each rth configuration

σ_{BD}^r is the stress of the BD coupled to strain ε_{BD}^r in each rth configuration

A_{AD} is the cross-section area of the beam AD

A_{BD} is the cross-section of the beam BD

ℓ_{AD}^r is the updated length of the AD beam at each rth configuration

ℓ_{BD}^r is the updated length of the BD beam at each rth configuration

Therefore, it is possible to define the strain energy of the global system as the sum of the single contributions, previously identified at each rth configuration.

$$U^r = U^r_{AD} + U^r_{BD} \quad \text{with} \quad r = 1...5 \tag{4.2.19}$$

As regards the loads' potential relevant to the external loads applied on the joint D and the coupled nodal displacements, one has at any configuration

$$W^r = P^r_{yD} v^r_D + P^r_{zD} w^r_D \tag{4.2.20}$$

where

P^r_{yD}, P^r_{zD} are the external load components applied in D leading to the rth configuration

v^r_D, w^r_D are the coupled nodal displacements at the rth configuration.

Whence one infers the TPE for each HVs

$$\Pi^r = U^r - W^r \quad \text{with} \quad r = 1,...,5 \tag{4.2.21}$$

Once computed the TPE for each HV, a new vector is searched for.

As the music improvisation process is characterized by three possible options like the repetition of a known harmony by the musician's memory, the adjustment of some pitches of an existing melody, or the reproduction of randomized notes, so in the analysed approach Geem et al. identified three possibilities to determine a new vector: *harmony memory, pitches adjustment, and randomization.*

In the first option one refers to an assigned accepted parameter $r_{par} \in [0,1]$. If it is close to 0, then it has a slow convergence; on the other hand, if the r_{par} is too close to 1, there is the possibility to have a wrong solution. Therefore, the accepted parameter is usually included between the values of 0,75-0,95.

In the second one, the pitches' adjustment, the new vector is determined through the generation of different solutions considering a bandwidth range b_{range} and a pitch-adjusting rate r_{pa}, that is

$$x_{new} = x_{old} + b_{range} \gamma \tag{4.2.22}$$

where

x_{new} is the searched new vector

x_{old} is the existing vector

γ is a number arbitrarily generated between $[-1,1]$.

To obtain an accurate solution a pitch-adjusting rate is assigned. Finally, the third option is similar to the second one, but it allows to find several solutions in order to reach the global optimum.

In this analysis, the new vector is generated starting from the existing ones in the HM. After that, the potential energy of the new vector is computed and evaluated. If it is better than that one of the corresponding starting vector, then it replaces the latter. The process is repeated up to convergence or as far as to achieve the imposed criterion. The new configuration is determined at the end of the iterative process. Subsequently the other unknown variables can be computed taking into account the equilibrium conditions, i.e. the stresses in the beams and the nodes reactions.

It is also possible to refer to other kinds of approaches about the TPE minimization problem, such as the *Sequential Quadratic Programming* (*S. Ohkubo et al., 1987*), the *Tree Search* (*A. Csebfalvi et al., 1999*), and so on; some researchers have proposed different procedures like the arbitrary search and simulated annealing algorithm (*Y.C. Toklu, 2004*) and the adaptive local search process (*Y.C. Toklu 2004*).

The report by *Toklu et al.* shows the algorithm developed and applied on a structure having geometric and mechanical non-linearity. The method is demonstrated to give good results also in case of instability phenomena and for several structures.

Starting from the general formulation, the expression of the TPE is considered referring to a plane pin-jointed structure

$$\Pi = \int_V e(\varepsilon)dV - \sum_{i=1}^{n_p} P_i u_i \tag{4.2.23}$$

remembering that

$$e(\varepsilon) = \int_0^\varepsilon \sigma(\varepsilon)d\varepsilon \tag{4.2.24}$$

where

$\sigma(\varepsilon)$ is the stress

$\mathcal{E}$ is the strain

V is the volume of the element

n_p is the number of applied loads

P_i are the applied external loads

u_i are the displacements coupled to the above mentioned loads

Eq. (4.2.23) represents the sum of the strain energy stored in the elements and the work produced by the applied loads for the coupled displacements, and is computed with reference to the deformed configuration.

Now, let consider a plane cable structure composed by m elements and n nodes, under n_p external loads.

Considering the element ij in the plane, where i and j denotes the ends with coordinates respectively given by (x_i, y_i) and (x_j, y_j), the initial length ℓ_{ij}^o is

$$\ell_{ij}^o = \sqrt{(x_j - x_i)^2 - (y_j - y_i)^2} \qquad (4.2.24)$$

consequently, if (u_i, v_i) and (u_j, v_j) denote the ends displacement components along the reference axes, the final length is given by

$$\ell_{ij} = \sqrt{(x_j - x_i + u_j - u_i)^2 + (y_j - y_i + v_j - v_i)^2} \qquad (4.2.25)$$

The stretching $\Delta\ell_{ij}$ is obtained as the difference by final and initial length

$$\Delta\ell_{ij} = \ell_{ij} - \ell_{ij}^\circ \qquad (4.2.26)$$

Therefore, the strain can be computed by the ratio in Eq. (4.2.6)

$$\varepsilon_{ij} = \frac{\Delta\ell_{ij}}{\ell_{ij}^o} \qquad (4.2.27)$$

Supposing known the ends, the strain can be easily identified and consequently the TPE can be computed for all elements as
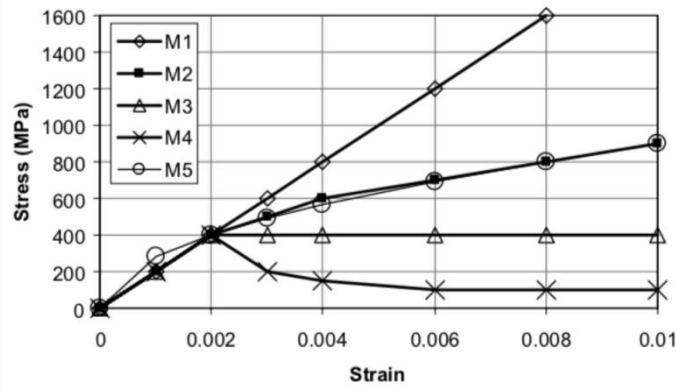
Figure 4.5: Stress- strain diagrams considered in the analysis- Toklu 2014

$$\Pi = \sum_{k=1}^{m} e_k A_k \ell_k - \sum_{i=1}^{n_p} P_i u_i \qquad\qquad (4.2.28)$$

The problem then consists of determining the displacements vector minimizing Eq. (4.2.28), satisfying the boundary conditions, represented by the constraints. The mechanical nonlinearity is implicitly taken into account since one refers to the deformed configuration. Actually the material properties are accounted for through the constitutive relations and Eq.(4.2.24). Therefore if the equations are given for the selected material, the possible mechanical non linearity may be easily implemented in the above shown formulation. One should notice that these relations are valid either for NT (No-Tension) or for NC (No-Compression) material.

Several combinations have been considered during experimental tests, allowing to identify materials that exhibit a symmetrical behaviour for both the solicitations (M1, M2, M5) and materials that, on the contrary, behave differently in tension (M3) and in compression (M4). In the latter case the different response of the tensile or compressive elements is considered.

The optimum problem, as formulated in the above, may be solved through a number of techniques as already emphasized. The application of the *Adaptive Local Search Method* (*ALSM*) is based on the identification of a variable domain where the optimal solution is searched for.

Starting from the assignment of a displacement field, applied on each node of the analysed structure and satisfying the boundary conditions, a new configuration is

identified, whence the elements' stretching, strains, strain densities and the TPE are computed, determining the best solution.

After this step a new displacement field is assigned, finding a new configuration and then the related TPE. The chosen displacement field during the process belongs to the previously defined domain.

If the updated TPE gives a value less than the preceding one, it substitutes the previous one, which has been considered the best solution till now. Otherwise another displacement set is identified and applied. The procedure is repeated up to convergence. A critical issue lies in the arbitrariness in the displacement field selection.

Therefore, to optimize the convergence, the following hypotheses can be made:

- without suitable steps into a trials series, at the greatest step a reduction factor $k_2 < 1$ is applied. The process ends when the dimension of the step is smaller than the predefined one.

- if the configuration is suitable within the defined domain, the multiplying factor $k_2 > 2$ is considered.

The described methodology can be applied for structures with mechanical and geometrical nonlinearity, and for structures either statically determined or with some instability; the algorithm does not require to solve matrix equations, and gives acceptable results, although referred to a local minimum rather than to the global one.

Some critical points are emerged, in particular referring to the relatively long execution times.

For solving the above introduced minimum problem, as an alternative, a number of methodologies are available belonging to the gradient method, such as the *Inverse Huang Algorithm* (IHA) (*S.T. Huang, 1989*).

The approach is based on two initial hypotheses:

- the cable net is in the elastic field
- the cable net is supposed anchored at supporting points that are perfectly fixed.

The approach allows to identify firstly the shape of the net loaded after the pretension and anchoring operations, and then to compute the internal forces of each cable at the final state. Moreover, if needed, it allows to design the net in order to sustain the nodal loads and the stretching forces without overloading or loosening any beam.

To determine the cable net configuration, one considers an ideal net having a linear-elastic behaviour, with elements resisting tensile and compressive forces, and fictitious

constraints for preventing the internal nodes displacements. At the boundary each element is subjected to a tensile force for anchoring to the external supporting joints. Hence the external cables undergo some non-null forces, unlike the other ones, which are not stressed.
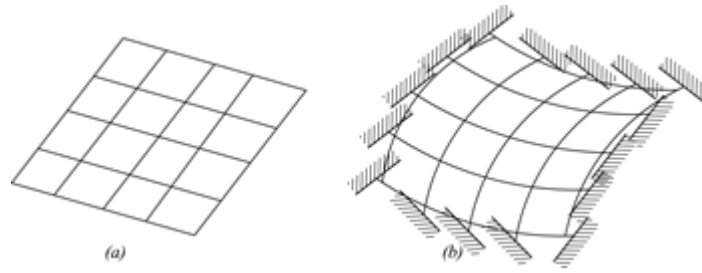
Figure 4.6: Cable net structure;(a) undeformed configuration of the free net; (b) deformed configuration of the constrained net.
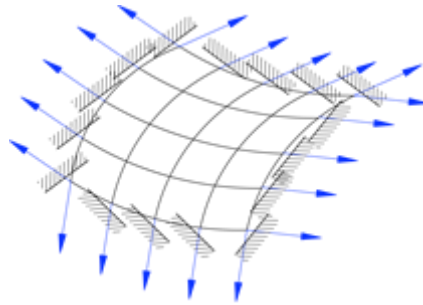
Figure 4.7: Cable net released with redistribution of internal forces.

Assuming that the beams are released then they endure a force redistribution obtaining a new equilibrium configuration of the entire system.

Therefore, the TPE functional Π is computed referring to the pretensioned system, and therefore the contribution of the pretension forces is considered

$$\Pi = U + V = \sum_{i=1}^{m} \left(U_i^o + F_i^o \Delta \ell_i + \frac{E_i A_i}{2 \ell_i^o} \Delta \ell_i^2 \right) - \mathbf{P}^t \mathbf{u} \qquad (4.2.29)$$

where

m is the beams number

U is the elastic energy of the beams

U^o is the elastic energy in the pretensioned cable

F_i^o are the pretensioned forces in the beams and it is $F_i^o = \dfrac{E_i A_i}{\ell_i^o}\left(\ell_i - \ell_i^o\right)$

$\Delta\ell_i$ is the stretching in the ith stressed beam

E_i is the Yong modulus in the ith beam

A_i is the cross-section area of the ith beam

ℓ_i^o is the length of the ith beam not stressed beam

$\mathbf{P}$ is the vector in n components of the nodal forces

$\mathbf{u}$ is the column vector of the nodal displacements components

The problem consists of finding the equilibrium configuration through the minimization of the energy by the *IHA*.

The following condition is checked

$$\nabla\Pi_{i+j}^T \nabla\Pi_{i+j} \leq a \tag{4.2.30}$$

where a is an arbitrary value.

The process is iterative up to the fitting of the criteria.

Once identified the TPE stationary point, represented by $\bar{\mathbf{x}} = \left(\bar{x}_{1x}, \bar{x}_{1y},..., \bar{x}_{jz}\right)$, both the final configuration of the ideal net and the cables' forces can be computed

$$\begin{bmatrix} \overline{X}_{1x} \\ \overline{X}_{1y} \\ \overline{X}_{1y} \\ \vdots \\ \overline{X}_{(j+1)z} \end{bmatrix} = \begin{bmatrix} u_{1x} \\ u_{1y} \\ u_{1z} \\ \vdots \\ u_{(j+1)z} \end{bmatrix} + \begin{bmatrix} \bar{x}_{1x} \\ \bar{x}_{1y} \\ \bar{x}_{1z} \\ \vdots \\ 0 \end{bmatrix} \tag{4.2.31}$$

$$\overline{\mathbf{X}} = \mathbf{u} + \vec{\mathbf{x}} \tag{4.2.32}$$

where

$\overline{\mathbf{X}}$ is the points' positions vector $\overline{\mathbf{X}} = \left(\overline{X}_{1x}, \overline{X}_{1y}, ..., \overline{X}_{(j+1)z}\right)$ related to the final configuration

$\mathbf{u}$ is the column vector $\mathbf{u} = \left(u_{1x}, u_{1y}, ..., u_{(j+1)z}\right)$ of the nodal displacement components

Eq. (4.2.31). (4.2.32) identify the nodes' coordinates of the net related to the assumed final configuration.

The cables' forces are given by

$$
\begin{bmatrix} F_1 \\ \vdots \\ F_i \\ \vdots \\ P_m \end{bmatrix} = \begin{bmatrix} F_1^0 \\ \vdots \\ F_i^0 \\ \vdots \\ F_m^0 \end{bmatrix} + \begin{bmatrix} \dfrac{E_1 A_1}{\ell_1} & & & & \\ & \ddots & & & \\ & & \dfrac{E_i A_i}{\ell_i} & & \\ & & & \ddots & \\ & & & & \dfrac{E_m A_m}{\ell_m} \end{bmatrix} \begin{bmatrix} \Delta\ell_1 \\ \vdots \\ \Delta\ell_i \\ \vdots \\ \Delta\ell_m \end{bmatrix}
\tag{4.2.33}
$$

where $\Delta\ell_1 ... \Delta\ell_m$ are the admissible stretching or shortening depending on $\overline{x}$.

So far, some simplifying hypotheses have been considered for the ideal net, concerned with the linear elasticity of the material, the resistance to tensile and compressive stresses, the possibility of exceeding the admissible forces ($F_{p,i}$).

Since in the real net the forces in the cables cannot exceed the admissible ranges, the following inequality needs should be verified, under the hypothesis of pure tension in the cables

$$
F_{p,i}(\text{lower bound}) \leq F_g \leq f_{p,i}(\text{upper bound})
\tag{4.2.34}
$$

or, in alternative, the following equivalent condition must be verified

$$
\varepsilon_{p,i}(\text{lower bound}) \leq \frac{\Delta\ell_i}{\ell_g^0} \leq \varepsilon_{p,i}(\text{upper bound})
\tag{4.2.35}
$$

which means that the admissible limit ranges of a defining domain must be complied with (ε is the admissible strain in the equivalent condition).

In order to satisfy Eq. (4.2.34)-(4.2.42), the cables length of the ideal net is modified. The process is iterative, changing step by step the length until Eq. (4.2.35) is verified. The process stops when all the cables are in tension, and the obtained value belongs to the limits of the admissible range Eq. (4.2.34).

4.3 Constrained minimization approaches

4.3.1   Basic relationships

Direct constrained optimization methodologies may be developed to evaluate the TPE minimum for a cable structure with m beams and t nodes, where n are free and s fixed respectively, and subject to loads applied only on the free nodes.

Any beam is assumed straight both in its undeformed and deformed configuration, and it undergoes only axial forces (positive if tensile and negative if compressive), under the hypothesis of constant stress and strain in the beam.

The structure (Fig. 4.8) is described in the plane reference system (Oyz), where the generalized nodal displacement components are identified, for the ith node, by v_i and w_i, respectively along the y and z axes and the coupled applied load components are denoted by $P_{y,i}$ and $P_{z,i}$.
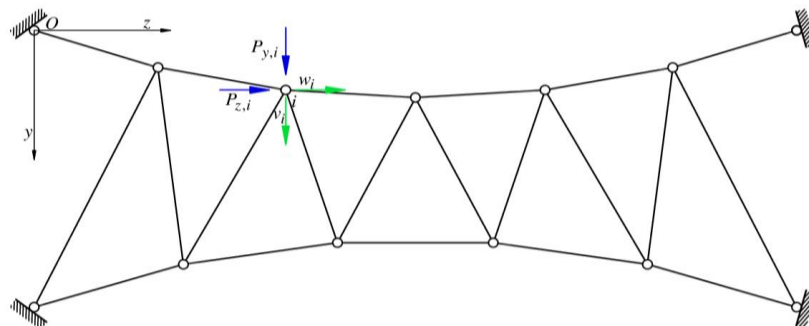
Figure 4.8: Plane cable structure.

The behaviour of each beam is highlighted through the relationship between the axial force and the length variation, for calculating the relevant energy, and then passing to the assembled structure.

4.3.1.1 Single beams' analysis

Let ℓ_{ij}^o be the initial length of the single beam ij connecting the i and j nodes shown in Fig.4.8 in its undeformed and deformed configurations.

Applying the overload **P**, the beam undergoes a configuration change corresponding to the length variation $\Delta\ell_{ij} = \ell_{ij} - \ell_{ij}^o$, where ℓ_{ij} is the updated length.

Consequently, it undergoes an axial force F_{ij}, supposed constant and positive in tension.
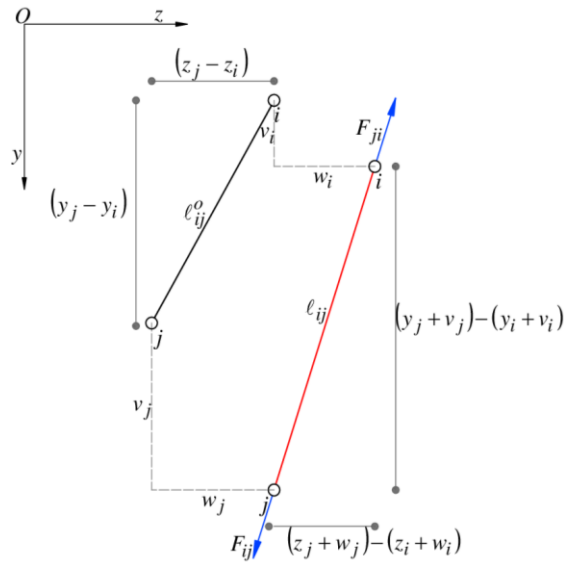
Figure 4.9: Undeformed and deformed beam configuration.

The following relations hold

$$\ell_{ij}^o = -\ell_{ji}^o \tag{4.3.1}$$

$$\ell_{ij}^o = \ell_{ji}^o \tag{4.3.2}$$

$$\ell_{ij} = -\ell_{ji} \tag{4.3.3}$$

$$\ell_{ij} = \ell_{ji} \tag{4.3.4}$$

$$\Delta\ell_{ij} = -\Delta\ell_{ji} \tag{4.3.5}$$

$$\Delta \ell_{ij} = \Delta \ell_{ji} \tag{4.3.6}$$

In particular, the initial ℓ_{ij}^o and final lengths can be explicited in the form

$$\ell_{ij}^o = \sqrt{\left(y_j - y_i\right)^2 + \left(z_j - z_i\right)^2} \tag{4.3.7}$$

$$\ell_{ij} = \sqrt{\left[\left(y_j + v_j\right) - \left(y_i + v_i\right)\right]^2 + \left[\left(z_j + w_j\right) - \left(z_i + w_i\right)\right]^2} \tag{4.3.8}$$

where

$\left(y_i, z_i\right)$ are the coordinates of the i node in the plane reference system

$\left(y_j, z_j\right)$ are the coordinates of the j node in the plane reference system

$\left(v_i, w_i\right)$ are the displacement components at the i node

$\left(v_j, w_j\right)$ are the displacement components at the j node

With reference to constitutive law of the considered material allowing to define the dependence of stress components on the strain ones $\sigma_{ij}\left(\varepsilon_{ij}\right)$, one may write the strain energy cumulated in the beam

$$U_{ij} = \int_V \int_0^{\varepsilon_{ij}} \sigma_{ij}\left(\varepsilon_{ij}\right) d\varepsilon_{ij} dV \tag{4.3.9}$$

which, in case of linear elastic material, turns into

$$U_{ij} = \frac{1}{2}\sigma_{ij}\varepsilon_{ij}A_{ij}\ell_{ij} = \frac{1}{2}E_{ij}\varepsilon_{ij}^2 A_{ij}\ell_{ij} \tag{4.3.10}$$

where

U_{ij} is the strain energy in the deformed beam ij

σ_{ij} is the uniform and constant stress related to the beam ij

ε_{ij} is the uniform and constant strain undergone by the beam ij after the load application

E_{ij} is the Young elasticity modulus of the beam ij depending on the material

A_{ij} the area of the cross-section of the beam ij

or

$$U_{ij} = \frac{1}{2} F_{ij} \Delta \ell_{ij} = \frac{E_{ij} A_{ij}}{\ell_{ij}} \Delta \ell_{ij}^2 \qquad (4.3.11)$$

where

F_{ij} is the internal force in the beam ij

Finally, assuming $h = ij$, the strain energy globally cumulated in the m beams of the structure is given by the sum of the single contributions $U_h = U_{ij}$

$$U = \sum_{h=1}^{m} U_h = \frac{1}{2} \sum_{h=1}^{m} F_h \Delta \ell_h \qquad (4.3.12)$$

The loads' potential energy relevant to the applied nodal loads P_j and the coupled nodal displacements u_j is globally for the n nodes

$$W = -\sum_{j=1}^{n} P_j u_j \qquad (4.3.13)$$

4.3.1.2 Assembled structure's energy

The TPE specialized for the given structure is then

$$\Pi = \frac{1}{2} \sum_{h=1}^{m} F_h \Delta \ell_h - \sum_{j=1}^{n} P_j u_j \qquad (4.3.14)$$

or in compact form

$$\Pi = \frac{1}{2} \mathbf{F}^T \Delta \ell - \mathbf{P}^T \mathbf{u} \qquad (4.3.15)$$

where

$\Delta \boldsymbol{\ell} = \begin{bmatrix} \Delta \ell_1 ... \Delta \ell_m \end{bmatrix}^T$ is the vector of the length variations

$\mathbf{F} = \begin{bmatrix} F_1 ... F_m \end{bmatrix}^T$ is the internal force vector

$\mathbf{u} = \begin{bmatrix} u_1 ... u_n \end{bmatrix}^T$ is the displacement vector of the free nodes

$\mathbf{P} = \begin{bmatrix} P_1 ... P_n \end{bmatrix}^T$ is the applied force vector acting on the free nodes

whence, since the compatibility relation holds $\Delta \boldsymbol{\ell} = \mathbf{Bu}$, with $\mathbf{B}$ the compatibility matrix, and according to the *principle of minimum TPE*

"in the set of displacement fields which satisfy the geometric compatibility, those which locally minimize the TPE also satisfy the equilibrium conditions and are stable equilibrium positions"(*Monforton, 1987*), one can formulate and solve the constrained optimization problem

$$Find \quad \underset{\Delta \boldsymbol{\ell}, \mathbf{u}}{Min} \langle \Pi \rangle = \underset{\Delta \boldsymbol{\ell}, \mathbf{u}}{Min} \left\langle \frac{1}{2} \mathbf{F}^T \Delta \boldsymbol{\ell} - \mathbf{P}^T \mathbf{u} \right\rangle$$

$$Sub \quad \Delta \boldsymbol{\ell} = \mathbf{Bu} \geq \mathbf{0}$$

(4.3.16)

including the condition on the sign of the length variations, which are required to be non negative, thus involving pure stretching.

4.3.2   Solution search

There are many different approaches to solve the constrained optimization problem. Heuristic, meta-heuristic methods can be found in the literature, in order to deal with the high nonlinearity characterizing these kinds of problems in structural engineering field. Here, we focuse on the search of the solution through the Kuhn-Tucker conditions. The main goal is to minimize the objective function observing the chosen and imposed constrained conditions (*Ohkbuco,1987*).

Usually the Kuhn-Tucker conditions are adopted for convex problems and convex constraints, represented by inequalities, equalities (*Rockafeller, 1975*) or both of them.

This approach can be considered as a generalization of the Lagrangian theory about the constrained optimization, and it is based on the use of linear relationship between objective and constraints (*Hanson, Mond, 1987*).

Let consider the differentiable scalar function $f(\mathbf{x})$ and $\mathbf{g}(\mathbf{x})$ the vector function in an open set $\mathbf{x} \in R^n$. Hence let set up the problem

$$Find \quad \underset{\mathbf{x}}{Min} \langle f(\mathbf{x}) \rangle$$

$$Sub \quad \mathbf{g}(\mathbf{x}) \leq \mathbf{0}$$

(4.3.17)

A vector $\boldsymbol{\lambda}_o$ does exist for minimal $\mathbf{x}_o$, such that

$$\nabla f_o(\mathbf{x}_o) + \boldsymbol{\lambda}_o J[\mathbf{g}(\mathbf{x}_o)] = \mathbf{0}$$

$$diag[\boldsymbol{\lambda}_o]\mathbf{g}(\mathbf{x}_o) = \mathbf{0}$$

$$\boldsymbol{\lambda}_o \geq \mathbf{0}$$

(4.3.18)

being $J[\mathbf{g}(\mathbf{x}_o)]$ the Jacobian matrix of $\mathbf{g}(\mathbf{x}_o)$ in $\mathbf{x}_o$.

It is important to put in evidence that in the convex problem the local optimum implies the global one.

4.3.3   The optimization problem and the Kuhn Tucker conditions

Usually the design optimization is defined as the procedure adopted to find the optimal parameters in order to identify the minimum (or the maximum) of the objective function, in the respect of a set of identified constraints.

In Eq.(4.3.16) the objective function identified in the energetic functional Π, the displacements as selected variables, and the imposed constraints are to be managed through Kuhn-Tucker conditions, which, in general yield necessary conditions for a minimum, but, if the involved functions are convex, then they are necessary and sufficient for a global minimum.

The constraints can be represented by the inequalities

$$g_j(x) \leq 0 \qquad \text{with } j = 1,..., p$$

(4.3.19)

and/or the equalities

$$h_r(x) = 0 \qquad \text{with} \quad r=1,...,q \tag{4.3.20}$$

where $g_j(x)$ and $h_r(x)$ are continuous functions endowed with first derivatives, representing the domain where the solution has to be searched for.

As known, the Kuhn- Tucker conditions are based on the linear relationship between the objective function and the constraint functions chosen in order to find the optimum.

These functions are combined in a *Lagrangian Function L*(x) defined as the sum of the objective function and the linear combination of the constrained conditions with unknown multipliers λ_j, μ_r.

Hence, the Lagrangian can be set in the form

$$L(\mathbf{x}, \boldsymbol{\lambda}, \boldsymbol{\mu}) = f(\mathbf{x}) + \sum_j \lambda_j g_j(\mathbf{x}) + \sum_r \mu_r h_r(\mathbf{x}) \tag{4.3.21}$$

and, omitting the explicit dependence on the variables, the Kuhn-Tucker conditions are written as

$$\frac{\partial L}{\partial x_i} = \frac{\partial f}{\partial x_i} + \sum_j \lambda_j \frac{\partial g_j}{\partial x_i} + \sum_r \mu_r \frac{\partial h_r}{\partial x_i} = 0$$

$$\left. \begin{array}{l} \lambda_j g_j = 0 \\ g_j \leq 0 \\ \lambda_j \geq 0 \end{array} \right\} \quad \forall j = 1,..., p \tag{4.3.22}$$

$$h_r = 0 \quad \forall r = 1,..., q$$

being $j=1...p$, $r=1...q$ constraint conditions and $i=1...n$ design variables.

With reference to Eq. (4.3.16), where the objective functional written in function of the main variables **u** is

$$f(\mathbf{u}) = \Pi(\mathbf{u}) = \frac{1}{2}\mathbf{F}^T\mathbf{B}\mathbf{u} - \mathbf{P}^T\mathbf{u} = \sum_{j=1}^{m} U_j(\mathbf{u}) - \mathbf{P}^T\mathbf{u} \tag{4.3.23}$$

the constraint conditions $g_j(\mathbf{u})$ are represented by the following inequalities

$$g_j(\mathbf{u}) = \sum_{s=1}^{n} B_{js}u_s \geq 0 \quad \forall j = 1,..., m \tag{4.3.24}$$

Thus the Lagrangian Function L can be written again in the forms below

$$L(\mathbf{u},\lambda) = \sum_{j=1}^{m} U_j(\mathbf{u}) - \mathbf{P}^T \mathbf{u} + \sum_{j=1}^{m} \lambda_j g_j(\mathbf{u})$$

$$L(\mathbf{u},\lambda) = \frac{1}{2}\sum_{j=1}^{m}\sum_{s=1}^{n}\sum_{t=1}^{n} C_j B_{js} B_{jt} u_s u_t - \sum_{s=1}^{n} P_s u_s + \sum_{j=1}^{m}\sum_{s=1}^{n} \lambda_j B_{js} u_s$$

$$(4.3.25)$$

Now, following Eq. (4.3.22), the Kuhn-Tucker conditions can be applied as follows

$$\frac{\partial L}{\partial u_k} = \sum_{j=1}^{m}\sum_{s=1}^{n} C_j B_{js} B_{jk} u_s - P_k u_k + \sum_{j=1}^{m} \lambda_j B_{jk} = 0 \quad ; \quad k = 1,....,n$$

$$\left.\begin{array}{l} \lambda_j g_j = \sum_{s=1}^{n} \lambda_j B_{js} u_s = 0 \\[2ex] g_j = \sum_{s=1}^{n} B_{js} u_s \geq 0 \\[2ex] \lambda_j \leq 0 \end{array}\right\} \quad \forall j = 1,..., m \qquad (4.3.26)$$

by solving the problem, the design variables $\mathbf{u}$ are computed.

Consequently, by substitution, the stretching and the forces in the beams can be identified, in order to obtain the balanced and compatible configuration subjected to the load and constraint condition considered.

4.4 An example

4.4.1 Initial geometry

With reference to the plane structure in Fig. 4.10, composed by $m = 3$ beams and $t = 4$ nodes, with $s = 3$ fixed and $n = 1$ free nodes, firstly the initial geometry is identified.
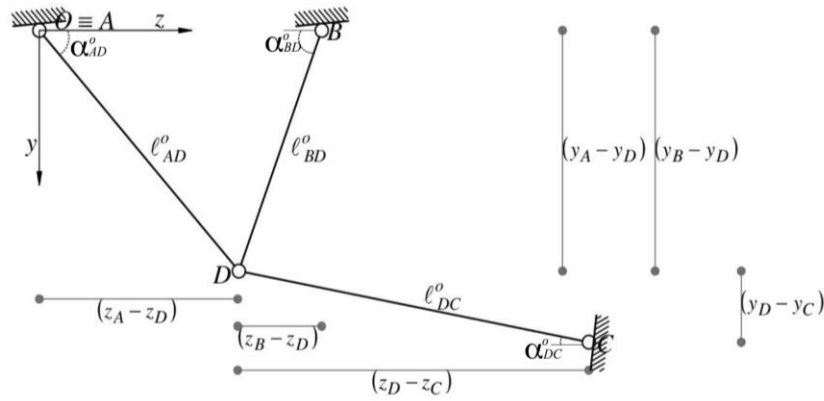
Figure 4.10: No-compression structure composed by m=3 beams, t=4 nodes with n=1 free node and s=3 fixed nodes. The structure is shown in its undeformed configuration in the reference system (Oyz).

The beams (AD, BD, CD), with the initial lengths $\ell^o_{AD}, \ell^o_{BD}, \ell^o_{CD}$, form the angles $\alpha^o_{AD}, \alpha^o_{BD}, \alpha^o_{CD}$ with the horizontal axis, in the reference plane system (*Oyz*).

The following geometric relations hold

$$\begin{aligned}\boldsymbol{\ell}_{AD} &= -\boldsymbol{\ell}_{DA} \\ \ell_{AD} &= \ell_{DA}\end{aligned}$$

(4.4.1 a)

$$\begin{aligned}\boldsymbol{\ell}_{BD} &= -\boldsymbol{\ell}_{DB} \\ \ell_{BD} &= \ell_{DB}\end{aligned}$$

(4.4.1 b)

$$\begin{aligned}\boldsymbol{\ell}_{CD} &= -\boldsymbol{\ell}_{DC} \\ \ell_{CD} &= \ell_{DC}\end{aligned}$$

(4.4.1.c)

with $\ell^o_{AD}, \ell^o_{BD}, \ell^o_{CD}$ the beam vectors in the initial configuration respectively from A to D, B to D and C to D (and hence, by changing the subscripts' positions, from D to A, D to B, D to C) and $\ell^o_{AD}, \ell^o_{BD}, \ell^o_{CD}$ the lengths of the beams AD, BD, CD in the initial configuration.

Since

$$A \equiv (0;0)$$
$$B \equiv (0; z_B)$$
$$C \equiv (y_c; z_C)$$
$$D \equiv (y_D; z_D)$$

(4.4.2)

the length of each beam can be computed

$$\ell^o_{AD} = \sqrt{(y_D - y_A)^2 + (z_D - z_A)^2} = \sqrt{(y_D)^2 + (z_D)^2}$$

(4.4.3 a)

$$\ell^o_{BD} = \sqrt{(y_D - y_B)^2 + (z_D - z_B)^2} = \sqrt{(y_D)^2 + (z_D - z_B)^2}$$

(4.4.3 b)

$$\ell^o_{CD} = \sqrt{(y_D - y_C)^2 + (y_D - y_C)^2}$$

(4.4.3 c)

The length vectors are then given

$$\ell^o_{AD} = \ell^o_{AD} \boldsymbol{\alpha}^o_{AD}$$

(4.4.4 a)

$$\ell^o_{BD} = \ell^o_{BD} \boldsymbol{\alpha}^o_{BD}$$

(4.4.4 b)

$$\ell^o_{CD} = \ell^o_{CD} \boldsymbol{\alpha}^o_{CD}$$

(4.4.4 c)

where

$\boldsymbol{\alpha}^o_{y,AD}, \boldsymbol{\alpha}^o_{y,BD}, \boldsymbol{\alpha}^o_{y,CD}$ are the (2×1) unit vectors of the beams in the reference system, with

components $\alpha^o_{y,AD}, \alpha^o_{y,BD}, \alpha^o_{y,CD}$ and $\alpha^o_{z,AD}, \alpha^o_{z,BD}, \alpha^o_{z,CD}$.

Furthermore, the following boundary conditions hold

$$\begin{cases} v_A = w_A = 0 \\ v_B = w_B = 0 \\ v_C = w_C = 0 \\ v_D \neq 0 \\ w_D \neq 0 \end{cases}$$

(4.4.5)

Moreover

A_{AD} is the cross-section area of the AD beam

A_{BD} is the cross-section area of the BD beam

A_{CD} is the cross-section area of the CD beam

and

E_{AD} is the Young elasticity modulus of the AD beam

E_{BD} is the Young elasticity modulus of the BD beam

E_{CD} is the Young elasticity modulus of the BD beam.

4.4.2   Updated geometry and mechanical features

The analysis is carried out considering the load $\mathbf{P}_D$, with $P_{y,D}, P_{z,D}$ plane components, applied on the free node D, and modulus

$$P_D = \sqrt{P_{y,D}^2 + P_{z,D}^2}$$

(4.4.6)

Due to the overload, the structure undergoes a configuration change moving from the initial geometry to deformed one, as shown in the Fig. 4.11.
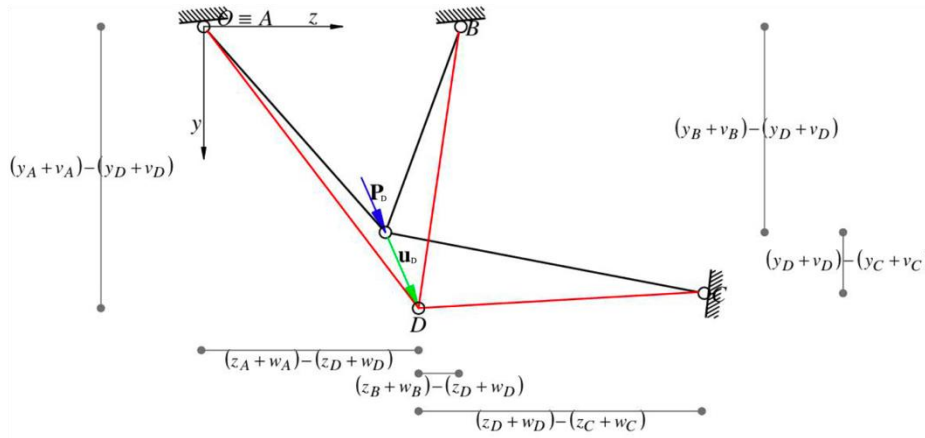
Figure 4.11: Undeformed and deformed configuration of the structure after the load application.

The free node displacement is identified by the vector $\mathbf{u}_D$ with modulus

$$u_D = \sqrt{v_D^2 + w_D^2} \tag{4.4.7}$$

where

v_D is the displacement component of the node D along the y axis

w_D is the displacement component of the node D along the z axis

Consequently the beams undergo the elongations $\Delta\ell_{ij}$ (with ij =AD, BD, CD) given by the difference among the final lengths (ℓ_{ij}, with ij=AD, BD, CD) and the initial ones in Eq. (4.4.3 a-b-c).

First of all, the updated lengths for each element are computed. Starting from AD

$$\ell_{AD} = \sqrt{(y_D + v_D - y_A - v_A)^2 + (z_D + w_D - z_A - w_A)^2} \tag{4.4.8}$$

taking into account the boundary conditions (Eq. 4.4.4) and Eq. (4.4.2), Eq. (4.4.8) can be written again in the following form

$$\ell_{AD} = \sqrt{(y_D + v_D)^2 + (z_D + w_D)^2} \tag{4.4.9}$$

Analogously, the final lengths of the other beams are defined

$$\ell_{BD} = \sqrt{(y_D + v_D - y_B - v_B)^2 + (z_D + w_D - z_B - w_B)^2}$$
$$\ell_{BD} = \sqrt{(y_D + v_D)^2 + (z_D + w_D - z_B)^2}$$

$$\ell_{BD} = \sqrt{(y_D + v_D)^2 + (z_D + w_D - z_B)^2} \tag{4.4.10}$$

$$\ell_{CD} = \sqrt{(y_D + v_D - y_C - v_C)^2 + (z_D + w_D - z_C - w_C)^2}$$
$$\ell_{CD} = \sqrt{(y_D + v_D - y_C)^2 + (z_D + w_D - z_C)^2}$$

$$\ell_{CD} = \sqrt{(y_D + v_D - y_C)^2 + (z_D + w_D - z_C)^2} \tag{4.4.11}$$

The elongations of each beam are inferred

$$\Delta\ell_{AD} = \ell_{AD} - \ell_{AD}^o \tag{4.4.12}$$

$$\Delta\ell_{BD} = \ell_{BD} - \ell_{BD}^o \tag{4.4.13}$$

$$\Delta \ell_{CD} = \ell_{CD} - \ell_{CD}^{o}$$ (4.4.14)

and collected in the vector of variation lengths including the stretching of each beam composing the structure

$$\Delta \boldsymbol{\ell} = [\Delta \ell_{AD}, \Delta \ell_{BD}, \Delta \ell_{CD}]^{T}$$ (4.4.15)

At the same time, the element is undergone by the axial forces

$$\mathbf{F}_{AD} = -\mathbf{F}_{DA}$$
$$F_{AD} = F_{DA}$$ (4.4.16)

$$\mathbf{F}_{BD} = -\mathbf{F}_{DB}$$
$$F_{BD} = F_{DB}$$ (4.4.17)

$$\mathbf{F}_{CD} = -\mathbf{F}_{DC}$$
$$F_{CD} = F_{DC}$$ (4.4.18)

being $\mathbf{F}_{AD}, \mathbf{F}_{BD}, \mathbf{F}_{CD}$ (and hence $\mathbf{F}_{DA}, \mathbf{F}_{DB}, \mathbf{F}_{DC}$) the vectors of the axial forces in each beam and F_{AD}, F_{BD}, F_{CD} the related intensities. Thus, a vector $\mathbf{F}$ including the axial forces is considered

$$\mathbf{F} = [F_{AD}, F_{BD}, F_{CD}]^{T}$$ (4.4.19)

As for the mechanical properties of the elements assuming a linear-elastic behaviour, the strains and the stresses are expressed as follows

$$\varepsilon_{AD} = \frac{\Delta \ell_{AD}}{\ell_{AD}}$$ (4.4.20)

$$\varepsilon_{BD} = \frac{\Delta \ell_{BD}}{\ell_{BD}}$$ (4.4.21)

$$\varepsilon_{CD} = \frac{\Delta \ell_{CD}}{\ell_{CD}}$$ (4.4.22)

and

$$\sigma_{AD} = \frac{F_{AD}}{A_{AD}}$$ (4.4.23)

$$\sigma_{BD} = \frac{F_{BD}}{A_{BD}}$$

(4.4.24)

$$\sigma_{CD} = \frac{F_{CD}}{A_{CD}}$$

(4.4.25)

where

$\varepsilon_{AD}, \varepsilon_{BD}, \varepsilon_{CD}$ are the strains along the axis beams, respectively AD, BD, CD;

$\sigma_{AD}, \sigma_{BD}, \sigma_{CD}$ are the axial stresses in the beams respectively AD, BD, CD.

Specializing the Hooke law for each one element, one gets

$$\sigma_{AD} = E_{AD}\varepsilon_{AD}$$

(4.4.26)

$$\sigma_{BD} = E_{BD}\varepsilon_{BD}$$

(4.4.27)

$$\sigma_{CD} = E_{CD}\varepsilon_{CD}$$

(4.4.28)

hence, the axial forces can be expressed as

$$F_{AD} = \frac{E_{AD}A_{AD}}{\ell_{AD}}\Delta\ell_{AD}$$

(4.4.29)

$$F_{BD} = \frac{E_{BD}A_{BD}}{\ell_{BD}}\Delta\ell_{BD}$$

(4.4.30)

$$F_{CD} = \frac{E_{CD}A_{CD}}{\ell_{CD}}\Delta\ell_{CD}$$

(4.4.31)

4.4.3   Potential energy of the structure

Following the procedure described in Par.4.4.1 to identify the strain energy, denoting by

U_{AD}, U_{BD}, U_{CD} respectively the strain energy of AD, BD and CD beams, and since

$$U_{AD} = e_{AD}A_{AD}\ell_{AD}$$

(4.4.32)

$$U_{BD} = e_{BD}A_{BD}\ell_{BD}$$

(4.4.33)

$$U_{CD} = e_{CD}A_{CD}\ell_{CD}$$

(4.4.34)

being

$$e_{AD} = \int_0^\varepsilon \sigma \cdot \varepsilon d\varepsilon = \frac{1}{2}\sigma_{AD}\varepsilon_{AD} \quad \text{the strain energy density of the beam AD}$$

$$e_{BD} = \int_0^\varepsilon \sigma \cdot \varepsilon d\varepsilon = \frac{1}{2}\sigma_{BD}\varepsilon_{BD} \quad \text{the strain energy density of the beam BD}$$

$$e_{CD} = \int_0^\varepsilon \sigma \cdot \varepsilon d\varepsilon = \frac{1}{2}\sigma_{CD}\varepsilon_{CD} \quad \text{the strain energy density of the beam CD}$$

or in equivalent form

$$U_{AD} = \frac{1}{2}F_{AD}\Delta\ell_{AD} \tag{4.4.35}$$

$$U_{BD} = \frac{1}{2}F_{BD}\Delta\ell_{BD} \tag{4.4.36}$$

$$U_{CD} = \frac{1}{2}F_{CD}\Delta\ell_{CD} \tag{4.4.37}$$

The strain energy of the global structure is given by the sum of each contribution; hence

$$U = U_{AD} + U_{BD} + U_{CD} \tag{4.4.38}$$

$$U = \left(e_{AD}A_{AD}\ell_{AD} + e_{BD}A_{BD}\ell_{BD} + e_{CD}A_{CD}\ell_{CD}\right) \tag{4.4.39}$$

or

$$U = \frac{1}{2}\left(F_{AD}\Delta\ell_{AD} + F_{BD}\Delta\ell_{BD} + F_{CD}\Delta\ell_{CD}\right) \tag{4.4.40}$$

Eq. (4.4.40) can be written again in the following form considering Eq. (4.4.15) and (4.4.19)

$$U = \frac{1}{2}\mathbf{F}^T\Delta\ell \tag{4.4.41}$$

Now let consider the loads' potential energy. Being $\mathbf{P}_D$ the load acting on the free node D, thus the loads' potential is easily calculated

$$W = W_D = -\mathbf{P}_D^T\mathbf{u}_D \tag{4.4.42}$$

where $\mathbf{u}_D$ is previously defined as the vector of the free node displacement.

Now the TPE equation for the global system is expressed by the sum of the global strain and loads' potential energies.

In particular, it is given by

$$\Pi = U + W \tag{4.4.43}$$

Therefore, taking into account Eqs. (4.4.41)-(4.4.42), Eq. (4.4.43) turns into

$$\Pi = \frac{1}{2}\mathbf{F}^T \Delta\ell - \mathbf{P}_D{}^T \mathbf{u}_D \tag{4.4.44}$$

where the main unknown variables are the stretching $\Delta\ell$ and the displacement $\mathbf{u}_D$.

Referring to the minimization of TPE, the variables $\Delta\ell$ and $\mathbf{u}_D$ can be identified by the minimization of the energetic function of the entire system, considering the compatibility equation expressed by the following relation

$$\Delta\ell = \mathbf{B}\mathbf{u}_D \text{ with } \mathbf{u}_D \text{ the displacement vector } \boldsymbol{u}_D = \begin{pmatrix} v_D \\ w_D \end{pmatrix} \tag{4.4.45}$$

$$\begin{pmatrix} \Delta\ell_{AD} \\ \Delta\ell_{BD} \\ \Delta\ell_{CD} \end{pmatrix} = \begin{pmatrix} b_{11} & b_{21} \\ b_{12} & b_{22} \\ b_{13} & b_{23} \end{pmatrix} \begin{pmatrix} v_D \\ w_D \end{pmatrix}$$

being $\mathbf{B}$ the compatibility matrix of $m \times 2n$ size.

Furthermore, the final lengths can be expressed in the following form

$$\Delta\ell_{AD} = \ell_{AD} - \ell^o_{AD} = b_{11}v_D + b_{12}w_D$$
$$\Delta\ell_{BD} = \ell_{BD} - \ell^o_{BD} = b_{21}v_D + b_{22}w_D$$
$$\Delta\ell_{CD} = \ell_{CD} - \ell^o_{CD} = b_{31}v_D + b_{32}w_D$$

Whence

$$\ell_{AD} - \ell^o_{AD} = b_{11}u_D \rightarrow \ell_{AD} = b_{11}v_D + b_{12}w_D + \ell^o_{AD}$$
$$\ell_{BD} - \ell^o_{BD} = b_{21}u_D \rightarrow \ell_{BD} = b_{21}v_D + b_{22}w_D + \ell^o_{BD}$$
$$\ell_{CD} - \ell^o_{CD} = b_{31}u_D \rightarrow \ell_{AD} = b_{31}v_D + b_{32}w_D + \ell^o_{CD}$$

$$\ell = \mathbf{B}\mathbf{u}_D + \ell^o \tag{4.4.46}$$

Then, considering Eq.(4.4.29-31), the vector **F** can be written as

$$\mathbf{F} = \begin{bmatrix} \dfrac{E_{AD}A_{AD}}{\ell_{AD}} \Delta\ell_{AD} \\[2mm] \dfrac{E_{BD}A_{BD}}{\ell_{BD}} \Delta\ell_{BD} \\[2mm] \dfrac{E_{CD}A_{CD}}{\ell_{CD}} \Delta\ell_{CD} \end{bmatrix}$$

After introducing the axial stiffness vector **R**

$$\mathbf{R} = \begin{bmatrix} \dfrac{E_{AD}A_{AD}}{\ell_{AD}} \\[2mm] \dfrac{E_{BD}A_{BD}}{\ell_{BD}} \\[2mm] \dfrac{E_{CD}A_{CD}}{\ell_{CD}} \end{bmatrix}$$

Then

$$\mathbf{F} = diag[\mathbf{R}]\Delta\ell = \mathbf{D}\Delta\ell$$

$$\mathbf{D} = diag[\mathbf{R}] = \begin{bmatrix} \dfrac{E_{AD}A_{AD}}{\ell_{AD}} & 0 & 0 \\[3mm] 0 & \dfrac{E_{BD}A_{BD}}{\ell_{BD}} & 0 \\[3mm] 0 & 0 & \dfrac{E_{CD}A_{CD}}{\ell_{CD}} \end{bmatrix}$$

and

$$\mathbf{F} = \mathbf{DBu}_D \qquad\qquad\qquad (4.4.47)$$

where

F is the axial forces vector with $m{\times}2$ size

B is the compatibility matrix with $m{\times}2n$ size

u$_D$ is the nodal displacements with vector $n{\times}2$ size

D is the stiffness matrix with $m{\times}m$ size

Moreover, by Eq. (4.4.46), the stiffness matrix $\mathbf{D}$ is defined as

$$\mathbf{D} = \begin{bmatrix} \dfrac{E_{AD}A_{AD}}{b_{11}v_D + b_{12}w_D + \ell^o_{AD}} & 0 & 0 \\[3mm] 0 & \dfrac{E_{BD}A_{BD}}{b_{21}v_D + b_{22}w_D + \ell^o_{BD}} & 0 \\[3mm] 0 & 0 & \dfrac{E_{CD}A_{CD}}{b_{31}v_D + b_{32}w_D + \ell^o_{CD}} \end{bmatrix} \qquad (4.4.48)$$

Thus, the optimization problem to find the unknown variables may be set as follows

$$Find \quad \underset{\mathbf{u}_D}{Min}\big\langle \Pi(\mathbf{u}_D)\big\rangle = \underset{\mathbf{u}_D}{Min}\Big\langle \frac{1}{2}\mathbf{F}^T(\mathbf{u}_D)\mathbf{B}\mathbf{u}_D - \mathbf{P}_D^T\mathbf{u}_D \Big\rangle$$

$$(4.4.49)$$

$$Sub \quad \mathbf{B}\mathbf{u}_D \geq \mathbf{0}$$

Therefore, taking into account Eq. (4.4.47), and by substituting into Eq. (4.4.49), one obtains the following expression of the $\Pi(\mathbf{u}_D)$

$$\Pi(\mathbf{u}_D) = \frac{1}{2}\big\{\mathbf{D}[\mathbf{B}\mathbf{u}_D]\big\}^T(\mathbf{B}\mathbf{u}_D) - \mathbf{P}_D^T\mathbf{u}_D \qquad (4.4.50)$$

which is a non-linear equation in the displacements unknown variables.

Hence, making it explicit, one gets

$$\Pi(\boldsymbol{u}_D) = \frac{1}{2}\left\{\begin{bmatrix} \dfrac{E_{AD}A_{AD}}{b_{11}v_D + \ell^o_{AD}} & 0 & 0 \\[2mm] 0 & \dfrac{E_{BD}A_{BD}}{b_{21}u_D + \ell^o_{BD}} & 0 \\[2mm] 0 & 0 & \dfrac{E_{CD}A_{CD}}{b_{31}v_D + b_{32}w_D + \ell^o_{CD}} \end{bmatrix} \begin{bmatrix} b_{11} & b_{21} \\ b_{12} & b_{22} \\ b_{13} & b_{23} \end{bmatrix}\begin{pmatrix} v_D \\ w_D \end{pmatrix}\right\}^T \left(\begin{bmatrix} b_{11} & b_{21} \\ b_{12} & b_{22} \\ b_{13} & b_{23} \end{bmatrix}\begin{pmatrix} v_D \\ w_D \end{pmatrix}\right) - P_{Dy}v_D - P_{Dz}W_D$$

$$\Pi(\boldsymbol{u}_D) = \frac{1}{2}\left\{\begin{bmatrix} \dfrac{E_{AD}A_{AD}}{b_{11}v_D + b_{12}w_D + \ell^o_{AD}} & 0 & 0 \\[2mm] 0 & \dfrac{E_{BD}A_{BD}}{b_{21}v_D + b_{22}w_D + \ell^o_{BD}} & 0 \\[2mm] 0 & 0 & \dfrac{E_{CD}A_{CD}}{b_{31}v_D + b_{32}w_D + \ell^o_{CD}} \end{bmatrix} \begin{bmatrix} b_{11}v_D + b_{12}w_D \\ b_{21}v_D + b_{22}w_D \\ b_{31}v_D + b_{32}w_D \end{bmatrix}\right\}^T \begin{bmatrix} b_{11}v_D + b_{12}w_D \\ b_{21}v_D + b_{22}w_D \\ b_{31}v_D + b_{32}w_D \end{bmatrix} - P_{Dy}v_D - P_{Dz}W_D$$

$$\Pi(\boldsymbol{u}_D) = \frac{1}{2}\left\{\begin{bmatrix} \dfrac{E_{AD}A_{AD}}{b_{11}v_D + b_{12}w_D + \ell^o_{AD}}(b_{11}v_D + b_{12}w_D) \\[2mm] \dfrac{E_{BD}A_{BD}}{b_{21}v_D + b_{22}w_D + \ell^o_{BD}}(b_{21}v_D + b_{22}w_D) \\[2mm] \dfrac{E_{CD}A_{CD}}{b_{31}v_D + b_{32}w_D + \ell^o_{CD}}(b_{31}v_D + b_{32}w_D) \end{bmatrix}\right\}^T \begin{bmatrix} b_{11}v_D + b_{12}w_D \\ b_{21}v_D + b_{22}w_D \\ b_{31}v_D + b_{32}w_D \end{bmatrix} - P_{Dy}v_D - P_{Dz}W_D$$

$$\Pi(\boldsymbol{u}_D) = \frac{1}{2}\left\{\left[\begin{array}{c} \dfrac{E_{AD}A_{AD}}{b_{11}v_D + b_{12}w_D + \ell^o_{AD}}(b_{11}v_D + b_{12}w_D) \\ \dfrac{E_{BD}A_{BD}}{b_{21}v_D + b_{22}w_D + \ell^o_{BD}}(b_{21}v_D + b_{22}w_D) \\ \dfrac{E_{CD}A_{CD}}{b_{31}v_D + b_{32}w_D + \ell^o_{CD}}(b_{31}v_D + b_{32}w_D) \end{array}\right]^T \left[\begin{array}{c} b_{11}v_D + b_{12}w_D \\ b_{21}v_D + b_{22}w_D \\ b_{31}v_D + b_{32}w_D \end{array}\right] - P_{Dy}v_D - P_{Dz}w_D \right\}$$

$$\Pi(\boldsymbol{u}_D) = \frac{1}{2}\left[\begin{array}{c} \dfrac{E_{AD}A_{AD}}{b_{11}v_D + b_{12}w_D + \ell^o_{AD}}(b_{11}v_D + b_{12}w_D)^2 + \dfrac{E_{BD}A_{BD}}{b_{21}v_D + b_{22}w_D + \ell^o_{BD}}(b_{21}v_D + b_{22}w_D)^2 + \\ + \dfrac{E_{CD}A_{CD}}{b_{31}v_D + b_{32}w_D + \ell^o_{CD}}(b_{31}v_D + b_{32}w_D)^2 \end{array}\right] - P_{Dy}v_D - P_{Dz}w_D$$

$$(4.4.51)$$

With

$$\left(b_{11}u_D + \ell^o_{AD}\right)\left(b_{21}u_D + \ell^o_{BD}\right)\left(b_{31}u_D + \ell^o_{CD}\right) \neq 0 \ ^{[18]} \qquad (4.4.52)$$

By solving the inequalities, the range of the admissible values of the design variables is identified, also by applying Kuhn-Tucker conditions.

---

[18]

$$\left(b_{11}u_D + \ell^o_{AD}\right)\left(b_{21}u_D + \ell^o_{BD}\right)\left(b_{31}u_D + \ell^o_{CD}\right) > 0$$

$$b_{11}b_{21}b_{31}u^3_D + b_{11}u_D\ell^o_{BD}\ell^o_{CD} + b_{21}u_D\ell^o_{AD}\ell^o_{CD} + b_{31}u_D\ell^o_{AD}\ell^o_{BD} + \ell^o_{AD}b_{21}b_{31}u^2_D +$$
$$+ \ell^o_{AD}\ell^o_{BD}\ell^o_{CD} + \ell^o_{BD}b_{31}b_{11}u^2_D + \ell^o_{CD}b_{11}b_{21}u^2_D \neq 0$$

$$b_{11}b_{21}b_{31}u^3_D + u^2_D\left(\ell^o_{AD}b_{21}b_{31} + \ell^o_{BD}b_{31}b_{11} + \ell^o_{CD}b_{11}b_{21}\right) + u_D\left(b_{11}\ell^o_{BD}\ell^o_{CD} + b_{21}\ell^o_{AD}\ell^o_{CD} + b_{31}\ell^o_{AD}\ell^o_{BD}\right) +$$
$$+ \ell^o_{AD}\ell^o_{BD}\ell^o_{CD} \neq 0$$

$$u_D[(b_{11}b_{21}b_{31}u^2_D) + (\ell^o_{AD}b_{21}b_{31} + \ell^o_{BD}b_{31}b_{11} + \ell^o_{CD}b_{11}b_{21})u_D + (b_{11}\ell^o_{BD}\ell^o_{CD} + b_{21}\ell^o_{AD}\ell^o_{CD} + b_{31}\ell^o_{AD}\ell^o_{BD})] +$$
$$+ \ell^o_{AD}\ell^o_{BD}\ell^o_{CD} \neq 0$$

$$u_D \neq 0$$

by assuming

$$h = (\ell^o_{AD}b_{21}b_{31} + \ell^o_{BD}b_{31}b_{11} + \ell^o_{CD}b_{11}b_{21})$$
$$a = b_{11}b_{21}b_{31}$$
$$c = (b_{11}\ell^o_{BD}\ell^o_{CD} + b_{21}\ell^o_{AD}\ell^o_{CD} + b_{31}\ell^o_{AD}\ell^o_{BD})$$

$$u_D = h \pm \sqrt{\frac{h^2 - 4ac}{2a}} \neq 0$$

The results, with the horizontal force equal to 10.000 N, are illustrated in the following figures, where the displacements are plotted with a amplification factor set to 10÷20.

Fig. 4.12a illustrates the system with all members fully reacting both in tension and compression, subject to the force P_{Dx} = 10 kN applied on node D, with the equilibrium configuration resulting from the small displacement analysis (Fig. 4.12b) and from iterated calculations converging towards true displacements results (Fig. 4.12c).

(a)   *(b)*   *(c)*
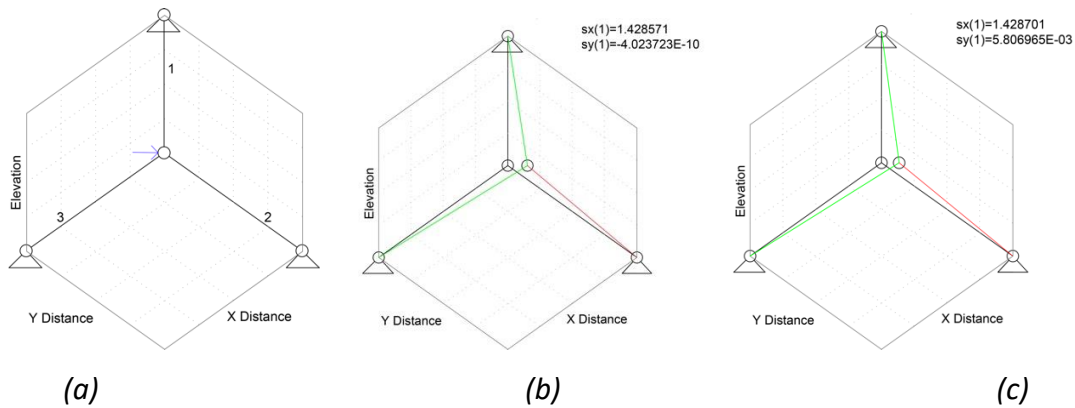
Figure. 4.12: Solutions with all bilaterally active members: a) The structural pattern; b) the small displacement solution; c) the iterated solution for effective, possibly large displacements. Amplifications of displacements are equal to 20.

One should notice that the rods plotted in green are in tension while the rods in red are compressed. The solution for small displacements is practically coincident with the effective displacements' one.

The second set of results solves the problem set in Eq.(4.4.49) -(4.4.50), corresponding to the case when the system is composed of cables that cannot resist compression. The results are depicted in Fig. 4.13.

sx(1)=4.284505
sy(1)=-1.427967

sx(1)=4.062129
sy(1)=-1.326584

(a)   (b)
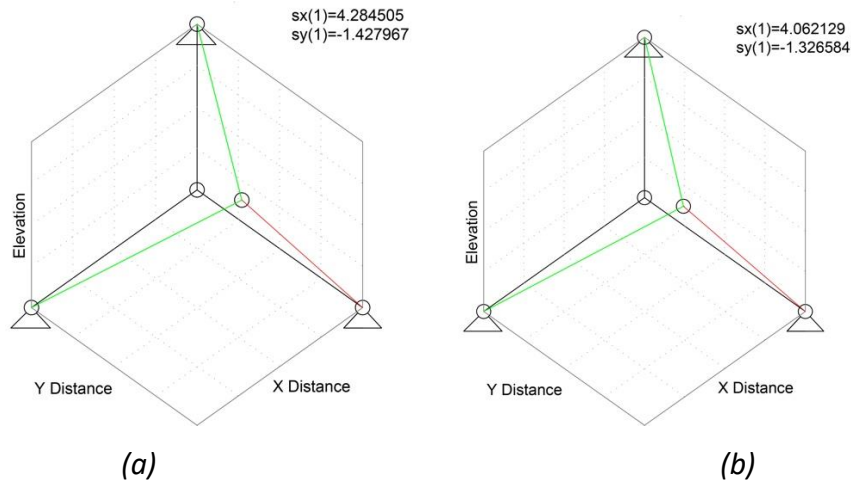
Figure 4.13; Solutions with all members unable to resist compression. a) the small displacement solution; b) the iterated solution for effective displacements. The green rods are in tension and are selected as effectively reactive. The red rod is acted on by a negligible force and does not actually contribute to equilibrium. Amplifications of displacements are equal to 10.

The final set of results considers the system composed by rods that cannot resist tension, i.e. solves the problem minimizing the energy functional in Eq.(4.4.49) but with the reversed constraint **Bu ≤ 0**. The relevant results are depicted in Fig. 4.14.

sx(1)=4.284505
sy(1)=1.427967

sx(1)=4.572097
sy(1)=1.557134

(a)   (b)
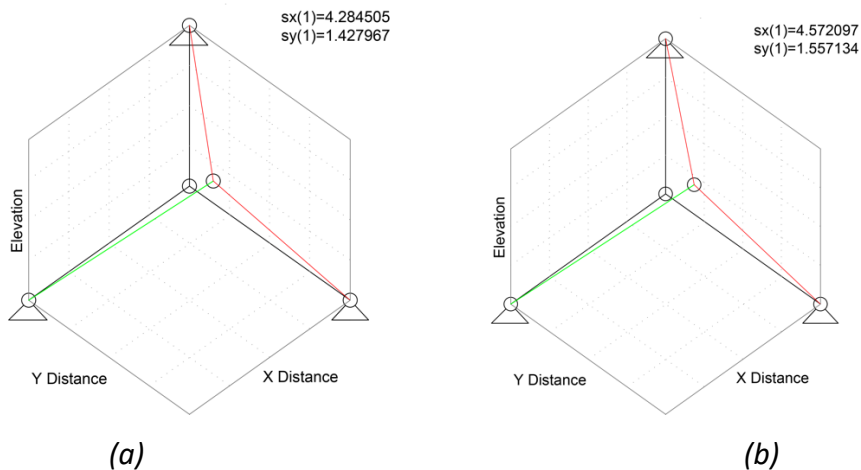
Fig. 4.14: Solutions with all members unable to resist tension. a) the small displacement solution; b) the iterated solution for effective displacements. The red rods are compressed and are selected as effectively reactive. The green rod is acted on by a negligible force and does not actually contribute to equilibrium. Amplifications of displacements are equal to 10.

The equilibrium paths of the different structural patterns are summarized in the following table

TABLE 4.4.1

Rods→	Bilateral		No-tension		No-compression	
Geometry→	Small	Actual	Small	Actual	Small	Actual
s_x (cm)	1.428	1.428	4.284	4.572	4.284	4.062
s_y(cm)	≈0	≈0	1.427	1.557	1.427	1.326
F_1 (N)	≈0	≈0	-10000	-10425	10000	9622
F_2 (N)	-7071	-7042	-14142	-14549	≈0	≈0
F_3 (N)	7071	7099	≈0	≈0	14142	13784

As one can deduct from the observation of the results, in the case of system unable to resist compression the change in the geometry improves the stiffness and the strength of the structure, so that in this case the small displacement analysis is on the safe side, while the opposite happens in the case of the no-tension system.

5. CALCULUS MODEL UNDER LARGE DISPLACEMENTS FOR CABLE STRUCTURES

5.1 Introduction

As highlighted in Chapter 1, in recent years cables as structural elements have been largely employed in architectonical and engineering buildings, both for the aesthetic quality and structural advantages (*Thai, Kim,2011*) such as the lightness, the elastic behaviour, the possibility of pretensioning, covering large spans and using minimum amounts of material with the maximum exploitation of the mechanical properties.

Cable systems are usually adopted as simple cables' systems for supporting structures for membrane roofs, shells or cable stayed bridges, as opposite curvature cable structures for big spans, and as cable-nets systems again for large spans' covering, as well as for supporting systems of glazed façades.

As known, these systems belong to the macro-category of tensile structures where purely tensile forces are involved (cables, membranes, cable and membrane structures, tensairity).

Although the many advantages, their geometric and/or mechanical non-linearity influences the response to the external actions making hard the static analysis. This is the main motivation of the increasing interest of researchers, who, starting from the identification of rigorous methods of modern mechanics for equilibrium, have been developing several approaches to identify the equilibrium shape of these structural systems both under the overloads and the pretension state.

For computational purposes, novel models have been proposed as well in matrix formulation basically falling under the displacements' and forces' approaches.

Usually, the most adopted models refer to the displacements' method, where the stiffness matrix is obtained by the assemblage operation. One demonstrated that this approach is careful about the structural analysis and it can be used for several shapes, load and constraint conditions (*Lan,1999*).

Actually, the analysis models can be divided in two typologies; those ones based on the classical formulation of the elastic catenary and those ones based on the discretization of the structure in finite elements.

In the first case, the equilibrium state of the continuum element suspended at the ends is mainly considered and analysed; it is important to highlight as the catenary approaches allow to identify the response of the structure also in case of seismic solicitations (*Abad et al, 2012*). One must put in evidence that the catenary approach is appropriate for very small curvatures (*Thai, Kim,2011*).

As concerns the discrete approaches the basic idea is to model the cables as composed of many segments connected to each other by joints. Consequently, different loads can be applied along the single segments, or at the joints, also considering lateral or not uniformly distributed loads, taking into account the geometric and mechanical non linearity, like for example the cross-section variation and the material resistance. In this case a higher number of the elements is required with respect to the first formulation (*Shoostari et al,2013*).

In the literature several approaches based on the catenary modelling of the cable can be found as for example the methods developed by O'Brien e Francis (*O' Brien e Francis, 1964*) and then by Jayaraman e Knudson (*Jayaraman e Knudson, 1981)*;

Recently some researchers have identified and characterized the tangent stiffness matrices and the internal forces vectors of the cables taking into account the self-weight of the cable, usually neglected both in the static and dynamic analyses.

Many other similar methods have been adapted to the specific problems, based on and rielaborating the equations of elastic catenary, minimizing the computational time, as those ones developed by Whang (*Whang et al, 2006*), Andreu (*Andreu et al, 2006*), Yang e Tsay (*Yang e Tsay, 2007*), Such (*Such et al, 2009*).

Other methodologies are based on FE approaches, refer to interpolation functions in order to describe the nonlinear behaviour of the structures both in continuum and discrete cases.

The continuum approach is largely used for small deflection cables with high level of pretension; the discrete one, instead, is largely applicable and is based on the use of

higher degree polynomials for the interpolation functions (*Chen et al., 2010*). Nevertheless, the formulation is hardest and then the tangent stiffness matrix and the internal forces vectors are obtained through isoparametric interpolation functions, by using the same number of parameters to describe the geometry and to interpolate.

The latter model is not properly appropriate to apply for great curvature cables, because, otherwise, it would imply a high number of elements increasing the computational effort (*Thai, Kim,2011*).

To evaluate the static behaviour of plane cable structures with opposite curvature, one largely refers to the FEM modeling and analysis.

In order to define the equilibrium configuration both in pretension and under the external loads, equilibrium and compatibility equations are solved by iterative processes, considering some simplifying hypotheses such as the possibility to neglect the terms with degree greater than one in the equilibrium equations and the self-weight of the beams.

In case of cable nets, after identified the geometry, their behaviour is analized, or considering them as three-dimensional discrete elements composed by several cables connected to each other and subject to nodal loads, or approximating their behaviour to the membrane one.

5.2 Plane systems

Adapting the considerations presented in Par.3.3 to plane systems, one may search for equilibrium shapes under live loads acting in the plane. Some results are illustrated for the cable system with opposite curvature in Fig. 5.1 loaded by in-plane nodal forces, after implementation of the relevant problem in a calculus code. In Fig.5.2 - 5.3 depicted results refer, respectively, to the application of the load components $P_y = 1$ and $P_x = 1$, with the force density ratio 1:1.
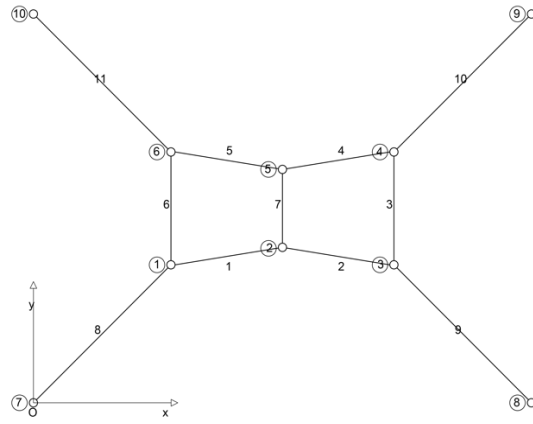
Figure 5.1: Topology scheme of a plane system.
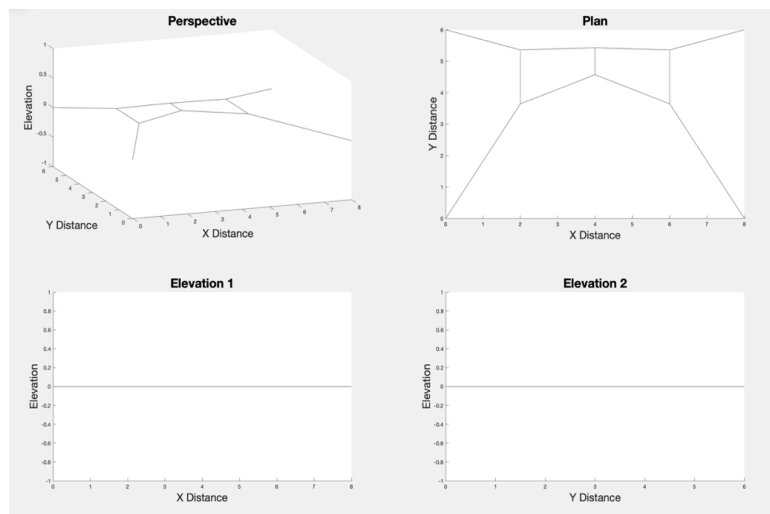
Figure 5.2: Equilibrium shape under the load $P_y=1$.
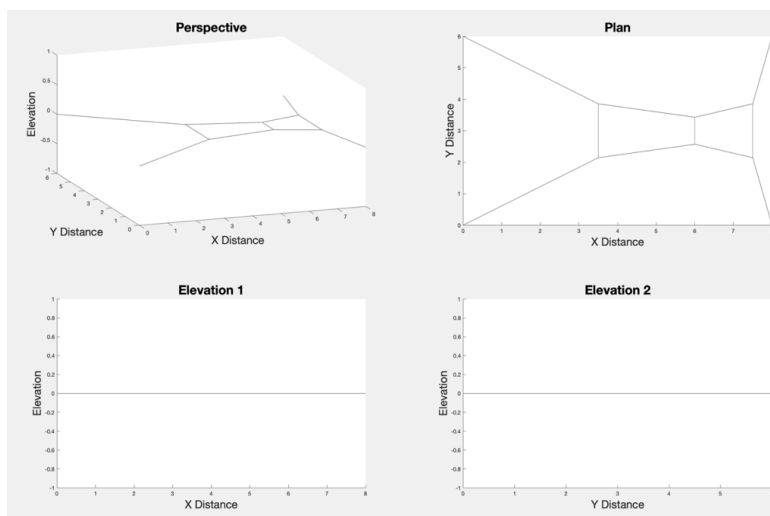
Figure 5.3: Equilibrium shape under the load $P_x=1$.
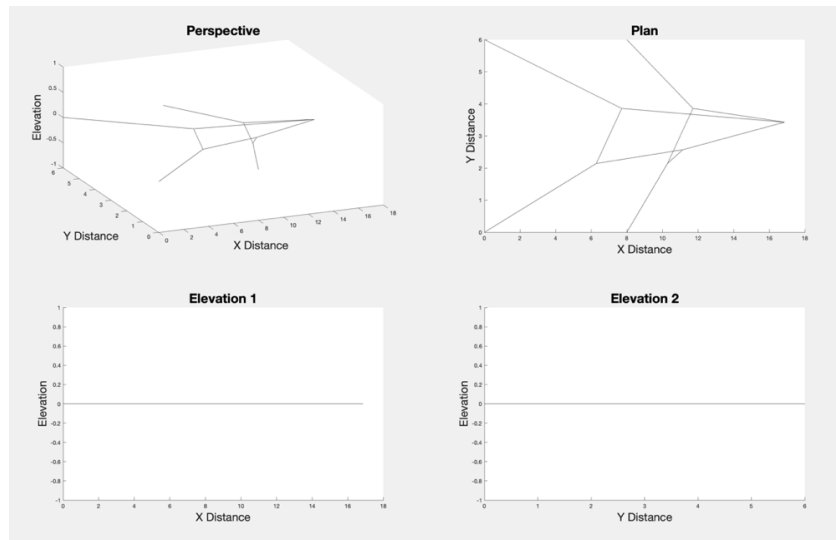
Figure 5.4: Equilibrium shape under the load $P_x=20$.

One also considers the case when the load $P_x = 20$ is applied on the node previously identified (node 5) determining the configuration shown in Fig.5.4. The ratio of the force density is 1:1.

In Fig.5.5 the shape due to the application of the loads $P_z=20$ and it is applied in the positive direction of z axis) only on the free node 5.
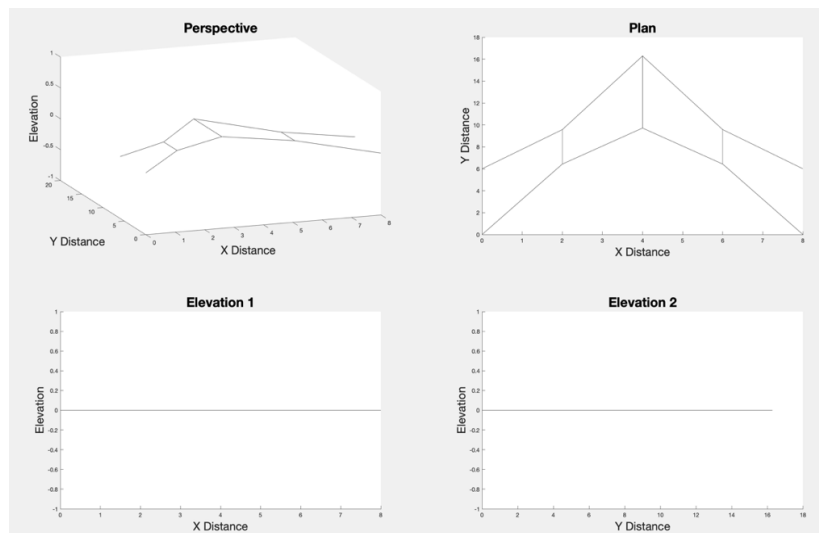
Figure 5.5: Equilibrium shape applying the load $P_z=20$

5.2.1 An overview of the basic approach

In this context, for analysing the static response of cable structures under external solicitations, the study and development of a calculus model suitable for the several typologies of tensile structures is focused on.

The approach is based on a matrix formulation in order to be then applied and developed, in the subsequent phase, on a structure composed by m cables, subject to the nodal loads and distorcing actions, where the self-weight of the elements is reported on the joints and the cables are considered straight both in the deformed and undeformed configurations.

The analysis is conducted in elastic field, thus initially neglecting the mechanical non-linearity of the elements, in order to identify the fundamental relationships in matrix form under large displacement.

The problem is started from a known static regime configuration, whence variations to displacements and distortions are applied leading to updating the structural configuration.

The first phase of this analysis is mainly devoted to the search and identification of the nonlinear geometric relation, in explicit form, between the balancing loads, necessary for the equilibrium in the varied configuration, and the applied displacements.

Two subsequent steps follow, referred to the single elements and the global structure.

In the single elements' analysis, the local variables and the main relations are introduced and identified, and, in particular, the relationship is inferred between the variation of the internal forces and of the positions of the free nodes of the element, expressed through the identification of the secant stiffness matrix, the secant geometric matrix and the secant distortions vector.

The second step concerns the transition to the global structure through an assembling procedure of the results from the first step, aiming at setting the relation of loads

ensuring the equilibrium in the deformed configuration, after the displacements' and distortions' application.

It must be pointed out that the fundamental identified equation is geometrically nonlinear, therefore a step by step procedure is developed to solve it under small loads' variations, that allow the linearization of the equation at any infinitesimal single step.

First of all, let consider a plane structure composed by *m* segments and *n* free joints in a known static regime. Starting form this configuration, a displacement $\Delta\mathbf{X}$ and distortion field $\Delta\mathbf{D}$ are applied in order to determine a change in the configuration of the structure, that may occur under the following three conditions:

- $\Delta\varepsilon = \dfrac{\Delta\ell}{\ell} \ll 1$, i.e. the deformations are very small

- Any segment has a linear elastic behaviour, thus the Hooke law holds

- The self-weight of the elements is neglected, and they are straight both in the undeformed and deformed configurations

In this phase, the analysis focuses on the identification of the load variation $\Delta\mathbf{P}(\Delta\mathbf{X})$ that ensures the equilibrium in the deformed configuration.

The single element is considered to identify the relation between internal forces and change of position at the free ends, through the introduction and definition of the stiffness secant elastic and geometric matrices[19] and the secant distortion vector, at the local level of the cable segment.

A non-linear equation is obtained, where the introduced entities depend on the imposed displacements.

To obtain the balancing loads' variation $\Delta\mathbf{P}(\Delta\mathbf{X})$, the assemblage of the system is performed introducing the Boolean matrix $\mathbf{A}$ depending only on the topology of the structure and where also the constraints are introduced.

---

[19] The matrices are defined as secant to put in evidence the dependence of the forces amplitude on the elements' stretching.

Finally, the relation between loads and displacements is identified

$$\Delta \mathbf{P} = \mathbf{K}_E^* \Delta \mathbf{U} + \mathbf{K}_G^* \Delta \mathbf{U} - \mathbf{Q} \Delta \mathbf{D} \qquad (5.2.1)$$

where $\mathbf{K}_E^*(\Delta \mathbf{X})$ denotes the elastic and $\mathbf{K}_E^*(\Delta \mathbf{X})$ the geometric stiffness matrix, and distortional secant one $\mathbf{Q}^*(\Delta \mathbf{X})$ of the global structure, depending on the imposed displacements. The identification of the mentioned matrixes and the solution procedure are illustrated in the following paragraphs.

5.2.1.1 Fundamental relationships

Let consider the plane cable structure shown in Fig.5.6, composed by $m = 11$ cables and $n = 6$ free nodes, and four fixed ends; let assume that the structure is in a known static regime.
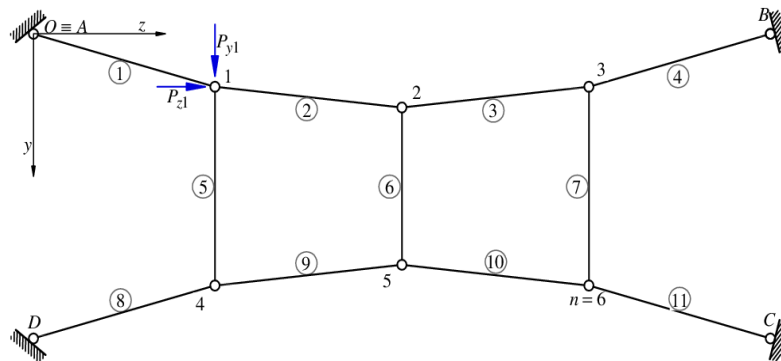
Figure 5.6: Cable structure under the application of nodal loads, in its known configuration in the plane (Oyz).

Let identify the following vectors in the place reference system (*Oyz*)

$$\mathbf{P}^T = \begin{bmatrix} P_{y1} & P_{z1} & P_{y2} & P_{z2} & \dots & \dots & P_{yn} & P_{zn} \end{bmatrix}$$
$$\mathbf{X}^T = \begin{bmatrix} y_1 & z_1 & y_2 & z_2 \dots & \dots y_n & z_n \end{bmatrix} \qquad (5.2.2)$$

$$\mathbf{F}^T = \begin{bmatrix} F_1 & F_2 & \dots & F_h & \dots & F_m \end{bmatrix}$$
$$\mathbf{D}^T = \begin{bmatrix} D_1 & D_2 & \dots & D_h & \dots & D_m \end{bmatrix} \qquad (5.2.3)$$

In the following the single cable segment is identified by the indexes of the end nodes ij (directed from i to j) rather than by the h index relevant to the hth element, that means for example $F_{56} = F_{10}$, $D_{56} = D_{10}$.

Let $\mathbf{P}^o$, $\mathbf{X}^o$, $\mathbf{F}^o$, $\mathbf{D}^o$ be the static and geometric entities describing the initial configuration Σ^o. One aims at finding the increment of the external loads $\Delta\mathbf{P}(\Delta\mathbf{X})$ necessary to keep the equilibrium in the new configuration, caused by the application of the geometry change $\Delta\mathbf{X}$ and possible additional distortions $\Delta\mathbf{D}$.

By assuming valid the hypotheses in Par. 5.2.1[20] , one denotes by

$\mathbf{f}_{ij}$ the force transmitted by the node i to the end node j in the beam ij.

$\mathbf{f}_{ji}$ the force transmitted by the node j to the end node i of the beam ij, such that $\mathbf{f}_{ij} = -\mathbf{f}_{ji}$ and $F_{ij} = F_{ji}$

F_{ij} the component $h = ij$ of the vector $\mathbf{F}_h$, representing the intensity of the force $\mathbf{f}_{ji}$

$\mathbf{f}_{ij}^o$ the force transmitted by the node i to the end node j in the beam ij inΣ^o

$\mathbf{f}_{ji}^o$ the force transmitted by the node j to the end node i of the beam ij in Σ^o , such that $\mathbf{f}_{ji}^o = -\mathbf{f}_{ij}^o$ and $F_{ji}^o = F_{ij}^o$

F_{ij}^o the component $h = ij$ of the vector $\mathbf{F}_h^o$, representing the intensity of the force $\mathbf{f}_{ij}^o$

For solving the problem, let firstly consider the element ij shown in Fig. 5.7.

---

[20] The deformations of all elements are small $\Delta\varepsilon = \dfrac{\Delta\ell}{\ell} << 1$.

The Hooke law is assumed valid; each cable segment is and keeps straight also in the deformed configuration.
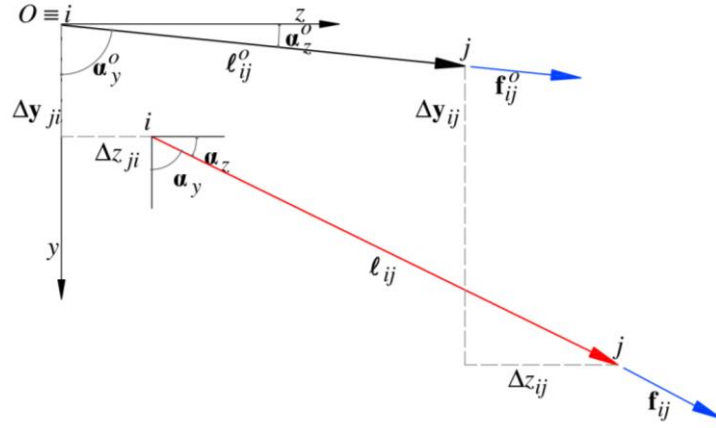
Figure 5.7: Undeformed and deformed configuration of the single element in the plane (Oyz).

The change of configuration from the initial known one Σ^o to the deformed one Σ is described by the difference vector

$$\Delta\mathbf{x}^d_{ij} = \begin{bmatrix} \Delta y_{ij} - \Delta y_{ji} \\ \Delta z_{ij} - \Delta z_{ji} \end{bmatrix} \tag{5.2.4}$$

whence

$$\ell_{ij} = \ell^o_{ij} + \Delta\mathbf{x}^d_{ij} \tag{5.2.5}$$

$$\Delta F_{ij} = \frac{E_{ij}A_{ij}}{\ell^\circ_{ij}}\left(\Delta\ell_{ij} - \Delta D_{ij}\right) = R_{ij}\left(\Delta\ell_{ij} - \Delta D_{ij}\right) \tag{5.2.6}$$

where

ℓ_{ij} is the length vector of the single cables in the deformed configuration directed from i to j

ℓ_{ji} is the length vector of the single cable in the deformed configuration directed from j to i, and such that $\ell_{ij} = -\ell_{ji}$ and $\ell_{ij} = \ell_{ji}$

ℓ_{ij} is the length of the beam ij in the deformed configuration

$\boldsymbol{\ell}_{ij}^o$ is the length vector of the single cable in the initial configuration, directed from i to j

$\boldsymbol{\ell}_{ji}^o$ is the length vector of the single cable directed form j to i, in the undeformed configuration, such that $\boldsymbol{\ell}_{ij}^o = -\boldsymbol{\ell}_{ij}^o$ and $\ell_{ij}^o = \ell_{ij}^o$

ℓ_{ij}^o is the initial length of the beam

ΔF_{ij} is the intensity of the force variation in the element

E_{ij} is the elasticity modulus of the element

A_{ij} is the cross section area of the element

$\Delta\ell_{ij}$ is the length variation of the element

ΔD_{ij} is the intensity of the distortion variation in the element

R_{ij} is the stiffness of the beam

One highlights that dependence by $\Delta\mathbf{x}_{ij}^d$ is omitted.

Let now consider the unit vector associated to the segment in the two configurations

$$
\begin{aligned}
\boldsymbol{\alpha}_{ij}^o &= \frac{\boldsymbol{\ell}_{ij}^o}{\ell_{ij}^o} = \begin{bmatrix} \alpha_{ij,y}^o \\ \alpha_{ij,z}^o \end{bmatrix} \quad in \ \Sigma^o \\
\boldsymbol{\alpha}_{ij} &= \frac{\boldsymbol{\ell}_{ij}}{\ell_{ij}} = \begin{bmatrix} \alpha_{ij,y} \\ \alpha_{ij,z} \end{bmatrix} \quad in \ \Sigma
\end{aligned}
\tag{5.2.7}
$$

whence the force vector $\mathbf{f}_{ij}$ can be expressed in the form

$$
\begin{aligned}
\mathbf{f}_{ij} &= F_{ij}\boldsymbol{\alpha}_{ij} = \left(F_{ij}^o + \Delta F_{ij}\right)\left(\boldsymbol{\alpha}_{ij}^o + \Delta\boldsymbol{\alpha}_{ij}\right) = \mathbf{f}_{ij}^o + \Delta F_{ij}\boldsymbol{\alpha}_{ij}^o + F_{ij}^o\Delta\boldsymbol{\alpha}_{ij} + \Delta F_{ij}\Delta\boldsymbol{\alpha}_{ij} \\
\Delta\mathbf{f}_{ij} &= \mathbf{f}_{ij} - \mathbf{f}_{ij}^o = \Delta F_{ij}\boldsymbol{\alpha}_{ij}^o + F_{ij}^o\Delta\boldsymbol{\alpha}_{ij} + \Delta F_{ij}\Delta\boldsymbol{\alpha}_{ij}
\end{aligned}
\tag{5.2.8}
$$

Analogously Eq. (5.2.5) can be written again in the form

$$\ell_{ij} = \ell_{ij}^o + \Delta\mathbf{x}_{ij}^d$$
$$\ell_{ij}\boldsymbol{\alpha}_{ij} = \ell_{ij}^o\boldsymbol{\alpha}_{ij}^o + \Delta\mathbf{x}_{ij}^d$$

(5.2.9)

And therefore the elongation is inferred [21]

$$\Delta\ell_{ij} = \ell_{ij} - \ell_{ij}^o = \boldsymbol{\alpha}_{ij}^{oT}\Delta\mathbf{x}_{ij}^d + \Delta\boldsymbol{\alpha}_{ij}^T\ell_{ij}$$

(5.2.10)

Taking into account Eq. (5.2.9), the variation of the versor is given by

$$\ell_{ij} = \ell_{ij}^o + \Delta\mathbf{x}_{ij}^d$$

$$\ell_{ij}\boldsymbol{\alpha}_{ij} = \ell_{ij}^o\boldsymbol{\alpha}_{ij}^o + \Delta\mathbf{x}_{ij}^d$$

$$\boldsymbol{\alpha}_{ij} = \frac{\ell_{ij}^o + \Delta\mathbf{x}_{ij}^d}{\ell_{ij}^o\left(1 + \Delta\varepsilon_{ij}\right)} = \frac{1}{\ell_{ij}^o}\left[\frac{\ell_{ij}^o + \Delta\mathbf{x}_{ij}^d}{\left(1 + \Delta\varepsilon_{ij}\right)}\right]$$

$$\Delta\boldsymbol{\alpha}_{ij} = \boldsymbol{\alpha}_{ij} - \boldsymbol{\alpha}_{ij}^o = \frac{\ell_{ij}^o + \Delta\mathbf{x}_{ij}^d}{\ell_{ij}^o\left(1 + \Delta\varepsilon_{ij}\right)} - \frac{\ell_{ij}^o}{\ell_{ij}^o} = \frac{1}{\ell_{ij}^o}\left[\frac{\ell_{ij}^o + \Delta\mathbf{x}_{ij}^d}{\left(1 + \Delta\varepsilon_{ij}\right)} - \ell_{ij}^o\right]$$

$$\Delta\boldsymbol{\alpha}_{ij} = \boldsymbol{\alpha}_{ij} - \boldsymbol{\alpha}_{ij}^o = \frac{\ell_{ij}^o + \Delta\mathbf{x}_{ij}^d}{\ell_{ij}^o\left(1 + \Delta\varepsilon_{ij}\right)} - \frac{\ell_{ij}^o}{\ell_{ij}^o} = \frac{1}{\ell_{ij}^o}\left[\frac{\ell_{ij}^o + \Delta\mathbf{x}_{ij}^d}{\left(1 + \Delta\varepsilon_{ij}\right)} - \ell_{ij}^o\right]$$

(5.2.11)

According to the small deformations hypothesis, whence

$$\frac{1}{1 + \Delta\varepsilon} \cong 1 - \Delta\varepsilon$$

(5.2.12)

Eq. (5.2.11) may be simplified

---

[21]

$$\ell_{ij} = \ell_{ij}^o + \Delta\mathbf{x}_{ij}^d$$

$$\ell_{ij}\boldsymbol{\alpha}_{ij} = \ell_{ij}^o\boldsymbol{\alpha}_{ij}^o + \Delta\mathbf{x}_{ij}^d$$

$$\boldsymbol{\alpha}_{ij}^T\ell_{ij}\boldsymbol{\alpha}_{ij} = \boldsymbol{\alpha}_{ij}^T\ell_{ij}^o\boldsymbol{\alpha}_{ij}^o + \boldsymbol{\alpha}_{ij}^T\Delta\mathbf{x}_{ij}^d = \left(\boldsymbol{\alpha}_{ij}^{oT} + \Delta\boldsymbol{\alpha}_{ij}^T\right)\ell_{ij}^o\boldsymbol{\alpha}_{ij}^o + \boldsymbol{\alpha}_{ij}^T\Delta\mathbf{x}_{ij}^d$$

$$\ell_{ij} - \ell_{ij}^o = \Delta\boldsymbol{\alpha}_{ij}^T\ell_{ij}^o\boldsymbol{\alpha}_{ij}^o + \boldsymbol{\alpha}_{ij}^T\Delta\mathbf{x}_{ij}^d$$

$$\Delta\ell_{ij} = \Delta\boldsymbol{\alpha}_{ij}^T\ell_{ij}^o\boldsymbol{\alpha}_{ij}^o + \boldsymbol{\alpha}_{ij}^T\Delta\mathbf{x}_{ij}^d$$

or:

$$\boldsymbol{\alpha}_{ij}^T\ell_{ij}\boldsymbol{\alpha}_{ij} = \boldsymbol{\alpha}_{ij}^T\ell_{ij}^o\boldsymbol{\alpha}_{ij}^o + \boldsymbol{\alpha}_{ij}^T\Delta\mathbf{x}_{ij}^d = \left(\boldsymbol{\alpha}_{ij}^{oT} + \Delta\boldsymbol{\alpha}_{ij}^T\right)\left(\ell_{ij}^o\boldsymbol{\alpha}_{ij}^o + \Delta\mathbf{x}_{ij}^d\right) =$$

$$= \boldsymbol{\alpha}_{ij}^{oT}\ell_{ij}^o\boldsymbol{\alpha}_{ij}^o + \boldsymbol{\alpha}_{ij}^{oT}\Delta\mathbf{x}_{ij}^d + \Delta\boldsymbol{\alpha}_{ij}^T\ell_{ij}^o\boldsymbol{\alpha}_{ij}^o + \Delta\boldsymbol{\alpha}_{ij}^T\Delta\mathbf{x}_{ij}^d$$

$$\ell_{ij} = \ell_{ij}^o + \boldsymbol{\alpha}_{ij}^{oT}\Delta\mathbf{x}_{ij}^d + \Delta\boldsymbol{\alpha}_{ij}^T\left(\ell_{ij}^o\boldsymbol{\alpha}_{ij}^o + \Delta\mathbf{x}_{ij}^d\right)$$

$$\Delta\ell_{ij} = \ell_{ij} - \ell_{ij}^o = \boldsymbol{\alpha}_{ij}^{oT}\Delta\mathbf{x}_{ij}^d + \Delta\boldsymbol{\alpha}_{ij}^T\ell_{ij}$$

$$\Delta\boldsymbol{\alpha}_{ij} = \boldsymbol{\alpha}_{ij} - \boldsymbol{\alpha}_{ij}^o = \frac{\boldsymbol{\ell}_{ij}^o + \Delta\mathbf{x}_{ij}^d}{\ell_{ij}^o\left(1 + \Delta\varepsilon_{ij}\right)} - \frac{\boldsymbol{\ell}_{ij}^o}{\ell_{ij}^o} = \frac{1}{\ell_{ij}^o}\left[\frac{\boldsymbol{\ell}_{ij}^o + \Delta\mathbf{x}_{ij}^d}{\left(1 + \Delta\varepsilon_{ij}\right)} - \boldsymbol{\ell}_{ij}^o\right]$$

$$\Delta\boldsymbol{\alpha}_{ij} = \frac{1}{\ell_{ij}^o}\left[\frac{\boldsymbol{\ell}_{ij}^o + \Delta\mathbf{x}_{ij}^d}{\left(1 + \Delta\varepsilon_{ij}\right)} - \boldsymbol{\ell}_{ij}^o\right] \cong \frac{1}{\ell_{ij}^o}\left[\left(\boldsymbol{\ell}_{ij}^o + \Delta\mathbf{x}_{ij}^d\right)\left(1 - \Delta\varepsilon_{ij}\right) - \boldsymbol{\ell}_{ij}^o\right] =$$

$$= \frac{1}{\ell_{ij}^o}\left[\boldsymbol{\ell}_{ij}^o + \Delta\mathbf{x}_{ij}^d - \Delta\varepsilon_{ij}\boldsymbol{\ell}_{ij}^o - \Delta\varepsilon_{ij}\Delta\mathbf{x}_{ij}^d - \boldsymbol{\ell}_{ij}^o\right]$$

$$\Delta\boldsymbol{\alpha}_{ij} = \frac{1}{\ell_{ij}^o}\left[\Delta\mathbf{x}_{ij}^d - \Delta\varepsilon_{ij}\boldsymbol{\ell}_{ij}\right] = \frac{1}{\ell_{ij}^o}\left[\Delta\mathbf{x}_{ij}^d - \frac{\Delta\ell_{ij}}{\ell_{ij}^o}\boldsymbol{\ell}_{ij}\right]$$

$$\Delta\boldsymbol{\alpha}_{ij} = \frac{1}{\ell_{ij}^o}\left[\Delta\mathbf{x}_{ij}^d - \frac{\Delta\ell_{ij}}{\ell_{ij}^o}\boldsymbol{\ell}_{ij}\right] \tag{5.2.13}$$

After substituting Eq. (3.2.13) in Eq. (5.2.10), one gets

$$\boldsymbol{\ell}_{ij} = \boldsymbol{\ell}_{ij}^o + \Delta\mathbf{x}_{ij}^d$$

$$\ell_{ij}\boldsymbol{\alpha}_{ij} = \ell_{ij}^o\boldsymbol{\alpha}_{ij}^o + \Delta\mathbf{x}_{ij}^d$$

$$\Delta\ell_{ij} = \ell_{ij} - \ell_{ij}^o = \boldsymbol{\alpha}_{ij}^{oT}\Delta\mathbf{x}_{ij}^d + \Delta\boldsymbol{\alpha}_{ij}^T\boldsymbol{\ell}_{ij} = \boldsymbol{\alpha}_{ij}^{oT}\Delta\mathbf{x}_{ij}^d + \boldsymbol{\ell}_{ij}^T\Delta\boldsymbol{\alpha}_{ij}$$

$$\Delta\boldsymbol{\alpha}_{ij} = \frac{1}{\ell_{ij}^o}\left[\Delta\mathbf{x}_{ij}^d - \Delta\varepsilon_{ij}\boldsymbol{\ell}_{ij}\right] = \frac{1}{\ell_{ij}^o}\left[\Delta\mathbf{x}_{ij}^d - \frac{\Delta\ell_{ij}}{\ell_{ij}^o}\boldsymbol{\ell}_{ij}\right]$$

$$\Delta\ell_{ij} = \boldsymbol{\alpha}_{ij}^{oT}\Delta\mathbf{x}_{ij}^d + \boldsymbol{\ell}_{ij}^T\frac{1}{\ell_{ij}^o}\left[\Delta\mathbf{x}_{ij}^d - \frac{\Delta\ell_{ij}}{\ell_{ij}^o}\boldsymbol{\ell}_{ij}\right] = \frac{\boldsymbol{\ell}_{ij}^{oT}}{\ell_{ij}^o}\Delta\mathbf{x}_{ij}^d + \boldsymbol{\ell}_{ij}^T\frac{1}{\ell_{ij}^o}\left[\Delta\mathbf{x}_{ij}^d - \frac{\Delta\ell_{ij}}{\ell_{ij}^o}\boldsymbol{\ell}_{ij}\right] =$$

$$= \frac{1}{\ell_{ij}^o}\left(\boldsymbol{\ell}_{ij}^{oT} + \boldsymbol{\ell}_{ij}^T\right)\Delta\mathbf{x}_{ij}^d - \frac{\Delta\ell_{ij}}{\ell_{ij}^{o2}}\boldsymbol{\ell}_{ij}^T\boldsymbol{\ell}_{ij}$$

$$\Delta\ell_{ij}\left(1 + \frac{\boldsymbol{\ell}_{ij}^T\boldsymbol{\ell}_{ij}}{\ell_{ij}^{o2}}\right) = \Delta\ell_{ij}\left(\frac{\ell_{ij}^{o2} + \boldsymbol{\ell}_{ij}^T\boldsymbol{\ell}_{ij}}{\ell_{ij}^{o2}}\right) = \frac{1}{\ell_{ij}^o}\left(\boldsymbol{\ell}_{ij}^{oT} + \boldsymbol{\ell}_{ij}^T\right)\Delta\mathbf{x}_{ij}^d$$

$$\Delta\ell_{ij} = \frac{1}{\ell_{ij}^o}\frac{\ell_{ij}^{o2}}{\ell_{ij}^{o2} + \boldsymbol{\ell}_{ij}^T\boldsymbol{\ell}_{ij}}\left(\boldsymbol{\ell}_{ij}^{oT} + \boldsymbol{\ell}_{ij}^T\right)\Delta\mathbf{x}_{ij}^d = \frac{\ell_{ij}^o}{\ell_{ij}^{o2} + \boldsymbol{\ell}_{ij}^T\boldsymbol{\ell}_{ij}}\left(\boldsymbol{\ell}_{ij}^{oT} + \boldsymbol{\ell}_{ij}^T\right)\Delta\mathbf{x}_{ij}^d \Rightarrow$$

$$\Delta\ell_{ij} = \frac{\ell_{ij}^o}{\ell_{ij}^{o2} + \boldsymbol{\ell}_{ij}^T\boldsymbol{\ell}_{ij}}\left(\boldsymbol{\ell}_{ij}^{oT} + \boldsymbol{\ell}_{ij}^T\right)\Delta\mathbf{x}_{ij}^d$$

$$\Delta\ell_{ij} = \frac{\ell_{ij}^o}{\ell_{ij}^{o2} + \boldsymbol{\ell}_{ij}^T\boldsymbol{\ell}_{ij}}\left(\boldsymbol{\ell}_{ij}^{oT} + \boldsymbol{\ell}_{ij}^T\right)\Delta\mathbf{x}_{ij}^d \tag{5.2.14}$$

Then, Eq. (5.2.14) is substituted in Eq.(5.2.13), whence

$$\Delta\boldsymbol{\alpha}_{ij} = \frac{1}{\ell^o_{ij}}\left[\Delta\mathbf{x}^d_{ij} - \frac{\Delta\ell_{ij}}{\ell^o_{ij}}\boldsymbol{\ell}_{ij}\right]$$

$$\Delta\ell_{ij} = \frac{\ell^o_{ij}}{\ell^{o2}_{ij} + \boldsymbol{\ell}^T_{ij}\boldsymbol{\ell}_{ij}}\left(\boldsymbol{\ell}^{oT}_{ij} + \boldsymbol{\ell}^T_{ij}\right)\Delta\mathbf{x}^d_{ij}$$

$$\Delta\boldsymbol{\alpha}_{ij} = \frac{1}{\ell^o_{ij}}\left[\Delta\mathbf{x}^d_{ij} - \frac{\left(\boldsymbol{\ell}^{oT}_{ij} + \boldsymbol{\ell}^T_{ij}\right)\Delta\mathbf{x}^d_{ij}}{\ell^{o2}_{ij} + \boldsymbol{\ell}^T_{ij}\boldsymbol{\ell}_{ij}}\boldsymbol{\ell}_{ij}\right]$$

$$\Delta\boldsymbol{\alpha}_{ij} = \frac{1}{\ell^o_{ij}}\Delta\mathbf{x}^d_{ij} - \frac{\left(\boldsymbol{\ell}^{oT}_{ij} + \boldsymbol{\ell}^T_{ij}\right)\Delta\mathbf{x}^d_{ij}}{\ell^{o2}_{ij} + \boldsymbol{\ell}^T_{ij}\boldsymbol{\ell}_{ij}}\frac{\boldsymbol{\ell}_{ij}}{\ell^o_{ij}}$$

$$\Delta\boldsymbol{\alpha}_{ij} = \frac{1}{\ell^o_{ij}}\Delta\mathbf{x}^d_{ij} - \frac{\left(\boldsymbol{\ell}^{oT}_{ij} + \boldsymbol{\ell}^T_{ij}\right)\Delta\mathbf{x}^d_{ij}}{\ell^{o2}_{ij} + \boldsymbol{\ell}^T_{ij}\boldsymbol{\ell}_{ij}}\frac{\boldsymbol{\ell}_{ij}}{\ell^o_{ij}} \qquad (5.2.15)$$

Since [22]

$$\left(\boldsymbol{\lambda}^T_{ij}\Delta\mathbf{x}^d_{ij}\right)\boldsymbol{\ell}_{ij} = \left(\boldsymbol{\ell}_{ij}\boldsymbol{\lambda}^T_{ij}\right)\Delta\mathbf{x}^d_{ij} \qquad (5.2.15b)$$

$\Delta\mathbf{f}$ can be computed for any assigned $\Delta\mathbf{x}^d$ using, in sequence, Eq. (5.2.5)$\rightarrow$ (5.2.14)$\rightarrow$ (5.2.6)$\rightarrow$ (5.2.15)$\rightarrow$ (5.2.8)[23]

---

[22] Actually, once considered three vectors

$$\left(\boldsymbol{\lambda}^T_{ij}\Delta\mathbf{x}^d_{ij}\right)\boldsymbol{\ell}_{ij} = \left(\boldsymbol{\ell}_{ij}\boldsymbol{\lambda}^T_{ij}\right)\Delta\mathbf{x}^d_{ij}$$

$$\left[\mathbf{a}^T\mathbf{b}\right]\mathbf{c} = \left[(a_1 \quad a_2)\binom{b_1}{b_2}\right]\binom{c_1}{c_2} = (a_1b_1 + a_2b_2)\binom{c_1}{c_2} = \binom{c_1a_1b_1 + c_1a_2b_2}{c_2a_1b_1 + c_2a_2b_2}$$

and, on the other side

$$\left[\mathbf{c}\mathbf{a}^T\right]\mathbf{b} = \left[\binom{c_1}{c_2}(a_1 \quad a_2)\right]\binom{b_1}{b_2} = \begin{bmatrix} c_1a_1 & c_1a_2 \\ c_2a_1 & c_2a_2 \end{bmatrix}\binom{b_1}{b_2} = \binom{c_1a_1b_1 + c_1a_2b_2}{c_2a_1b_1 + c_2a_2b_2}$$

and therefore
$$\left[\mathbf{a}^T\mathbf{b}\right]\mathbf{c} = \left[\mathbf{c}\mathbf{a}^T\right]\mathbf{b}$$

$$\boldsymbol{\ell}_{ij} = \boldsymbol{\ell}^O_{ij} + \Delta\mathbf{x}^d_{ij} \quad (5.2.5)$$

[23]
$$\boldsymbol{\lambda}^T_{ij} = \frac{\boldsymbol{\ell}^{oT}_{ij} + \boldsymbol{\ell}^T_{ij}}{\ell^{o2}_{ij} + \boldsymbol{\ell}^T_{ij}\boldsymbol{\ell}_{ij}}$$

$$\Delta\ell_{ij} = \frac{\ell^o_{ij}}{\ell^{o2}_{ij} + \boldsymbol{\ell}^T_{ij}\boldsymbol{\ell}_{ij}}\left(\boldsymbol{\ell}^{oT}_{ij} + \boldsymbol{\ell}^T_{ij}\right)\Delta\mathbf{x}^d_{ij} = \ell^o_{ij}\boldsymbol{\lambda}^T_{ij}\Delta\mathbf{x}^d_{ij} \quad (5.2.14)$$

$$\Delta\mathbf{f}_{ij} = R_{ij}\boldsymbol{\ell}_{ij}\boldsymbol{\lambda}_{ij}^T\Big[\mathbf{I} - \Delta\mathbf{x}_{ij}^d\boldsymbol{\lambda}_{ij}^T\Big]\Delta\mathbf{x}_{ij}^d + \frac{F_{ij}^o}{\ell_{ij}^o}\Big(\mathbf{I} - \boldsymbol{\ell}_{ij}\boldsymbol{\lambda}_{ij}^T\Big)\Delta\mathbf{x}_{ij}^d - \frac{R_{ij}}{\ell_{ij}^o}\Delta D_{ij}\Big(1 - \boldsymbol{\lambda}_{ij}^T\Delta\mathbf{x}_{ij}^d\Big)\boldsymbol{\ell}_{ij} \qquad (5.2.16)$$

$$\Delta F_{ij} = \frac{E_{ij}A_{ij}}{\ell_{ij}^\circ}\Big(\Delta\ell_{ij} - \Delta D_{ij}\Big) = R_{ij}\Big(\Delta\ell_{ij} - \Delta D_{ij}\Big)(5.2.6)$$

$$\Delta F_{ij} = R_{ij}\Big(\ell_{ij}^O\boldsymbol{\lambda}_{ij}^T\Delta\mathbf{x}_{ij}^d - \Delta D_{ij}\Big)(5.2.15)$$

$$\Delta\boldsymbol{\alpha}_{ij} = \frac{1}{\ell_{ij}^o}\Delta\mathbf{x}_{ij}^d - \frac{\Big(\boldsymbol{\ell}_{ij}^{oT} + \boldsymbol{\ell}_{ij}^T\Big)\Delta\mathbf{x}_{ij}^d}{\ell_{ij}^{o2} + \boldsymbol{\ell}_{ij}^T\boldsymbol{\ell}_{ij}}\frac{\boldsymbol{\ell}_{ij}}{\ell_{ij}^o}$$

$$\Delta\boldsymbol{\alpha}_{ij} = \frac{1}{\ell_{ij}^o}\Delta\mathbf{x}_{ij}^d - \boldsymbol{\lambda}_{ij}^T\Delta\mathbf{x}_{ij}^d\frac{\boldsymbol{\ell}_{ij}}{\ell_{ij}^o}$$

$$\Delta\mathbf{f}_{ij} = \mathbf{f}_{ij} - \mathbf{f}_{ij}^O = \Delta F_{ij}\boldsymbol{\alpha}_{ij}^O + F_{ij}^O\Delta\boldsymbol{\alpha}_{ij} + \Delta F_{ij}\Delta\boldsymbol{\alpha}_{ij}(5.2.8)$$

$$\Delta\mathbf{f}_{ij} = R_{ij}\Big(\ell_{ij}^o\boldsymbol{\lambda}_{ij}^T\Delta\mathbf{x}_{ij}^d - \Delta D_{ij}\Big)\boldsymbol{\alpha}_{ij}^o + F_{ij}^o\Bigg(\frac{1}{\ell_{ij}^o}\Delta\mathbf{x}_{ij}^d - \boldsymbol{\lambda}_{ij}^T\Delta\mathbf{x}_{ij}^d\frac{\boldsymbol{\ell}_{ij}}{\ell_{ij}^o}\Bigg) + R_{ij}\Big(\ell_{ij}^o\boldsymbol{\lambda}_{ij}^T\Delta\mathbf{x}_{ij}^d - \Delta D_{ij}\Big)\Bigg(\frac{1}{\ell_{ij}^o}\Delta\mathbf{x}_{ij}^d - \boldsymbol{\lambda}_{ij}^T\Delta\mathbf{x}_{ij}^d\frac{\boldsymbol{\ell}_{ij}}{\ell_{ij}^o}\Bigg) =$$

$$= R_{ij}\ell_{ij}^o\boldsymbol{\lambda}_{ij}^T\Delta\mathbf{x}_{ij}^d\boldsymbol{\alpha}_{ij}^o - R_{ij}\Delta D_{ij}\boldsymbol{\alpha}_{ij}^o + F_{ij}^o\Bigg(\frac{1}{\ell_{ij}^o}\Delta\mathbf{x}_{ij}^d - \boldsymbol{\lambda}_{ij}^T\Delta\mathbf{x}_{ij}^d\frac{\boldsymbol{\ell}_{ij}}{\ell_{ij}^o}\Bigg) + R_{ij}\ell_{ij}^o\boldsymbol{\lambda}_{ij}^T\Delta\mathbf{x}_{ij}^d\Bigg(\frac{1}{\ell_{ij}^o}\Delta\mathbf{x}_{ij}^d - \boldsymbol{\lambda}_{ij}^T\Delta\mathbf{x}_{ij}^d\frac{\boldsymbol{\ell}_{ij}}{\ell_{ij}^o}\Bigg) - R_{ij}\Delta D_{ij}\Bigg(\frac{1}{\ell_{ij}^o}\Delta\mathbf{x}_{ij}^d - \boldsymbol{\lambda}_{ij}^T\Delta\mathbf{x}_{ij}^d\frac{\boldsymbol{\ell}_{ij}}{\ell_{ij}^o}\Bigg) =$$

$$= R_{ij}\ell_{ij}^o\boldsymbol{\lambda}_{ij}^T\Delta\mathbf{x}_{ij}^d\boldsymbol{\alpha}_{ij}^o + R_{ij}\ell_{ij}^o\boldsymbol{\lambda}_{ij}^T\Delta\mathbf{x}_{ij}^d\Bigg(\frac{1}{\ell_{ij}^o}\Delta\mathbf{x}_{ij}^d - \boldsymbol{\lambda}_{ij}^T\Delta\mathbf{x}_{ij}^d\frac{\boldsymbol{\ell}_{ij}}{\ell_{ij}^o}\Bigg) + F_{ij}^o\Bigg(\frac{1}{\ell_{ij}^o}\Delta\mathbf{x}_{ij}^d - \boldsymbol{\lambda}_{ij}^T\Delta\mathbf{x}_{ij}^d\frac{\boldsymbol{\ell}_{ij}}{\ell_{ij}^o}\Bigg) - R_{ij}\Delta D_{ij}\Bigg(\frac{1}{\ell_{ij}^o}\Delta\mathbf{x}_{ij}^d - \boldsymbol{\lambda}_{ij}^T\Delta\mathbf{x}_{ij}^d\frac{\boldsymbol{\ell}_{ij}}{\ell_{ij}^o} + \boldsymbol{\alpha}_{ij}^o\Bigg) =$$

$$= R_{ij}\ell_{ij}^o\boldsymbol{\lambda}_{ij}^T\Delta\mathbf{x}_{ij}^d\boldsymbol{\alpha}_{ij}^o + R_{ij}\ell_{ij}^o\boldsymbol{\lambda}_{ij}^T\Delta\mathbf{x}_{ij}^d\Bigg(\frac{1}{\ell_{ij}^o}\Delta\mathbf{x}_{ij}^d - \boldsymbol{\lambda}_{ij}^T\Delta\mathbf{x}_{ij}^d\frac{\boldsymbol{\ell}_{ij}}{\ell_{ij}^o}\Bigg) + F_{ij}^o\Bigg(\frac{1}{\ell_{ij}^o}\Delta\mathbf{x}_{ij}^d - \boldsymbol{\lambda}_{ij}^T\Delta\mathbf{x}_{ij}^d\frac{\boldsymbol{\ell}_{ij}}{\ell_{ij}^o}\Bigg) - \frac{R_{ij}}{\ell_{ij}^o}\Delta D_{ij}\Big(\Delta\mathbf{x}_{ij}^d - \boldsymbol{\lambda}_{ij}^T\Delta\mathbf{x}_{ij}^d\boldsymbol{\ell}_{ij} + \ell_{ij}^o\boldsymbol{\alpha}_{ij}^o\Big) =$$

$$= R_{ij}\ell_{ij}^o\boldsymbol{\lambda}_{ij}^T\Delta\mathbf{x}_{ij}^d\boldsymbol{\alpha}_{ij}^o + \frac{1}{\ell_{ij}^o}R_{ij}\ell_{ij}^o\boldsymbol{\lambda}_{ij}^T\Delta\mathbf{x}_{ij}^d\Delta\mathbf{x}_{ij}^d - R_{ij}\ell_{ij}^o\boldsymbol{\lambda}_{ij}^T\Delta\mathbf{x}_{ij}^d\boldsymbol{\lambda}_{ij}^T\Delta\mathbf{x}_{ij}^d\frac{\boldsymbol{\ell}_{ij}}{\ell_{ij}^o} + \frac{F_{ij}^o}{\ell_{ij}^o}\Big(\Delta\mathbf{x}_{ij}^d - \boldsymbol{\lambda}_{ij}^T\Delta\mathbf{x}_{ij}^d\boldsymbol{\ell}_{ij}\Big) - \frac{R_{ij}}{\ell_{ij}^o}\Delta D_{ij}\Big(1 - \boldsymbol{\lambda}_{ij}^T\Delta\mathbf{x}_{ij}^d\Big)\boldsymbol{\ell}_{ij} =$$

$$= R_{ij}\boldsymbol{\lambda}_{ij}^T\Delta\mathbf{x}_{ij}^d\Big(\ell_{ij}^o\boldsymbol{\alpha}_{ij}^o + \Delta\mathbf{x}_{ij}^d\Big) - R_{ij}\boldsymbol{\lambda}_{ij}^T\Delta\mathbf{x}_{ij}^d\boldsymbol{\lambda}_{ij}^T\Delta\mathbf{x}_{ij}^d\boldsymbol{\ell}_{ij} + \frac{F_{ij}^o}{\ell_{ij}^o}\Big(\Delta\mathbf{x}_{ij}^d - \boldsymbol{\lambda}_{ij}^T\Delta\mathbf{x}_{ij}^d\boldsymbol{\ell}_{ij}\Big) - \frac{R_{ij}}{\ell_{ij}^o}\Delta D_{ij}\Big(1 - \boldsymbol{\lambda}_{ij}^T\Delta\mathbf{x}_{ij}^d\Big)\boldsymbol{\ell}_{ij} =$$

$$= R_{ij}\boldsymbol{\lambda}_{ij}^T\Delta\mathbf{x}_{ij}^d\Big(\boldsymbol{\ell}_{ij} - \boldsymbol{\lambda}_{ij}^T\Delta\mathbf{x}_{ij}^d\boldsymbol{\ell}_{ij}\Big) + \frac{F_{ij}^o}{\ell_{ij}^o}\Big(\Delta\mathbf{x}_{ij}^d - \boldsymbol{\lambda}_{ij}^T\Delta\mathbf{x}_{ij}^d\boldsymbol{\ell}_{ij}\Big) - \frac{R_{ij}}{\ell_{ij}^o}\Delta D_{ij}\Big(1 - \boldsymbol{\lambda}_{ij}^T\Delta\mathbf{x}_{ij}^d\Big)\boldsymbol{\ell}_{ij}$$

$$\Big[\mathbf{a}^T\mathbf{b}\Big]\mathbf{c} = \Big[\mathbf{c}\mathbf{a}^T\Big]\mathbf{b}$$

$$\Delta\mathbf{f}_{ij} = R_{ij}\Big(\boldsymbol{\lambda}_{ij}^T\Delta\mathbf{x}_{ij}^d\Big)\boldsymbol{\ell}_{ij} - R_{ij}\Big(\boldsymbol{\lambda}_{ij}^T\Delta\mathbf{x}_{ij}^d\Big)\boldsymbol{\lambda}_{ij}^T\Delta\mathbf{x}_{ij}^d\boldsymbol{\ell}_{ij} + \frac{F_{ij}^o}{\ell_{ij}^o}\Big(\Delta\mathbf{x}_{ij}^d - \boldsymbol{\lambda}_{ij}^T\Delta\mathbf{x}_{ij}^d\boldsymbol{\ell}_{ij}\Big) - \frac{R_{ij}}{\ell_{ij}^o}\Delta D_{ij}\Big(1 - \boldsymbol{\lambda}_{ij}^T\Delta\mathbf{x}_{ij}^d\Big)\boldsymbol{\ell}_{ij} =$$

$$= R_{ij}\Big(\boldsymbol{\ell}_{ij}\boldsymbol{\lambda}_{ij}^T\Big)\Delta\mathbf{x}_{ij}^d - R_{ij}\Big(\boldsymbol{\lambda}_{ij}^T\Delta\mathbf{x}_{ij}^d\Big)\Big(\boldsymbol{\ell}_{ij}\boldsymbol{\lambda}_{ij}^T\Big)\Delta\mathbf{x}_{ij}^d + \frac{F_{ij}^o}{\ell_{ij}^o}\Big(\Delta\mathbf{x}_{ij}^d - \Big(\boldsymbol{\ell}_{ij}\boldsymbol{\lambda}_{ij}^T\Big)\Delta\mathbf{x}_{ij}^d\Big) - \frac{R_{ij}}{\ell_{ij}^o}\Delta D_{ij}\Big(1 - \boldsymbol{\lambda}_{ij}^T\Delta\mathbf{x}_{ij}^d\Big)\boldsymbol{\ell}_{ij} =$$

$$= R_{ij}\Big(\boldsymbol{\ell}_{ij}\boldsymbol{\lambda}_{ij}^T\Big)\Delta\mathbf{x}_{ij}^d - R_{ij}\Big(\boldsymbol{\ell}_{ij}\boldsymbol{\lambda}_{ij}^T\Big)\Big(\boldsymbol{\lambda}_{ij}^T\Delta\mathbf{x}_{ij}^d\Big)\Delta\mathbf{x}_{ij}^d + \frac{F_{ij}^o}{\ell_{ij}^o}\Big(\Delta\mathbf{x}_{ij}^d - \Big(\boldsymbol{\ell}_{ij}\boldsymbol{\lambda}_{ij}^T\Big)\Delta\mathbf{x}_{ij}^d\Big) - \frac{R_{ij}}{\ell_{ij}^o}\Delta D_{ij}\Big(1 - \boldsymbol{\lambda}_{ij}^T\Delta\mathbf{x}_{ij}^d\Big)\boldsymbol{\ell}_{ij} =$$

$$= R_{ij}\Big(\boldsymbol{\ell}_{ij}\boldsymbol{\lambda}_{ij}^T\Big)\Delta\mathbf{x}_{ij}^d - R_{ij}\Big(\boldsymbol{\ell}_{ij}\boldsymbol{\lambda}_{ij}^T\Big)\Big(\Delta\mathbf{x}_{ij}^d\boldsymbol{\lambda}_{ij}^T\Big)\Delta\mathbf{x}_{ij}^d + \frac{F_{ij}^o}{\ell_{ij}^o}\Big(\Delta\mathbf{x}_{ij}^d - \Big(\boldsymbol{\ell}_{ij}\boldsymbol{\lambda}_{ij}^T\Big)\Delta\mathbf{x}_{ij}^d\Big) - \frac{R_{ij}}{\ell_{ij}^o}\Delta D_{ij}\Big(1 - \boldsymbol{\lambda}_{ij}^T\Delta\mathbf{x}_{ij}^d\Big)\boldsymbol{\ell}_{ij} =$$

$$\Delta\mathbf{f}_{ij} = R_{ij}\boldsymbol{\ell}_{ij}\boldsymbol{\lambda}_{ij}^T\Big[\mathbf{I} - \Delta\mathbf{x}_{ij}^d\boldsymbol{\lambda}_{ij}^T\Big]\Delta\mathbf{x}_{ij}^d + \frac{F_{ij}^o}{\ell_{ij}^o}\Big(\mathbf{I} - \boldsymbol{\ell}_{ij}\boldsymbol{\lambda}_{ij}^T\Big)\Delta\mathbf{x}_{ij}^d - \frac{R_{ij}}{\ell_{ij}^o}\Delta D_{ij}\Big(1 - \boldsymbol{\lambda}_{ij}^T\Delta\mathbf{x}_{ij}^d\Big)\boldsymbol{\ell}_{ij}$$

with

$$\boldsymbol{\lambda}_{ij}^T = \frac{\boldsymbol{\ell}_{ij}^{oT} + \boldsymbol{\ell}_{ij}^T}{\ell_{ij}^{o2} + \boldsymbol{\ell}_{ij}^T \boldsymbol{\ell}_{ij}} = \frac{\boldsymbol{\ell}_{ij}^{oT} + \boldsymbol{\ell}_{ij}^T}{\ell_{ij}^{o2} + \ell_{ij}^2} \quad ; \quad \boldsymbol{\lambda}_{ij} = \frac{\boldsymbol{\ell}_{ij}^o + \boldsymbol{\ell}_{ij}}{\ell_{ij}^{o2} + \boldsymbol{\ell}_{ij}^T \boldsymbol{\ell}_{ij}} = \frac{\boldsymbol{\ell}_{ij}^o + \boldsymbol{\ell}_{ij}}{\ell_{ij}^{o2} + \ell_{ij}^2} \qquad (5.2.17)$$

Eq. (5.2.16) refers to the action of the *ij* beam on the node *j*; to obtain the action on the node *i* by the same beam, one refers to Eq.(5.2.16) again and applies an indexes' permutation, taking into account that

$$\Delta\mathbf{f}_{ij} = -\Delta\mathbf{f}_{ji} \ ;$$

$$\boldsymbol{\ell}_{ij} = -\boldsymbol{\ell}_{ji} \ ;$$

$$\boldsymbol{\lambda}_{ij}^T = -\boldsymbol{\lambda}_{ji}^T \ ;$$

$$(5.2.18)$$

$$\Delta\mathbf{x}_{ij}^d = -\Delta\mathbf{x}_{ji}^d$$

and

$$F_{ij}^o = F_{ji}^o \ ;$$

$$\ell_{ij}^o = \ell_{ji}^o \ ;$$

$$\Delta D_{ij} = \Delta D_{ji};$$

$$(5.2.19)$$

$$R_{ij} = R_{ji}$$

$$\Delta\mathbf{f}_{ij} = R_{ij}\ell_{ij}\lambda_{ij}^{T}\left[\mathbf{I} - \Delta\mathbf{x}_{ij}^{d}\lambda_{ij}^{T}\right]\Delta\mathbf{x}_{ij}^{d} + \frac{F_{ij}^{O}}{\ell_{ij}^{o}}\left(\mathbf{I} - \ell_{ij}\lambda_{ij}^{T}\right)\Delta\mathbf{x}_{ij}^{d} - \frac{R_{ij}}{\ell_{ij}^{o}}\Delta D_{ij}\left(1 - \lambda_{ij}^{T}\Delta\mathbf{x}_{ij}^{d}\right)\ell_{ij}$$

$$\Delta\mathbf{f}_{ij} = -\Delta\mathbf{f}_{ji} \; ; \; R_{ij} = R_{ji} \; ; \; \ell_{ij} = -\ell_{ji} \; ; \; \lambda_{ij}^{T} = -\lambda_{ji}^{T} \; ; \; \Delta\mathbf{x}_{ij}^{d} = -\Delta\mathbf{x}_{ji}^{d} \; ; \; F_{ij}^{O} = F_{ji}^{O} \; ; \; \ell_{ij}^{o} = \ell_{ji}^{o} \; ;$$

$$\Delta D_{ij} = \Delta D_{ji}$$

$$-\Delta\mathbf{f}_{ji} = -R_{ji}\ell_{ji}\lambda_{ji}^{T}\left[\mathbf{I} - \Delta\mathbf{x}_{ji}^{d}\lambda_{ji}^{T}\right]\Delta\mathbf{x}_{ji}^{d} - \frac{F_{ji}^{O}}{\ell_{ji}^{o}}\left(\mathbf{I} - \ell_{ji}\lambda_{ji}^{T}\right)\Delta\mathbf{x}_{ji}^{d} + \frac{R_{ji}}{\ell_{ji}^{o}}\Delta D_{ji}\left(1 - \lambda_{ji}^{T}\Delta\mathbf{x}_{ji}^{d}\right)\ell_{ji}$$

definitively

$$\Delta\mathbf{f}_{ji} = R_{ji}\ell_{ji}\lambda_{ji}^{T}\left[\mathbf{I} - \Delta\mathbf{x}_{ji}^{d}\lambda_{ji}^{T}\right]\Delta\mathbf{x}_{ji}^{d} + \frac{F_{ji}^{O}}{\ell_{ji}^{o}}\left(\mathbf{I} - \ell_{ji}\lambda_{ji}^{T}\right)\Delta\mathbf{x}_{ji}^{d} - \frac{R_{ji}}{\ell_{ji}^{o}}\Delta D_{ji}\left(1 - \lambda_{ji}^{T}\Delta\mathbf{x}_{ji}^{d}\right)\ell_{ji}$$

or, also,

$$\Delta\mathbf{f}_{ji} = R_{ij}\ell_{ij}\lambda_{ij}^{T}\left[\mathbf{I} - \Delta\mathbf{x}_{ij}^{d}\lambda_{ij}^{T}\right]\Delta\mathbf{x}_{ji}^{d} + \frac{F_{ij}^{O}}{\ell_{ij}^{o}}\left(\mathbf{I} - \ell_{ij}\lambda_{ij}^{T}\right)\Delta\mathbf{x}_{ji}^{d} - \frac{R_{ij}}{\ell_{ij}^{o}}\Delta D_{ij}\left(1 - \lambda_{ij}^{T}\Delta\mathbf{x}_{ij}^{d}\right)\ell_{ji}$$

or, as in Eq. (5.2.18)

$$\Delta\mathbf{f}_{ji} = R_{ij}\ell_{ij}\lambda_{ij}^{T}\left[\mathbf{I} - \Delta\mathbf{x}_{ij}^{d}\lambda_{ij}^{T}\right]\Delta\mathbf{x}_{ji}^{d} + \frac{F_{ij}^{O}}{\ell_{ij}^{o}}\left(\mathbf{I} - \ell_{ij}\lambda_{ij}^{T}\right)\Delta\mathbf{x}_{ji}^{d} + \frac{R_{ij}}{\ell_{ij}^{o}}\Delta D_{ij}\left(1 - \lambda_{ij}^{T}\Delta\mathbf{x}_{ij}^{d}\right)\ell_{ij}$$

$$\Delta\mathbf{f}_{ji} = R_{ij}\ell_{ij}\lambda_{ij}^{T}\left[\mathbf{I} - \Delta\mathbf{x}_{ij}^{d}\lambda_{ij}^{T}\right]\Delta\mathbf{x}_{ji}^{d} + \frac{F_{ij}^{o}}{\ell_{ij}^{o}}\left(\mathbf{I} - \ell_{ij}\lambda_{ij}^{T}\right)\Delta\mathbf{x}_{ji}^{d} + \frac{R_{ij}}{\ell_{ij}^{o}}\Delta D_{ij}\left(1 - \lambda_{ij}^{T}\Delta\mathbf{x}_{ij}^{d}\right)\ell_{ij} \qquad (5.2.20)$$

The variation of the internal forces of the *ij* beam can be completely represented by the vector $\Delta\mathbf{n}_{ij}$ that includes the variation of the internal forces at both the element ends

$$\Delta\mathbf{n}_{ij}^{T} = \left[\Delta\mathbf{f}_{ij}^{T} \; \vdots \; \Delta\mathbf{f}_{ji}^{T}\right] = \left[\Delta f_{ij,x} \; \vdots \; \Delta f_{ij,y} \; \vdots \; \Delta f_{ji,x} \; \vdots \; \Delta f_{ji,y}\right] \qquad (5.2.21)$$

Anagously $\Delta\mathbf{u}_{ij}$ denotes the vector that includes the 4 imposed displacements at both the ends, paying attention on Eq. (5.2.4) for that is

$$\Delta\mathbf{x}_{ij}^{d} = \begin{bmatrix} \Delta y_{ij} - \Delta y_{ji} \\ \Delta z_{ij} - \Delta z_{ji} \end{bmatrix}$$

$$\Delta\mathbf{x}_{ij}^{d} = \left[\mathbf{I} \; \vdots \; -\mathbf{I}\right]\Delta\mathbf{u}_{ij} \quad ; \quad \Delta\mathbf{x}_{ji}^{d} = \left[-\mathbf{I} \; \vdots \; \mathbf{I}\right]\Delta\mathbf{u}_{ij} \qquad (5.2.22)$$

being $\Delta\mathbf{u}_{ij} = -\Delta\mathbf{u}_{ji}$

one has

$$\Delta\mathbf{x}_{ij}^d = \begin{bmatrix} \mathbf{I} & \vdots & -\mathbf{I} \end{bmatrix}\Delta\mathbf{u}_{ij} \quad ; \quad \Delta\mathbf{x}_{ji}^d = \begin{bmatrix} -\mathbf{I} & \vdots & \mathbf{I} \end{bmatrix}\Delta\mathbf{u}_{ij}$$

$$\Delta\mathbf{x}_{ij}^d = \begin{bmatrix} \Delta y_{ij} - \Delta y_{ji} \\ \Delta z_{ij} - \Delta z_{ji} \end{bmatrix} ; \quad \Delta\mathbf{x}_{ji}^d = \begin{bmatrix} \Delta y_{ji} - \Delta y_{ij} \\ \Delta z_{ji} - \Delta z_{ij} \end{bmatrix}$$

$$\Delta\mathbf{u}_{ij}^T = \begin{bmatrix} \Delta y_{ij} & \Delta z_{ij} & \Delta y_{ji} & \Delta z_{ji} \end{bmatrix}$$

$$\begin{bmatrix} \mathbf{I} & \vdots & -\mathbf{I} \end{bmatrix}\Delta\mathbf{u}_{ij} = \begin{bmatrix} 1 & 0 & -1 & 0 \\ 0 & 1 & 0 & -1 \end{bmatrix}\begin{pmatrix} \Delta y_{ij} \\ \Delta z_{ij} \\ \Delta y_{ji} \\ \Delta z_{ji} \end{pmatrix} = \begin{bmatrix} \Delta y_{ij} - \Delta y_{ji} \\ \Delta z_{ij} - \Delta z_{ji} \end{bmatrix} = \Delta\mathbf{x}_{ij}^d$$

$$\begin{bmatrix} -\mathbf{I} & \vdots & \mathbf{I} \end{bmatrix}\Delta\mathbf{u}_{ij} = \begin{bmatrix} -1 & 0 & 1 & 0 \\ 0 & -1 & 0 & 1 \end{bmatrix}\begin{pmatrix} \Delta y_{ij} \\ \Delta z_{ij} \\ \Delta y_{ji} \\ \Delta z_{ji} \end{pmatrix} = \begin{bmatrix} \Delta y_{ji} - \Delta y_{ij} \\ \Delta z_{ji} - \Delta z_{ij} \end{bmatrix} = \Delta\mathbf{x}_{ji}^d$$

The dependence of $\Delta\mathbf{n}_{ij}$ on $\Delta\mathbf{u}_{ij}$ can be expressed by a single matrix relation, by assembling Eq. (5.2.16) relevant to ij to the analogous Eq. (5.2.20), and considering Eq. (5.2.21) and Eq. (5.2.22)

$$\Delta\mathbf{n}_{ij}^T = \begin{bmatrix} \Delta\mathbf{f}_{ij}^T & \vdots & \Delta\mathbf{f}_{ji}^T \end{bmatrix} = \begin{bmatrix} \Delta f_{ij,x} & \vdots & \Delta f_{ij,y} & \vdots & \Delta f_{ji,x} & \vdots & \Delta f_{ji,y} \end{bmatrix}$$

$$\Delta\mathbf{f}_{ij} = R_{ij}\boldsymbol{\ell}_{ij}\boldsymbol{\lambda}_{ij}^T\begin{bmatrix} \mathbf{I} - \Delta\mathbf{x}_{ij}^d\boldsymbol{\lambda}_{ij}^T \end{bmatrix}\Delta\mathbf{x}_{ij}^d + \frac{F_{ij}^o}{\ell_{ij}^o}\left(\mathbf{I} - \boldsymbol{\ell}_{ij}\boldsymbol{\lambda}_{ij}^T\right)\Delta\mathbf{x}_{ij}^d - \frac{R_{ij}}{\ell_{ij}^o}\Delta D_{ij}\left(1 - \boldsymbol{\lambda}_{ij}^T\Delta\mathbf{x}_{ij}^d\right)\boldsymbol{\ell}_{ij}$$

$$\Delta\mathbf{f}_{ji} = R_{ij}\boldsymbol{\ell}_{ij}\boldsymbol{\lambda}_{ij}^T\begin{bmatrix} \mathbf{I} - \Delta\mathbf{x}_{ij}^d\boldsymbol{\lambda}_{ij}^T \end{bmatrix}\Delta\mathbf{x}_{ji}^d + \frac{F_{ij}^o}{\ell_{ij}^o}\left(\mathbf{I} - \boldsymbol{\ell}_{ij}\boldsymbol{\lambda}_{ij}^T\right)\Delta\mathbf{x}_{ji}^d + \frac{R_{ij}}{\ell_{ij}^o}\Delta D_{ij}\left(1 - \boldsymbol{\lambda}_{ij}^T\Delta\mathbf{x}_{ij}^d\right)\boldsymbol{\ell}_{ij}$$

$$\Delta\mathbf{n}_{ij} = \begin{bmatrix} \Delta\mathbf{f}_{ij} \\ \Delta\mathbf{f}_{ji} \end{bmatrix} = \left\{ R_{ij}\begin{bmatrix} \boldsymbol{\ell}_{ij}\boldsymbol{\lambda}_{ij}^T\begin{bmatrix} \mathbf{I} - \Delta\mathbf{x}_{ij}^d\boldsymbol{\lambda}_{ij}^T \end{bmatrix} & \vdots & \mathbf{0} \\ \hline \mathbf{0} & \vdots & \boldsymbol{\ell}_{ij}\boldsymbol{\lambda}_{ij}^T\begin{bmatrix} \mathbf{I} - \Delta\mathbf{x}_{ij}^d\boldsymbol{\lambda}_{ij}^T \end{bmatrix} \end{bmatrix} + \begin{bmatrix} \frac{F_{ij}^o}{\ell_{ij}^o}\begin{bmatrix} \mathbf{I} - \boldsymbol{\ell}_{ij}\boldsymbol{\lambda}_{ij}^T & \vdots & \mathbf{0} \\ \hline \mathbf{0} & \vdots & \mathbf{I} - \boldsymbol{\ell}_{ij}\boldsymbol{\lambda}_{ij}^T \end{bmatrix} \end{bmatrix} \right\}\begin{bmatrix} \mathbf{I} & \vdots & -\mathbf{I} \\ \hline -\mathbf{I} & \vdots & \mathbf{I} \end{bmatrix}\Delta\mathbf{u}_{ij} +$$

$$- \frac{R_{ij}}{\ell_{ij}^o}\left(1 - \boldsymbol{\lambda}_{ij}^T\Delta\mathbf{x}_{ij}^d\right)\begin{bmatrix} \boldsymbol{\ell}_{ij} \\ \hline -\boldsymbol{\ell}_{ij} \end{bmatrix}\Delta D_{ij}$$

$$\Delta\mathbf{n}_{ij} = \begin{bmatrix} \Delta\mathbf{f}_{ij} \\ \Delta\mathbf{f}_{ji} \end{bmatrix} = \left\{ R_{ij}\begin{bmatrix} \boldsymbol{\ell}_{ij}\boldsymbol{\lambda}_{ij}^T\big[\mathbf{I}-\Delta\mathbf{x}_{ij}^d\boldsymbol{\lambda}_{ij}^T\big] & \mathbf{0} \\ \mathbf{0} & \boldsymbol{\ell}_{ij}\boldsymbol{\lambda}_{ij}^T\big[\mathbf{I}-\Delta\mathbf{x}_{ij}^d\boldsymbol{\lambda}_{ij}^T\big] \end{bmatrix} + \\ + \dfrac{F_{ij}^o}{\ell_{ij}^o}\begin{bmatrix} \mathbf{I}-\boldsymbol{\ell}_{ij}\boldsymbol{\lambda}_{ij}^T & \mathbf{0} \\ \mathbf{0} & \mathbf{I}-\boldsymbol{\ell}_{ij}\boldsymbol{\lambda}_{ij}^T \end{bmatrix} \right\} \begin{bmatrix} \mathbf{I} & -\mathbf{I} \\ -\mathbf{I} & \mathbf{I} \end{bmatrix}\Delta\mathbf{u}_{ij} +$$

$$-\dfrac{R_{ij}}{\ell_{ij}^o}\Big(1-\boldsymbol{\lambda}_{ij}^T\Delta\mathbf{x}_{ij}^d\Big)\begin{bmatrix} \boldsymbol{\ell}_{ij} \\ -\boldsymbol{\ell}_{ij} \end{bmatrix}\Delta D_{ij}$$

(5.2.23)

Eq. (5.2.23) can be synthetically written in the form

$$\Delta\mathbf{n}_{ij} = \mathbf{k}_{Eij}^*\Delta\mathbf{u}_{ij} + \mathbf{k}_{Gij}^*\Delta\mathbf{u}_{ij} - \mathbf{q}_{ij}^*\Delta D_{ij} \tag{5.2.24}$$

where[24]

$$\mathbf{k}_{Eij}^*(\Delta\mathbf{x}_{ij}^d) = R_{ij}\left\{\boldsymbol{\ell}_{ij}\boldsymbol{\lambda}_{ij}^T\big[\mathbf{I}-\Delta\mathbf{x}_{ij}^d\boldsymbol{\lambda}_{ij}^T\big]\right\}\begin{bmatrix} \mathbf{I} & -\mathbf{I} \\ -\mathbf{I} & \mathbf{I} \end{bmatrix} = \mathbf{k}_{Eij}^*\big(\Delta\mathbf{x}_{ij}^d\big)^{[25]} \tag{5.2.25}$$

---

[24]

$$\Delta\mathbf{n}_{ij}^T = \begin{bmatrix} \Delta\mathbf{f}_{ij}^T & \Delta\mathbf{f}_{ji}^T \end{bmatrix} = \begin{bmatrix} \Delta f_{ij,x} & \Delta f_{ij,y} & \Delta f_{ji,x} & \Delta f_{ji,y} \end{bmatrix}$$

$$\Delta\mathbf{f}_{ij} = R_{ij}\boldsymbol{\ell}_{ij}\boldsymbol{\lambda}_{ij}^T\Big[\mathbf{I}-\Delta\mathbf{x}_{ij}^d\boldsymbol{\lambda}_{ij}^T\Big]\Delta\mathbf{x}_{ij}^d + \dfrac{F_{ij}^O}{\ell_{ij}^o}\Big(\mathbf{I}-\boldsymbol{\ell}_{ij}\boldsymbol{\lambda}_{ij}^T\Big)\Delta\mathbf{x}_{ij}^d - \dfrac{R_{ij}}{\ell_{ij}^o}\Delta D_{ij}\Big(1-\boldsymbol{\lambda}_{ij}^T\Delta\mathbf{x}_{ij}^d\Big)\boldsymbol{\ell}_{ij}$$

$$\Delta\mathbf{f}_{ji} = R_{ij}\boldsymbol{\ell}_{ij}\boldsymbol{\lambda}_{ij}^T\Big[\mathbf{I}-\Delta\mathbf{x}_{ij}^d\boldsymbol{\lambda}_{ij}^T\Big]\Delta\mathbf{x}_{ji}^d + \dfrac{F_{ij}^O}{\ell_{ij}^o}\Big(\mathbf{I}-\boldsymbol{\ell}_{ij}\boldsymbol{\lambda}_{ij}^T\Big)\Delta\mathbf{x}_{ji}^d + \dfrac{R_{ij}}{\ell_{ij}^o}\Delta D_{ij}\Big(1-\boldsymbol{\lambda}_{ij}^T\Delta\mathbf{x}_{ij}^d\Big)\boldsymbol{\ell}_{ij}$$

$$\Delta\mathbf{n}_{ij} = \begin{bmatrix} \Delta\mathbf{f}_{ij} \\ \Delta\mathbf{f}_{ji} \end{bmatrix} = \left\{ R_{ij}\begin{bmatrix} \boldsymbol{\ell}_{ij}\boldsymbol{\lambda}_{ij}^T\big[\mathbf{I}-\Delta\mathbf{x}_{ij}^d\boldsymbol{\lambda}_{ij}^T\big] & \mathbf{0} \\ \mathbf{0} & \boldsymbol{\ell}_{ij}\boldsymbol{\lambda}_{ij}^T\big[\mathbf{I}-\Delta\mathbf{x}_{ij}^d\boldsymbol{\lambda}_{ij}^T\big] \end{bmatrix} + \\ + \dfrac{F_{ij}^O}{\ell_{ij}^o}\begin{bmatrix} \mathbf{I}-\boldsymbol{\ell}_{ij}\boldsymbol{\lambda}_{ij}^T & \mathbf{0} \\ \mathbf{0} & \mathbf{I}-\boldsymbol{\ell}_{ij}\boldsymbol{\lambda}_{ij}^T \end{bmatrix} \right\} \begin{bmatrix} \mathbf{I} & -\mathbf{I} \\ -\mathbf{I} & \mathbf{I} \end{bmatrix}\Delta\mathbf{u}_{ij} +$$

$$-\dfrac{R_{ij}}{\ell_{ij}^o}\Big(1-\boldsymbol{\lambda}_{ij}^T\Delta\mathbf{x}_{ij}^d\Big)\begin{bmatrix} \boldsymbol{\ell}_{ij} \\ -\boldsymbol{\ell}_{ij} \end{bmatrix}\Delta D_{ij}$$

$$\mathbf{k}_{Eij}^* = R_{ij}\left\{\boldsymbol{\ell}_{ij}\boldsymbol{\lambda}_{ij}^T\big[\mathbf{I}-\Delta\mathbf{x}_{ij}^d\boldsymbol{\lambda}_{ij}^T\big]\right\}\begin{bmatrix} \mathbf{I} & -\mathbf{I} \\ -\mathbf{I} & \mathbf{I} \end{bmatrix} = \mathbf{k}_{Eij}^*\big(\Delta\mathbf{x}_{ij}^d\big)$$

$$\mathbf{k}_{Gij}^* = \dfrac{F_{ij}^O}{\ell_{ij}^o}\Big\{\mathbf{I}-\boldsymbol{\ell}_{ij}\boldsymbol{\lambda}_{ij}^T\Big\}\begin{bmatrix} \mathbf{I} & -\mathbf{I} \\ -\mathbf{I} & \mathbf{I} \end{bmatrix} = \mathbf{k}_{Gij}^*\big(\Delta\mathbf{x}_{ij}^d\big)$$

$$\mathbf{q}_{ij}^* = \dfrac{R_{ij}}{\ell_{ij}^o}\Big(1-\boldsymbol{\lambda}_{ij}^T\Delta\mathbf{x}_{ij}^d\Big)\begin{bmatrix} \boldsymbol{\ell}_{ij} \\ -\boldsymbol{\ell}_{ij} \end{bmatrix} = \mathbf{q}_{ij}^*\big(\Delta\mathbf{x}_{ij}^d\big)$$

[25] Elastic secant stiffness matrix of the beam *ij;*

$$\mathbf{k}_{Gij}^*(\Delta\mathbf{x}_{ij}^d) = \frac{F_{ij}^o}{\ell_{ij}^o}\left\{\mathbf{I} - \boldsymbol{\ell}_{ij}\boldsymbol{\lambda}_{ij}^T\right\}\begin{bmatrix} \mathbf{I} & \vdots & -\mathbf{I} \\ \hline -\mathbf{I} & \vdots & \mathbf{I} \end{bmatrix} = \mathbf{k}_{Gij}^*\left(\Delta\mathbf{x}_{ij}^d\right)^{26} \tag{5.2.26}$$

$$\mathbf{q}_{ij}^*(\Delta\mathbf{x}_{ij}^d) = \frac{R_{ij}}{\ell_{ij}^o}\left(1 - \boldsymbol{\lambda}_{ij}^T\Delta\mathbf{x}_{ij}^d\right)\begin{bmatrix} \boldsymbol{\ell}_{ij} \\ \hline -\boldsymbol{\ell}_{ij} \end{bmatrix} = \mathbf{q}_{ij}^*\left(\Delta\mathbf{x}_{ij}^d\right)^{27} \tag{5.2.27}$$

The matrices included in the graph parentheses with 2x2 size in Eq. (5.2.5)-(5.2.26) are assumed as common multipliers of the identity sub-matrices in the right square parentheses. Understood the dependence on $\Delta\mathbf{x}_{ij}^d$

$$\begin{aligned}\mathbf{k}_{Eij}^* &= R_{ij}\left\{\boldsymbol{\ell}_{ij}\boldsymbol{\lambda}_{ij}^T\left[\mathbf{I} - \Delta\mathbf{x}_{ij}^d\boldsymbol{\lambda}_{ij}^T\right]\right\}\begin{bmatrix} \mathbf{I} & \vdots & -\mathbf{I} \\ \hline -\mathbf{I} & \vdots & \mathbf{I} \end{bmatrix} = \\ &= R_{ij}\boldsymbol{\ell}_{ij}\boldsymbol{\lambda}_{ij}^T\begin{bmatrix} \mathbf{I} - \Delta\mathbf{x}_{ij}^d\boldsymbol{\lambda}_{ij}^T & \vdots & -\left(\mathbf{I} - \Delta\mathbf{x}_{ij}^d\boldsymbol{\lambda}_{ij}^T\right) \\ \hline -\left(\mathbf{I} - \Delta\mathbf{x}_{ij}^d\boldsymbol{\lambda}_{ij}^T\right) & \vdots & \mathbf{I} - \Delta\mathbf{x}_{ij}^d\boldsymbol{\lambda}_{ij}^T \end{bmatrix}\end{aligned} \tag{5.2.25b}$$

$$\mathbf{k}_{Gij}^* = \frac{F_{ij}^o}{\ell_{ij}^o}\left\{\mathbf{I} - \boldsymbol{\ell}_{ij}\boldsymbol{\lambda}_{ij}^T\right\}\begin{bmatrix} \mathbf{I} & \vdots & -\mathbf{I} \\ \hline -\mathbf{I} & \vdots & \mathbf{I} \end{bmatrix} = \frac{F_{ij}^o}{\ell_{ij}^o}\begin{bmatrix} \mathbf{I} - \boldsymbol{\ell}_{ij}\boldsymbol{\lambda}_{ij}^T & \vdots & -\left(\mathbf{I} - \boldsymbol{\ell}_{ij}\boldsymbol{\lambda}_{ij}^T\right) \\ \hline -\left(\mathbf{I} - \boldsymbol{\ell}_{ij}\boldsymbol{\lambda}_{ij}^T\right) & \vdots & \mathbf{I} - \boldsymbol{\ell}_{ij}\boldsymbol{\lambda}_{ij}^T \end{bmatrix} \tag{5.2.26b}$$

5.2.1.2 Assembled system

Denoting by $\Delta\mathbf{x}$ the vector in $4m$ components that includes the prefixed order sub-vectors $\Delta\mathbf{u}_{ij} \equiv \Delta\mathbf{u}_h$

$$\Delta\mathbf{x}^T = \left[..... \; \vdots \; \Delta\mathbf{u}_{ij}^T \; \vdots \; .....\right] = \left[..... \; \vdots \; \Delta y_{ij} \quad \Delta z_{ij} \quad \Delta y_{ji} \quad \Delta z_{ji} \; \vdots \; .....\right] \tag{5.2.28}$$

and $\Delta\mathbf{U}$ the vector that includes in $2n$ components the imposed displacements at the free nodes, allowing the configuration change $\Sigma^o \rightarrow \Sigma$.

After introducing the topological matrix $\mathbf{A}\,(4m\times2n)$ whose elements are 0 or 1 (Boolean matrix), according to compatibility

$$\Delta\mathbf{x} = \mathbf{A}\Delta\mathbf{U} \tag{5.2.29}$$

---

[26] Geometric secant stiffness matrix of the beam *ij*;

[27] Distortional secant vector of the beam *ij*.

The ground constraint of a structural element lead to nullify two components of the relevant $\Delta\mathbf{x}$ for each change of configuration. Thus, the two related rows of $\mathbf{A}$ are all made of zeros.

Let consider the $4m$ components vector

$$\Delta\mathbf{N}^T = \begin{bmatrix} ..... & \vdots & \Delta\mathbf{n}_{ij}^T & \vdots & ..... \end{bmatrix} = \begin{bmatrix} ..... & \vdots & \Delta n_{ij,y} & \Delta n_{ij,z} & \Delta n_{ji,y} & \Delta n_{ji,z} & \vdots & ..... \end{bmatrix} \qquad (5.2.30)$$

which includes as subvectors, in the same order of $\Delta\mathbf{x}$, all the vectors $\Delta\mathbf{n}_{ij} \equiv \Delta\mathbf{n}_h$ ($h = 1,\ldots m$) with reference to the different beams.

Denoting by $\Delta\mathbf{P}$ the added external loads vector, requested for the configuration change $\Sigma^\circ \to \Sigma$, which is the vector that, at each node, balances the vector sum of the forces $\Delta\mathbf{n}_{ij}$ transmitted to the node by the beam here converging.

One easily notes that the relation between forces and loads represents the equilibrium equation, where the equilibrium matrix is the transposed of $\mathbf{A}$

$$\Delta\mathbf{P} = \mathbf{A}^T \Delta\mathbf{N} \qquad (5.2.31)$$

Denoting by $\mathbf{diag}\lfloor \mathbf{k}_{ij} \rfloor$ the matrix made of all zeros except for the matrices $\mathbf{k}_{ij}$ placed in the diagonal positions, Eq. (5.2.24) is assembled in the unique relation referring to the definitions given in Eqs. (5.2.28) – (5.2.29) and Eqs. (5.2.25)-(5.2.27)

$$\Delta\mathbf{N} = \mathbf{diag}\lfloor \mathbf{k}_{E,ij}^* \rfloor \Delta\mathbf{x} + \mathbf{diag}\lfloor \mathbf{k}_{G,ij}^* \rfloor \Delta\mathbf{x} - \mathbf{diag}\lfloor \mathbf{q}_{ij}^* \rfloor \Delta\mathbf{D} \qquad (5.2.32)$$

Substituting Eq. (5.2.29) and Eq. (5.2.31) in Eq. (5.2.32), one gets

$$\Delta \mathbf{N} = \mathbf{diag}\!\left[\mathbf{k}_{E,ij}^{*}\right]\!\Delta \mathbf{x} + \mathbf{diag}\!\left[\mathbf{k}_{G,ij}^{*}\right]\!\Delta \mathbf{x} - \mathbf{diag}\!\left[\mathbf{q}_{ij}^{*}\right]\!\Delta \mathbf{D}$$

$$\Delta \mathbf{x} = \mathbf{A}\Delta \mathbf{U}$$

$$\Delta \mathbf{N} = \mathbf{diag}\!\left[\mathbf{k}_{E,ij}^{*}\right]\!\mathbf{A}\Delta \mathbf{U} + \mathbf{diag}\!\left[\mathbf{k}_{G,ij}^{*}\right]\!\mathbf{A}\Delta \mathbf{U} - \mathbf{diag}\!\left[\mathbf{q}_{ij}^{*}\right]\!\Delta \mathbf{D}$$

$$\Delta \mathbf{P} = \mathbf{A}^{T}\Delta \mathbf{N} = \left\{\mathbf{A}^{T}\mathbf{diag}\!\left[\mathbf{k}_{E,ij}^{*}\right]\!\mathbf{A}\right\}\!\Delta \mathbf{U} + \left\{\mathbf{A}^{T}\mathbf{diag}\!\left[\mathbf{k}_{G,ij}^{*}\right]\!\mathbf{A}\right\}\!\Delta \mathbf{U} - \left\{\mathbf{A}^{T}\mathbf{diag}\!\left[\mathbf{q}_{ij}^{*}\right]\right\}\!\Delta \mathbf{D}$$

$$\Delta \mathbf{P} = \mathbf{K}_{E}^{*}\Delta \mathbf{U} + \mathbf{K}_{G}^{*}\Delta \mathbf{U} - \mathbf{Q}^{*}\Delta \mathbf{D}$$

with

$$\mathbf{K}_{E}^{*} = \mathbf{A}^{T}\mathbf{diag}\!\left[\mathbf{k}_{E,ij}^{*}\right]\!\mathbf{A}$$

$$\mathbf{K}_{G}^{*} = \mathbf{A}^{T}\mathbf{diag}\!\left[\mathbf{k}_{G,ij}^{*}\right]\!\mathbf{A}$$

$$\mathbf{Q}^{*} = \mathbf{A}^{T}\mathbf{diag}\!\left[\mathbf{q}_{ij}^{*}\right]$$

$$\Delta \mathbf{P} = \mathbf{K}_{E}^{*}\Delta \mathbf{U} + \mathbf{K}_{G}^{*}\Delta \mathbf{U} - \mathbf{Q}^{*}\Delta \mathbf{D} \tag{5.2.33}$$

By assuming

$$\mathbf{K}_{E}^{*} = \mathbf{A}^{T}\mathbf{diag}\!\left[\mathbf{k}_{E,ij}^{*}\right]\!\mathbf{A} = \mathbf{K}_{E}^{*}(\Delta \mathbf{U})^{[28]} \tag{5.2.34}$$

$$\mathbf{K}_{G}^{*} = \mathbf{A}^{T}\mathbf{diag}\!\left[\mathbf{k}_{G,ij}^{*}\right]\!\mathbf{A} = \mathbf{K}_{G}^{*}(\Delta \mathbf{U})^{[29]} \tag{5.2.35}$$

$$\mathbf{Q}^{*} = \mathbf{A}^{T}\mathbf{diag}\!\left[\mathbf{q}_{ij}^{*}\right] = \mathbf{Q}^{*}(\Delta \mathbf{U})^{[30]} \tag{5.2.36}$$

Eq. (5.2.33) solves the problem formulated in Par.5.2.1.1

One can observe that it is strongly non-linear because the introduced matrix depends on displacements, which implies that the problem cannot be solved for given loads' $\Delta \mathbf{P}$ and distortions'' $\Delta \mathbf{D}$ variations n order to obtain the relevant variation of configuration $\Delta \mathbf{X}$.

Therefore a procedure to linearize Eq. (5.2.33) is adopted in order to get the change of configuration $\Delta \mathbf{X}$ under given load variations $\Delta \mathbf{P}$.

---

[28] Global elastic secant stiffness matrix

[29] Global geometric secant stiffness matrix

[30] Global distortional secant matrix

5.2.2   Step by step approaches

With reference to the know configuration, let consider some infinitesimal variations which allow to linearize Eq. (5.2.33) , and, then, to identify the tangent stiffness elastic and geometric matrices and the non-singular and invertible stiffness matrix $\mathbf{K} = \mathbf{K}_E + \mathbf{K}_G$.

The problem is solved by given infinitesimal load variations, identifying the coupled joints' displacements and consequently the relevant change of configuration.

Variations are considered arbitrarily small and the symbol Δ is substituted by d.

The vector $\boldsymbol{\lambda}$, Eq. (5.2.17) firstly, turn into, except for infinitesimals

$$\boldsymbol{\lambda}_{ij}^T = \frac{\boldsymbol{\ell}_{ij}^{oT} + \boldsymbol{\ell}_{ij}^T}{\ell_{ij}^{o2} + \boldsymbol{\ell}_{ij}^T \boldsymbol{\ell}_{ij}} = \frac{\boldsymbol{\ell}_{ij}^{oT} + \boldsymbol{\ell}_{ij}^T}{\ell_{ij}^{o2} + \ell_{ij}^2} \quad ; \quad \boldsymbol{\lambda}_{ij} = \frac{\boldsymbol{\ell}_{ij}^o + \boldsymbol{\ell}_{ij}}{\ell_{ij}^{o2} + \boldsymbol{\ell}_{ij}^T \boldsymbol{\ell}_{ij}} = \frac{\boldsymbol{\ell}_{ij}^o + \boldsymbol{\ell}_{ij}}{\ell_{ij}^{o2} + \ell_{ij}^2} \tag{5.2.17}$$

$$\boldsymbol{\lambda}_{ij} = \frac{\boldsymbol{\ell}_{ij}^o + \boldsymbol{\ell}_{ij}}{\ell_{ij}^{o2} + \ell_{ij}^2} = \frac{2\boldsymbol{\ell}_{ij}^o}{2\ell_{ij}^{o2}} = \frac{1}{\ell_{ij}^o} \frac{\boldsymbol{\ell}_{ij}^o}{\ell_{ij}^o} = \frac{1}{\ell_{ij}^o} \boldsymbol{\alpha}_{ij}^o$$

$$\boldsymbol{\lambda}_{ij}^T = \frac{\boldsymbol{\ell}_{ij}^{oT} + \boldsymbol{\ell}_{ij}^T}{\ell_{ij}^{o2} + \ell_{ij}^2} = \frac{2\boldsymbol{\ell}_{ij}^{oT}}{2\ell_{ij}^{o2}} = \frac{1}{\ell_{ij}^o} \boldsymbol{\alpha}_{ij}^{oT}$$

$$\boldsymbol{\lambda}_{ij} = \frac{1}{\ell_{ij}^o} \boldsymbol{\alpha}_{ij}^o \quad ; \quad \boldsymbol{\lambda}_{ij}^T = \frac{1}{\ell_{ij}^o} \boldsymbol{\alpha}_{ij}^{oT} \tag{5.2.37}$$

Analogously, Eq. (5.2.24) can be written again

$$\Delta \mathbf{n}_{ij} = \mathbf{k}_{Eij}^* \Delta \mathbf{u}_{ij} + \mathbf{k}_{Gij}^* \Delta \mathbf{u}_{ij} - \mathbf{q}_{ij}^* \Delta D_{ij} \tag{3.2.24}$$

$$\Delta \mathbf{n}_{ij} = \mathbf{k}_{Eij} d\mathbf{u}_{ij} + \mathbf{k}_{Gij} d\mathbf{u}_{ij} - \mathbf{q}_{ij} dD_{ij} \tag{5.2.38}$$

where the matrices are independent of $d\mathbf{x}_{ij}^d$ and assume the form (with ()* denoting the quantities under large displacements)

$$\mathbf{k}^*_{Eij} = R_{ij} \left\{ \boldsymbol{\ell}_{ij} \boldsymbol{\lambda}^T_{ij} \left[\mathbf{I} - \Delta\mathbf{x}^d_{ij} \boldsymbol{\lambda}^T_{ij} \right] \right\} \begin{bmatrix} \mathbf{I} & -\mathbf{I} \\ -\mathbf{I} & \mathbf{I} \end{bmatrix} = \mathbf{k}^*_{Eij}\left(\Delta\mathbf{x}^d_{ij}\right)$$

$$\mathbf{k}_{Eij} = R_{ij} \left\{ \ell^o_{ij} \frac{1}{\ell^o_{ij}} \boldsymbol{\alpha}^{oT}_{ij} \left[\mathbf{I} - d\mathbf{x}^d_{ij} \frac{1}{\ell^o_{ij}} \boldsymbol{\alpha}^{oT}_{ij} \right] \right\} \begin{bmatrix} \mathbf{I} & -\mathbf{I} \\ -\mathbf{I} & \mathbf{I} \end{bmatrix}$$

$$\mathbf{k}_{Eij} = R_{ij} \left\{ \boldsymbol{\alpha}^o_{ij} \boldsymbol{\alpha}^{oT}_{ij} \right\} \begin{bmatrix} \mathbf{I} & -\mathbf{I} \\ -\mathbf{I} & \mathbf{I} \end{bmatrix}$$

developing

$$\mathbf{k}_{Eij} = R_{ij} \left\{ \boldsymbol{\alpha}^o_{ij} \boldsymbol{\alpha}^{oT}_{ij} \right\} \begin{bmatrix} \mathbf{I} & -\mathbf{I} \\ -\mathbf{I} & \mathbf{I} \end{bmatrix} = R_{ij} \begin{bmatrix} \alpha^o_{ij,y} \\ \alpha^o_{ij,z} \end{bmatrix} \begin{bmatrix} \alpha^o_{ij,y} & \alpha^o_{ij,z} \end{bmatrix} \begin{bmatrix} \mathbf{I} & -\mathbf{I} \\ -\mathbf{I} & \mathbf{I} \end{bmatrix} =$$

$$= R_{ij} \begin{bmatrix} \alpha^{o2}_{ij,y} & \alpha^o_{ij,y}\alpha^o_{ij,z} \\ \alpha^o_{ij,z}\alpha^o_{ij,y} & \alpha^{o2}_{ij,z} \end{bmatrix} \begin{bmatrix} \mathbf{I} & -\mathbf{I} \\ -\mathbf{I} & \mathbf{I} \end{bmatrix} =$$

$$= R_{ij} \begin{bmatrix} \alpha^{o2}_{ij,y} & \alpha^o_{ij,y}\alpha^o_{ij,z} & -\alpha^{o2}_{ij,y} & -\alpha^o_{ij,y}\alpha^o_{ij,z} \\ \alpha^o_{ij,z}\alpha^o_{ij,y} & \alpha^{o2}_{ij,z} & -\alpha^o_{ij,z}\alpha^o_{ij,y} & -\alpha^{o2}_{ij,z} \\ -\alpha^{o2}_{ij,y} & -\alpha^o_{ij,y}\alpha^o_{ij,z} & \alpha^{o2}_{ij,y} & \alpha^o_{ij,y}\alpha^o_{ij,z} \\ -\alpha^o_{ij,z}\alpha^o_{ij,y} & -\alpha^{o2}_{ij,z} & \alpha^o_{ij,z}\alpha^o_{ij,y} & \alpha^{o2}_{ij,z} \end{bmatrix}$$

$$\mathbf{k}_{Eij} = R_{ij} \left\{ \boldsymbol{\alpha}^o_{ij} \boldsymbol{\alpha}^{oT}_{ij} \right\} \begin{bmatrix} \mathbf{I} & -\mathbf{I} \\ -\mathbf{I} & \mathbf{I} \end{bmatrix}{}^{[31]} \qquad\qquad (5.2.39)$$

---

[31] Tangent elastic stiffness matrix

$$\mathbf{k}^*_{Gij} = \frac{F^o_{ij}}{\ell^o_{ij}} \left\{ \mathbf{I} - \boldsymbol{\ell}_{ij} \boldsymbol{\lambda}^T_{ij} \right\} \left[\begin{array}{c|c} \mathbf{I} & -\mathbf{I} \\ \hline -\mathbf{I} & \mathbf{I} \end{array} \right] = \mathbf{k}^*_{Gij} \left(\Delta \mathbf{x}^d_{ij} \right)$$

$$\mathbf{k}_{Gij} = \frac{F^o_{ij}}{\ell^o_{ij}} \left\{ \mathbf{I} - \boldsymbol{\ell}^o_{ij} \frac{1}{\ell^o_{ij}} \boldsymbol{\alpha}^{oT}_{ij} \right\} \left[\begin{array}{c|c} \mathbf{I} & -\mathbf{I} \\ \hline -\mathbf{I} & \mathbf{I} \end{array} \right]$$

$$\mathbf{k}_{Gij} = \frac{F^o_{ij}}{\ell^o_{ij}} \left\{ \mathbf{I} - \boldsymbol{\alpha}^o_{ij} \boldsymbol{\alpha}^{oT}_{ij} \right\} \left[\begin{array}{c|c} \mathbf{I} & -\mathbf{I} \\ \hline -\mathbf{I} & \mathbf{I} \end{array} \right]$$

developing

$$\mathbf{k}_{Gij} = \frac{F^o_{ij}}{\ell^o_{ij}} \left\{ \mathbf{I} - \boldsymbol{\alpha}^o_{ij} \boldsymbol{\alpha}^{oT}_{ij} \right\} \left[\begin{array}{c|c} \mathbf{I} & -\mathbf{I} \\ \hline -\mathbf{I} & \mathbf{I} \end{array} \right] =$$

$$= \frac{F^o_{ij}}{\ell^o_{ij}} \left\{ \left[\begin{array}{c|c} 1 & 0 \\ \hline 0 & 1 \end{array} \right] - \left[\begin{array}{c|c} \alpha^{o2}_{ij,y} & \alpha^o_{ij,y}\alpha^o_{ij,z} \\ \hline \alpha^o_{ij,z}\alpha^o_{ij,y} & \alpha^{o2}_{ij,z} \end{array} \right] \right\} \left[\begin{array}{c|c} \mathbf{I} & -\mathbf{I} \\ \hline -\mathbf{I} & \mathbf{I} \end{array} \right] =$$

$$= \frac{F^o_{ij}}{\ell^o_{ij}} \left\{ \left[\begin{array}{c|c} 1-\alpha^{o2}_{ij,y} & -\alpha^o_{ij,y}\alpha^o_{ij,z} \\ \hline -\alpha^o_{ij,z}\alpha^o_{ij,y} & 1-\alpha^{o2}_{ij,z} \end{array} \right] \right\} \left[\begin{array}{c|c} \mathbf{I} & -\mathbf{I} \\ \hline -\mathbf{I} & \mathbf{I} \end{array} \right] =$$

$$= \frac{F^o_{ij}}{\ell^o_{ij}} \left\{ \left[\begin{array}{c|c} \alpha^{o2}_{ij,z} & -\alpha^o_{ij,y}\alpha^o_{ij,z} \\ \hline -\alpha^o_{ij,z}\alpha^o_{ij,y} & \alpha^{o2}_{ij,y} \end{array} \right] \right\} \left[\begin{array}{c|c} \mathbf{I} & -\mathbf{I} \\ \hline -\mathbf{I} & \mathbf{I} \end{array} \right] =$$

$$= \frac{F^o_{ij}}{\ell^o_{ij}} \left[\begin{array}{cc|cc} \alpha^{o2}_{ij,z} & -\alpha^o_{ij,y}\alpha^o_{ij,z} & -\alpha^{o2}_{ij,z} & \alpha^o_{ij,y}\alpha^o_{ij,z} \\ -\alpha^o_{ij,z}\alpha^o_{ij,y} & \alpha^{o2}_{ij,y} & \alpha^o_{ij,z}\alpha^o_{ij,y} & -\alpha^{o2}_{ij,y} \\ \hline -\alpha^{o2}_{ij,z} & \alpha^o_{ij,y}\alpha^o_{ij,z} & \alpha^{o2}_{ij,z} & -\alpha^o_{ij,y}\alpha^o_{ij,z} \\ \alpha^o_{ij,z}\alpha^o_{ij,y} & -\alpha^{o2}_{ij,y} & -\alpha^o_{ij,z}\alpha^o_{ij,y} & \alpha^{o2}_{ij,y} \end{array} \right]$$

$$\mathbf{k}_{Gij} = \frac{F^o_{ij}}{\ell^o_{ij}} \left\{ \mathbf{I} - \boldsymbol{\alpha}^o_{ij} \boldsymbol{\alpha}^{oT}_{ij} \right\} \left[\begin{array}{c|c} \mathbf{I} & -\mathbf{I} \\ \hline -\mathbf{I} & \mathbf{I} \end{array} \right]^{32} \tag{5.2.40}$$

$$\mathbf{q}^*_{ij} = \frac{R_{ij}}{\ell^o_{ij}} \left(1 - \boldsymbol{\lambda}^T_{ij} \Delta \mathbf{x}^d_{ij} \right) \left[\begin{array}{c} \boldsymbol{\ell}_{ij} \\ \hline -\boldsymbol{\ell}_{ij} \end{array} \right] = \mathbf{q}^*_{ij} \left(\Delta \mathbf{x}^d_{ij} \right)$$

$$\mathbf{q}_{ij} = \frac{R_{ij}}{\ell^o_{ij}} \left(1 - \frac{1}{\ell^o_{ij}} \boldsymbol{\alpha}^{oT}_{ij} d\mathbf{x}^d_{ij} \right) \left[\begin{array}{c} \boldsymbol{\ell}^o_{ij} \\ \hline -\boldsymbol{\ell}^o_{ij} \end{array} \right] =$$

$$= \frac{R_{ij}}{\ell^o_{ij}} \left[\begin{array}{c} \boldsymbol{\ell}^o_{ij} \\ \hline -\boldsymbol{\ell}^o_{ij} \end{array} \right] = R_{ij} \left[\begin{array}{c} \boldsymbol{\alpha}^{oT}_{ij} \\ \hline -\boldsymbol{\alpha}^{oT}_{ij} \end{array} \right]$$

$$\mathbf{q}_{ij} = R_{ij} \left[\begin{array}{c} \boldsymbol{\alpha}^{oT}_{ij} \\ \hline -\boldsymbol{\alpha}^{oT}_{ij} \end{array} \right]$$

---

[32] Geometric tangent stiffness matrix

$$\mathbf{q}_{ij} = R_{ij} \begin{bmatrix} \boldsymbol{\alpha}_{ij}^{oT} \\ -\boldsymbol{\alpha}_{ij}^{oT} \end{bmatrix}^{33} \tag{5.2.41}$$

Remembering Eq. (5.2.7)

$$\boldsymbol{\alpha}_{ij}^{o} = \frac{\boldsymbol{\ell}_{ij}^{o}}{\ell_{ij}^{o}} = \begin{bmatrix} \alpha_{ij,y}^{o} \\ \alpha_{ij,z}^{o} \end{bmatrix}$$

$$\boldsymbol{\alpha}_{ij} = \frac{\boldsymbol{\ell}_{ij}}{\ell_{ij}} = \begin{bmatrix} \alpha_{ij,y} \\ \alpha_{ij,z} \end{bmatrix} \tag{5.2.7}$$

one observes that

$$\boldsymbol{\alpha}_{ij}^{o} \boldsymbol{\alpha}_{ij}^{oT} = \begin{bmatrix} \alpha_{ij,y}^{o2} & \alpha_{ij,y}^{o} \alpha_{ij,z}^{o} \\ \alpha_{ij,z}^{o} \alpha_{ij,y}^{o} & \alpha_{ij,z}^{o2} \end{bmatrix} \tag{5.2.42}$$

As for the global structure, the relation between loads and displacements Eq. (5.2.33) turns into

$$d\mathbf{P} = \mathbf{K}_E d\mathbf{U} + \mathbf{K}_G d\mathbf{U} - \mathbf{Q} d\mathbf{D} \tag{5.2.43}$$

where

$$\mathbf{K}_E = \mathbf{A}^T \mathbf{diag}[\mathbf{k}_{E,ij}] \mathbf{A} \tag{5.2.44}$$

$$\mathbf{K}_G = \mathbf{A}^T \mathbf{diag}[\mathbf{k}_{G,ij}] \mathbf{A} \tag{5.2.45}$$

$$\mathbf{Q} = \mathbf{A}^T \mathbf{diag}[\mathbf{q}_{ij}] \tag{5.2.46}$$

One gets the total tangent stiffness matrix

$$\mathbf{K} = \mathbf{K}_E + \mathbf{K}_G \quad ; \quad \det[\mathbf{K}] \neq 0 \quad ; \quad eig[\mathbf{K}] > 0 \tag{5.2.47}$$

which is assumed to be non singular and positive defined, as ordinarily usual under the assumed hypotheses.

Finally, Eq. (5.2.43) can be solved by $d\mathbf{U}$

---

[33] Distortional tangent stiffness vector

$$d\mathbf{U} = \mathbf{K}^{-1}\big(d\mathbf{P} + \mathbf{Q}d\mathbf{D}\big) \tag{5.2.48}$$

The elongations of the single elements and therefore the increments of the internal forces are also to be considered.

About the elongations, Eq. (5.2.14) is taken into account, remembering Eq. (5.2.37) and Eq. (5.2.20)

$$\Delta\ell_{ij} = \frac{\ell_{ij}^{o}}{\ell_{ij}^{o2} + \ell_{ij}^{T}\ell_{ij}}\big(\ell_{ij}^{oT} + \ell_{ij}^{T}\big)\Delta\mathbf{x}_{ij}^{d} \tag{5.2.14}$$

$$\lambda_{ij}^{T} = \frac{\ell_{ij}^{oT} + \ell_{ij}^{T}}{\ell_{ij}^{o2} + \ell_{ij}^{2}} = \frac{2\ell_{ij}^{oT}}{2\ell_{ij}^{o2}} = \frac{1}{\ell_{ij}^{o}}\boldsymbol{\alpha}_{ij}^{oT} \tag{5.2.37}$$

$$\Delta\mathbf{x}_{ij}^{d} = \big[\mathbf{I} \ \vdots \ -\mathbf{I}\big]\Delta\mathbf{u}_{ij} \quad ; \quad \Delta\mathbf{x}_{ji}^{d} = \big[-\mathbf{I} \ \vdots \ \mathbf{I}\big]\Delta\mathbf{u}_{ij} \tag{5.2.20}$$

$$d\ell_{ij} = \boldsymbol{\alpha}_{ij}^{oT}d\mathbf{x}_{ij}^{d} = \boldsymbol{\alpha}_{ij}^{oT}\big[\mathbf{I} \ \vdots \ -\mathbf{I}\big]d\mathbf{u}_{ij} = \big[\boldsymbol{\alpha}_{ij}^{oT} \ \vdots \ -\boldsymbol{\alpha}_{ij}^{oT}\big]d\mathbf{u}_{ij} \tag{5.2.49}$$

one considers the *m* elongations' vector

$$d\mathbf{L} = \big[d\ell_{1} \ \vdots \ ..... \ \vdots \ d\ell_{ij=h} \ \vdots \ \ \vdots \ d\ell_{m}\big] \tag{5.2.50}$$

By considering Eq. (5.2.27)

$$\Delta\mathbf{x} = \mathbf{A}\Delta\mathbf{U} \tag{5.2.27}$$

one can write again (remembering the definition in Eq. (5.2.26) of $\Delta\mathbf{x}$, here $d\mathbf{x}$)

$$\Delta\mathbf{x}^{T} = \big[..... \ \vdots \ \Delta\mathbf{u}_{ij}^{T} \ \vdots \ .....\big] = \big[..... \ \vdots \ \Delta y_{ij} \quad \Delta z_{ij} \quad \Delta y_{ji} \quad \Delta z_{ji} \ \vdots \ .....\big] \tag{5.2.26}$$

$$d\ell_{ij} = \boldsymbol{\alpha}_{ij}^{oT}d\mathbf{x}_{ij}^{d} = \boldsymbol{\alpha}_{ij}^{oT}\big[\mathbf{I} \ \vdots \ -\mathbf{I}\big]d\mathbf{u}_{ij} = \big[\boldsymbol{\alpha}_{ij}^{oT} \ \vdots \ -\boldsymbol{\alpha}_{ij}^{oT}\big]d\mathbf{u}_{ij}$$

$$d\mathbf{x} = \mathbf{A}d\mathbf{U}$$

$$d\mathbf{L} = diag\big[\boldsymbol{\alpha}_{ij}^{oT} \ \vdots \ -\boldsymbol{\alpha}_{ij}^{oT}\big]d\mathbf{x} = diag\big[\boldsymbol{\alpha}_{ij}^{oT} \ \vdots \ -\boldsymbol{\alpha}_{ij}^{oT}\big]\mathbf{A}d\mathbf{U}$$

$$\mathbf{B} = diag\big[\boldsymbol{\alpha}_{ij}^{oT} \ \vdots \ -\boldsymbol{\alpha}_{ij}^{oT}\big]\mathbf{A}$$

$$d\mathbf{L} = \mathbf{B}d\mathbf{U}$$

$$d\mathbf{L} = \mathbf{B}d\mathbf{U} \tag{5.2.51}$$

where $\mathbf{B}$ denotes the compatibility matrix ($m \times 2n$) depending on the geometry of the configuration Σ^o

$$\mathbf{B} = diag\left[\boldsymbol{\alpha}_{ij}^{oT} \;\vdots\; -\boldsymbol{\alpha}_{ij}^{oT}\right]\mathbf{A} \tag{5.2.52}$$

The forces' variations $d\mathbf{F}$ are expressed in function of $d\mathbf{L}$ and $d\mathbf{D}$, by assembling the m scalar equations Eq.(5.2.6) for $ij = h = 1,\ldots.m,$ and one gets

$$d\mathbf{F} = diag\lfloor R_{ij}\rfloor(d\mathbf{L} - d\mathbf{D}) \tag{5.2.53}$$

5.2.3   Solution procedure

On the basis of the relations developed in the above, one sets up a calculus method for solving the main problem of these kind of structures, i.e. identifying the displacements for each given load condition.

Actually, by starting from the known initial configuration Σ^o, its change into the new one Σ occurs after the application of the loads $\Delta\mathbf{P}$ and distortions $\Delta\mathbf{D}$, which may be regarded as given by the sum of a number of load conditions: one considers. Then let consider a load story given by an additive sequence of s increments of loads and distortions.

$$\begin{aligned}\Delta\mathbf{P} &= \Delta^1\mathbf{P} + \Delta^2\mathbf{P} + \ldots\ldots + \Delta^s\mathbf{P}\\ \Delta\mathbf{D} &= \Delta^1\mathbf{D} + \Delta^2\mathbf{D} + \ldots\ldots + \Delta^s\mathbf{D}\end{aligned} \tag{5.2.54}$$

The final state Σ can be reached going through a series of intermediate conditions

$$\Sigma^o \to \Sigma^1\left(\Delta^1\mathbf{P},\Delta^1\mathbf{D}\right) \to \Sigma^2\left(\Delta^1\mathbf{P}+\Delta^2\mathbf{P},\Delta^1\mathbf{D}+\Delta^2\mathbf{D}\right) \to \ldots\ldots \to \Sigma = \Sigma^s\left(\Delta\mathbf{P},\Delta\mathbf{D}\right) \tag{5.2.55}$$

Thus, once chosen $\Delta^r\mathbf{P}$ sufficiently small, then the passage from the situation Σ^{r-1} to the subsequent one Σ^r can be analized by the linear equations Eq.(5.2.48)-(5.2.53) in Par.5.2.1

$$d\mathbf{U} = \mathbf{K}^{-1}\left(d\mathbf{P} + \mathbf{Q}d\mathbf{D}\right) \tag{5.2.48}$$

$$d\ell_{ij} = \boldsymbol{\alpha}_{ij}^{oT}d\mathbf{x}_{ij}^d = \boldsymbol{\alpha}_{ij}^{oT}\left[\mathbf{I} \;\vdots\; -\mathbf{I}\right]d\mathbf{u}_{ij} = \left[\boldsymbol{\alpha}_{ij}^{oT} \;\vdots\; -\boldsymbol{\alpha}_{ij}^{oT}\right]d\mathbf{u}_{ij} \tag{5.2.49}$$

$$d\mathbf{L} = \begin{bmatrix} d\ell_1 & \vdots & ..... & \vdots & d\ell_{ij=h} & \vdots & & \vdots & d\ell_m \end{bmatrix} \tag{5.2.50}$$

$$d\mathbf{L} = \mathbf{B}d\mathbf{U} \tag{5.2.51}$$

$$\mathbf{B} = diag\left[\boldsymbol{\alpha}_{ij}^{oT} \quad \vdots \quad -\boldsymbol{\alpha}_{ij}^{oT}\right]\mathbf{A} \tag{5.2.52}$$

$$d\mathbf{F} = diag\left[R_{ij}\right](d\mathbf{L} - d\mathbf{D}) \tag{5.2.53}$$

After r steps, by summing up the partial results, one gets

$$\begin{aligned} (\Delta\mathbf{U})^r &= \Delta^1\mathbf{U} + \Delta^2\mathbf{U} + ... + \Delta^r\mathbf{U} \\ (\Delta\mathbf{F})^r &= \Delta^1\mathbf{F} + \Delta^2\mathbf{F} + ... + \Delta^r\mathbf{F} \\ (\Delta\mathbf{L})^r &= \Delta^1\mathbf{L} + \Delta^2\mathbf{L} + ... + \Delta^r\mathbf{L} \end{aligned} \tag{5.2.56}$$

The final results identifying Σ are obtained when $r = s$

$$\begin{aligned} \Delta\mathbf{U} &= (\Delta\mathbf{U})^s \\ \Delta\mathbf{F} &= (\Delta\mathbf{F})^s \\ \Delta\mathbf{L} &= (\Delta\mathbf{L})^s \end{aligned} \tag{5.2.57}$$

5.2.4   Example

In the following an example is presented for analytically treating the above illustrated theoretical calculus model. Let consider a plane structure composed by $m = 2$ beams and $n = 1$ free nodes (Fig.5.8), in a known static regime[34]
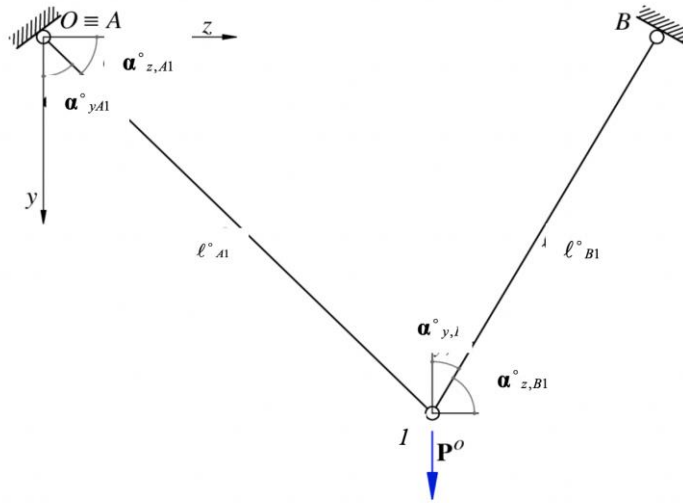
Figure 5.8: Plane cable structure in the initial configuration loaded at the free node in the known static regime.

Let consider the following entities in the initial configuration, where

$\mathbf{P}^{oT} = \begin{bmatrix} P^o_{y,1} & 0 \end{bmatrix}$ is the vector of the initial loads applied on the free nodes, in *2n* components, in the initial configuration

$\mathbf{X}^{oT} = \begin{bmatrix} y^o & z^o \end{bmatrix}$ is the position vector of the free nodes in *2n* components, in the initial configuration

$\mathbf{F}^{0T} = \begin{bmatrix} f^0_{A1} & f^0_{B1} \end{bmatrix}$ is the vector of the forces in the *m* beams, in the initial configuration

---

[34] In the following, the dependence on $\Delta\mathbf{x}^d_{A1}$ in the analysis of the single beam, and on $\Delta\mathbf{X}$ in the global structure aanalysis are omitted.

$\mathbf{D}^{0T} = \begin{bmatrix} D^0_{A1} & D^0_{B1} \end{bmatrix}$ is the vector of the distortions in the m beams in the initial configuration

As shown in the previous paragraphs, after identifying the initial configuration in a static known regime, a change of position $\Delta\mathbf{X}$ of the free node is applied leading to a new geometry of the structure and consequently to new static conditions. Let also consider a variation of distortion in the beams (Fig.5.9).

The transition from the undeformed to the deformed configuration occurs under the hypotheses (Par. 5.2.1):

a. $\Delta\varepsilon = \dfrac{\Delta\ell}{\ell} \ll 1$, which means that the deformations in any beam are very small

b.   Each beam has an elastic linear behavior

c.   Any cable segment is straight both in undeformed and deformed configurations.
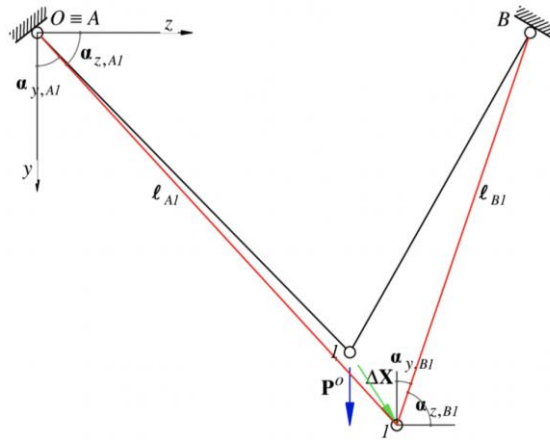
Figure 5.9: Deformed configuration (in red) due to the application of the position change of the free node.

Hence, the variation of the external nodal load $\Delta\mathbf{P}(\Delta\mathbf{X})$ is searched for, in order to ensure the equilibrium in the deformed configuration (Fig. 5.8).
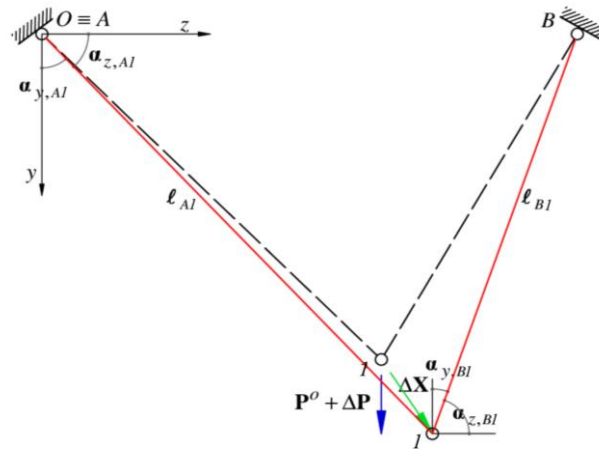
Figure 5.10: Cable structure in the deformed configuration (continuous line).

Denoted by

$\mathbf{P} = \mathbf{P}^o + \Delta\mathbf{P}$ the vector of the applied nodal load in the deformed configuration

$\mathbf{X} = \mathbf{X}^o + \Delta\mathbf{X}$ the vector of the updates position of the free node in the deformed configuration

$\mathbf{D} = \mathbf{D}^o + \Delta\mathbf{D}$ the vector of the distortions in the beams in the deformed configuration

One follows the two steps of the analysis in Par. 5.2.1, hence, firstly, the study of the single elements with the identification of the relations between the internal forces' variations and the free node position change, and, then, the study of the global structure, where the assemblage operation is dealt with by introducing the topological matrix $\mathbf{A}$, finally, allowing to identify the relation between the load increments imposed position changes of the free node.

5.2.4.1 Single elements' analysis

Let first of all consider the beam A1 in Fig.5.11 and its deformed configuration described by the vector $\Delta\mathbf{x}_{A1}^d$ after the application of $\Delta\mathbf{X}$
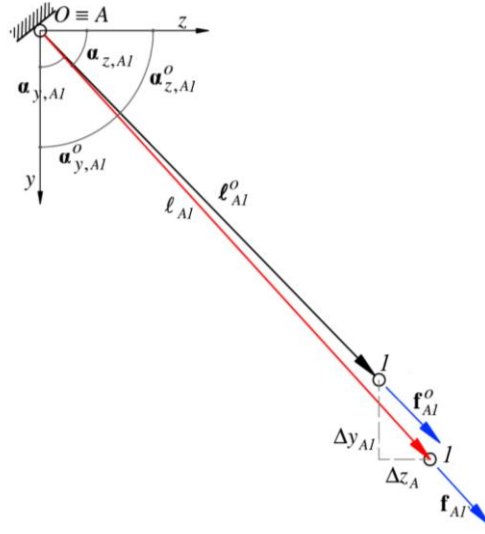
Figure 5.11: A1 beam in its initial and deformed configuration.

$$\Delta \mathbf{x}_{A1}^{d} = \begin{bmatrix} \Delta y_{A1} - \Delta y_{1A} \\ \Delta z_{A1} - \Delta z_{1A} \end{bmatrix} = \begin{bmatrix} \Delta y_{A1} \\ \Delta z_{A1} \end{bmatrix}$$
(5.2.58)

The boundary conditions in A, as a restrained node, are

$$\Delta y_{A1} = 0$$
$$\Delta z_{A1} = 0$$

Consequently, by omitting the dependence of the following entities by $\Delta \mathbf{x}_{A1}^{d}$, one gets

$$\ell_{A1} = \ell_{A1}^{o} + \Delta \mathbf{x}_{A1}^{d}$$
(5.2.59)

$$\Delta F_{A1} = \frac{E_{A1} A_{A1}}{\ell_{A1}} (\Delta \ell_{A1} - \Delta D_{A1}) = R_{A1} (\Delta \ell_{A1} - \Delta D_{A1})$$
(5.2.60)

where

ℓ_{A1} is the beam vector *A1*, directed from *A* to *1* in the deformed configuration

ℓ_{A1}^{o} is the beam vector *A1* directed from *A* to *1* in the initial configuration

ΔF_{A1} is the magnitude of the force variation in the beam *A1*

R_{A1} is the axial stiffness in the beam *A1*

$\Delta \ell_{A1}$ is the modulus of the length variation of the beam *A1*

ΔD_{A1} is the modulus of variation of the distortions in the beam *A1*

In this first step, one focuses on the identification of the variations of the internal forces

$$\Delta \mathbf{f}_{A1}(\Delta \mathbf{x}_{A1}^{d}) \tag{5.2.61}$$

$$\Delta \mathbf{f}_{B1}(\Delta \mathbf{x}_{B1}^{d}) \tag{5.2.62}$$

whence, remembering Eq. (5.2.16) in Par. 3.2,

$$\Delta \mathbf{f}_{A1} = R_{A1} \ell_{A1} \lambda_{A1}^{T} \left[\mathbf{I} - \Delta \mathbf{x}_{A1}^{d} \lambda_{A1}^{T} \right] \Delta \mathbf{x}_{A1}^{d} + \frac{F_{A1}^{o}}{\ell_{A1}^{o}} \left[\mathbf{I} - \ell_{A1} \lambda_{A1}^{T} \right] \Delta \mathbf{x}_{A1}^{d} -$$

$$+ \frac{R_{A1}}{\ell_{A1}^{o}} \ell_{A1} (1 - \lambda_{A1}^{T} \Delta \mathbf{x}_{A1}^{d}) \Delta D_{A1} \tag{5.2.63}$$

where

I is the identity matrix in 2×2 dimensions

$\boldsymbol{\lambda}$ is the vector $\dfrac{1}{\ell_{A1}^{o2} + \ell_{A1}^{T} \ell_{A1}} \left(\ell_{A1}^{o} + \ell_{A1} \right)$

Hence, the variation of the internal force in the analysed beam *A1* from the end 1 to *A* is inferred obtained through indexes' permutation

$$\Delta \mathbf{f}_{1A} = R_{A1} \ell_{A1} \lambda_{A1}^{T} \left[\mathbf{I} - \Delta \mathbf{x}_{A1}^{d} \lambda_{A1}^{T} \right] \Delta \mathbf{x}_{1A}^{d} + \frac{F_{A1}^{o}}{\ell_{A1}^{o}} \left[\ell_{A1} \lambda_{A1}^{T} \right] \Delta \mathbf{x}_{1A}^{d} -$$

$$- \frac{R_{A1}}{\ell_{A1}^{o}} \ell_{A1} (1 - \lambda_{A1}^{T} \Delta \mathbf{x}_{A1}^{d}) \Delta D_{A1}$$

Once determined the internal forces' variations at the ends of the considered beam, one re-assembles the structure, in such a way to evaluate the variation of nodal load necessary for the equilibrium of the structure in the updated configuration.

One considers the $4m$ components vector $\Delta\mathbf{n}_{A1}$ that embeds the variations of the internal forces at the ends the beam $A1$

$$\Delta\mathbf{n}_{A1} = \begin{bmatrix} \Delta\mathbf{f}_{A1} \\ \Delta\mathbf{f}_{1A} \end{bmatrix} = \begin{bmatrix} \Delta F_{A1,y} \\ \Delta F_{A1,z} \\ \Delta F_{1A,y} \\ \Delta F_{1A,z} \end{bmatrix} \tag{5.2.65}$$

Since

$$\Delta\mathbf{x}_{A1}^d = \begin{bmatrix} 1 & 0 & -1 & 0 \\ 0 & 1 & 0 & -1 \end{bmatrix} \begin{bmatrix} \Delta y_{A1} \\ \Delta z_{A1} \\ \Delta y_{1A} \\ \Delta z_{1A} \end{bmatrix} = \begin{bmatrix} \Delta y_{A1} - \Delta y_{1A} \\ \Delta z_{A1} - \Delta z_{1A} \end{bmatrix} \tag{5.2.66}$$

$$\rightarrow \Delta\mathbf{x}_{A1}^d = \begin{bmatrix} \mathbf{I} & \vdots & -\mathbf{I} \end{bmatrix}\Delta\mathbf{u}_{A1} \tag{5.2.67}$$

$$\rightarrow \Delta\mathbf{x}_{1A}^d = \begin{bmatrix} -\mathbf{I} & \vdots & \mathbf{I} \end{bmatrix}\Delta\mathbf{u}_{A1} \tag{5.2.68}$$

with $\Delta\mathbf{u}_{A1}$ of the 4 components displacement vector.

Thus the internal force vector can be written in the form

$$\Delta\mathbf{n}_{A1} = \left\{ R_{A1} \begin{bmatrix} \ell_{A1}\lambda_{A1}^T\left[\mathbf{I} - \Delta\mathbf{x}_{A1}^d\lambda_{A1}^T\right] & \mathbf{0} \\ \mathbf{0} & \ell_{A1}\lambda_{A1}^T\left[\mathbf{I} - \Delta\mathbf{x}_{A1}^d\lambda_{A1}^T\right] \end{bmatrix} + \frac{F_{A1}^o}{\ell_{A1}^o}\begin{bmatrix} \left[\mathbf{I} - \ell_{A1}\lambda_{A1}^T\right] & \mathbf{0} \\ \mathbf{0} & \left[\mathbf{I} - \ell_{A1}\lambda_{A1}^T\right] \end{bmatrix} \right\} \begin{bmatrix} \mathbf{I} & -\mathbf{I} \\ -\mathbf{I} & \mathbf{I} \end{bmatrix}\Delta\mathbf{u}_{A1} -$$
$$+ \frac{R_{A1}}{\ell_{A1}^o}(1 - \lambda_{A1}^T\Delta\mathbf{x}_{A1}^d)\begin{bmatrix} \ell_{A1} \\ -\ell_{A1} \end{bmatrix}\Delta D_{A1} \tag{5.2.69}$$

where one can identify the following matrices

$$\mathbf{k}_{E,A1}^* = R_{A1}\left\{\ell_{AC}\lambda_{AC}^T\left[\mathbf{I} - \Delta\mathbf{x}_{AC}^d\lambda_{AC}^T\right]\right\}\begin{bmatrix} \mathbf{I} & -\mathbf{I} \\ -\mathbf{I} & \mathbf{I} \end{bmatrix}$$

$$\mathbf{k}_{G,A1}^* = \frac{F_{A1}^0}{\ell_{A1}^0}\left\{\mathbf{I} - \ell_{A1}\lambda_{A1}^T\right\}\begin{bmatrix} \mathbf{I} & -\mathbf{I} \\ -\mathbf{I} & \mathbf{I} \end{bmatrix} \tag{5.2.70}$$

$$\mathbf{q}_{A1}^* = \frac{R_{A1}}{\ell_{A1}^0}(1 - \lambda_{A1}^T\Delta\mathbf{x}_{A1}^d)\begin{bmatrix} \ell_{A1} \\ -\ell_{A1} \end{bmatrix}$$

which are respectively the stiffness elastic and geometric secant matrices, and the secant distortion vector of the beam $A1$.

By writing Eq. (5.2.69) in a compact form, it turns into

$$\Delta \mathbf{n}_{A1} = \mathbf{k}_{E,A1}^{*} \Delta \mathbf{u}_{A1} + \mathbf{k}_{G,A1}^{*} \Delta \mathbf{u}_{A1} - \mathbf{q}_{A1}^{*} \Delta \mathbf{D}_{A1} \tag{5.2.71}$$

As concerns the other beam $B1$ of the structure, its change of geometry is given by

$$\Delta \mathbf{x}_{B1}^{d} = \begin{bmatrix} \Delta y_{B1} - \Delta y_{1B} \\ \Delta z_{B1} - \Delta z_{1B} \end{bmatrix} = \begin{bmatrix} \Delta y_{B1} \\ \Delta z_{B1} \end{bmatrix} \tag{5.2.72}$$

with boundary conditions in B

$$\begin{aligned} \Delta y_{1B} &= 0 \\ \Delta z_{1B} &= 0 \end{aligned} \tag{5.2.73}$$

Whence, $\Delta \mathbf{f}_{B1}$ is given in the form

$$\Delta \mathbf{f}_{B1} = R_{B1} \ell_{B1} \lambda_{B1}^{T} \left[\mathbf{I} - \Delta \mathbf{x}_{B1}^{d} \lambda_{B1}^{T} \right] \Delta \mathbf{x}_{B1}^{d} + \frac{F_{B1}^{o}}{\ell_{B1}^{o}} \left[\mathbf{I} - \ell_{B1} \lambda_{B1}^{T} \right] \Delta \mathbf{x}_{B1}^{d} -$$

$$+ \frac{R_{B1}}{\ell_{B1}^{o}} \ell_{B1} (1 - \lambda_{B1}^{T} \Delta \mathbf{x}_{B1}^{d}) \Delta D_{B1} \tag{5.2.74}$$

and then, by permuting the indexes, one gets $\Delta \mathbf{f}_{1B}$

$$\Delta \mathbf{f}_{1B} = R_{B1} \ell_{B1} \lambda_{B1}^{T} \left[\mathbf{I} - \Delta \mathbf{x}_{B1}^{d} \lambda_{B1}^{T} \right] \Delta \mathbf{x}_{1B}^{d} + \frac{F_{B1}^{o}}{\ell_{B1}^{o}} \left[\ell_{B1} \lambda_{B1}^{T} \right] \Delta \mathbf{x}_{1B}^{d} -$$

$$- \frac{R_{B1}}{\ell_{B1}^{o}} \ell_{B1} (1 - \lambda_{B1}^{T} \Delta \mathbf{x}_{B1}^{d}) \Delta D_{B1} \tag{3.6.18}$$

where

$\mathbf{I}$ is the identity matrix in 2×2 dimensions

$\boldsymbol{\lambda}$ is the vector $\dfrac{1}{\ell_{B1}^{o2} + \ell_{B1}^{T} \ell_{B1}} \left(\ell_{B1}^{o} + \ell_{B1} \right)$.

thus, the vector $\Delta \mathbf{n}_{B1}$ is introduced

$$\Delta \mathbf{n}_{B1} = \begin{bmatrix} \Delta \mathbf{f}_{B1} \\ \Delta \mathbf{f}_{1B} \end{bmatrix} = \begin{bmatrix} \Delta F_{B1,y} \\ \Delta F_{B1,z} \\ \Delta F_{1B,y} \\ \Delta F_{1B,z} \end{bmatrix} \tag{5.2.75}$$

By considering the vector of displacements $\Delta \mathbf{u}_{B1}$ one gets

$$\Delta\mathbf{x}_{B1}^d = \begin{bmatrix} 1 & 0 & -1 & 0 \\ 0 & 1 & 0 & -1 \end{bmatrix} \begin{bmatrix} \Delta y_{B1} \\ \Delta z_{B1} \\ \Delta y_{1B} \\ \Delta z_{1B} \end{bmatrix} = \begin{bmatrix} \Delta y_{B1} - \Delta y_{1B} \\ \Delta z_{B1} - \Delta z_{1B} \end{bmatrix} \tag{5.2.75}$$

i.e.

$$\Delta\mathbf{x}_{B1}^d = \begin{bmatrix} \mathbf{I} & \vdots & -\mathbf{I} \end{bmatrix} \Delta\mathbf{u}_{B1} \tag{5.2.76}$$

$$\Delta\mathbf{x}_{1B}^d = \begin{bmatrix} \mathbf{I} & \vdots & -\mathbf{I} \end{bmatrix} \Delta\mathbf{u}_{B1} \tag{5.2.77}$$

Then

$$\Delta\mathbf{n}_{B1} = \left\{ R_{B1} \begin{bmatrix} \boldsymbol{\ell}_{B1} \lambda_{B1}^T [\mathbf{I} - \Delta\mathbf{x}_{B1}^d \lambda_{B1}^T] & \mathbf{0} \\ \mathbf{0} & \boldsymbol{\ell}_{BC} \lambda_{B1}^T [\mathbf{I} - \Delta\mathbf{x}_{B1}^d \lambda_{B1}^T] \end{bmatrix} + \right.$$
$$\left. + \frac{F_{B1}^o}{\ell_{B1}^o} \begin{bmatrix} [\mathbf{I} - \boldsymbol{\ell}_{B1} \lambda_{B1}^T] & \mathbf{0} \\ \mathbf{0} & [\mathbf{I} - \boldsymbol{\ell}_{B1} \lambda_{B1}^T] \end{bmatrix} \right\} \begin{bmatrix} \mathbf{I} & -\mathbf{I} \\ -\mathbf{I} & \mathbf{I} \end{bmatrix} \Delta\mathbf{u}_{B1} -$$
$$+ \frac{R_{B1}}{\ell_{B1}^o} (1 - \lambda_{B1}^T \Delta\mathbf{x}_{B1}^d) \begin{bmatrix} \boldsymbol{\ell}_{B1} \\ -\boldsymbol{\ell}_{B1} \end{bmatrix} \Delta D_{B1} \tag{5.2.78}$$

In the compact form

$$\Delta\mathbf{n}_{B1} = \mathbf{k}_{E,B1}^* \Delta\mathbf{u}_{B1} + \mathbf{k}_{G,B1}^* \Delta\mathbf{u}_{B1} - \mathbf{q}_{B1}^* \Delta D_{B1} \tag{5.2.79}$$

with

$$\mathbf{k}_{E,B1}^* = R_{B1} \left\{ \boldsymbol{\ell}_{B1} \lambda_{B1}^T [\mathbf{I} - \Delta\mathbf{x}_{B1}^d \lambda_{B1}^T] \right\} \begin{bmatrix} \mathbf{I} & -\mathbf{I} \\ -\mathbf{I} & \mathbf{I} \end{bmatrix}$$

$$\mathbf{k}_{G,B1}^* = \frac{F_{B1}^0}{\ell_{B1}^0} \left\{ [\mathbf{I} - \boldsymbol{\ell}_{B1} \lambda_{B1}^T] \right\} \begin{bmatrix} \mathbf{I} & -\mathbf{I} \\ -\mathbf{I} & \mathbf{I} \end{bmatrix} \tag{5.2.80}$$

$$\mathbf{q}_{B1}^* = \frac{R_{B1}}{\ell_{B1}^0} (1 - \lambda_{B1}^T \Delta\mathbf{x}_{B1}^d) \begin{bmatrix} \boldsymbol{\ell}_{B1} \\ -\boldsymbol{\ell}_{B1} \end{bmatrix}$$

which are, respectively, the stiffness elastic and geometric secant matrixes, and the secant distortion vector referred to the *B1* beam.

5.2.4.2 Global structure's analysis: identification of the main entities

To pass to the analysis of the entire structure, let now consider embedding the previously identified displacement and force vector of each cable segment

$$\Delta \mathbf{x} = \begin{bmatrix} \Delta \mathbf{u}_{A1} \\ \Delta \mathbf{u}_{B1} \end{bmatrix} = \begin{bmatrix} \Delta y_{A1} \\ \Delta z_{A1} \\ \Delta y_{1A} \\ \Delta z_{1A} \\ \Delta y_{B1} \\ \Delta z_{B1} \\ \Delta y_{1B} \\ \Delta z_{1B} \end{bmatrix} \quad (5.2.81)$$

$$\Delta \mathbf{N} = \begin{bmatrix} \Delta \mathbf{n}_{A1} \\ \Delta \mathbf{n}_{B1} \end{bmatrix} = \begin{bmatrix} \Delta F_{A1,y} \\ \Delta F_{A1,z} \\ \Delta F_{1A,y} \\ \Delta F_{1A,z} \\ \Delta F_{B1,y} \\ \Delta F_{B1,z} \\ \Delta F_{1B,y} \\ \Delta F_{1B,z} \end{bmatrix} \quad (5.2.82)$$

Two linear compatibility and equilibrium relations may be set through the Boolean matrix $\mathbf{A}$ ($4m \times 2n$), and its transposed one $\mathbf{A}^T$ ($2n \times 4m$). $\mathbf{A}$ is made of 0 and 1 and depends on the topology, with 1 for the free nodes.

Hence, by considering the structure shown in Fig. 5.12 and its constraint conditions
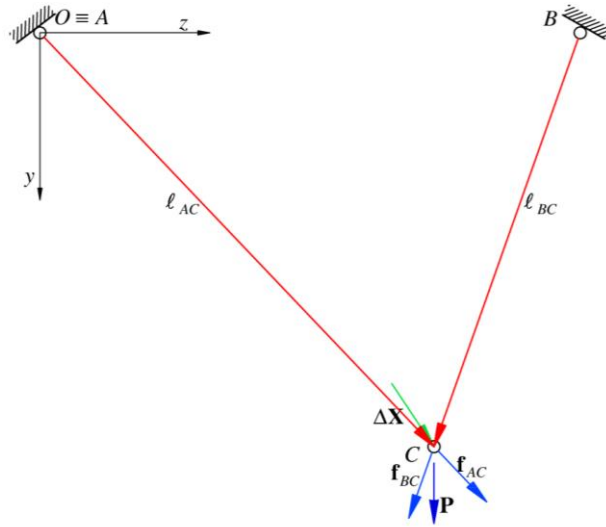
Figure 5.12: Deformed global structure.

the **A** matrix is given by

$$
\mathbf{A} =
\begin{bmatrix}
1 & 0 \\
0 & 1 \\
0 & 0 \\
0 & 0 \\
1 & 0 \\
0 & 1 \\
0 & 0 \\
0 & 0
\end{bmatrix}
\begin{matrix}
1 \\
\\
A \\
\\
1 \\
\\
B
\end{matrix}
\tag{5.2.83}
$$

Thus the compatibility relation can be written

$$\Delta\mathbf{x} = \mathbf{A}\Delta\mathbf{U} \tag{5.2.84}$$

and, taking into account Eq. (5.2.82), the equilibrium is

$$\Delta\mathbf{P} = \mathbf{A}^T\Delta\mathbf{N} \tag{5.2.85}$$

By remembering Eq. (5.2.32)

$$\Delta\mathbf{N} = diag[\mathbf{k}^*_{E,ij}]\Delta\mathbf{x} + diag[\mathbf{k}^*_{G,ij}]\Delta\mathbf{x} - diag[\mathbf{q}^*_{ij}]\Delta\mathbf{D}$$

where $diag[\;]$ denotes the matrix in the square parentheses arranged in diagonal position

$$\Delta\mathbf{N} = \begin{bmatrix} \mathbf{k}_{E,A1}^{*} & \mathbf{0} \\ \mathbf{0} & \mathbf{k}_{E,B1}^{*} \end{bmatrix} \Delta\mathbf{x} + \begin{bmatrix} \mathbf{k}_{G,A1}^{*} & \mathbf{0} \\ \mathbf{0} & \mathbf{k}_{G,B1}^{*} \end{bmatrix} \Delta\mathbf{x} - \begin{bmatrix} \mathbf{q}_{A1}^{*} & \mathbf{0} \\ \mathbf{0} & \mathbf{q}_{B1}^{*} \end{bmatrix} \Delta\mathbf{D} \tag{5.2.86}$$

Moreover, substituting Eq. (5.2.83) into Eq. (5.2.86), one gets

$$\Delta\mathbf{N} = \begin{bmatrix} \mathbf{k}_{E,A1}^{*} & \mathbf{0} \\ \mathbf{0} & \mathbf{k}_{E,B1}^{*} \end{bmatrix} \mathbf{A}\Delta\mathbf{U} + \begin{bmatrix} \mathbf{k}_{G,A1}^{*} & \mathbf{0} \\ \mathbf{0} & \mathbf{k}_{G,B1}^{*} \end{bmatrix} \mathbf{A}\Delta\mathbf{U} - \begin{bmatrix} \mathbf{q}_{A1}^{*} & \mathbf{0} \\ \mathbf{0} & \mathbf{q}_{B1}^{*} \end{bmatrix} \Delta\mathbf{D} \tag{5.2.87}$$

and one gets

$$\Delta\mathbf{P} = \mathbf{A}^{T} \begin{bmatrix} \mathbf{k}_{E,A1}^{*} & \mathbf{0} \\ \mathbf{0} & \mathbf{k}_{E,B1}^{*} \end{bmatrix} \mathbf{A}\Delta\mathbf{U} + \mathbf{A}^{T} \begin{bmatrix} \mathbf{k}_{G,A1}^{*} & \mathbf{0} \\ \mathbf{0} & \mathbf{k}_{G,B1}^{*} \end{bmatrix} \mathbf{A}\Delta\mathbf{U} - \mathbf{A}^{T} \begin{bmatrix} \mathbf{q}_{A1}^{*} & \mathbf{0} \\ \mathbf{0} & \mathbf{q}_{B1}^{*} \end{bmatrix} \Delta\mathbf{D} \tag{5.2.88}$$

where

$$\mathbf{K}_{E}^{*} = \mathbf{A}^{T} diag[\mathbf{k}_{E,ij}^{*}]\mathbf{A} \tag{5.2.89a}$$

$$\mathbf{K}_{G}^{*} = \mathbf{A}^{T} diag[\mathbf{k}_{G,ij}^{*}]\mathbf{A} \tag{5.2.89b}$$

$$\mathbf{Q} = diag[\mathbf{q}_{ij}^{*}] \tag{5.2.89c}$$

Whence one can write

$$\Delta\mathbf{P} = \mathbf{K}_{E}^{*}\Delta\mathbf{U} + \mathbf{K}_{G}^{*}\Delta\mathbf{U} - \mathbf{Q}^{*}\Delta\mathbf{D} \tag{5.2.90}$$

To solve the above equation, one assumes that the distortions are equal to 0

$$\Delta\mathbf{D} = \mathbf{0}$$
$$\mathbf{Q}^{*}\Delta\mathbf{D} = \mathbf{0} \tag{5.2.91}$$

Eq.(5.2.90) turns then into

$$\Delta\mathbf{P} = \mathbf{K}_{E}^{*}\Delta\mathbf{U} + \mathbf{K}_{G}^{*}\Delta\mathbf{U} \tag{5.2.92}$$

After identified the variation of the external load by Eq. (5.2.92), through a small incremental step (**p**) the first variaton of **P** is computed by

$$d\mathbf{P}^1 = \Delta\mathbf{P} + \mathbf{p} \qquad\qquad (5.2.93)$$

The trigger value is considered to proceed step by step, and then the coupled displacement can be identified by inverting the stiffeness matrix given by

$$\mathbf{K} = \mathbf{K}_E + \mathbf{K}_G \qquad\qquad (5.2.94)$$

finally obtaining

$$d\mathbf{U}^1 = \mathbf{K}^{-1} d\mathbf{P}^1 \qquad\qquad (5.2.95)$$

Eq. (5.2.95) denotes the infinitesimal step applied to the structure, repeating the above presented calculus procedure for then indivituating a new load condition. The procedure continues up to convergence, that is when the difference between two subsequent solutions is very small

$$d\mathbf{P}^{r+1} - d\mathbf{P}^r < |t| \qquad\qquad (5.2.96)$$

where

$d\mathbf{P}^{r+1}$ is the load variation at the subsequent step $r+1$

$d\mathbf{P}^r$ is the load variation at the preceding step r

$|t|$ is a tolerance value assumed for a valid solution.

5.3 Three-dimensional systems

When referring to 3D structures, one may apply and extend to spatial schemes what developed in Par.3.3 for 2D structures, and one may, thus, develop the general setup for finding equilibrium shapes under different load conditions in the three-dimensional case. As an example one refers to the topology illustrated in Fig. 5.13 subject to out-of-plane loads, and one synthetically presents in the following the relevant results, after suitably implementing the problem in the related calculus code.
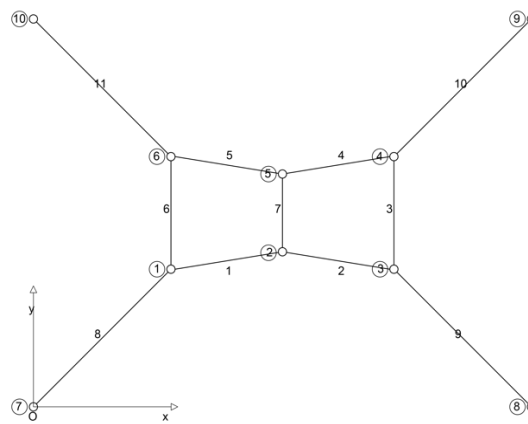
5.13: Topology scheme.

In Fig. 5.14 the configuration is reported, due to the application of out-of-plane load P_z = 1 in the upward direction with a ratio in edge and internal branches equal to 1:1.
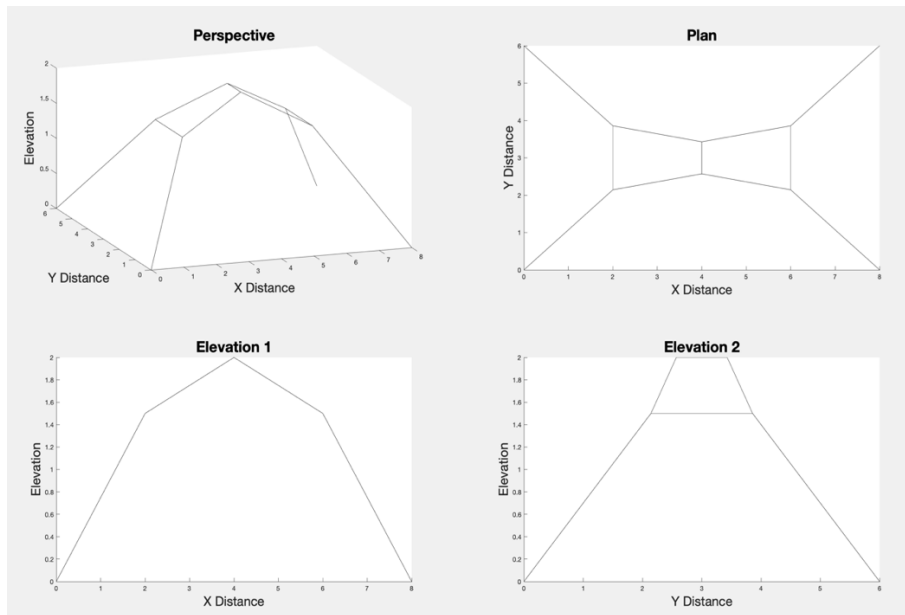
Figure 5.14 : Equilibrium shape under the out-plane load P_z=1 in the upward direction. The ratio in the edge to the internal branches is q=1:1.

Fig. 5.15 depicts the shape assumed by the structure under the application of the out-of-plane load $P_z = 20$ in the upward direction on a single free node (free node 5).
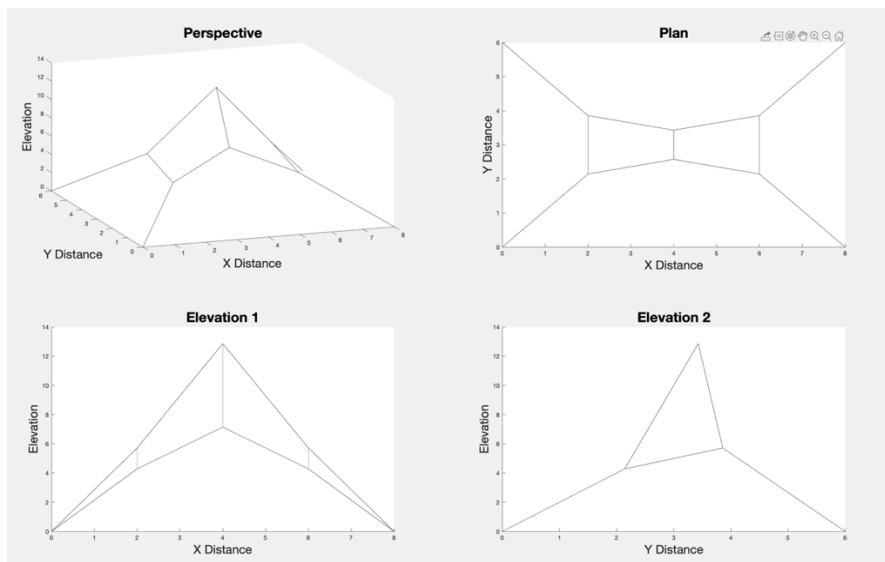
Figure 5.15: Equilibrium shape under the load P_z=20 in the upward direction , applied only on the free node 5.
The ratio in the edge to the internal branches is q=1:1.

5.3.1 Implementation

In the following the methodology described for a plane cable system with opposed curvature is extended to a three-dimensional system case, shown in Fig.5.16-17, and we will demonstrate its validity.
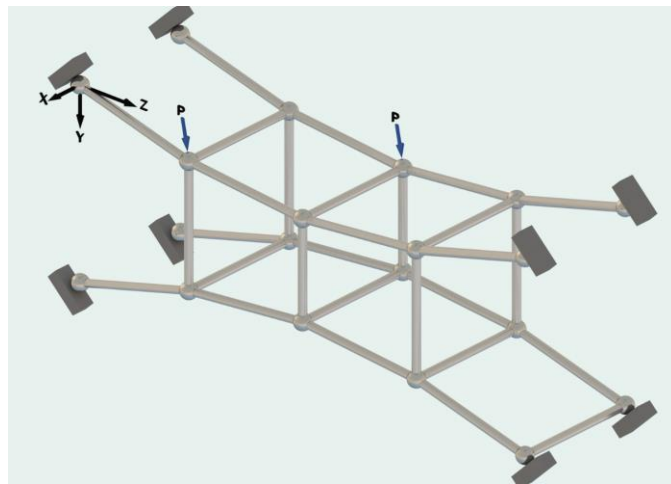
Figure 5.16: 3D model of a cable system with opposite curvature.

Thus, keeping the same definitions and symbols given for the plane case in the previous Par.(5.2.1)-(5.2.2), the problem is formulated for a cable structure in the three-dimensional space (Fig.5.17).
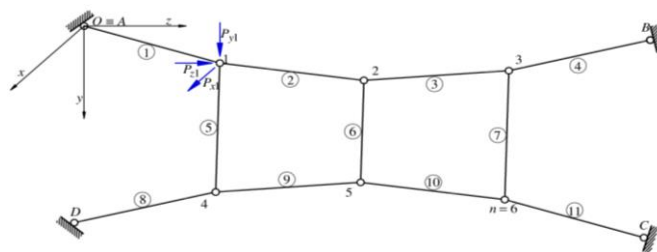
Figure 5.17 Lateral view of the Cable structure in the reference system Oxyz.

The entities introduced for a two-dimensional system are extended to the three-dimensional one, referring to the system (Oxyz)

$$\mathbf{P}^T = \begin{bmatrix} P_{x1} & P_{y1} & P_{z1} & P_{x2} & P_{y2} & P_{z2} & ... & ... & P_{xn} & P_{yn} & P_{zn} \end{bmatrix}$$

$$\mathbf{X}^T = \begin{bmatrix} x_1 & y_1 & z_1 & x_2 & y_2 & z_2 & ... & ... & x_n & y_n & z_n \end{bmatrix}$$

(5.3.1)

$$\mathbf{F}^T = \begin{bmatrix} F_1 & F_2 & ... & F_h & ... & F_m \end{bmatrix}$$

$$\mathbf{D}^T = \begin{bmatrix} D_1 & D_2 & ... & D_h & ... & D_m \end{bmatrix}$$

(5.3.2)

As seen, the change of configuration from Σ^o to Σ for a single element ij (Fig. 5.18) is described by the vector

$$\Delta\mathbf{x}_{ij}^d = \begin{bmatrix} \Delta x_{ij} - \Delta x_{ji} \\ \Delta y_{ij} - \Delta y_{ji} \\ \Delta z_{ij} - \Delta z_{ji} \end{bmatrix}$$

(5.3.3)
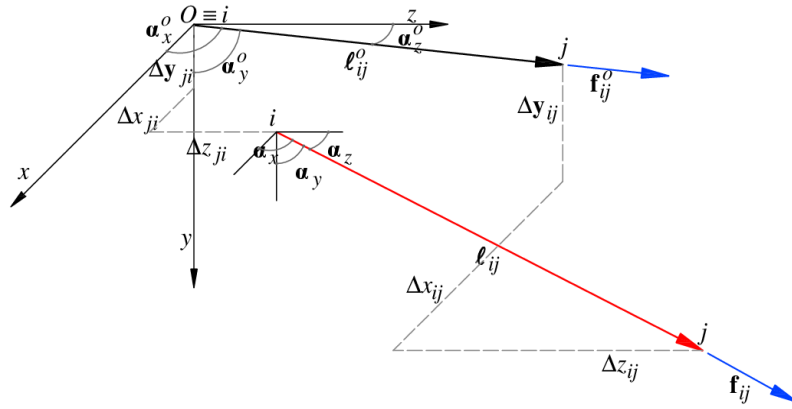
Figure 5.18: Undeformed and deformed configuration of the beam due to the change of configuration applied on the entire structure, in the reference system (Oxyz).

The length vector of the element ij in the deformed shape and the entity of the force variation are given by

$$\ell_{ij} = \ell_{ij}^o + \Delta\mathbf{x}_{ij}^d$$

(5.3.4)

$$\Delta F_{ij} = \frac{E_{ij} A_{ij}}{\ell^{\circ}_{ij}} \left(\Delta\ell_{ij} - \Delta D_{ij} \right) = R_{ij} \left(\Delta\ell_{ij} - \Delta D_{ij} \right) \tag{5.3.5}$$

By introducing the versors

$$\boldsymbol{\alpha}^{o}_{ij} = \frac{\ell^{o}_{ij}}{\ell^{o}_{ij}} = \begin{bmatrix} \alpha^{o}_{ij,x} \\ \alpha^{o}_{ij,y} \\ \alpha^{o}_{ij,z} \end{bmatrix} \quad in \ \ \Sigma^{o}$$

$$\boldsymbol{\alpha}_{ij} = \frac{\ell_{ij}}{\ell_{ij}} = \begin{bmatrix} \alpha_{ij,x} \\ \alpha_{ij,y} \\ \alpha_{ij,z} \end{bmatrix} \quad in \ \ \Sigma \tag{5.3.6}$$

the force vector in ij can be written again

$$\mathbf{f}_{ij} = F_{ij}\boldsymbol{\alpha}_{ij} = \left(F^{o}_{ij} + \Delta F_{ij} \right)\left(\boldsymbol{\alpha}^{o}_{ij} + \Delta\boldsymbol{\alpha}_{ij} \right) = \mathbf{f}^{o}_{ij} + \Delta F_{ij}\boldsymbol{\alpha}^{o}_{ij} + F^{o}_{ij}\Delta\boldsymbol{\alpha}_{ij} + \Delta F_{ij}\Delta\boldsymbol{\alpha}_{ij}$$

$$\Delta\mathbf{f}_{ij} = \mathbf{f}_{ij} - \mathbf{f}^{o}_{ij} = \Delta F_{ij}\boldsymbol{\alpha}^{o}_{ij} + F^{o}_{ij}\Delta\boldsymbol{\alpha}_{ij} + \Delta F_{ij}\Delta\boldsymbol{\alpha}_{ij} \tag{5.3.7}$$

Similarly, Eq. (5.3.4) turns into

$$\ell_{ij} = \ell^{o}_{ij} + \Delta\mathbf{x}^{d}_{ij}$$

$$\ell_{ij}\boldsymbol{\alpha}_{ij} = \ell^{o}_{ij}\boldsymbol{\alpha}^{o}_{ij} + \Delta\mathbf{x}^{d}_{ij} \tag{5.3.8}$$

Hence, the length variation is computed

$$\ell_{ij} = \ell^{o}_{ij} + \Delta\mathbf{x}^{d}_{ij}$$

$$\ell_{ij}\boldsymbol{\alpha}_{ij} = \ell^{o}_{ij}\boldsymbol{\alpha}^{o}_{ij} + \Delta\mathbf{x}^{d}_{ij}$$

$$\boldsymbol{\alpha}^{T}_{ij}\ell_{ij}\boldsymbol{\alpha}_{ij} = \boldsymbol{\alpha}^{T}_{ij}\ell^{o}_{ij}\boldsymbol{\alpha}^{o}_{ij} + \boldsymbol{\alpha}^{T}_{ij}\Delta\mathbf{x}^{d}_{ij} = \left(\boldsymbol{\alpha}^{oT}_{ij} + \Delta\boldsymbol{\alpha}^{T}_{ij} \right)\ell^{o}_{ij}\boldsymbol{\alpha}^{o}_{ij} + \boldsymbol{\alpha}^{T}_{ij}\Delta\mathbf{x}^{d}_{ij}$$

$$\ell_{ij} - \ell^{o}_{ij} = \Delta\boldsymbol{\alpha}^{T}_{ij}\ell^{o}_{ij}\boldsymbol{\alpha}^{o}_{ij} + \boldsymbol{\alpha}^{T}_{ij}\Delta\mathbf{x}^{d}_{ij}$$

$$\Delta\ell_{ij} = \Delta\boldsymbol{\alpha}^{T}_{ij}\ell^{o}_{ij}\boldsymbol{\alpha}^{o}_{ij} + \boldsymbol{\alpha}^{T}_{ij}\Delta\mathbf{x}^{d}_{ij}$$

or :

$$\boldsymbol{\alpha}^{T}_{ij}\ell_{ij}\boldsymbol{\alpha}_{ij} = \boldsymbol{\alpha}^{T}_{ij}\ell^{o}_{ij}\boldsymbol{\alpha}^{o}_{ij} + \boldsymbol{\alpha}^{T}_{ij}\Delta\mathbf{x}^{d}_{ij} = \left(\boldsymbol{\alpha}^{oT}_{ij} + \Delta\boldsymbol{\alpha}^{T}_{ij} \right)\left(\ell^{o}_{ij}\boldsymbol{\alpha}^{o}_{ij} + \Delta\mathbf{x}^{d}_{ij} \right) =$$

$$= \boldsymbol{\alpha}^{oT}_{ij}\ell^{o}_{ij}\boldsymbol{\alpha}^{o}_{ij} + \boldsymbol{\alpha}^{oT}_{ij}\Delta\mathbf{x}^{d}_{ij} + \Delta\boldsymbol{\alpha}^{T}_{ij}\ell^{o}_{ij}\boldsymbol{\alpha}^{o}_{ij} + \Delta\boldsymbol{\alpha}^{T}_{ij}\Delta\mathbf{x}^{d}_{ij}$$

$$\ell_{ij} = \ell^{o}_{ij} + \boldsymbol{\alpha}^{oT}_{ij}\Delta\mathbf{x}^{d}_{ij} + \Delta\boldsymbol{\alpha}^{T}_{ij}\left(\ell^{o}_{ij}\boldsymbol{\alpha}^{o}_{ij} + \Delta\mathbf{x}^{d}_{ij} \right)$$

$$\Delta \ell_{ij} = \ell_{ij} - \ell_{ij}^{o} = \boldsymbol{\alpha}_{ij}^{oT} \Delta \mathbf{x}_{ij}^{d} + \Delta \boldsymbol{\alpha}_{ij}^{T} \ell_{ij} \qquad (5.3.9)$$

Following the same developments like in the plane case, the variation of the versor is obtained by Eq. (5.3.8)

$$\boldsymbol{\ell}_{ij} = \boldsymbol{\ell}_{ij}^{o} + \Delta \mathbf{x}_{ij}^{d}$$

$$\ell_{ij} \boldsymbol{\alpha}_{ij} = \ell_{ij}^{o} \boldsymbol{\alpha}_{ij}^{o} + \Delta \mathbf{x}_{ij}^{d}$$

$$\boldsymbol{\alpha}_{ij} = \frac{\boldsymbol{\ell}_{ij}^{o} + \Delta \mathbf{x}_{ij}^{d}}{\ell_{ij}^{o} \left(1 + \Delta \varepsilon_{ij}\right)} = \frac{1}{\ell_{ij}^{o}} \left[\frac{\boldsymbol{\ell}_{ij}^{o} + \Delta \mathbf{x}_{ij}^{d}}{\left(1 + \Delta \varepsilon_{ij}\right)} \right]$$

$$\Delta \boldsymbol{\alpha}_{ij} = \boldsymbol{\alpha}_{ij} - \boldsymbol{\alpha}_{ij}^{o} = \frac{\boldsymbol{\ell}_{ij}^{o} + \Delta \mathbf{x}_{ij}^{d}}{\ell_{ij}^{o} \left(1 + \Delta \varepsilon_{ij}\right)} - \frac{\boldsymbol{\ell}_{ij}^{o}}{\ell_{ij}^{o}} = \frac{1}{\ell_{ij}^{o}} \left[\frac{\boldsymbol{\ell}_{ij}^{o} + \Delta \mathbf{x}_{ij}^{d}}{\left(1 + \Delta \varepsilon_{ij}\right)} - \boldsymbol{\ell}_{ij}^{o} \right] \qquad (5.3.10)$$

Because of small deformation hypothesis

$$\frac{1}{1 + \Delta \varepsilon} \cong 1 - \Delta \varepsilon \qquad (5.3.11)$$

Eq. (5.3.10) is simplified into

$$\Delta \boldsymbol{\alpha}_{ij} = \boldsymbol{\alpha}_{ij} - \boldsymbol{\alpha}_{ij}^{o} = \frac{\boldsymbol{\ell}_{ij}^{o} + \Delta \mathbf{x}_{ij}^{d}}{\ell_{ij}^{o} \left(1 + \Delta \varepsilon_{ij}\right)} - \frac{\boldsymbol{\ell}_{ij}^{o}}{\ell_{ij}^{o}} = \frac{1}{\ell_{ij}^{o}} \left[\frac{\boldsymbol{\ell}_{ij}^{o} + \Delta \mathbf{x}_{ij}^{d}}{\left(1 + \Delta \varepsilon_{ij}\right)} - \boldsymbol{\ell}_{ij}^{o} \right]$$

$$\Delta \boldsymbol{\alpha}_{ij} = \frac{1}{\ell_{ij}^{o}} \left[\frac{\boldsymbol{\ell}_{ij}^{o} + \Delta \mathbf{x}_{ij}^{d}}{\left(1 + \Delta \varepsilon_{ij}\right)} - \boldsymbol{\ell}_{ij}^{o} \right] \cong \frac{1}{\ell_{ij}^{o}} \left[\left(\boldsymbol{\ell}_{ij}^{o} + \Delta \mathbf{x}_{ij}^{d}\right)\left(1 - \Delta \varepsilon_{ij}\right) - \boldsymbol{\ell}_{ij}^{o} \right] =$$

$$= \frac{1}{\ell_{ij}^{o}} \left[\boldsymbol{\ell}_{ij}^{o} + \Delta \mathbf{x}_{ij}^{d} - \Delta \varepsilon_{ij} \boldsymbol{\ell}_{ij}^{o} - \Delta \varepsilon_{ij} \Delta \mathbf{x}_{ij}^{d} - \boldsymbol{\ell}_{ij}^{o} \right]$$

$$\Delta \boldsymbol{\alpha}_{ij} = \frac{1}{\ell_{ij}^{o}} \left[\Delta \mathbf{x}_{ij}^{d} - \Delta \varepsilon_{ij} \boldsymbol{\ell}_{ij} \right] = \frac{1}{\ell_{ij}^{o}} \left[\Delta \mathbf{x}_{ij}^{d} - \frac{\Delta \ell_{ij}}{\ell_{ij}^{o}} \boldsymbol{\ell}_{ij} \right]$$

$$\Delta \boldsymbol{\alpha}_{ij} = \frac{1}{\ell_{ij}^{o}} \left[\Delta \mathbf{x}_{ij}^{d} - \frac{\Delta \ell_{ij}}{\ell_{ij}^{o}} \boldsymbol{\ell}_{ij} \right] \qquad (5.3.12)$$

and Eq. (5.3.9) turns into

$$\boldsymbol{\ell}_{ij} = \boldsymbol{\ell}_{ij}^{o} + \Delta \mathbf{x}_{ij}^{d}$$

$$\ell_{ij} \boldsymbol{\alpha}_{ij} = \ell_{ij}^{o} \boldsymbol{\alpha}_{ij}^{o} + \Delta \mathbf{x}_{ij}^{d}$$

$$\Delta \ell_{ij} = \ell_{ij} - \ell_{ij}^{o} = \boldsymbol{\alpha}_{ij}^{oT} \Delta \mathbf{x}_{ij}^{d} + \Delta \boldsymbol{\alpha}_{ij}^{T} \boldsymbol{\ell}_{ij} = \boldsymbol{\alpha}_{ij}^{oT} \Delta \mathbf{x}_{ij}^{d} + \boldsymbol{\ell}_{ij}^{T} \Delta \boldsymbol{\alpha}_{ij}$$

$$\Delta \boldsymbol{\alpha}_{ij} = \frac{1}{\ell_{ij}^{o}} \left[\Delta \mathbf{x}_{ij}^{d} - \Delta \varepsilon_{ij} \boldsymbol{\ell}_{ij} \right] = \frac{1}{\ell_{ij}^{o}} \left[\Delta \mathbf{x}_{ij}^{d} - \frac{\Delta \ell_{ij}}{\ell_{ij}^{o}} \boldsymbol{\ell}_{ij} \right]$$

$$\Delta \ell_{ij} = \boldsymbol{\alpha}_{ij}^{oT} \Delta \mathbf{x}_{ij}^{d} + \boldsymbol{\ell}_{ij}^{T} \frac{1}{\ell_{ij}^{o}} \left[\Delta \mathbf{x}_{ij}^{d} - \frac{\Delta \ell_{ij}}{\ell_{ij}^{o}} \boldsymbol{\ell}_{ij} \right] = \frac{\boldsymbol{\ell}_{ij}^{oT}}{\ell_{ij}^{o}} \Delta \mathbf{x}_{ij}^{d} + \boldsymbol{\ell}_{ij}^{T} \frac{1}{\ell_{ij}^{o}} \left[\Delta \mathbf{x}_{ij}^{d} - \frac{\Delta \ell_{ij}}{\ell_{ij}^{o}} \boldsymbol{\ell}_{ij} \right] =$$

$$= \frac{1}{\ell_{ij}^{o}} \left(\boldsymbol{\ell}_{ij}^{oT} + \boldsymbol{\ell}_{ij}^{T} \right) \Delta \mathbf{x}_{ij}^{d} - \frac{\Delta \ell_{ij}}{\ell_{ij}^{o2}} \boldsymbol{\ell}_{ij}^{T} \boldsymbol{\ell}_{ij}$$

$$\Delta \ell_{ij} \left(1 + \frac{\boldsymbol{\ell}_{ij}^{T} \boldsymbol{\ell}_{ij}}{\ell_{ij}^{o2}} \right) = \Delta \ell_{ij} \left(\frac{\ell_{ij}^{o2} + \boldsymbol{\ell}_{ij}^{T} \boldsymbol{\ell}_{ij}}{\ell_{ij}^{o2}} \right) = \frac{1}{\ell_{ij}^{o}} \left(\boldsymbol{\ell}_{ij}^{oT} + \boldsymbol{\ell}_{ij}^{T} \right) \Delta \mathbf{x}_{ij}^{d}$$

$$\Delta \ell_{ij} = \frac{1}{\ell_{ij}^{o}} \frac{\ell_{ij}^{o2}}{\ell_{ij}^{o2} + \boldsymbol{\ell}_{ij}^{T} \boldsymbol{\ell}_{ij}} \left(\boldsymbol{\ell}_{ij}^{oT} + \boldsymbol{\ell}_{ij}^{T} \right) \Delta \mathbf{x}_{ij}^{d} = \frac{\ell_{ij}^{o}}{\ell_{ij}^{o2} + \boldsymbol{\ell}_{ij}^{T} \boldsymbol{\ell}_{ij}} \left(\boldsymbol{\ell}_{ij}^{oT} + \boldsymbol{\ell}_{ij}^{T} \right) \Delta \mathbf{x}_{ij}^{d}$$

$$\Delta \ell_{ij} = \frac{\ell_{ij}^{o}}{\ell_{ij}^{o2} + \boldsymbol{\ell}_{ij}^{T} \boldsymbol{\ell}_{ij}} \left(\boldsymbol{\ell}_{ij}^{oT} + \boldsymbol{\ell}_{ij}^{T} \right) \Delta \mathbf{x}_{ij}^{d} \tag{5.3.13}$$

For removing the elongation in Eq. (5.3.12) by Eq. (5.3.13), one gets the new expression

$$\Delta \boldsymbol{\alpha}_{ij} = \frac{1}{\ell_{ij}^{o}} \left[\Delta \mathbf{x}_{ij}^{d} - \frac{\Delta \ell_{ij}}{\ell_{ij}^{o}} \boldsymbol{\ell}_{ij} \right]$$

$$\Delta \ell_{ij} = \frac{\ell_{ij}^{o}}{\ell_{ij}^{o2} + \boldsymbol{\ell}_{ij}^{T} \boldsymbol{\ell}_{ij}} \left(\boldsymbol{\ell}_{ij}^{oT} + \boldsymbol{\ell}_{ij}^{T} \right) \Delta \mathbf{x}_{ij}^{d}$$

$$\Delta \boldsymbol{\alpha}_{ij} = \frac{1}{\ell_{ij}^{o}} \left[\Delta \mathbf{x}_{ij}^{d} - \frac{\left(\boldsymbol{\ell}_{ij}^{oT} + \boldsymbol{\ell}_{ij}^{T} \right) \Delta \mathbf{x}_{ij}^{d}}{\ell_{ij}^{o2} + \boldsymbol{\ell}_{ij}^{T} \boldsymbol{\ell}_{ij}} \boldsymbol{\ell}_{ij} \right]$$

$$\Delta \boldsymbol{\alpha}_{ij} = \frac{1}{\ell_{ij}^{o}} \Delta \mathbf{x}_{ij}^{d} - \frac{\left(\boldsymbol{\ell}_{ij}^{oT} + \boldsymbol{\ell}_{ij}^{T} \right) \Delta \mathbf{x}_{ij}^{d}}{\ell_{ij}^{o2} + \boldsymbol{\ell}_{ij}^{T} \boldsymbol{\ell}_{ij}} \frac{\boldsymbol{\ell}_{ij}}{\ell_{ij}^{o}}$$

$$\Delta \boldsymbol{\alpha}_{ij} = \frac{1}{\ell_{ij}^{o}} \Delta \mathbf{x}_{ij}^{d} - \frac{\left(\boldsymbol{\ell}_{ij}^{oT} + \boldsymbol{\ell}_{ij}^{T} \right) \Delta \mathbf{x}_{ij}^{d}}{\ell_{ij}^{o2} + \boldsymbol{\ell}_{ij}^{T} \boldsymbol{\ell}_{ij}} \frac{\boldsymbol{\ell}_{ij}}{\ell_{ij}^{o}} \tag{5.3.14}$$

The force variation in the element ij at the node j is

$$\Delta\mathbf{f}_{ij} = R_{ij}\ell_{ij}\boldsymbol{\lambda}_{ij}^T\left[\mathbf{I} - \Delta\mathbf{x}_{ij}^d\boldsymbol{\lambda}_{ij}^T\right]\Delta\mathbf{x}_{ij}^d + \frac{F_{ij}^o}{\ell_{ij}^o}\left(\mathbf{I} - \ell_{ij}\boldsymbol{\lambda}_{ij}^T\right)\Delta\mathbf{x}_{ij}^d - \frac{R_{ij}}{\ell_{ij}^o}\Delta D_{ij}\left(1 - \boldsymbol{\lambda}_{ij}^T\Delta\mathbf{x}_{ij}^d\right)\ell_{ij} \qquad (5.3.15)$$

By remembering Eq. (5.3.17)

$$\boldsymbol{\lambda}_{ij}^T = \frac{\ell_{ij}^{oT} + \ell_{ij}^T}{\ell_{ij}^{o2} + \ell_{ij}^T\ell_{ij}} = \frac{\ell_{ij}^{oT} + \ell_{ij}^T}{\ell_{ij}^{o2} + \ell_{ij}^2} \quad ; \quad \boldsymbol{\lambda}_{ij} = \frac{\ell_{ij}^o + \ell_{ij}}{\ell_{ij}^{o2} + \ell_{ij}^T\ell_{ij}} = \frac{\ell_{ij}^o + \ell_{ij}}{\ell_{ij}^{o2} + \ell_{ij}^2} \qquad (5.3.16)$$

the action on the node i is obtained by the permutation of indexes

$$\Delta\mathbf{f}_{ij} = R_{ij}\ell_{ij}\boldsymbol{\lambda}_{ij}^T\left[\mathbf{I} - \Delta\mathbf{x}_{ij}^d\boldsymbol{\lambda}_{ij}^T\right]\Delta\mathbf{x}_{ij}^d + \frac{F_{ij}^o}{\ell_{ij}^o}\left(\mathbf{I} - \ell_{ij}\boldsymbol{\lambda}_{ij}^T\right)\Delta\mathbf{x}_{ij}^d - \frac{R_{ij}}{\ell_{ij}^o}\Delta D_{ij}\left(1 - \boldsymbol{\lambda}_{ij}^T\Delta\mathbf{x}_{ij}^d\right)\ell_{ij}$$

$$\Delta\mathbf{f}_{ij} = -\Delta\mathbf{f}_{ji} \quad ; \quad R_{ij} = R_{ji} \quad ; \quad \ell_{ij} = -\ell_{ji} \ ; \ \boldsymbol{\lambda}_{ij}^T = -\boldsymbol{\lambda}_{ji}^T \ ; \ \Delta\mathbf{x}_{ij}^d = -\Delta\mathbf{x}_{ji}^d \quad ; \quad F_{ij}^o = F_{ji}^o \quad ; \quad \ell_{ij}^o = \ell_{ji}^o \quad ;$$

$$\Delta D_{ij} = \Delta D_{ji}$$

$$-\Delta\mathbf{f}_{ji} = -R_{ji}\ell_{ji}\boldsymbol{\lambda}_{ji}^T\left(\mathbf{I} - \Delta\mathbf{x}_{ji}^d\boldsymbol{\lambda}_{ji}^T\right)\Delta\mathbf{x}_{ji}^d - \frac{F_{ji}^o}{\ell_{ji}^o}\left(\mathbf{I} - \ell_{ji}\boldsymbol{\lambda}_{ji}^T\right)\Delta\mathbf{x}_{ji}^d + \frac{R_{ji}}{\ell_{ji}^o}\Delta D_{ji}\left(1 - \boldsymbol{\lambda}_{ji}^T\Delta\mathbf{x}_{ji}^d\right)\ell_{ji}$$

definitively

$$\Delta\mathbf{f}_{ji} = R_{ji}\ell_{ji}\boldsymbol{\lambda}_{ji}^T\left[\mathbf{I} - \Delta\mathbf{x}_{ji}^d\boldsymbol{\lambda}_{ji}^T\right]\Delta\mathbf{x}_{ji}^d + \frac{F_{ji}^o}{\ell_{ji}^o}\left(\mathbf{I} - \ell_{ji}\boldsymbol{\lambda}_{ji}^T\right)\Delta\mathbf{x}_{ji}^d - \frac{R_{ji}}{\ell_{ji}^o}\Delta D_{ji}\left(1 - \boldsymbol{\lambda}_{ji}^T\Delta\mathbf{x}_{ji}^d\right)\ell_{ji}$$

or

$$\Delta\mathbf{f}_{ji} = R_{ij}\ell_{ij}\boldsymbol{\lambda}_{ij}^T\left[\mathbf{I} - \Delta\mathbf{x}_{ij}^d\boldsymbol{\lambda}_{ij}^T\right]\Delta\mathbf{x}_{ji}^d + \frac{F_{ij}^o}{\ell_{ij}^o}\left(\mathbf{I} - \ell_{ij}\boldsymbol{\lambda}_{ij}^T\right)\Delta\mathbf{x}_{ji}^d - \frac{R_{ij}}{\ell_{ij}^o}\Delta D_{ij}\left(1 - \boldsymbol{\lambda}_{ij}^T\Delta\mathbf{x}_{ij}^d\right)\ell_{ji}$$

or as

$$\Delta\mathbf{f}_{ji} = R_{ij}\ell_{ij}\boldsymbol{\lambda}_{ij}^T\left[\mathbf{I} - \Delta\mathbf{x}_{ij}^d\boldsymbol{\lambda}_{ij}^T\right]\Delta\mathbf{x}_{ji}^d + \frac{F_{ij}^o}{\ell_{ij}^o}\left(\mathbf{I} - \ell_{ij}\boldsymbol{\lambda}_{ij}^T\right)\Delta\mathbf{x}_{ji}^d + \frac{R_{ij}}{-\ell_{ij}^o}\Delta D_{ij}\left(1 - \boldsymbol{\lambda}_{ij}^T\Delta\mathbf{x}_{ij}^d\right)\ell_{ij}$$

$$\Delta\mathbf{f}_{ji} = R_{ij}\ell_{ij}\boldsymbol{\lambda}_{ij}^T\left[\mathbf{I} - \Delta\mathbf{x}_{ij}^d\boldsymbol{\lambda}_{ij}^T\right]\Delta\mathbf{x}_{ji}^d + \frac{F_{ij}^o}{\ell_{ij}^o}\left(\mathbf{I} - \ell_{ij}\boldsymbol{\lambda}_{ij}^T\right)\Delta\mathbf{x}_{ji}^d + \frac{R_{ij}}{\ell_{ij}^o}\Delta D_{ij}\left(1 - \boldsymbol{\lambda}_{ij}^T\Delta\mathbf{x}_{ij}^d\right)\ell_{ij} \qquad (5.3.17)$$

The vector of the internal force variation at the ends of the beam ij turns into

$$\Delta\mathbf{n}_{ij}^T = \left[\Delta\mathbf{f}_{ij}^T \ \vdots \ \Delta\mathbf{f}_{ji}^T\right] = \left[\Delta f_{ij,x} \ \vdots \ \Delta f_{ij,y} \ \vdots \ \Delta f_{ij,z} \ \vdots \ \Delta f_{ji,x} \ \vdots \ \Delta f_{ji,y} \ \vdots \ \Delta f_{ji,z}\right] \qquad (5.3.18)$$

Analogously $\Delta\mathbf{u}_{ij}$ denotes the vector of the 6 components of the imposed displacements at the ends. Observing that for Eq. (5.3.3)

$$\Delta \mathbf{x}_{ij}^{d} = \begin{bmatrix} \Delta x_{ij} - \Delta x_{ji} \\ \Delta y_{ij} - \Delta y_{ji} \\ \Delta z_{ij} - \Delta z_{ji} \end{bmatrix} \qquad (5.3.3)$$

$$\Delta \mathbf{x}_{ij}^{d} = \begin{bmatrix} \mathbf{I} & \vdots & -\mathbf{I} \end{bmatrix} \Delta \mathbf{u}_{ij} \quad ; \quad \Delta \mathbf{x}_{ji}^{d} = \begin{bmatrix} -\mathbf{I} & \vdots & \mathbf{I} \end{bmatrix} \Delta \mathbf{u}_{ij} \qquad (5.3.19)$$

and

$$\Delta \mathbf{x}_{ij}^{d} = \begin{bmatrix} \mathbf{I} & \vdots & -\mathbf{I} \end{bmatrix} \Delta \mathbf{u}_{ij} \quad ; \quad \Delta \mathbf{x}_{ji}^{d} = \begin{bmatrix} -\mathbf{I} & \vdots & \mathbf{I} \end{bmatrix} \Delta \mathbf{u}_{ij}$$

$$\Delta \mathbf{x}_{ij}^{d} = \begin{bmatrix} \Delta x_{ij} - \Delta x_{ji} \\ \Delta y_{ij} - \Delta y_{ji} \\ \Delta z_{ij} - \Delta z_{ji} \end{bmatrix} \quad ; \quad \Delta \mathbf{x}_{ji}^{d} = \begin{bmatrix} \Delta x_{ji} - \Delta x_{ij} \\ \Delta y_{ji} - \Delta y_{ij} \\ \Delta z_{ji} - \Delta z_{ij} \end{bmatrix}$$

$$\Delta \mathbf{u}_{ij}^{T} = \begin{bmatrix} \Delta x_{ij} & \Delta y_{ij} & \Delta z_{ij} & \Delta x_{ji} & \Delta y_{ji} & \Delta z_{ji} \end{bmatrix}$$

$$\begin{bmatrix} \mathbf{I} & \vdots & -\mathbf{I} \end{bmatrix} \Delta \mathbf{u}_{ij} = \begin{bmatrix} 1 & 0 & 0 & -1 & 0 & 0 \\ 0 & 1 & 0 & 0 & -1 & 0 \\ 0 & 0 & 1 & 0 & 0 & -1 \end{bmatrix} \begin{pmatrix} \Delta x_{ij} \\ \Delta y_{ij} \\ \Delta z_{ij} \\ \Delta x_{ji} \\ \Delta y_{ji} \\ \Delta z_{ji} \end{pmatrix} = \begin{bmatrix} \Delta x_{ij} - \Delta x_{ji} \\ \Delta y_{ij} - \Delta y_{ji} \\ \Delta z_{ij} - \Delta z_{ji} \end{bmatrix} = \Delta \mathbf{x}_{ij}^{d}$$

$$\begin{bmatrix} -\mathbf{I} & \vdots & \mathbf{I} \end{bmatrix} \Delta \mathbf{u}_{ij} = \begin{bmatrix} 1 & 0 & 0 & -1 & 0 & 0 \\ 0 & 1 & 0 & 0 & -1 & 0 \\ 0 & 0 & 1 & 0 & 0 & -1 \end{bmatrix} \begin{pmatrix} \Delta x_{ij} \\ \Delta y_{ij} \\ \Delta z_{ij} \\ \Delta x_{ji} \\ \Delta y_{ji} \\ \Delta z_{ji} \end{pmatrix} = \begin{bmatrix} \Delta x_{ji} - \Delta x_{ij} \\ \Delta y_{ji} - \Delta y_{ij} \\ \Delta z_{ji} - \Delta z_{ij} \end{bmatrix} = \Delta \mathbf{x}_{ji}^{d}$$

the dependence between $\Delta \mathbf{n}_{ij}$ and $\Delta \mathbf{u}_{ij}$ is inferred in the form

$$\Delta\mathbf{n}_{ij}^T = \left[\Delta\mathbf{f}_{ij}^T \;\vdots\; \Delta\mathbf{f}_{ji}^T\right] = \left[\Delta f_{ij,x} \;\vdots\; \Delta f_{ij,y} \;\vdots\; \Delta f_{ij,z} \;\vdots\; \Delta f_{ji,x} \;\vdots\; \Delta f_{ji,y} \;\vdots\; \Delta f_{ji,z}\right]$$

$$\Delta\mathbf{f}_{ij} = R_{ij}\ell_{ij}\boldsymbol{\lambda}_{ij}^T\left[\mathbf{I} - \Delta\mathbf{x}_{ij}^d\boldsymbol{\lambda}_{ij}^T\right]\Delta\mathbf{x}_{ij}^d + \frac{F_{ij}^o}{\ell_{ij}^o}\left(\mathbf{I} - \ell_{ij}\boldsymbol{\lambda}_{ij}^T\right)\Delta\mathbf{x}_{ij}^d - \frac{R_{ij}}{\ell_{ij}^o}\Delta D_{ij}\left(1 - \boldsymbol{\lambda}_{ij}^T\Delta\mathbf{x}_{ij}^d\right)\ell_{ij}$$

$$\Delta\mathbf{f}_{ji} = R_{ij}\ell_{ij}\boldsymbol{\lambda}_{ij}^T\left[\mathbf{I} - \Delta\mathbf{x}_{ij}^d\boldsymbol{\lambda}_{ij}^T\right]\Delta\mathbf{x}_{ji}^d + \frac{F_{ij}^o}{\ell_{ij}^o}\left(\mathbf{I} - \ell_{ij}\boldsymbol{\lambda}_{ij}^T\right)\Delta\mathbf{x}_{ji}^d + \frac{R_{ij}}{\ell_{ij}^o}\Delta D_{ij}\left(1 - \boldsymbol{\lambda}_{ij}^T\Delta\mathbf{x}_{ij}^d\right)\ell_{ij}$$

$$\Delta\mathbf{n}_{ij} = \begin{bmatrix}\Delta\mathbf{f}_{ij}\\\Delta\mathbf{f}_{ji}\end{bmatrix} = \left\{R_{ij}\begin{bmatrix}\ell_{ij}\boldsymbol{\lambda}_{ij}^T\left[\mathbf{I}-\Delta\mathbf{x}_{ij}^d\boldsymbol{\lambda}_{ij}^T\right] & \vdots & \mathbf{0}\\ \cdots & & \cdots\\ \mathbf{0} & \vdots & \ell_{ij}\boldsymbol{\lambda}_{ij}^T\left[\mathbf{I}-\Delta\mathbf{x}_{ij}^d\boldsymbol{\lambda}_{ij}^T\right]\end{bmatrix} + \atop +\frac{F_{ij}^o}{\ell_{ij}^o}\begin{bmatrix}\mathbf{I}-\ell_{ij}\boldsymbol{\lambda}_{ij}^T & \vdots & \mathbf{0}\\ \cdots & & \cdots\\ \mathbf{0} & \vdots & \mathbf{I}-\ell_{ij}\boldsymbol{\lambda}_{ij}^T\end{bmatrix}\right\}\begin{bmatrix}\mathbf{I} & \vdots & -\mathbf{I}\\ -\mathbf{I} & \vdots & \mathbf{I}\end{bmatrix}\Delta\mathbf{u}_{ij} +$$

$$-\frac{R_{ij}}{\ell_{ij}^o}\left(1-\boldsymbol{\lambda}_{ij}^T\Delta\mathbf{x}_{ij}^d\right)\begin{bmatrix}\ell_{ij}\\ \cdots\\ -\ell_{ij}\end{bmatrix}\Delta D_{ij}$$

$$\Delta\mathbf{n}_{ij} = \begin{bmatrix}\Delta\mathbf{f}_{ij}\\\Delta\mathbf{f}_{ji}\end{bmatrix} = \left\{R_{ij}\begin{bmatrix}\ell_{ij}\boldsymbol{\lambda}_{ij}^T\left[\mathbf{I}-\Delta\mathbf{x}_{ij}^d\boldsymbol{\lambda}_{ij}^T\right] & \vdots & \mathbf{0}\\ \cdots & & \cdots\\ \mathbf{0} & \vdots & \ell_{ij}\boldsymbol{\lambda}_{ij}^T\left[\mathbf{I}-\Delta\mathbf{x}_{ij}^d\boldsymbol{\lambda}_{ij}^T\right]\end{bmatrix} + \atop +\frac{F_{ij}^o}{\ell_{ij}^o}\begin{bmatrix}\mathbf{I}-\ell_{ij}\boldsymbol{\lambda}_{ij}^T & \vdots & \mathbf{0}\\ \cdots & & \cdots\\ \mathbf{0} & \vdots & \mathbf{I}-\ell_{ij}\boldsymbol{\lambda}_{ij}^T\end{bmatrix}\right\}\begin{bmatrix}\mathbf{I} & \vdots & -\mathbf{I}\\ -\mathbf{I} & \vdots & \mathbf{I}\end{bmatrix}\Delta\mathbf{u}_{ij} + \tag{5.3.20}$$

$$-\frac{R_{ij}}{\ell_{ij}^o}\left(1-\boldsymbol{\lambda}_{ij}^T\Delta\mathbf{x}_{ij}^d\right)\begin{bmatrix}\ell_{ij}\\ \cdots\\ -\ell_{ij}\end{bmatrix}\Delta D_{ij}$$

Taking into account that here the secant stiffness matrices and vector assume different dimensions, they are defined as

$$\Delta\mathbf{n}_{ij} = \mathbf{k}_{Eij}^*\Delta\mathbf{u}_{ij} + \mathbf{k}_{Gij}^*\Delta\mathbf{u}_{ij} - \mathbf{q}_{ij}^*\Delta D_{ij} \tag{5.3.21}$$

$$\Delta\mathbf{n}_{ij}^T = \left[\Delta\mathbf{f}_{ij}^T \;\vdots\; \Delta\mathbf{f}_{ji}^T\right] = \left[\Delta f_{ij,x} \;\vdots\; \Delta f_{ij,y} \;\vdots\; \Delta f_{ij,z} \;\vdots\; \Delta f_{ji,x} \;\vdots\; \Delta f_{ji,y} \;\vdots\; \Delta f_{ji,z}\right]$$

$$\Delta\mathbf{f}_{ij} = R_{ij}\ell_{ij}\boldsymbol{\lambda}_{ij}^T\left[\mathbf{I} - \Delta\mathbf{x}_{ij}^d\boldsymbol{\lambda}_{ij}^T\right]\Delta\mathbf{x}_{ij}^d + \frac{F_{ij}^o}{\ell_{ij}^o}\left(\mathbf{I} - \ell_{ij}\boldsymbol{\lambda}_{ij}^T\right)\Delta\mathbf{x}_{ij}^d - \frac{R_{ij}}{\ell_{ij}^o}\Delta D_{ij}\left(1 - \boldsymbol{\lambda}_{ij}^T\Delta\mathbf{x}_{ij}^d\right)\ell_{ij}$$

$$\Delta\mathbf{f}_{ji} = R_{ij}\ell_{ij}\boldsymbol{\lambda}_{ij}^T\left[\mathbf{I} - \Delta\mathbf{x}_{ij}^d\boldsymbol{\lambda}_{ij}^T\right]\Delta\mathbf{x}_{ji}^d + \frac{F_{ij}^o}{\ell_{ij}^o}\left(\mathbf{I} - \ell_{ij}\boldsymbol{\lambda}_{ij}^T\right)\Delta\mathbf{x}_{ji}^d + \frac{R_{ij}}{\ell_{ij}^o}\Delta D_{ij}\left(1 - \boldsymbol{\lambda}_{ij}^T\Delta\mathbf{x}_{ij}^d\right)\ell_{ij}$$

$$\Delta\mathbf{n}_{ij} = \begin{bmatrix}\Delta\mathbf{f}_{ij}\\\Delta\mathbf{f}_{ji}\end{bmatrix} = \left\{R_{ij}\begin{bmatrix}\ell_{ij}\boldsymbol{\lambda}_{ij}^T\left[\mathbf{I}-\Delta\mathbf{x}_{ij}^d\boldsymbol{\lambda}_{ij}^T\right] & \vdots & \mathbf{0}\\ \cdots & & \cdots\\ \mathbf{0} & \vdots & \ell_{ij}\boldsymbol{\lambda}_{ij}^T\left[\mathbf{I}-\Delta\mathbf{x}_{ij}^d\boldsymbol{\lambda}_{ij}^T\right]\end{bmatrix} + \atop +\frac{F_{ij}^o}{\ell_{ij}^o}\begin{bmatrix}\mathbf{I}-\ell_{ij}\boldsymbol{\lambda}_{ij}^T & \vdots & \mathbf{0}\\ \cdots & & \cdots\\ \mathbf{0} & \vdots & \mathbf{I}-\ell_{ij}\boldsymbol{\lambda}_{ij}^T\end{bmatrix}\right\}\begin{bmatrix}\mathbf{I} & \vdots & -\mathbf{I}\\ -\mathbf{I} & \vdots & \mathbf{I}\end{bmatrix}\Delta\mathbf{u}_{ij} +$$

$$-\frac{R_{ij}}{\ell_{ij}^o}\left(1-\boldsymbol{\lambda}_{ij}^T\Delta\mathbf{x}_{ij}^d\right)\begin{bmatrix}\ell_{ij}\\ \cdots\\ -\ell_{ij}\end{bmatrix}\Delta D_{ij}$$

$$\mathbf{k}^{*}_{Eij} = R_{ij}\left\{ \boldsymbol{\ell}_{ij}\boldsymbol{\lambda}^{T}_{ij}\left[\mathbf{I} - \Delta\mathbf{x}^{d}_{ij}\boldsymbol{\lambda}^{T}_{ij}\right]\right\}\left[\begin{array}{c|c} \mathbf{I} & -\mathbf{I} \\ \hline -\mathbf{I} & \mathbf{I} \end{array}\right] = \mathbf{k}^{*}_{Eij}\left(\Delta\mathbf{x}^{d}_{ij}\right) \tag{5.3.22}$$

$$\mathbf{k}^{*}_{Gij} = \frac{F^{o}_{ij}}{\ell^{o}_{ij}}\left\{\mathbf{I} - \boldsymbol{\ell}_{ij}\boldsymbol{\lambda}^{T}_{ij}\right\}\left[\begin{array}{c|c} \mathbf{I} & -\mathbf{I} \\ \hline -\mathbf{I} & \mathbf{I} \end{array}\right] = \mathbf{k}^{*}_{Gij}\left(\Delta\mathbf{x}^{d}_{ij}\right) \tag{5.3.23}$$

$$\mathbf{q}^{*}_{ij} = \frac{R_{ij}}{\ell^{o}_{ij}}\left(1 - \boldsymbol{\lambda}^{T}_{ij}\Delta\mathbf{x}^{d}_{ij}\right)\left[\begin{array}{c} \boldsymbol{\ell}_{ij} \\ \hline -\boldsymbol{\ell}_{ij} \end{array}\right] = \mathbf{q}^{*}_{ij}\left(\Delta\mathbf{x}^{d}_{ij}\right) \tag{5.3.24}$$

Actually, the matrices appearing in the graph parentheses are with 3×3 size, and they have the same function as described in Par. 5.2.1.

5.3.1   Assembled system

In order to consider the global structure the vector $\Delta\mathbf{x}$ is introduced, which now includes the $6m$ components of the sub vectors $\Delta u_{ij} \equiv \Delta u_h$

$$\Delta\mathbf{x}^{T} = \left[..... \vdots \Delta\mathbf{u}^{T}_{ij} \vdots .....\right] = \left[..... \vdots \Delta x_{ij} \quad \Delta y_{ij} \quad \Delta z_{ij} \quad \Delta x_{ji} \quad \Delta y_{ji} \quad \Delta z_{ji} \vdots .....\right] \tag{5.3.25}$$

and the vector $\Delta\mathbf{U}$ of the $3n$ imposed displacements at the free nodes.

Hence the relation between $\Delta\mathbf{x}$ and $\Delta\mathbf{U}$ is expressed through the topological matrix $\mathbf{A}$ ($6m \times n$),

$$\Delta\mathbf{x} = \mathbf{A}\Delta\mathbf{U} \tag{5.3.26}$$

At constrained nodes, the relevant components of $\Delta\mathbf{x}$ are zero in any change of configuration, and then the related rows in $\mathbf{A}$ are equal to 0 as well.

Let considers the $6m$ components vector

$$\Delta\mathbf{N}^{T} = \left[..... \vdots \Delta\mathbf{n}^{T}_{ij} \vdots .....\right] = \left[..... \vdots \Delta n_{ij,x} \quad \Delta n_{ij,y} \quad \Delta n_{ij,z} \quad \Delta n_{ji,x} \quad \Delta n_{ji,y} \quad \Delta n_{ij,z} \vdots .....\right] \tag{5.3.27}$$

which includes the sub vectors $\Delta\mathbf{n}_{ij} \equiv \Delta\mathbf{n}_h$ ($h = 1,...m$) in the same order of $\Delta\mathbf{x}$, related to the several segments. The variation of the external load $\Delta\mathbf{P}$ is inferred through equilibrium by the transpose of $\mathbf{A}$

$$\Delta \mathbf{P} = \mathbf{A}^{\mathrm{T}} \Delta \mathbf{N} \tag{5.3.28}$$

With reference to the definition of $\mathbf{diag[k_{ij}]}$[35] and to Eq. (5.3.21), (5.3.25)-(5.3.27), (5.3.22)-(5.3.24), one gets

$$\Delta \mathbf{N} = \mathbf{diag}\!\left[\mathbf{k}^{*}_{E,ij}\right]\!\Delta \mathbf{x} + \mathbf{diag}\!\left[\mathbf{k}^{*}_{G,ij}\right]\!\Delta \mathbf{x} - \mathbf{diag}\!\left[\mathbf{q}^{*}_{ij}\right]\!\Delta \mathbf{D} \tag{5.3.29}$$

$$\Delta \mathbf{N} = \mathbf{di\,ag}\!\left[\mathbf{k}^{*}_{E,ij}\right]\!\Delta \mathbf{x} + \mathbf{di\,ag}\!\left[\mathbf{k}^{*}_{G,ij}\right]\!\Delta \mathbf{x} - \mathbf{di\,ag}\!\left[\mathbf{q}^{*}_{ij}\right]\!\Delta \mathbf{D}$$

$$\Delta \mathbf{x} = \mathbf{A}\Delta \mathbf{U}$$

$$\Delta \mathbf{N} = \mathbf{di\,ag}\!\left[\mathbf{k}^{*}_{E,ij}\right]\!\mathbf{A}\Delta \mathbf{U} + \mathbf{di\,ag}\!\left[\mathbf{k}^{*}_{G,ij}\right]\!\mathbf{A}\Delta \mathbf{U} - \mathbf{di\,ag}\!\left[\mathbf{q}^{*}_{ij}\right]\!\Delta \mathbf{D}$$

Whence the solving equation is identified

$$\Delta \mathbf{P} = \mathbf{A}^{T}\Delta \mathbf{N} = \left\{\mathbf{A}^{T}\mathbf{diag}\!\left[\mathbf{k}^{*}_{E,ij}\right]\!\mathbf{A}\right\}\!\Delta \mathbf{U} + \left\{\mathbf{A}^{T}\mathbf{diag}\!\left[\mathbf{k}^{*}_{G,ij}\right]\!\mathbf{A}\right\}\!\Delta \mathbf{U} - \left\{\mathbf{A}^{T}\mathbf{diag}\!\left[\mathbf{q}^{*}_{ij}\right]\right\}\!\Delta \mathbf{D}$$

$$\Delta \mathbf{P} = \mathbf{K}^{*}_{E}\Delta \mathbf{U} + \mathbf{K}^{*}_{G}\Delta \mathbf{U} - \mathbf{Q}^{*}\Delta \mathbf{D} \tag{5.3.30}$$

with

$$\mathbf{K}^{*}_{E} = \mathbf{A}^{T}\mathbf{diag}\!\left[\mathbf{k}^{*}_{E,ij}\right]\!\mathbf{A} = \mathbf{K}^{*}_{E}(\Delta \mathbf{U}) \tag{5.3.31}$$

$$\mathbf{K}^{*}_{G} = \mathbf{A}^{T}\mathbf{diag}\!\left[\mathbf{k}^{*}_{G,ij}\right]\!\mathbf{A} = \mathbf{K}^{*}_{G}(\Delta \mathbf{U}) \tag{5.3.32}$$

$$\mathbf{Q}^{*} = \mathbf{A}^{T}\mathbf{diag}\!\left[\mathbf{q}^{*}_{ij}\right] = \mathbf{Q}^{*}(\Delta \mathbf{U}) \tag{5.3.33}$$

Hence the step by step approach in Par.5.2.2 is applied, taking into account that

1. $\mathbf{k}_{Eij} = R_{ij}\left\{\boldsymbol{\alpha}^{o}_{ij}\boldsymbol{\alpha}^{oT}_{ij}\right\}\begin{bmatrix} \mathbf{I} & \vdots & -\mathbf{I} \\ \hline -\mathbf{I} & \vdots & \mathbf{I} \end{bmatrix}$ is the elastic tangent stiffness matrix of the element

   ij

---

[35] The matrix is made by zeros except for the diagonal positions, where the sub-matrices $\mathbf{k}_{ij}$ are placed.

$$
\mathbf{k}^{*}_{Eij} = R_{ij}\left\{ \boldsymbol{\ell}_{ij}\boldsymbol{\lambda}^{T}_{ij}\left[\mathbf{I} - \Delta\mathbf{x}^{d}_{ij}\boldsymbol{\lambda}^{T}_{ij}\right]\right\}\begin{bmatrix}\mathbf{I} & -\mathbf{I}\\ -\mathbf{I} & \mathbf{I}\end{bmatrix} = \mathbf{k}^{*}_{Eij}\left(\Delta\mathbf{x}^{d}_{ij}\right)
$$

$$
\mathbf{k}_{Eij} = R_{ij}\left\{ \boldsymbol{\ell}^{o}_{ij}\frac{1}{\boldsymbol{\ell}^{o}_{ij}}\boldsymbol{\alpha}^{oT}_{ij}\left[\mathbf{I} - d\mathbf{x}^{d}_{ij}\frac{1}{\boldsymbol{\ell}^{o}_{ij}}\boldsymbol{\alpha}^{oT}_{ij}\right]\right\}\begin{bmatrix}\mathbf{I} & -\mathbf{I}\\ -\mathbf{I} & \mathbf{I}\end{bmatrix}
$$

$$
\mathbf{k}_{Eij} = R_{ij}\left\{ \boldsymbol{\alpha}^{o}_{ij}\boldsymbol{\alpha}^{oT}_{ij}\right\}\begin{bmatrix}\mathbf{I} & -\mathbf{I}\\ -\mathbf{I} & \mathbf{I}\end{bmatrix}
$$

$$
\mathbf{k}_{Eij} = R_{ij}\left\{ \boldsymbol{\alpha}^{o}_{ij}\boldsymbol{\alpha}^{oT}_{ij}\right\}\begin{bmatrix}\mathbf{I} & -\mathbf{I}\\ -\mathbf{I} & \mathbf{I}\end{bmatrix} = R_{ij}\begin{bmatrix}\alpha^{o}_{ij,x}\\ \alpha^{o}_{ij,y}\\ \alpha^{o}_{ij,z}\end{bmatrix}\begin{bmatrix}\alpha^{o}_{ij,x} & \alpha^{o}_{ij,y} & \alpha^{o}_{ij,z}\end{bmatrix}\begin{bmatrix}\mathbf{I} & -\mathbf{I}\\ -\mathbf{I} & \mathbf{I}\end{bmatrix} =
$$

$$
= R_{ij}\begin{bmatrix}\alpha^{o2}_{ij,x} & \alpha^{o}_{ij,x}\alpha^{o}_{ij,y} & \alpha^{o}_{ij,x}\alpha^{o}_{ij,z}\\ \alpha^{o}_{ij,y}\alpha^{o}_{ij,x} & \alpha^{o2}_{ij,y} & \alpha^{o}_{ij,y}\alpha^{o}_{ij,z}\\ \alpha^{o}_{ij,z}\alpha^{o}_{ij,x} & \alpha^{o}_{ij,z}\alpha^{o}_{ij,y} & \alpha^{o2}_{ij,z}\end{bmatrix}\begin{bmatrix}\mathbf{I} & -\mathbf{I}\\ -\mathbf{I} & \mathbf{I}\end{bmatrix} =
$$

$$
= R_{ij}\begin{bmatrix}\alpha^{o2}_{ij,x} & \alpha^{o}_{ij,x}\alpha^{o}_{ij,y} & \alpha^{o}_{ij,x}\alpha^{o}_{ij,z} & -\alpha^{o2}_{ij,x} & -\alpha^{o}_{ij,x}\alpha^{o}_{ij,y} & -\alpha^{o}_{ij,x}\alpha^{o}_{ij,z}\\ \alpha^{o}_{ij,y}\alpha^{o}_{ij,x} & \alpha^{o2}_{ij,y} & \alpha^{o}_{ij,y}\alpha^{o}_{ij,z} & -\alpha^{o}_{ij,y}\alpha^{o}_{ij,x} & -\alpha^{o2}_{ij,y} & -\alpha^{o}_{ij,y}\alpha^{o}_{ij,z}\\ \alpha^{o}_{ij,z}\alpha^{o}_{ij,x} & \alpha^{o}_{ij,z}\alpha^{o}_{ij,y} & \alpha^{o2}_{ij,z} & -\alpha^{o}_{ij,z}\alpha^{o}_{ij,x} & -\alpha^{o}_{ij,z}\alpha^{o}_{ij,y} & -\alpha^{o2}_{ij,z}\\ -\alpha^{o2}_{ij,x} & -\alpha^{o}_{ij,x}\alpha^{o}_{ij,y} & -\alpha^{o}_{ij,x}\alpha^{o}_{ij,z} & \alpha^{o2}_{ij,x} & \alpha^{o}_{ij,x}\alpha^{o}_{ij,y} & \alpha^{o}_{ij,x}\alpha^{o}_{ij,z}\\ -\alpha^{o}_{ij,y}\alpha^{o}_{ij,x} & -\alpha^{o2}_{ij,y} & -\alpha^{o}_{ij,y}\alpha^{o}_{ij,z} & \alpha^{o}_{ij,y}\alpha^{o}_{ij,x} & \alpha^{o2}_{ij,y} & \alpha^{o}_{ij,y}\alpha^{o}_{ij,z}\\ -\alpha^{o}_{ij,z}\alpha^{o}_{ij,x} & -\alpha^{o}_{ij,z}\alpha^{o}_{ij,y} & -\alpha^{o2}_{ij,z} & \alpha^{o}_{ij,z}\alpha^{o}_{ij,x} & \alpha^{o}_{ij,z}\alpha^{o}_{ij,y} & \alpha^{o2}_{ij,z}\end{bmatrix}
$$

2. $\mathbf{k}_{Gij} = \dfrac{F^{o}_{ij}}{\boldsymbol{\ell}^{o}_{ij}}\left\{\mathbf{I} - \boldsymbol{\alpha}^{o}_{ij}\boldsymbol{\alpha}^{oT}_{ij}\right\}\begin{bmatrix}\mathbf{I} & -\mathbf{I}\\ -\mathbf{I} & \mathbf{I}\end{bmatrix}$ is the eometric tangent stiffness matrix of the

element ij

$$\mathbf{k}^*_{Gij} = \frac{F^o_{ij}}{\ell^o_{ij}} \left\{ \mathbf{I} - \boldsymbol{\ell}_{ij} \boldsymbol{\lambda}^T_{ij} \right\} \left[\begin{array}{c|c} \mathbf{I} & -\mathbf{I} \\ \hline -\mathbf{I} & \mathbf{I} \end{array} \right] = \mathbf{k}^*_{Gij}\left(\Delta \mathbf{x}^d_{ij}\right)$$

$$\mathbf{k}_{Gij} = \frac{F^o_{ij}}{\ell^o_{ij}} \left\{ \mathbf{I} - \boldsymbol{\ell}^o_{ij} \frac{1}{\ell^o_{ij}} \boldsymbol{\alpha}^{oT}_{ij} \right\} \left[\begin{array}{c|c} \mathbf{I} & -\mathbf{I} \\ \hline -\mathbf{I} & \mathbf{I} \end{array} \right]$$

$$\mathbf{k}_{Gij} = \frac{F^o_{ij}}{\ell^o_{ij}} \left\{ \mathbf{I} - \boldsymbol{\alpha}^o_{ij} \boldsymbol{\alpha}^{oT}_{ij} \right\} \left[\begin{array}{c|c} \mathbf{I} & -\mathbf{I} \\ \hline -\mathbf{I} & \mathbf{I} \end{array} \right]$$

$$\mathbf{k}_{Gij} = \frac{F^o_{ij}}{\ell^o_{ij}} \left\{ \mathbf{I} - \boldsymbol{\alpha}^o_{ij} \boldsymbol{\alpha}^{oT}_{ij} \right\} \left[\begin{array}{c|c} \mathbf{I} & -\mathbf{I} \\ \hline -\mathbf{I} & \mathbf{I} \end{array} \right] =$$

$$= \frac{F^o_{ij}}{\ell^o_{ij}} \left\{ \begin{bmatrix} 1 & 0 & 0 \\ 0 & 1 & 0 \\ 0 & 0 & 1 \end{bmatrix} - \left[\begin{array}{c|c|c} \alpha^{o2}_{ij,x} & \alpha^o_{ij,x}\alpha^o_{ij,y} & \alpha^o_{ij,x}\alpha^o_{ij,z} \\ \hline \alpha^o_{ij,y}\alpha^o_{ij,x} & \alpha^{o2}_{ij,y} & \alpha^o_{ij,y}\alpha^o_{ij,z} \\ \hline \alpha^o_{ij,z}\alpha^o_{ij,x} & \alpha^o_{ij,z}\alpha^o_{ij,y} & \alpha^{o2}_{ij,z} \end{array} \right] \right\} \left[\begin{array}{c|c} \mathbf{I} & -\mathbf{I} \\ \hline -\mathbf{I} & \mathbf{I} \end{array} \right] =$$

$$= \frac{F^o_{ij}}{\ell^o_{ij}} \left\{ \left[\begin{array}{c|c|c} 1-\alpha^{o2}_{ij,x} & -\alpha^o_{ij,x}\alpha^o_{ij,y} & -\alpha^o_{ij,x}\alpha^o_{ij,z} \\ \hline -\alpha^o_{ij,y}\alpha^o_{ij,x} & 1-\alpha^{o2}_{ij,y} & -\alpha^o_{ij,y}\alpha^o_{ij,z} \\ \hline -\alpha^o_{ij,z}\alpha^o_{ij,x} & -\alpha^o_{ij,z}\alpha^o_{ij,y} & 1-\alpha^{o2}_{ij,z} \end{array} \right] \right\} \left[\begin{array}{c|c} \mathbf{I} & -\mathbf{I} \\ \hline -\mathbf{I} & \mathbf{I} \end{array} \right] =$$

$$= \frac{F^o_{ij}}{\ell^o_{ij}} \left\{ \left[\begin{array}{c|c|c} (\alpha^{o2}_{ij,y}+\alpha^{o2}_{ij,z}) & -\alpha^o_{ij,x}\alpha^o_{ij,y} & -\alpha^o_{ij,x}\alpha^o_{ij,z} \\ \hline -\alpha^o_{ij,y}\alpha^o_{ij,x} & (\alpha^{o2}_{ij,x}+\alpha^{o2}_{ij,z}) & -\alpha^o_{ij,y}\alpha^o_{ij,z} \\ \hline -\alpha^o_{ij,z}\alpha^o_{ij,x} & -\alpha^o_{ij,z}\alpha^o_{ij,y} & (\alpha^{o2}_{ij,x}+\alpha^{o2}_{ij,y}) \end{array} \right] \right\} \left[\begin{array}{c|c} \mathbf{I} & -\mathbf{I} \\ \hline -\mathbf{I} & \mathbf{I} \end{array} \right] =$$

$$= \frac{F^o_{ij}}{\ell^o_{ij}} \left[\begin{array}{ccc|ccc} (\alpha^{o2}_{ij,y}+\alpha^{o2}_{ij,z}) & -\alpha^o_{ij,x}\alpha^o_{ij,y} & -\alpha^o_{ij,x}\alpha^o_{ij,z} & -(\alpha^{o2}_{ij,y}+\alpha^{o2}_{ij,z}) & \alpha^o_{ij,x}\alpha^o_{ij,y} & \alpha^o_{ij,x}\alpha^o_{ij,z} \\ -\alpha^o_{ij,y}\alpha^o_{ij,x} & (\alpha^{o2}_{ij,x}+\alpha^{o2}_{ij,z}) & -\alpha^o_{ij,y}\alpha^o_{ij,z} & \alpha^o_{ij,y}\alpha^o_{ij,x} & -(\alpha^{o2}_{ij,x}+\alpha^{o2}_{ij,z}) & \alpha^o_{ij,y}\alpha^o_{ij,z} \\ -\alpha^o_{ij,z}\alpha^o_{ij,x} & -\alpha^o_{ij,z}\alpha^o_{ij,y} & (\alpha^{o2}_{ij,x}+\alpha^{o2}_{ij,y}) & \alpha^o_{ij,z}\alpha^o_{ij,x} & \alpha^o_{ij,z}\alpha^o_{ij,y} & -(\alpha^{o2}_{ij,x}+\alpha^{o2}_{ij,y}) \\ \hline -(\alpha^{o2}_{ij,y}+\alpha^{o2}_{ij,z}) & \alpha^o_{ij,x}\alpha^o_{ij,y} & \alpha^o_{ij,x}\alpha^o_{ij,z} & (\alpha^{o2}_{ij,y}+\alpha^{o2}_{ij,z}) & -\alpha^o_{ij,x}\alpha^o_{ij,y} & -\alpha^o_{ij,x}\alpha^o_{ij,z} \\ \alpha^o_{ij,y}\alpha^o_{ij,x} & -(\alpha^{o2}_{ij,x}+\alpha^{o2}_{ij,z}) & \alpha^o_{ij,y}\alpha^o_{ij,z} & -\alpha^o_{ij,y}\alpha^o_{ij,x} & (\alpha^{o2}_{ij,x}+\alpha^{o2}_{ij,z}) & -\alpha^o_{ij,y}\alpha^o_{ij,z} \\ \alpha^o_{ij,z}\alpha^o_{ij,x} & \alpha^o_{ij,z}\alpha^o_{ij,y} & -(\alpha^{o2}_{ij,x}+\alpha^{o2}_{ij,y}) & -\alpha^o_{ij,z}\alpha^o_{ij,x} & -\alpha^o_{ij,z}\alpha^o_{ij,y} & (\alpha^{o2}_{ij,x}+\alpha^{o2}_{ij,y}) \end{array} \right]$$

3. $\mathbf{q}_{ij} = R_{ij} \left[\begin{array}{c} \boldsymbol{\alpha}^{oT}_{ij} \\ \hline -\boldsymbol{\alpha}^{oT}_{ij} \end{array} \right]$ is the distortional tangent vector of the element ij

$$\mathbf{q}^*_{ij} = \frac{R_{ij}}{\ell^o_{ij}} \left(1 - \boldsymbol{\lambda}^T_{ij}\Delta\mathbf{x}^d_{ij} \right) \left[\begin{array}{c} \boldsymbol{\ell}_{ij} \\ \hline -\boldsymbol{\ell}_{ij} \end{array} \right] = \mathbf{q}^*_{ij}\left(\Delta\mathbf{x}^d_{ij}\right)$$

$$\mathbf{q}_{ij} = \frac{R_{ij}}{\ell^o_{ij}} \left(1 - \frac{1}{\ell^o_{ij}} \boldsymbol{\alpha}^{oT}_{ij} d\mathbf{x}^d_{ij} \right) \left[\begin{array}{c} \boldsymbol{\ell}^o_{ij} \\ \hline -\boldsymbol{\ell}^o_{ij} \end{array} \right] =$$

$$= \frac{R_{ij}}{\ell^o_{ij}} \left[\begin{array}{c} \boldsymbol{\ell}^o_{ij} \\ \hline -\boldsymbol{\ell}^o_{ij} \end{array} \right] = R_{ij} \left[\begin{array}{c} \boldsymbol{\alpha}^{oT}_{ij} \\ \hline -\boldsymbol{\alpha}^{oT}_{ij} \end{array} \right]$$

$$\mathbf{q}_{ij} = R_{ij} \left[\begin{array}{c} \boldsymbol{\alpha}^{oT}_{ij} \\ \hline -\boldsymbol{\alpha}^{oT}_{ij} \end{array} \right]$$

Remembering Eq. (5.2.51)

$$d\mathbf{L} = \mathbf{B}d\mathbf{U}$$

with

$$\mathbf{B} = diag\left[\boldsymbol{\alpha}_{ij}^{oT} \;\vdots\; -\boldsymbol{\alpha}_{ij}^{oT}\right]\mathbf{A} \text{ the compatibility matrix } (m{\times}3n)$$

5.3.2 The elastic and distortional stiffness matrix

The distortional effects, which have been neglected in Par.5.2.3 in order to solve Eq. (5.2.33) in Par. 5.2.1.2, are considered in the following.

Let consider Eq.(5.2.16) in Par. 5.2.1

$$\Delta\mathbf{f}_{ij} = R_{ij}\ell_{ij}\boldsymbol{\lambda}_{ij}^T\left[\mathbf{I} - \Delta\mathbf{x}_{ij}^d\boldsymbol{\lambda}_{ij}^T\right]\Delta\mathbf{x}_{ij}^d + \frac{F_{ij}^o}{\ell_{ij}^o}\left(\mathbf{I} - \ell_{ij}\boldsymbol{\lambda}_{ij}^T\right)\Delta\mathbf{x}_{ij}^d - \frac{R_{ij}}{\ell_{ij}^o}\Delta D\left(1 - \boldsymbol{\lambda}_{ij}^T\Delta\mathbf{x}_{ij}^d\right)\ell_{ij} \qquad (5.2.16)$$

By assembling all the terms depending on the axial stiffness *R,* one gets

$$\Delta\mathbf{f}_{ij} = R_{ij}\left[\ell_{ij}\boldsymbol{\lambda}_{ij}^T\mathbf{I}\Delta\mathbf{x}_{ij}^d - \ell_{ij}\boldsymbol{\lambda}_{ij}^T\Delta\mathbf{x}_{ij}^d\boldsymbol{\lambda}_{ij}^T\Delta\mathbf{x}_{ij}^d - \Delta D\frac{\ell_{ij}}{\ell_{ij}^o} + \Delta D\boldsymbol{\lambda}_{ij}^T\Delta\mathbf{x}_{ij}^d\frac{\ell_{ij}}{\ell_{ij}^o}\right] + $$
$$+\frac{F_{ij}^o}{\ell_{ij}^o}\left(\mathbf{I} - \ell_{ij}\boldsymbol{\lambda}_{ij}^T\right)\Delta\mathbf{x}_{ij}^d \qquad (5.3.34)$$

Hence, by moving the terms independent by the $\Delta\mathbf{x}_{ij}^d$ to the left and by considering Eq.(5.2.5) in Par.5.2.1), Eq.(5.3.34) can be re-written

$$\Delta\mathbf{f}_{ij} + \frac{R_{ij}}{\ell_{ij}^o}\Delta D_{ij}\ell_{ij} = R_{ij}\left[\ell_{ij}\boldsymbol{\lambda}_{ij}^T\mathbf{I}\Delta\mathbf{x}_{ij}^d - \ell_{ij}\boldsymbol{\lambda}_{ij}^T\Delta\mathbf{x}_{ij}^d\boldsymbol{\lambda}_{ij}^T\Delta\mathbf{x}_{ij}^d + \frac{1}{\ell_{ij}^o}\Delta D_{ij}\boldsymbol{\lambda}_{ij}^T\Delta\mathbf{x}_{ij}^d\ell_{ij}\right] + \frac{F_{ij}^o}{\ell_{ij}^o}\left(\mathbf{I} - \ell_{ij}\boldsymbol{\lambda}_{ij}^T\right)\Delta\mathbf{x}_{ij}^d$$

$$\Delta\mathbf{f}_{ij} + \frac{R_{ij}}{\ell_{ij}^o}\Delta D_{ij}\left(\ell_{ij}^o + \Delta\mathbf{x}_{ij}^d\right) = R_{ij}\left[\ell_{ij}\boldsymbol{\lambda}_{ij}^T\mathbf{I}\Delta\mathbf{x}_{ij}^d - \ell_{ij}\boldsymbol{\lambda}_{ij}^T\Delta\mathbf{x}_{ij}^d\boldsymbol{\lambda}_{ij}^T\Delta\mathbf{x}_{ij}^d + \frac{1}{\ell_{ij}^o}\Delta D_{ij}\boldsymbol{\lambda}_{ij}^T\Delta\mathbf{x}_{ij}^d\ell_{ij}\right] + \frac{F_{ij}^o}{\ell_{ij}^o}\left(\mathbf{I} - \ell_{ij}\boldsymbol{\lambda}_{ij}^T\right)\Delta\mathbf{x}_{ij}^d$$

$$\Delta\mathbf{f}_{ij} + \frac{R_{ij}}{\ell_{ij}^o}\Delta D_{ij}\ell_{ij}^o = R_{ij}\left\{\left[\ell_{ij}\boldsymbol{\lambda}_{ij}^T\mathbf{I}\Delta\mathbf{x}_{ij}^d - \ell_{ij}\boldsymbol{\lambda}_{ij}^T\Delta\mathbf{x}_{ij}^d\boldsymbol{\lambda}_{ij}^T\Delta\mathbf{x}_{ij}^d + \frac{1}{\ell_{ij}^o}\Delta D_{ij}\boldsymbol{\lambda}_{ij}^T\Delta\mathbf{x}_{ij}^d\ell_{ij}\right] - \frac{1}{\ell_{ij}^o}\Delta D_{ij}\Delta\mathbf{x}_{ij}^d\right\} + \frac{F_{ij}^o}{\ell_{ij}^o}\left(\mathbf{I} - \ell_{ij}\boldsymbol{\lambda}_{ij}^T\right)\Delta\mathbf{x}_{ij}^d$$

$$\Delta\mathbf{f}_{ij} + \frac{R_{ij}}{\ell_{ij}^o}\Delta D_{ij}\ell_{ij}^o = R_{ij}\left\{\left[\ell_{ij}\boldsymbol{\lambda}_{ij}^T\mathbf{I}\Delta\mathbf{x}_{ij}^d - \ell_{ij}\boldsymbol{\lambda}_{ij}^T\Delta\mathbf{x}_{ij}^d\boldsymbol{\lambda}_{ij}^T\Delta\mathbf{x}_{ij}^d + \frac{1}{\ell_{ij}^o}\Delta D_{ij}\boldsymbol{\lambda}_{ij}^T\Delta\mathbf{x}_{ij}^d\ell_{ij}\right] - \frac{1}{\ell_{ij}^o}\Delta D_{ij}\Delta\mathbf{x}_{ij}^d\right\} +$$
$$+\frac{F_{ij}^o}{\ell_{ij}^o}\left(\mathbf{I} - \ell_{ij}\boldsymbol{\lambda}_{ij}^T\right)\Delta\mathbf{x}_{ij}^d \qquad (5.3.35)$$

Whence

$$\Delta\mathbf{f} + \frac{R_{ij}}{\ell_{ij}^{\circ}}\Delta D_{ij}\boldsymbol{\ell}_{ij}^{\circ} = R_{ij}\left\{\boldsymbol{\ell}_{ij}\boldsymbol{\lambda}_{ij}^{T}\left[\mathbf{I}\left(1+\frac{1}{\ell_{ij}^{\circ}}\Delta D_{ij}\right)-\Delta\mathbf{x}_{ij}^{d}\boldsymbol{\lambda}_{ij}^{T}\right]-\mathbf{I}\frac{1}{\ell_{ij}^{\circ}}\Delta D_{ij}\right\}\Delta\mathbf{x}_{ij}^{d} + \frac{F_{ij}^{o}}{\ell_{ij}^{\circ}}\left(\mathbf{I}-\boldsymbol{\ell}_{ij}\boldsymbol{\lambda}_{ij}^{T}\right)\Delta\mathbf{x}_{ij}^{d}$$

$$(5.3.36)$$

Setting

$$\Delta\mathbf{f}_{ij}^{D} = \frac{R_{ij}}{\ell_{ij}^{\circ}}\Delta D_{ij}\boldsymbol{\ell}_{ij}^{\circ}$$

i.e. the axial distortional forces, Eq. (5.36) turns into

$$\Delta\mathbf{f} + \Delta\mathbf{f}_{ij}^{D} = R_{ij}\left\{\boldsymbol{\ell}_{ij}\boldsymbol{\lambda}_{ij}^{T}\left[\mathbf{I}\left(1+\frac{1}{\ell_{ij}^{\circ}}\Delta D_{ij}\right)-\Delta\mathbf{x}_{ij}^{d}\boldsymbol{\lambda}_{ij}^{T}\right]-\mathbf{I}\frac{1}{\ell_{ij}^{\circ}}\Delta D_{ij}\right\}\Delta\mathbf{x}_{ij}^{d} + \frac{F_{ij}^{o}}{\ell_{ij}^{\circ}}\left(\mathbf{I}-\boldsymbol{\ell}_{ij}\boldsymbol{\lambda}_{ij}^{T}\right)\Delta\mathbf{x}_{ij}^{d} \qquad (5.3.37)$$

Denoting by

$$\mathbf{k}_{E,ij}^{*D} = R_{ij}\left\{\boldsymbol{\ell}_{ij}\boldsymbol{\lambda}_{ij}^{T}\left[\mathbf{I}\left(1+\frac{1}{\ell_{ij}^{\circ}}\Delta D_{ij}\right)-\Delta\mathbf{x}_{ij}^{d}\boldsymbol{\lambda}_{ij}^{T}\right]-\mathbf{I}\frac{1}{\ell_{ij}^{\circ}}\Delta D_{ij}\right\} \qquad (5.3.38)$$

the modified secant elastic stiffness matrix due to the effects of the distortions, one has

$$\Delta\mathbf{f}_{ij} + \Delta\mathbf{f}_{ij}^{D} = \mathbf{k}_{E,ij}^{*D}\Delta\mathbf{x}_{ij}^{d} + \mathbf{k}_{G,ij}^{*}\Delta\mathbf{x}_{ij}^{d} \qquad (5.3.39)$$

Following the considerations made in the Par. 5.2.1, Eq.(5.2.33), one has

$$\Delta\mathbf{N}^{DT} = \left[\ldots \vdots \Delta\mathbf{n}_{ij}^{DT} \vdots \ldots\right] \qquad (5.3.40)$$

Where

$$\Delta\mathbf{n}_{ij}^{D} = \begin{bmatrix} \Delta\mathbf{f}_{ij}^{D} \\ \Delta\mathbf{f}_{ji}^{D} \end{bmatrix} \qquad (5.3.41)$$

and

$$\Delta\mathbf{P}^{D} = \mathbf{A}^{T}\Delta\mathbf{N}^{D} \qquad (5.3.42)$$

which is the equilibrium equation between the variation of distortional loads and the distortional forces.

For the entire structure one has

$$\Delta \mathbf{N} + \Delta \mathbf{N}^D = diag\left[\mathbf{k}_{E,ij}^{*D}\right]\Delta \mathbf{x} + diag\left[\mathbf{k}_{G,ij}^{*}\right]\Delta \mathbf{x} \tag{5.3.43}$$

whence, because of compatibility

$$\Delta \mathbf{x} = \mathbf{A}\Delta \mathbf{U}$$

$$\Delta \mathbf{N} + \Delta \mathbf{N}^D = diag\left[\mathbf{k}_{E,ij}^{*D}\right]\mathbf{A}\Delta \mathbf{U} + diag\left[\mathbf{k}_{G,ij}^{*}\right]\mathbf{A}\Delta \mathbf{U} \tag{5.3.44}$$

As regards the equilibrium, remembering that

$$\Delta \mathbf{P} = \mathbf{A}^T \Delta \mathbf{N}$$

one gets

$$\Delta \mathbf{P} + \Delta \mathbf{P}^D = \mathbf{A}^T \Delta \mathbf{N} + \mathbf{A}^T \Delta \mathbf{N}^D$$

$$\Delta \mathbf{P} + \Delta \mathbf{P}^D = \mathbf{A}^T \left(\Delta \mathbf{N} + \Delta \mathbf{N}^D\right)$$

$$\Delta \mathbf{P} + \Delta \mathbf{P}^D = \mathbf{A}^T \left(diag\left[\mathbf{k}_{E,ij}^{*D}\right]\mathbf{A}\Delta \mathbf{U} + diag\left[\mathbf{k}_{G,ij}^{*}\right]\mathbf{A}\Delta \mathbf{U}\right)$$

$$\Delta \mathbf{P} + \Delta \mathbf{P}^D = \mathbf{A}^T diag\left[\mathbf{k}_{E,ij}^{*D}\right]\mathbf{A}\Delta \mathbf{U} + \mathbf{A}^T diag\left[\mathbf{k}_{G,ij}^{*}\right]\mathbf{A}\Delta \mathbf{U} \tag{5.3.45}$$

By considering that

$$\mathbf{K}_E^{*D} = \mathbf{A}^T diag\left[\mathbf{k}_{E,ij}^{*D}\right]\mathbf{A} \tag{5.3.46}$$

$$\mathbf{K}_G^{*} = \mathbf{A}^T diag\left[\mathbf{k}_{G,ij}^{*}\right]\mathbf{A} \tag{5.3.47}$$

are respectively the secant elastic stiffness matrix with the distorting effects, and the secant geometric stiffness one, Eq. (5.3.45) can be written

$$\Delta \mathbf{P} + \Delta \mathbf{P}^D = \mathbf{K}_E^{*D}\Delta \mathbf{U} + \mathbf{K}_G^{*}\Delta \mathbf{U} \tag{5.3.48}$$

Assuming

$$\Delta \mathbf{P}_{Tot} = \Delta \mathbf{P} + \Delta \mathbf{P}^D \tag{5.3.49}$$

Eq.(5.3.48) written including the distortional effects as distortional loads, turns into

$$\Delta \mathbf{P}_{Tot} = \mathbf{K}_E^{*D} \Delta \mathbf{U} + \mathbf{K}_G^* \Delta \mathbf{U} \tag{5.3.50}$$

The solving procedure previously described holds also for Eq. (5.3.50), and the same considerations are valid also in the 3D extension, taking into account the different size of the matrices.

6. AN OVERVIEW ON THE DYNAMIC BEHAVIOUR OF CABLE TENSILE SYSTEMS

Aiming at emphasizing the dynamic behavior of tensile structures, in the following the performance of cable tensile roof is investigated through the analysis of a study case which is referred to.

The executed investigation focuses on the vibration modes of the selected study case, paying attention, mainly, to the deformed configurations, frequencies and periods. The accidental loads referred to in the analysis are identified as concerns the Italian Instructions NTC2008. The analyzed structure is an open system, and, in this case, it is undergone by an asymmetrical load.

6.1 General description of the study case

Firstly, the geometry and the materials of the study case have been identified and described in the following. The structure refers to a tensile roof designed for covering a large space in Tokyo. It is an open system, as previously mentioned, and it is composed of steel frames and cables. Fig. 6.1 shows that it is a symmetrical cable structure with opposite curvature where the connecting cables are arranged along the vertical direction.
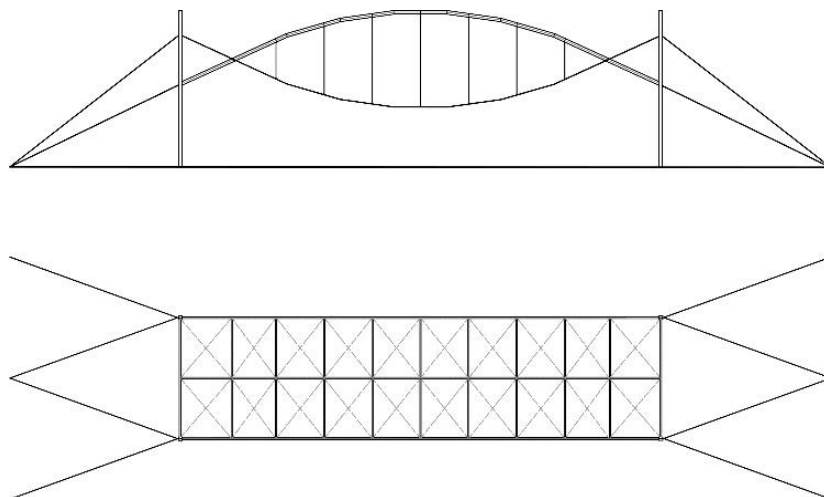
Figure 6.1: Plan and vertical views of the structural scheme.

The geometry is characterized by an arch structure composed by steel elements consisting of beams, piles and cables. The covering is in PVC material. It presents a

span of 40000 mm, a depth of 10000 mm, reaching a height of 13000 mm. For the piles HEM300 are used and IPE300 and IPE200 for the beams. The diameter of cables is 10 mm or 40 mm based on their arrangement and structural function. In Fig.6.2 the lateral view is shown.
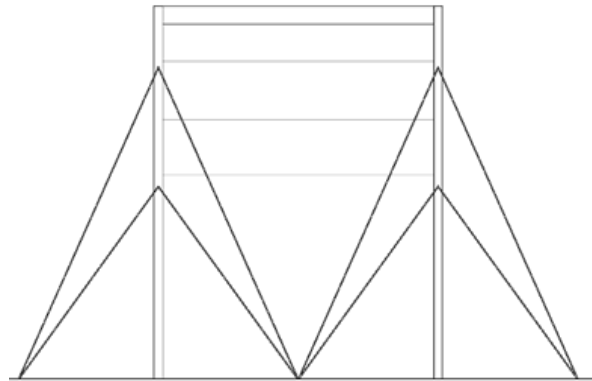
Figure 6.2: Lateral view of the structural scheme.

The distance between the cable elements amounts to 10000 mm, reaching a total depth of 20000 mm, as highlighted in Fig. 6.4. Moreover, the connecting cables present a different length along the arcade (Fig. 6.3).
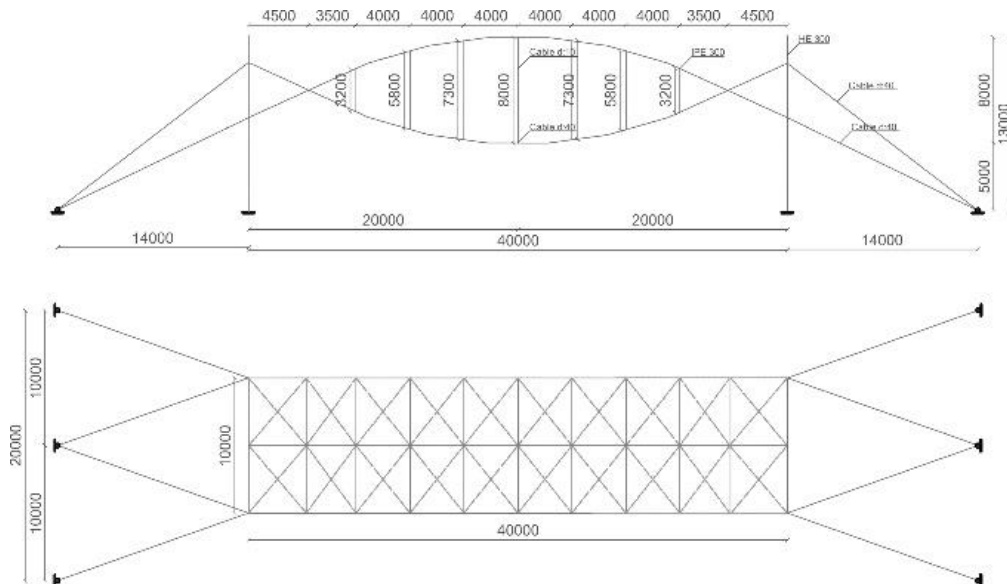
Figure 6.3: Plan and frontal views of the structural scheme.
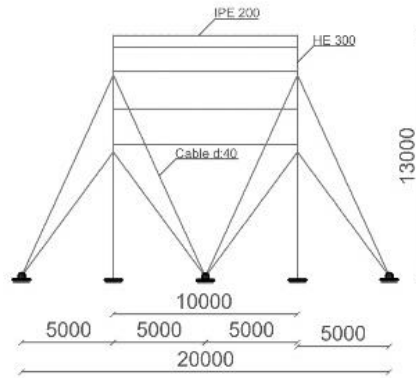
Figure 6.4: Lateral view of the structural scheme.

The analysis has been conducted according to the Italian Regulations, in particular:

Law November, 5th 1971: "Norme per la disciplina delle opere di conglomerato cementizio armato, normale e precompresso ed a struttura metallica" (Regulation about the reinforced concrete, concrete and pre-pressed concrete buildings and steel frame structures);

D.M. (Ministerial Decree) Transport Infrastructures January, 14th 2008 : "Norme tecniche per le Costruzioni" (Technical regulation about the buildings);

Furthermore some indications belonging to the **Circolare 2 febbraio 2009 n. 617 del Ministero delle Infrastrutture e dei Trasporti** have been considered:

"Istruzioni per l'applicazione delle 'Norme Tecniche delle Costruzioni' di cui al D.M. 14 gennaio 2008". (Instructions about the application of the Technical Regulation about the buildings; DM 2008/01/14).

6.1.1   Materials

Then the materials composing the elements have been identified, as follows:

-S355

-Stainless steel

-PVC

in order to evaluate the following mechanical properties:

- Weight per Unit of Volume

- Mass per Unit of Volume

-Young Modulus (E)

- Coefficient of Poisson (v)

- Shear Modulus (G)

- Coefficient of thermal expansion (α)

- Yield tensile stress (f_{yk})

The stress/strain graph is shown in Fig. 6.9.

6.1.2   Regularity of the structure

Table 6.1 summarizes the principal features of the plan and height regularity for the study case, according to Italian Regulations (Par.6.1).

Table 6.1: Check of the plan regularity

Plan regularity of the the structure	
The plan configuration appears symmetric along the two perpendicular directions, according to the mass and stiffness distribution.	YES
The ratio between the sides of a rectangle that inscribe the plan is less than 4. (b_{tot} = 68000 mm; h_{tot} = 20000 mm; b_{tot}/h_{tot} =3,4)	YES
No dimension of any recesses or protrusions exceeding 25% of the construction dimension in the corresponding direction.	YES
The horizontal elements can be considered infinitely rigid in their plane with respect to the vertical elements and sufficiently resistant.	YES

Height regularity of the structure	
All the resistant vertical systems extend along all the height of the building.	YES

6.1.3   Load Conditions

As concerns the loads applied on the structure, they are subdivided in permanent and accidental loads.

To the first category the following loads belong:

-   G_1: the structural elements self- weight (cables, beams, piles)
-   G_2: the un-structural elements self-weight
-   T: the pre- tension in the cables

To the second one the following loads belong:

-   L: accidental loads.

The considered load condition is given by

$$G_1 + G_2 + T + L \tag{6.1}$$

The loads evaluation has been made according to the DM 2008, except for the permanent ones, whose evaluation has been made according to the final dimensions of the structure.

6.2 Modelling

A FEM model has been developed for the study case, in order to evaluate its response under the accidental asymmetrical loads.
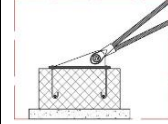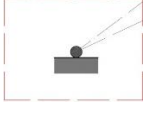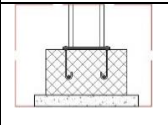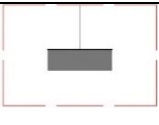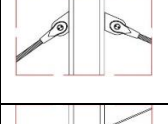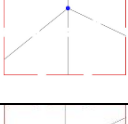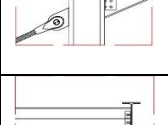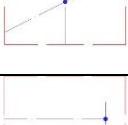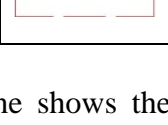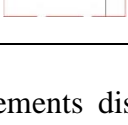
After the definition of the geometry and materials of the elements, and the constraint conditions, the model has been realized with SAP2000 using frames, cables and shell elements.

The lateral sloping and the vertical cables are modelled like a straight frame, divided in ten segments in correspondence of the nodes which link the cable to the vertical ones.

The elements respect the number and the arrangement supposed in the design phase step. The roof surface has been modelled through shell elements with membrane behaviour. It has been divided in a regular mesh.

Moreover, the elements are linked to each other through joints, as shown in Table 6.2.

Table 6.2: Main constraint conditions

	Constraint [U=0;Φ=0]	Hinge [U=0;Φ≠0]	Joints

In Fig. 6.5-8, one shows the model and the different elements distinguished by the different colors.

Legend

■ Frame

■ Cable

■ Shell
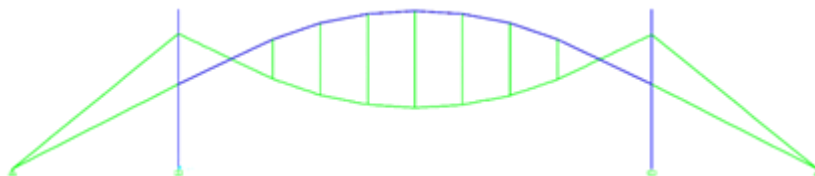
Figure 6.5: Model-Frontal view.
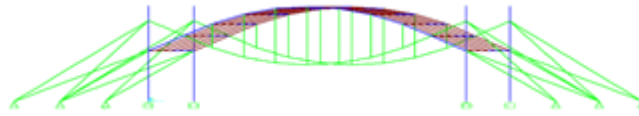
Figure 6.6: Model-Perspective view.
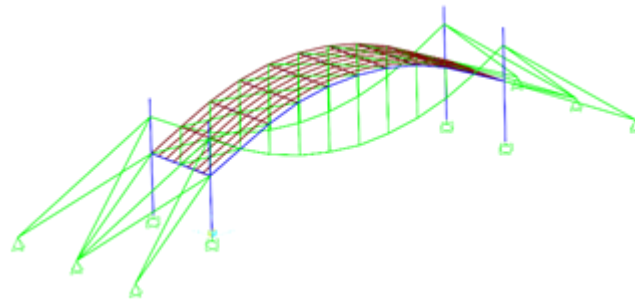
Figure 6.7: Axonometric view.
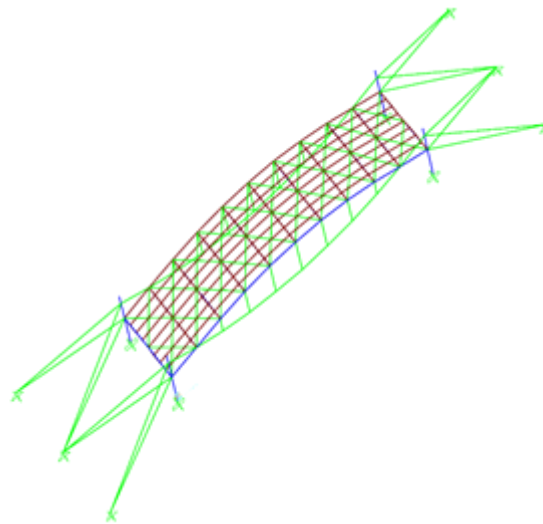
Figure 6.8: Model- Bird's eye view.

In *Table 6.3* and *Table 6.4* the number and type of elements and the number of the constrained points used in the model are shown respectively.

Table 6.3: Type and number of elements

ELEMENTS	N° OF ELEMENTS
Frames	46

Cables	90
Shell	80
Nodes	131

For the piles the use of the HEM300 is adopted; instead for the principal beams the IPE300 and for the secondary beams IPE200 are used.

In *Table 6.5* the geometrical features of the above mentioned elements are shown.

Table 6.5: Geometrical features of the frame elements
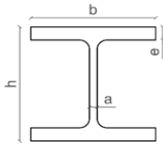
		h	B	a	e
		[mm]	[mm]	[mm]	[mm]
	IPE300	300	150	7,1	10,7
	IPE200	200	100	5,6	8,5
	HEM300	340	310	21	39

6.2.1   Materials' properties

Then the mechanical parameters of the materials have been considered, summarized in Tables 8 and 9. Moreover, in Fig. 6.9 the stress/strain graph of the steel material used in the model is shown.

Table 8: Weight and mass

Material	Weight per unit volume	Mass per unit volume
	$[kN/m^3]$	$[kN/m^3]$
S355	77	7,849
Steel	77,5	7,902

Table 9: Properties Data

Material	E	ν	α	G
	kN/m^2	-	°C	kN/m^2
S355	2,1E+8	0,3	12E-6	80769231
Steel	2E+8	0,3	16	76923077

Legend

■ Axial Stress/Strain Curve

■ Share Stress/Strain Curve
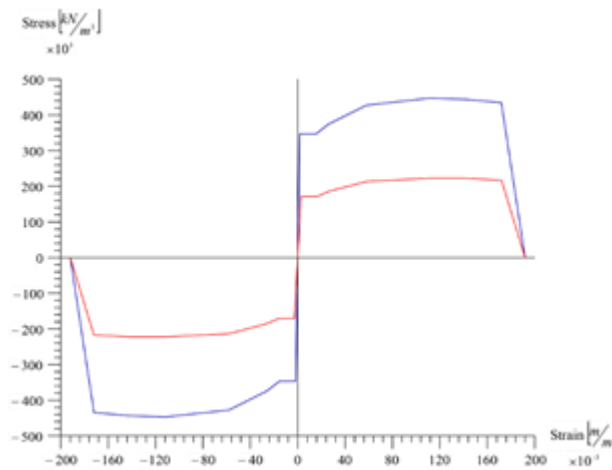
Figure 6.9: Stress/strain graph of adopted steel material.

6.2.2 Load Conditions

As concerns the load condition, the self-weight of the structure and the accidental loads have been considered.

The self-weight has been calculated by the program, by considering the self-weight of the roof like an overload on the structure and including the pretension in the cable in the class of the permanent loads.

About the accidental loads, an asymmetrical load one has been applied on the structure, classified in the class of live loads.
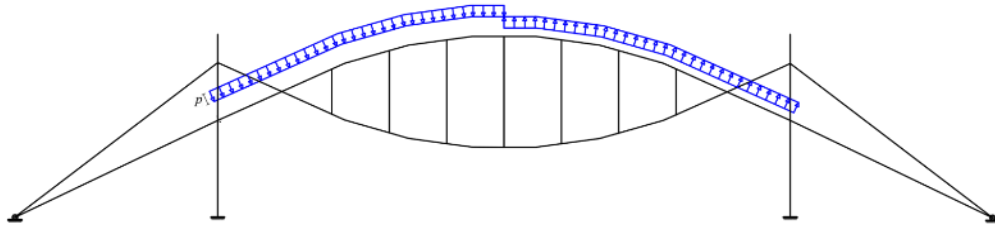
Figure 6.10: Accidental load condition.

Table 6.10: Load condition

Type of load	
Self- weight	The self-weight of the structure is calculated by the program
G2	0,009 kN/m²
Live	q_{sk}=1,30kN/m²

The value of the accidental loads has been calculated according to the NTC2008.

A snow load has been supposed on the roof.

According to the NTC2008 for a snow load, considering the different zones, one has

1. $a_s \leq 200 \rightarrow q_{sk} = 0.60 kN/m^2$ (6.2)

2. $a_s \geq 200 \rightarrow q_{sk} = 0.51\left[1+\left(\dfrac{a_s}{481}\right)^2\right]kN/m^2$ (6.3)

where

a_s is the height of the zone

q_{sk} is the snow load

Therefore, one has considered a snow load given by

$$a_s = 600 \tag{6.4}$$

$$q_{sk} = 0.51\left[1 + \left(600\big/481\right)^2\right] = 1.30 kN/m^2 \tag{6.5}$$

The uniform asymmetrical load has been applied on the model in terms of nodal loads. Fig. 6.11 shows how the asymmetrical loads have been calculated for each node of the roof surface.
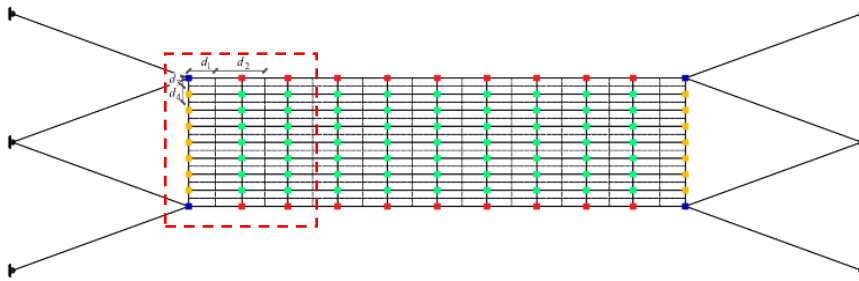
Figure 6.11: Nodal loads on the roof surface.
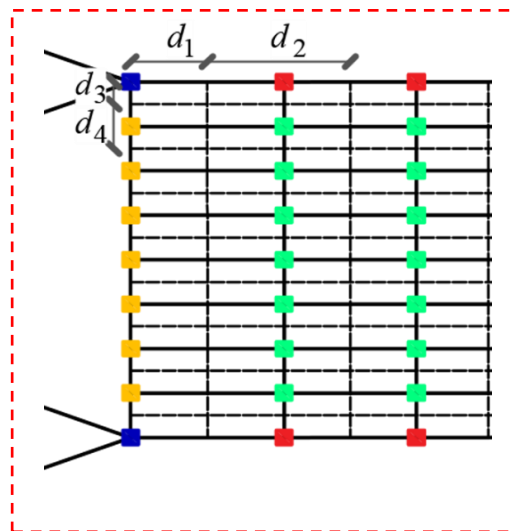
Figure 6.12: Detail of the nodal loads condition.

The value of the nodal loads has been analytically calculated as follows.

Firstly, three types of nodes on the roof surface have been identified:

1. External nodes

2.Longitudinal boundary nodes

3. Transversal boundary nodes

4. Inner nodes

For each of them, the value of the load has been determined as follows:

■ $p \cdot d_1 \cdot d_2$

■ $p \cdot d_2 \cdot d_3$

■ $p \cdot d_4 \cdot d_1$

■ $p \cdot d_2 \cdot d_4$

The roof overload has been considered also applied on the nodes, following the same procedure.

6.3 Modal analysis

The modal analysis of the structure has been developed under the given load conditions.

In order to identify the different vibration modes of the structure, one has considered the following masses:

1. Self- weight of the structural elements (G_1)

2. Overload of the roof (G_2)

3. Accidental loads (L)

Therefore, the total mass is:

G_1:

Piles: $w \cdot A \cdot H \cdot n$ [kN]

Beams: $w \cdot A \cdot \ell \cdot n$ [kN]

Cables: $w \cdot A \cdot \ell \cdot n$ [kN]

G_2:

Roof surface: $g_R \cdot A$ [kN]

where:

w: weight of the material of the element in kN/m^3

A: area of the element in m^2

H: height of the element in m

n: number of the elements

l: length of the elements in m

g_r: gravity load of the roof in kN/m^2

In order to assign this mass to the structures, one has identified the different loads in the MASS SOURCE (M2), given by:

Elements and additional masses (G_1)
From load (G_2+L)

After that, the number of modes according to the eigen vectors has been identified.

6.4 Numerical results

In Figs. 6.13-24, one reports the results obtained by the modal analysis in terms of deformed shapes (displacements in mm), frequencies(Cyc/sec) and periods (sec.).
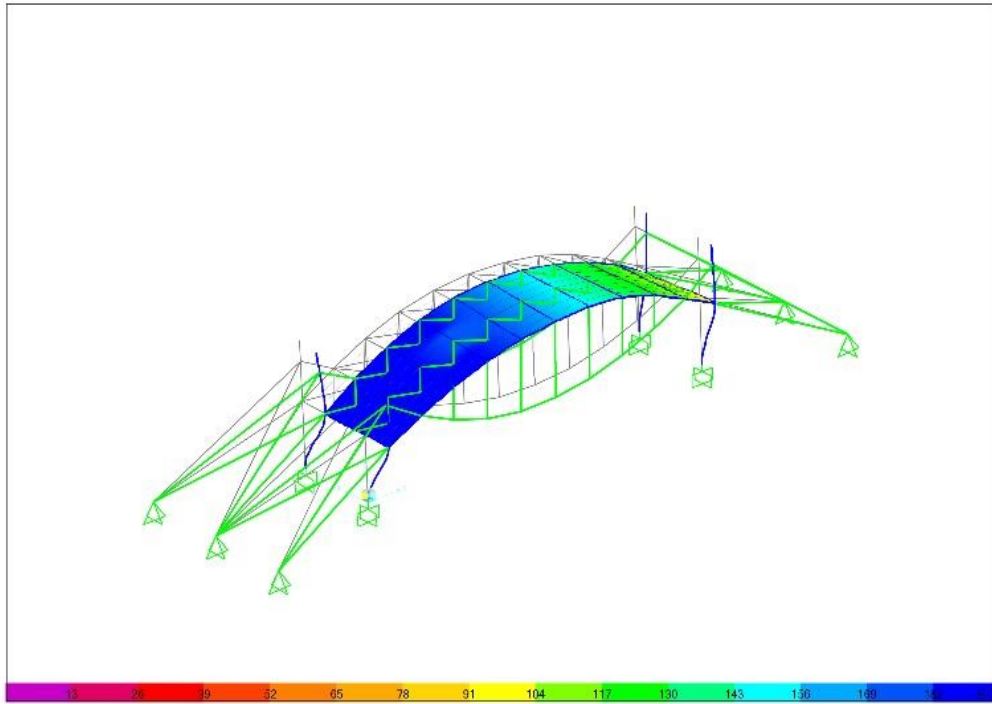
Figure 6.13: Mode 1.
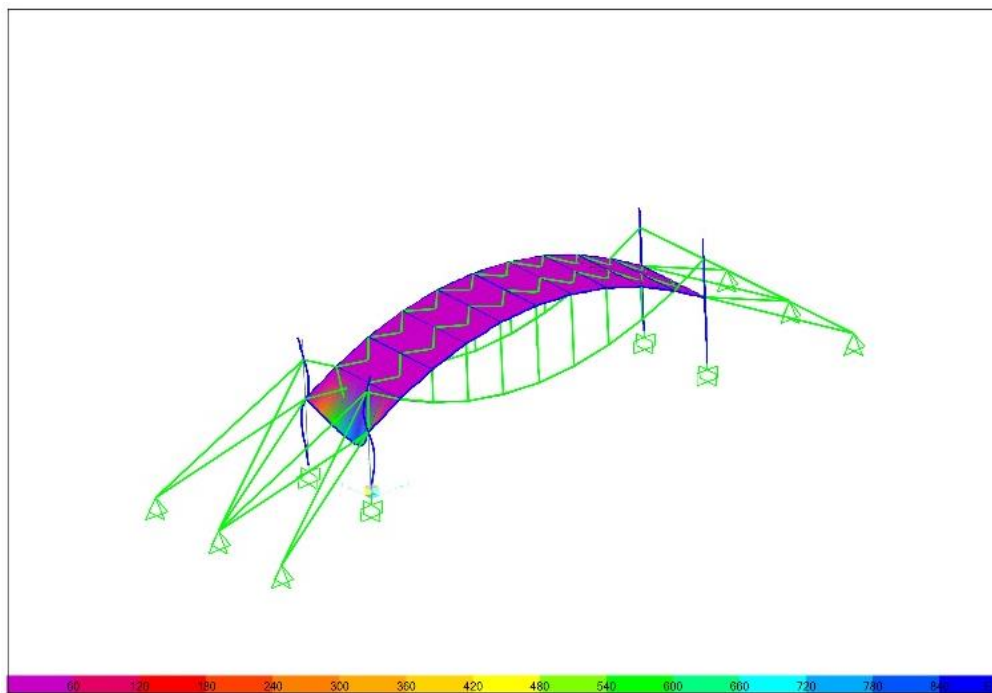
Figure 6.14: Mode 2.
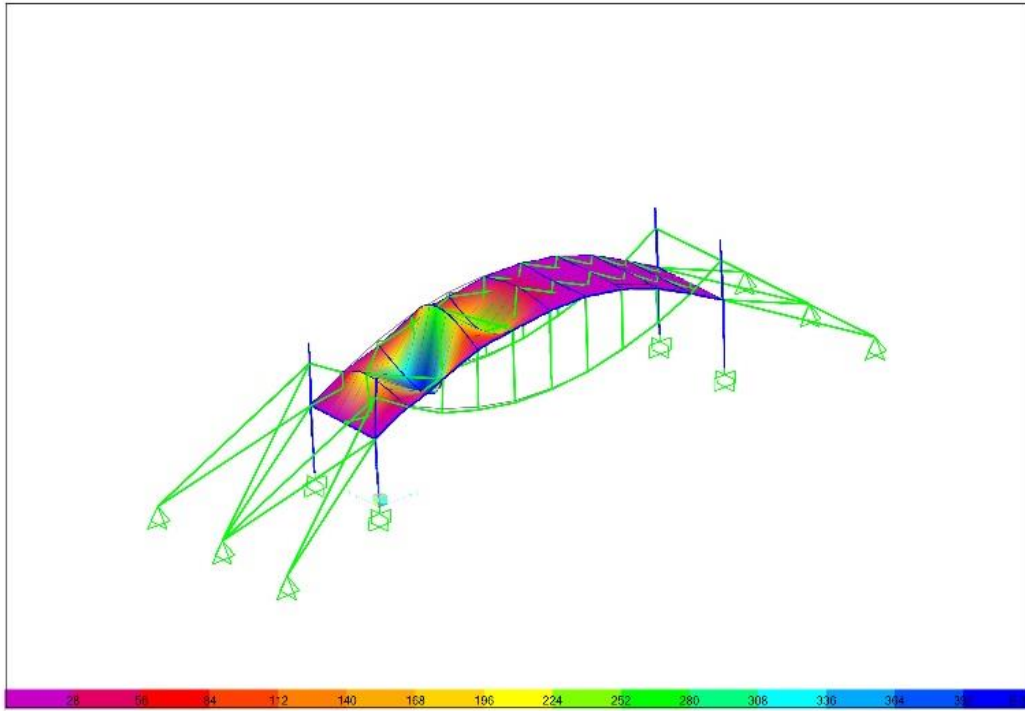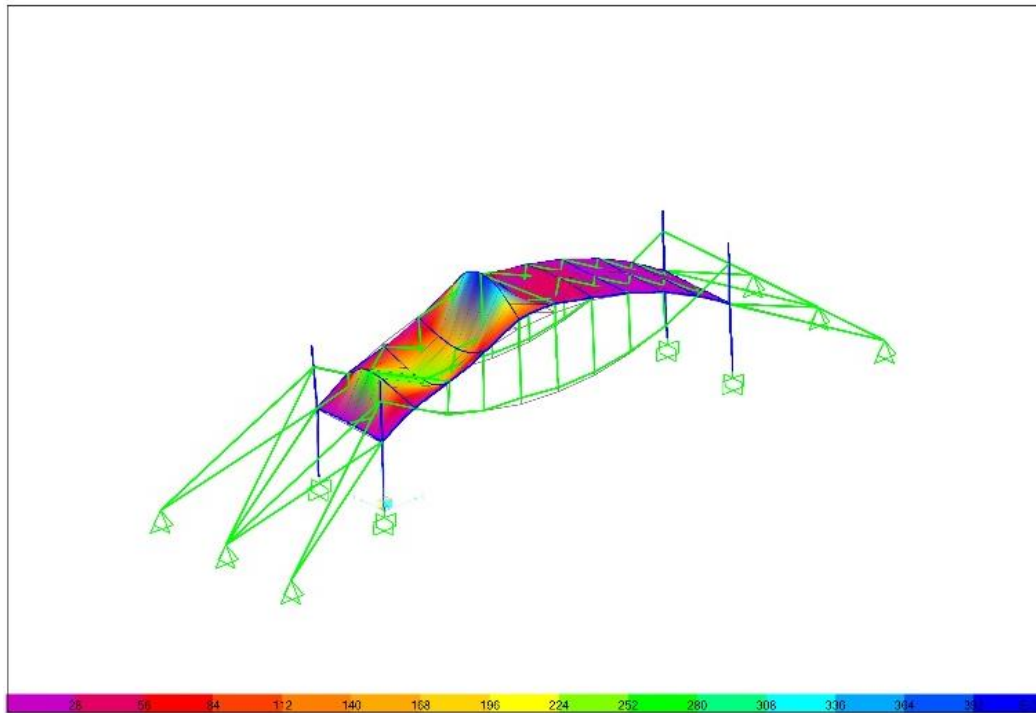
Figure 6.15: Mode 3.
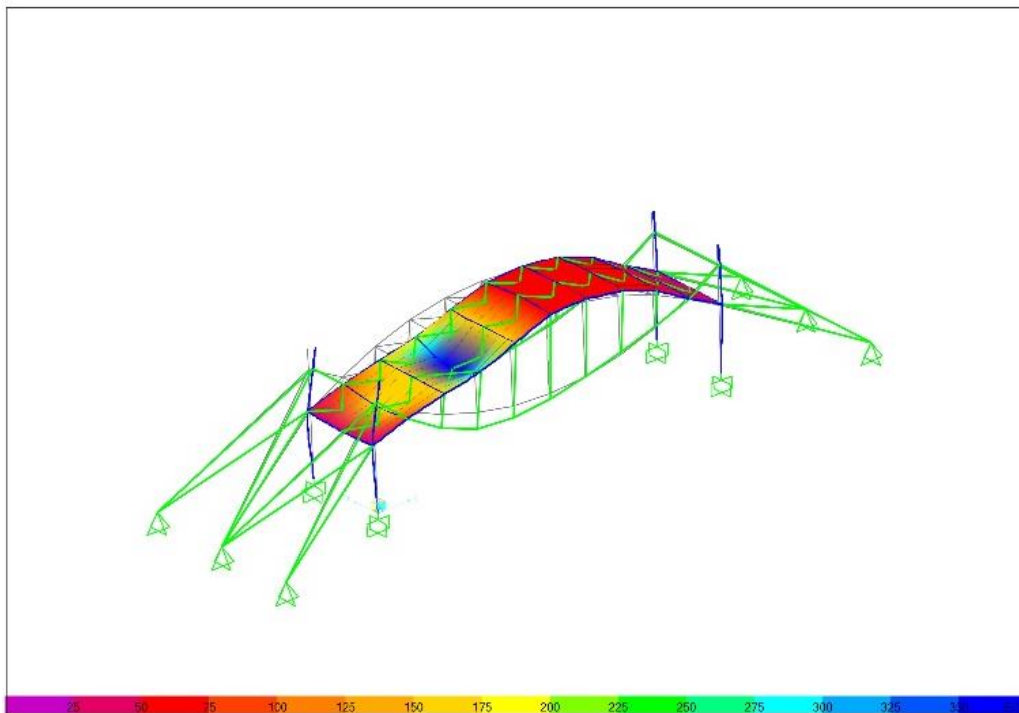
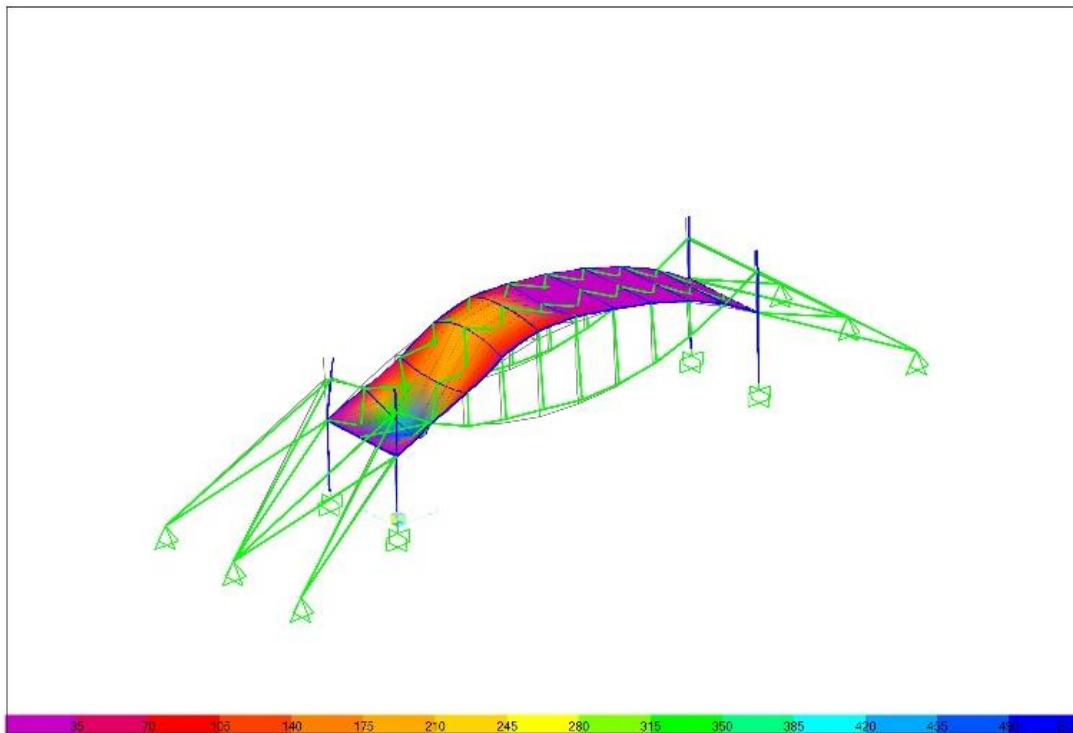*Figure 6.16: Mode 4.*

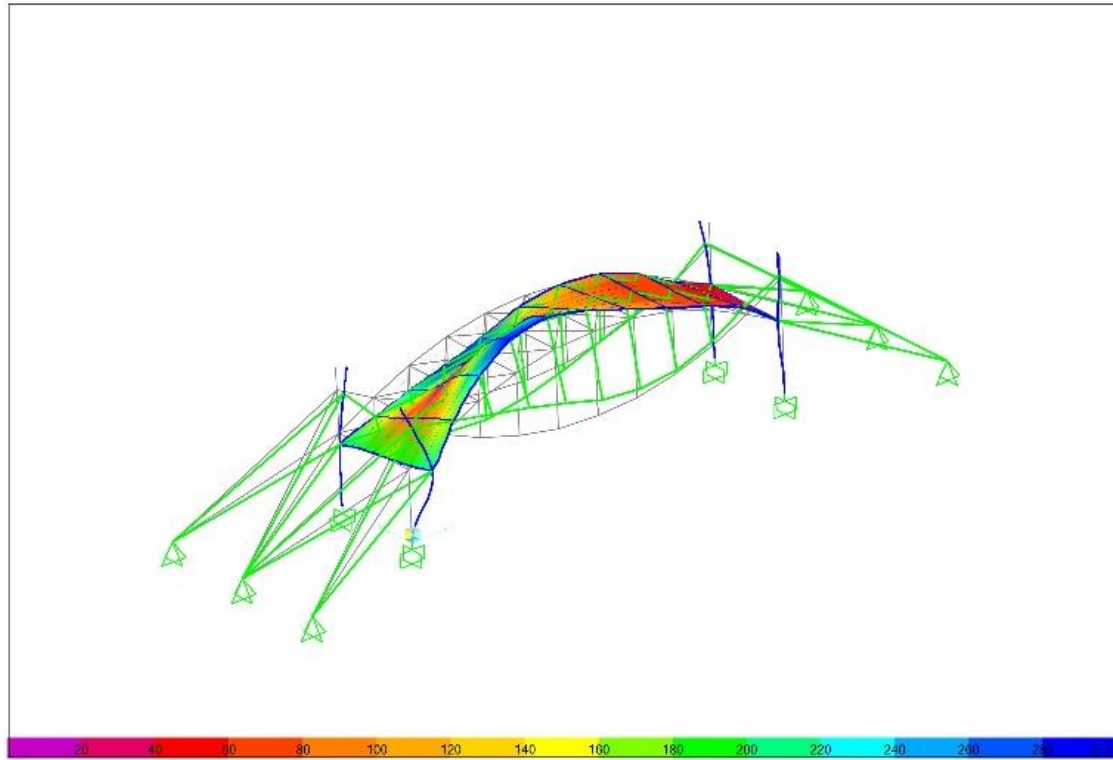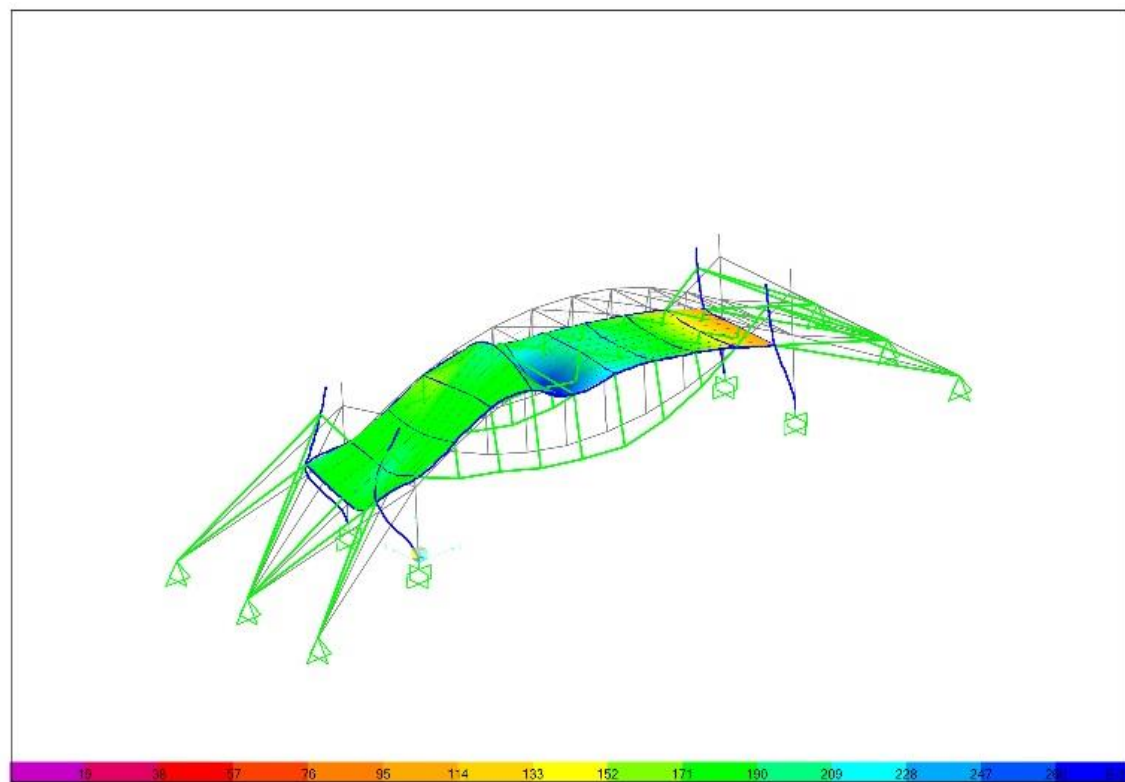*Figure 6.17: Mode 5.*

Figure 6.18: Mode 6.

Figure 6.19: Mode 7.
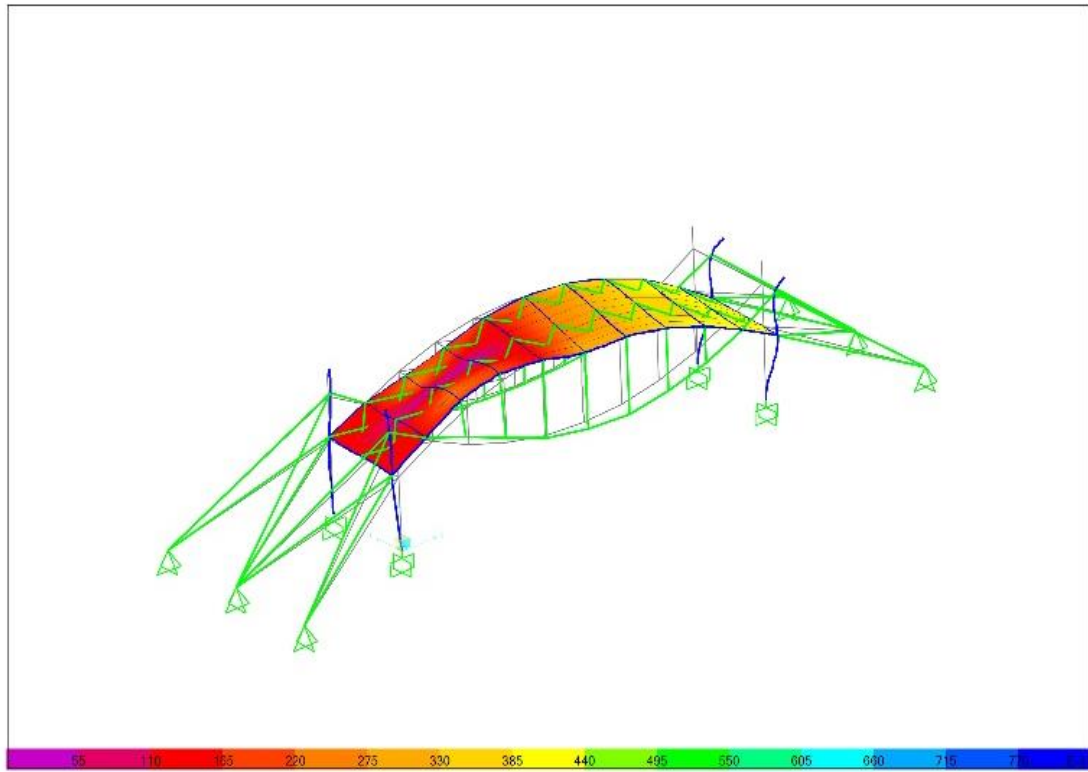

Figure 6.20: Mode 8.
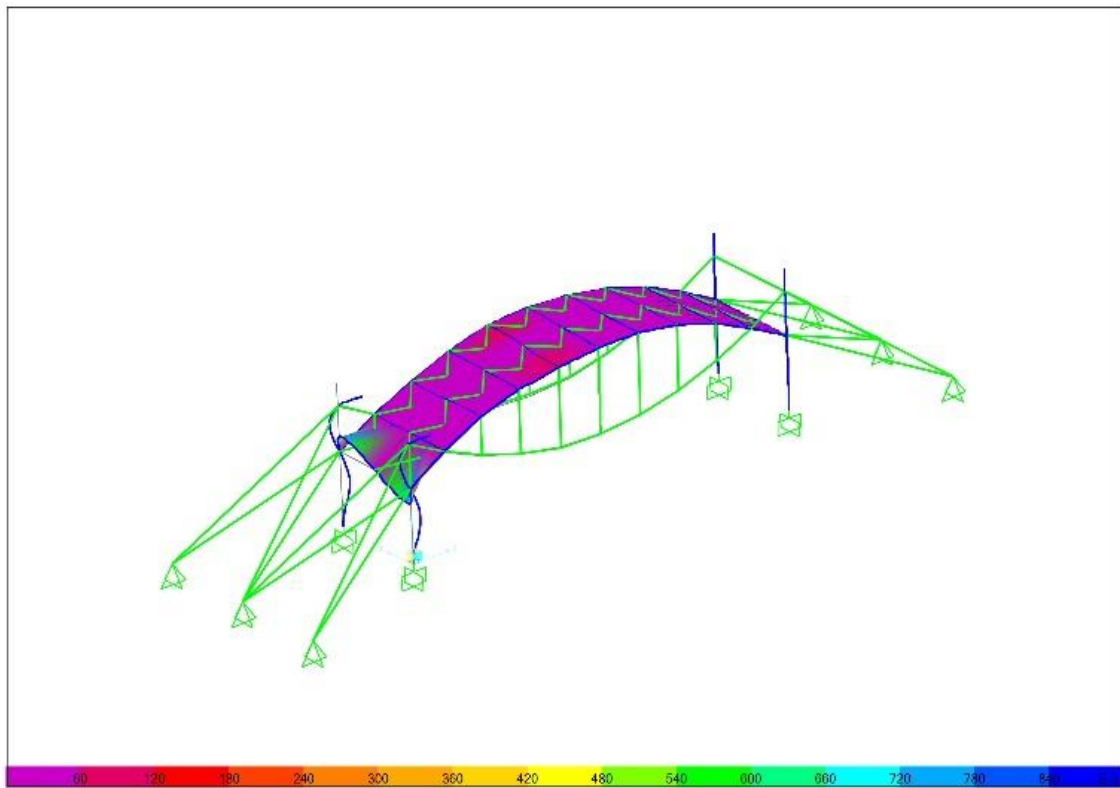
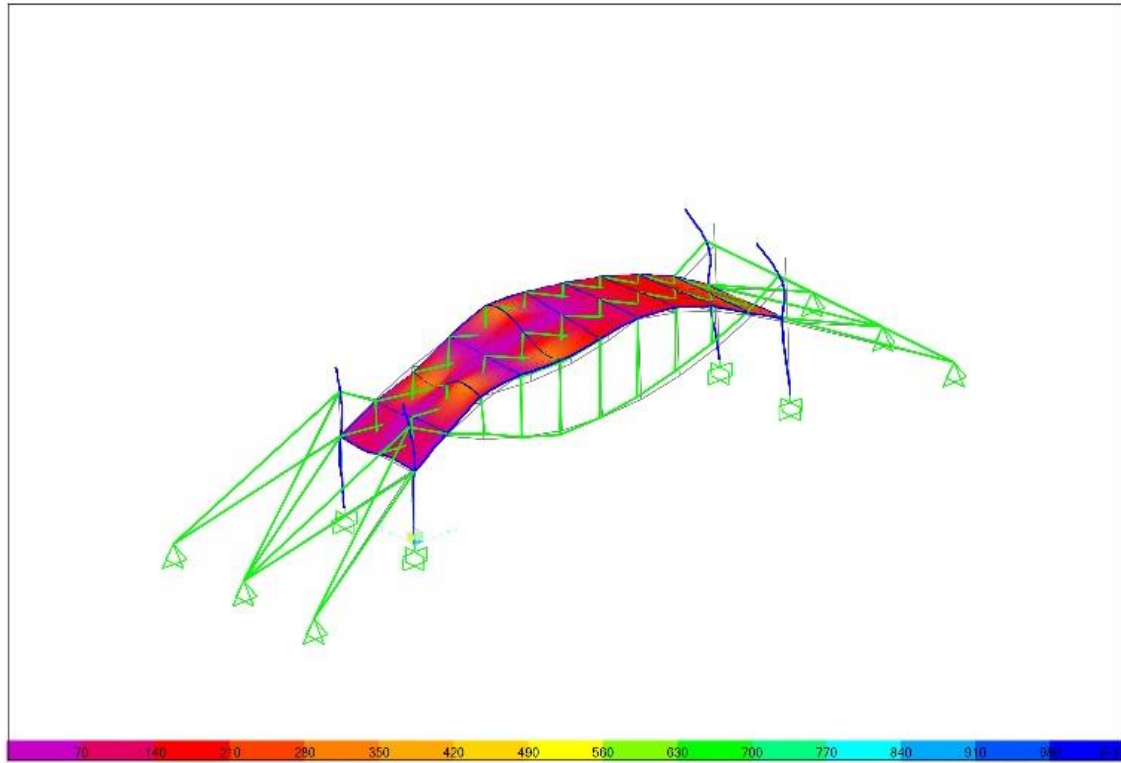*Figure 6.21: Mode 9.*

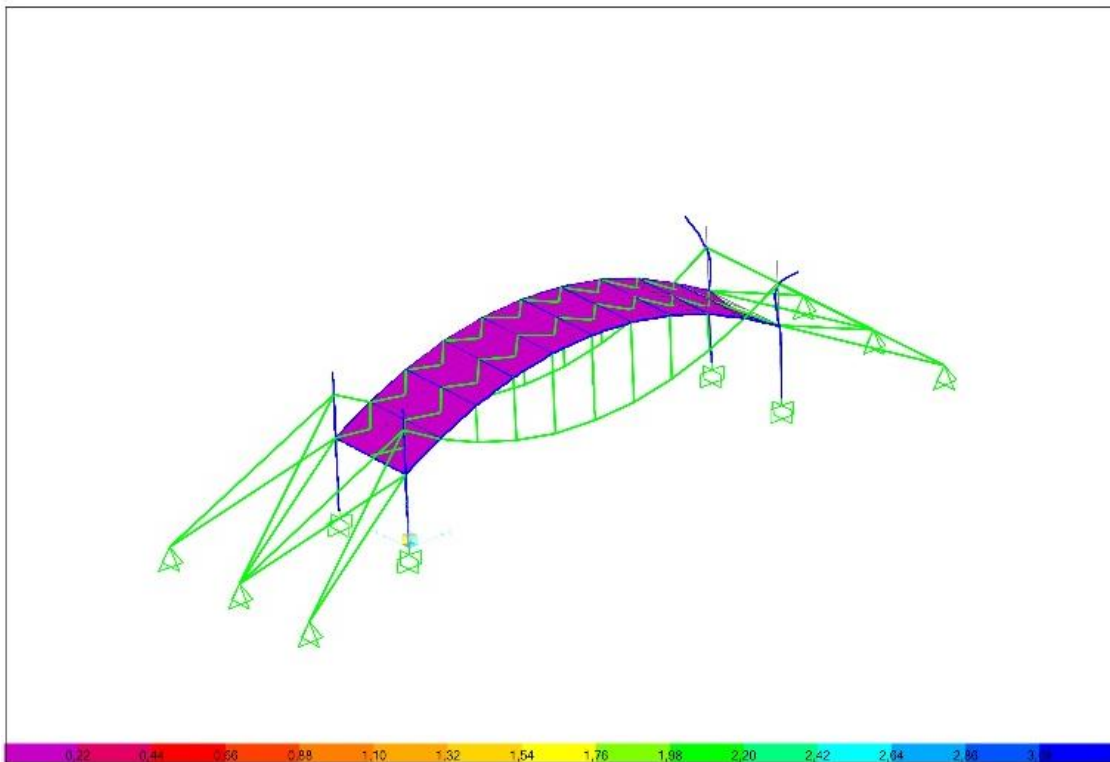*Figure 6.22: Mode 10.*

Figure 6.23: Mode 11.

Figure 6.24: Mode 12.

In the modal analysis 24 vibration modes have been considered, here depicting the first 12 modes.

In Table 6.11 and Table 6.12 the obtained results are shown.

Table 6.11: Modal Load Participation Ratios

OutputCase	ItemType	Item	Static	Dynamic
Text	Text	Text	Percent	Percent
MODAL	Acceleration	UX	71,4232	99,3969
MODAL	Acceleration	UY	96,5346	99,9492
MODAL	Acceleration	UZ	65,9536	88,7967

Table 6.12: Period and frequencies

StepType	StepNum	Period	Frequency	CircFreq
Text	Unitless	Sec	Cyc/sec	rad/sec
Mode	1	0,557161	1,7948	11,277
Mode	2	0,422132	2,3689	14,884
Mode	3	0,32747	3,0537	19,187
Mode	4	0,312177	3,2033	20,127
Mode	5	0,283351	3,5292	22,175
Mode	6	0,249995	4,0001	25,133
Mode	7	0,198076	5,0486	31,721
Mode	8	0,177829	5,6234	35,333
Mode	9	0,161133	6,206	38,994
Mode	10	0,136697	7,3154	45,964
Mode	11	0,131833	7,5853	47,66
Mode	12	0,120482	8,3	52,15

7 CONCLUSIONS

Tensile structures represent special kinds of architectural and engineering systems. They had a rapid spread during the years due to their advantages as lightness, simple and fast installation, maximum use of the materials' mechanical properties. These structures are mainly characterized by cables or cables systems as structural elements, and they can be classified in cable structures, including simple cable, cable with opposite curvature, and cable nets; membrane structures, tensegrity, and tesairity. Their application field is various and for the above-mentioned features, these structures require particular attention about the design and behaviour analysis comparing to the other ones typologies. It implicated an increasing interest of the researcher about their structural analysis. The form-finding process is a fundamental step in the design of these systems searching the equilibrium shape according to the load conditions. As known that the tensile structures are hypostatic systems, where the forces depend on the deformations; therefore, the small displacements hypothesis doesn't hold, and the calculus gets complicated.

Several approaches have been developed and improved in the years, starting from the results obtained by the study about the equilibrium of the rope. In particular, the methods can be divided into catenary, FEM, and energy approaches.

Some procedures have been analyzed in this dissertation, investigating the current state of the art; theoretical description and calculus demonstration of the statements have been presented at the beginning chapters, to highlight the advantages and disadvantages of the methodologies available in the literature.

Paying attention mainly to the cable structures, simple, with opposite curvature and cable-nets, the examined methods model the structural elements or as a continuum or a discrete one. The first case is referred to as the catenary approaches where the cable is considered as a continuum element suspended from the ends; it is demonstrated that this method is proposed for the cable with small curvature.

The second one, instead, starts from the assumption that the cable can be divided into several segments linked to each other through joints; the loads are applied along each segment or on the nodes, taking into account the geometrical and/or mechanical non-linearity. However, even if in this case some simplifications in the calculus can be obtained, the number of elements grows up, increasing the computational time. Hence,

to solve this aspect, several matrix methods have been proposed, searching for the tangent stiffness matrix and largely referring to FEM modeling. These two types of approaches (continuum or discrete) have been considered also for the cable nets systems; they can be considered or as a continuum approximating their behaviour to the membrane one, or considering the system composed by several segments interconnected to each other at the joints, and therefore considering the nodal solicitation.

As concerns the energy approaches, they are widely used in the structural engineering field, mainly to describe the non-linear behaviour of these kinds of structures under the large displacements hypothesis and by employing the mathematical variational problems. Based on the Minimum Total Potential Energy Principle, several methods have been analyzed and demonstrated in this thesis, in particular ones referred to as Harmony search.

After classified the different typologies of the tensile structures and the deep investigation performed about statics of these structural systems, in particular focusing on the cable ones, different procedures are proposed and described.

Firstly, a constrained optimization methodology has been developed and explained for a 2D cable system composed of m straight beams and t nodes, where n are free and s are fixed. It is loaded at the free nodes in a plane reference system; the analysis has been conducted first on the single beam composing the structure and then on the global system to identify the energy functional to minimize to obtain the equilibrated and compatible shape. The solution is founded through a constrained optimization problem solved by referring to the Kuhn-Tucker conditions, identifying the displacements as the unknown variables and the constraints conditions as the inequalities. The Lagrangian function has been obtained finding the global minimum of the energy functional. The approach has been applied to a simple structure to highlight the advantages of the described procedure.

Successively, to evaluate the static response of the above-mentioned cable structure, both in 2D and 3D systems, the research is focused on the study and the development of a calculus model in large displacements and small deformations, considering the geometrical non-linearity and the elastic field.

The method is in a matrix form and starts from a known static regime of the plane structure, on which a configuration change is applied, updating the structural shape.

Taking into account that the deformations are small, the self-weight of the element is neglected, and the Hooke law holds, the procedure is divided into two steps: the first one focuses on the analysis of the single beams leading to the identification of the relationship between variation of the internal forces and the position of the free nodes, through the secant stiffness matrices, elastic and geometric, and the distortion secant vector.

The second phase is characterized by an assemblage operation, identifying the geometrical non-linear relationship of the loads ensuring the equilibrium in the deformed configuration, and the displacements, expressed by the secant stiffness matrices, elastic and geometric, and the distortion one.

The problem has been solved through a step by step procedure allowing to linearize the equation at any infinitesimal single step, under small loads' variation.

Once the distorting variations have been neglected and then their contribution has been considered, identifying a distorting stiffness matrix, and considering the distortion as the distorting loads.

The method has been applied to a simple structure and then extended to the three-dimensional case confirming the expected results.

Finally, an overview of the dynamic behaviour of the tensile structure has been dealt with, analyzing the vibration modes of a study case.

Paying the base for future developments and improvements, this research is aimed to put in evidence the special behaviour of the tensile structure, with particular attention on statics of cables ones, proposing methodologies proper to their structural analysis and suitable to several typologies belonging to these structural categories

8   REFERENCES

M.S.A. Abad, A. Shoostari, V. Esnmaeili, A. N. Riabi, *Nonlinear analysis of cable structures under general loadings*, Finite Elements in Analysis and design, Vol. 73, pp. 11-19, 2013.

M. S. A. Abad, A. Shooshtari, V. Esmaeili, A. Naghavi Riabi, *Material and geometric nonlinear dynamic analysis of cable structures under seismic excitations*, in: 15th World Conference on Earthquake Engineering, Lisbon, Portugal, 2012.

M. S. A. Abad, A. Shooshtari, V. Esmaeili, A. Naghavi Riabi, *Non-linear analysis of cable structures under general loadings*, Finite Elements in Analisys and Design, n.73, pp 11-19,2013.

G. Aboul-Nasr, S.A Mourad, *An extended force-density method for form finding of constrained cable-nets*, Case Studies in Structural Engineering, vol. 3, pp. 19-23, 2015.

Y. An, B.F. Spencer Jr., J. Ou, *A Test Method for Damage Diagnosis of Suspension Bridge Suspender Cables*, Comput. Civil Infr. Eng. n.30, pp.771-784,2015.

A. Andreu, L. Gil, P.Roca, *A new deformable catenary element for the analysis of cable structures*, Comput. Structu. n. 84, pp.1182-1890, 2006.

M. Asgar Batthi, *Advanced Topics in Finite Element Analysis of Structures: With Mathematica and Matlab Computations*, Wiley, 2006.

G. Bekdas, R. Temur, Y.C. Toklu, *Analysis of truss structures via total potential optimization implemented with teaching learning based optimization algorithm,* 3rd International Conference on Optimization Techniques in Engineering (OTENG '15), Rome, November 7-9, 2015.

P. Benedikt, R. Wuchner, K.Bletzinger, *Advances in the form-finding of structural membranes*, Procedia Engineering, vol. 155, pp. 332-341, 2016.

H. Berger, *Light structures- Structures of light, The Art and Engineering of Tensile Architecture*, AulhorHouse,1996.

J. Bernoulli, *Solutio problematis funicolarii*, Acta Eruditorum, Lipsia, 1690, p. 274-276).

R. R. Bradshaw, *History of the analysis of cable net structures*, Structures Congress 2005 April 20-24, 2005, New York, New York, United States.

N. J. Branaman, V. Arcarob, H. Adelic, *A unified approach for analysis of cable and tensegrity structures using memoryless quasi-newton minimization of total strain energy,*Engn Struct. n. 179, pp. 332-340,2019.

F.K. Brogner, *Analysis of tension structures*, Pmt. Second Conference Matrix Method Structural Mech. AFFDL-TR68-150, Wright-Patterson A.F.B., pp. 1253-1270, Ohio, 1968.

F.K. Brogner, R.H. Mallet, M.D. Minich, L.A. Schimdt, *Development and evaluation of energy search methods in nonlinear structural analysis*, AFFDL-TR65-I 13, Wright-Patterson A.F.B., Ohio (1965).

H. A. Buchholdt, *An Introduction to Cable Roof Structures-Second Edition*, Cap. 6, pp. 72-98, ICE Publishing, United Kingdom, 1998.

H.A. Buchholdt et al., *A gradient method with-flexible boundaries*, Proceeding of International Conference of Tension-Roof Structures, London, 1974.

P. Campanella, *Involucro tessile e comfort ambientale. Potenzialità e limiti delle chiusure a membrana pretesa*, Tesi di dottorato,2011.

A. Capasso*, Atopic Architecture and Membrane Structures, Sign and signs of a new building archetype between ethics and form*,2014.

H. Chi Tran, J. Lee, *Advanced Form-Finding for cable-nets structures*, Int. J. of Solids and Struct., vol. 47, pp. 1785-1794, 2010.

J. Chilton*, Form-finding and fabric forming in the work of Heinz Isler*, 2th International Conference on Flexible Formwork, pp. 84-91, 2012.

W. Chunjiang, W. Renpeng, D. Shilin, Q. Ruojun, *A new catenary cable element*, Int. J. Space Struct. n. 18, pp.269-275, 2003.

R. Carter, *Boat remains and maritime trade in the Persian gulf during sixth and fifth millemnia BC*, Antiquity, Vol.80, pp.52-63, 2006.

D. Cobo del arco, A. C. Aparicio, *Preliminary static anlalysis of suspension bridges*, Engineering Structures, Vol. 23, pp. 1096-1103, 2001.

R. Connelly, M. Terrell, *Globally rigid symmetric tensegrities,* Structural Topology, vol. 21, pp. 59-78, 1995.

A. Cunha, E. Caetano, R. Delgado, *Dynamic tests on large cable-stayed bridge*, Journal Bridge Engineering, 6, 54–62,2001.

Y.M. Desai, N. Popplewell, A.H. Shah, D.N. Buragohain, *Geometric nonlinear static analysis of cable supported structures*, Comput. Struct. n. 29, pp.1001-1009,1988.

S. Dong, Y. Zhao, D. Xing, *Application and development of modern long-span space structures in China*, Frontier of Structural Engineering, Vol.6, pp. 224-239, 2012.

S.E. El-Lishani, H. Nooshin, P. Disney, *Investigating the statical stability of pin- jointes structures using genetic algorithm*, Int. J. of Spacing Structures, Vol. 20, pp.53-68,2005.

B. Forster, M. Mollaert, A. Zannelli, *Progettare con le membrane*, Maggioli Editore, 2007.

Z.W. Geem, J.H. Kim, G.V. Loganathan, *A new heuristic optimization algorithm: Harmoni search*, Simulation, Vol.11, pp.60-68, 2001.

E. Giusti, *Il calcolo infinitesimale tra Leibniz e Newton*, Rendiconti del seminario di matematica, 1988.

A. Gottfried, *Le Strutture*, Hoepli, Milano, 2001.

S. Guess, *The stiffness of prestressed framework: Aunifying approach*, Int. J. of Solids and Struct. n. 43,pp.842-854,2006.

M.A. Hanson, B. Mond, *Necessary and Sufficient Conditions in Constrained Optimization*, Mathematical Programming, Vol.37, pp. 51-58, 1987.

S. Hernandez, J.M.M. Tur, *Tensegrity Frameworks: Static analysis review*, Mechanism and Machine Theory, pp. 1-40, 2009.

E. Hernandez- Montes, R.Jurado-Pina, E. Bayo, *Topological Mapping for Tension Structures*, Journal of Structural Engineering, Vol132, 2006.

C. Huygens, *Lettera a Leibniz del 9 ottobre 1690*, Oeuvres compl`etes, L'Aia, Societ´e hollandaise des Sciences, 1895.

Y. Kanno, M. Ohsaki, *Minimum principle of complementary energy for nonlinear elastic cable networks with geometrical nonlinearities, Journal of Optimization Theory Application, Vol.126, pp. 617-641*, 2005.

T. Kawada, *History of the Modern Suspension Bridge: Solving the Dilemma between Economy and Stiffness*, ASCE Publication: Reston, VA, USA, 2010.

K. Koohestani, *Form-finding of a tensegrity structure via genetic algorithm*, Int. J. of Solids and Structures, vol.49, pp. 739-747, 2012.

K. Koohestani, S.D. Guest, *A new approach to the analytical an numerical form finding of tensegrity structures,* Inte. J. of Solids and Struct., vol. 50, pp. 2995-3007, 2013.

A.S.K. Kwan, *A new Approach to geometric nonlinearity of cable structures*, Computer and Structures, Vol. 67,1998

T.T. Lan, *Space Frame Structures, Structural Engineering Handbook*, Ed. Chen Wai-Fah, CRC Press LLC, 1999.

L. Liao, B. Du, *Finite element analysis of cable-truss structures*, in: 51st AIAA/ASME/ASCE/AHS/ASC Structures, Structural Dynamics, and Materials Conference, Orlando, Florida, USA, 2010.

I. Liddell, *Frei Otto and the development of gridshell, Case Studies* in Structural Engineering, vol.4, pp. 39-49, 2015.

Y. Liu, B. Zwingmann, M. Schlaich, *Carbon Fiber Reinforced Polymer for Cable Structures- A review*, Polymers, Vol. 6, pp.2078-2099,2015.

Q. Mac, M. Ohsakid, Z. Chena, X. Yanc, *Step-by-step unbalanced force iteration method for cable-strut structure with irregular shape,* Eng. Struct. n.177, pp.331-344,2018.

M. Majowiecki, *Tension Structures: Jawerth System*, Acier Stahl Steel, pp.169-177,1971.

R.H. Mallet, L.A. Schimdt, *Nonlinear structural analysis by energy search*, Journal of Structural Division ASCE, Vol. 93, pp.221-234, 1967.

R. Mandic, G. Hadzi-Nikovic and S. Coric, *Investigation of the behaviour of the cable-stayed bridge under test load,* Geofizika, Vol.28,2011.

M. Masic, R.E. Skelton, P.E. Gill, *Optimization of tensegrity structures*, Int. J. of Solids and Structures, vol. 43, pp.4687-4703, 2006.

M. Masic, R.E. Skelton, P.E. Gill, *Algebraic tensegrity form finding,* Int. J.l of Solids and Structures, vol.42, pp.4883-4858,2005.

M. Miki, K. Kawaguchi, *Extended Force density method for form-finding of tension structures*, J. of the International Association for Shell and Spatial Structures, pp.291-303, 2010.

G. R. Monforton, N. M. El-Hakim, *Analysis of truss-cable structures*, Computers and Structures, Vol. 11, pag. 327-335, 1980.

A. Micheletti, W.O. Williams, *A marching procedure for form-finding for tensegrity structures,* J. of Mechanics of Materials and Structures, vol.2, n°5, pp. 101-123, 2007.

W.T. O' Brien, A.J. Francis, *Cable movements under two-dimensional loads*, J. Struct. Div., ASCE n.90, pp.89-124,1964.

J. Ochesendorf and P. Block, *Exploring shell forms*, in Shell Structures for Architecture: Form Finding and Optimization, pp-7-12, 2014.

F.Otto, K. F. Schleyer, *Tensostrutture: calcolo di funi, reti di funi e strutture di funi,* 1972.

M. Pagitz, J.M.M. Tur, *Finite element based form-finding algorithm for tensegrity structures*, Int. J. of Solids and Structures, vol.46, pp. 3235-3240, 2009.

C. Paul, H. Lipson, F.J.V. Cuevas, *Evolutionary form-finding of tensegrity structures,* Proceedings of the 7th annual conference on Genetic and evolutionary computation, NY, USA, pp.3-10, 2005.

H.-J Scheck,., *The force density method for form finding and computation of general networks*, Int.l J. of Space Structures, vol.14, pp. 79-87, 1999.

L.A. Schimdt, F.K. Brogner, R.L. Fox, *Finite structural analysis using plate and shell discrete elements*, The American institute of Aeronautics and Astronautics Journal, Vol. 6, pp.781-791, 1968.

N. Srinil, G. Rega, S. Chucheepsakui, *Three-dimensional non linear coupling and dynamic tension in large- diameter tree vibration of arbitrary sagged cables*, J. Sound Vib. N.269, pp.823-852, 2004.

G.D. Stefanou, *Dynamic response of tension cable structures due to wind loads*, Comput. Struct. n. 43, pp.365–372,1992.

M. Such, J. R. J. Octavio, A. Carnicero, O. Lopez-Garcia, *An approach based on the catenary equation to deal with static analysis of three dimensional cable structures*, Engineering Structures, Vol. 31, pp. 2162-2170, 2009.

K. Takamatsu, T. Takeuchi, T. Kumagai, T. Ogawa, *Response Evaluation of Seismically Isolates Lattice Domes using Amplification Factors*, International Association for Shell and Spatial Structures, Symposium 2009.

T. Takeuchi, K. Okada, T. Ogawa, *Seismic Response evaluation of freedom lattice shell roofs with supporting substructures*, J. of Struct. Construction Eng., Vol.81,2016.

H.T. Thai, S.E. Kim, *Nonlinear static and dynamic analysis of cable structure*, Finite Element in Analysis and Design, Vol. 47, pp. 237-246, 2011.

H.T. Thai, S. E. Kim, *Non-linear static dynamic analysis of cable structures*, Finite Elem. Anal. Des. n.47, pp. 237-246,2011.

A.G. Tibert, S. Pellegrino, *Review of Form-Finding Methods for Tensegrity Structures,* Int. J. of Space Structures, vol. 18 n.4, pp. 209-223, 2003.

G. Tibert, *Numerical Analysis of Cable Roof Structures*, KTH, 1999.

T. Teramoto, H. Kitamura, H.Harada,T. Takeuchi*, Design and Construction of glass cubes using dot point glacing system*, AIJ Journal of Technology and Design,Vol.2, 1996.

Y.C. Toklu, G. Bekdas, R. Temur, *Analysis of cable structures trough energy minimization*, Structural Engineering and Mechanics, Vol. 62, pp. 749-758, 2017.

Y. Cengiz Toklu, G. Bekdaş and R. Temür, *Analysis of cable structures through energy minimization,* Struct.l Eng. Mechanics, n. 6, pp.749-758, 2017.

F. Treyssède, *Finite element modeling of temperature load effects on the vibration of local modes in multi-cable structures*, J. of Sound and Vibration n.413, pp.191-204,2018.

D.S. Wakefield, *Engineering analysis of tension structures: theory and practice*, Engineering Structures, Vol.21, pp. 680-690, 1999.

C. Wang, R. Wang, S. Dong, R. Qian, *A new catenary element, International Journal of Space Structures*, Vol. 18, pp.269-275, 2003.

C. Wang, R. Wang, S. Dong., R. Qian, *A new catenary cable element*, International Journal of Space and Strructures, Vol.18, pp. 269-275, 2003.

P.H. Wang, H.T. Lin, T.Y. Tang, *Study on non-linear analysis a highly redundant cable stayed bridge*, Comput. Struct. n.80, pp.165-182,2002.

C. Williams, *What is a shell?*, in Shell Structures for Atchitecture: Form Finding and Optimization, pp27-31, 2014

J. C. Wilson, W. Gravelle, *Modelling of a cable-stayed bridge for dynamic analysis*, Earthq. Eng. Struct. Dyn. n.20, 707-721,1991.

M. Yamamoto, B.S. Gan, K. Fujita, J. Kurokawa, *A Genetic Algorithm Based Form-Finding of Tensegrity Structure, Procedia Engineering*, vol. 14, pp.2949-2956, 2011.

J.Y. Zhang, M. Ohsaki, *Adaptive force density method for form-finding problem of tensegrity structures*, Int.l J. of Solids and Structures, vol. 4, pp.5658-5673, 2006.

J.Y. Zhang, M. Ohsaki, Y. Kanno, *A direct approach to design of geometry and forces of tensegrity systems*, Int. J. of Solids and Structures, vol. 43, pp.2260-2278, 2006.

https://www.google.com/search?q=cable+structures&rlz=1C1CAFA_enIT762IT762&s xsrf=ALeKk00epg-C_NQm9xnS1S-WPXrgvdjXgw:1583998755669&source=lnms&tbm=isch&sa=X&ved=2ahUKEwjQ3Z -Zt5ToAhWIrIsKHR-FC_cQ_AUoAXoECBEQAw

https://www.pinterest.it/search/pins/?q=cable%20structures&rs=typed&term_meta[]= cable%7Ctyped&term_meta[]=structures%7Ctyped

https://www.pinterest.it/search/pins/?q=tensile%20structures&rs=typed&term_meta[] =tensile%7Ctyped&term_meta[]=structures%7Ctyped